Laboratory Study of Optimized Concrete Pavement Mixtures

Dr. Konstantin Sobolev, Mohamadreza Moini , Dr. Scott Muzenski,
Dr. Rani Pradoto, Dr. Marina Kozhukhova, Dr. Ismael Flores-Vivian
University of Wisconsin - Milwaukee

Dr. Steven Cramer, Le Pham
University of Wisconsin - Madison

Dr. Ahmed Faheem
Temple University/Bloom Companies, LLC

WisDOT ID no. 0092-13-04
August 2015

RESEARCH & LIBRARY UNIT

WISCONSIN HIGHWAY RESEARCH PROGRAM

WISCONSIN DOT
PUTTING RESEARCH TO WORK

Disclaimer

This research was funded by the Wisconsin Department of Transportation and the Federal Highway Administration through the Wisconsin Highway Research Program under Project 0092-13-04. The content of this report reflect the views of the authors who are responsible for the facts and accuracy of the data presented herein. The contents do not necessarily reflect the official views of the Wisconsin Department of Transportation or the Federal Highway Administration at the time of publication.

This document is disseminated under the sponsorship of the Department of Transportation in the interest of information exchange. The United States Government assumes no liability for its contents or use thereof. This report does not constitute a standard, specification or regulation.

The United States Government does not endorse products or manufacturers. Trade and manufacturers' names appear in this report only because they are considered essential to the object of the document.

Technical Report Documentation Page

1. Report No. WHRP 0092-13-04	2. Government Accession No	3. Recipient's Catalog No
4. Title and Subtitle Laboratory Study of Optimized Concrete Pavement Mixtures		5. Report Date December 2015 6. Performing Organization Code Wisconsin Highway Research Program
7. Authors Konstantin Sobolev, Mohamadreza Moini, Steve Cramer, Ismael Flores-Vivian, Scott Muzenski, Rani Pradoto, Ahmed Fahim, Le Pham, Marina Kozhukhova		8. Performing Organization Report No.
9. Performing Organization Name and Address UW-Milwaukee UW- Madison Temple University / Bloom		10. Work Unit No. (TRAIS) 11. Contract or Grant No. WisDOT SPR# 0092-13-04
12. Sponsoring Agency Name and Address Wisconsin Department of Transportation Research & Library Unit 4802 Sheboygan Ave. Rm 104 Madison, WI 53707		13. Type of Report and Period Covered Final Report 2012-2015 14. Sponsoring Agency Code
15. Supplementary Notes		

16. Abstract

Recent research supported by the Wisconsin Department of Transportation (WisDOT) concluded that concrete produced with reduced cementitious materials content had an adequate durability; however, tested mixes frequently demonstrated poor workability. As a result, a need was identified for a multi-faceted approach to optimize the mixture proportions for low-slump concrete in pavements in order to realize the benefits related to reduced cementitious material content. The reported approach includes the use of supplementary cementitious materials (SCMs), optimized aggregate gradations, and the use of superplasticizers (high-range water reducing admixtures).

Current WisDOT practice minimizes the use of portland cement through replacement with SCMs, but does not address the use optimized aggregate gradation or superplasticizers. Therefore, additional research was conducted to support the development of specifications inclusive of these factors to improve the performance and sustainability of concrete paving mixtures used in Wisconsin. This research project evaluated the feasibility of expanding current specifications to incorporate the optimized superplasticized concrete in sustainable concrete paving applications. Furthermore, the goal of the reported study was to produce the guidelines for optimizing concrete mix design by evaluating the performance of a range of concrete mixtures.

The performance evaluation of optimized concrete included the workability (slump), air content, compressive and flexural strength, freeze-thaw resistance, and rapid chloride permeability in accordance with the relevant AASHTO or ASTM standards. Finally, the reported research recommended the selection of aggregate gradations and superplasticizing admixtures in low-slump concrete with reduced cementitious materials intended for paving applications.

17. Keywords	18. Distribution Statement
optimization, low cement concrete, aggregates, admixtures, superplasticizer, supplementary cementitious materials, compressive strength, durability, air-void analysis	No restriction. This document is available to the public through the National Technical Information Service 5285 Port Royal Road Springfield VA 22161

18. Security classif.(of this report)	19. Security classif. (of this page)	20. No. of Pages	21. Price
Unclassified	Unclassified	184	Gratis

Form DOT F 1700.7 (8-72) Reproduction of completed page authorized

EXECUTIVE SUMMARY

Other than water, portland cement concrete is the most used commodity. Major parts of civil and transportation infrastructure, including bridges, roadway pavements, dams, and buildings are made of concrete. Because of wide-scale applications of these important structures in different climatic zones and associated exposures, concrete durability is often of major concern. In 2013, the study of American Society of Civil Engineers (ASCE) estimated that one-third of America's major roads are in poor or mediocre condition [1]. The same article reports that annual investments of $170 billion on roads and $20.5 billion for bridges are needed to substantially improve the condition of infrastructure. In addition to durability concerns, the production of portland cement is associated with the emissions of approximately one cubic meter of carbon dioxide per ton (plus NO_x and SO_x). Therefore, replacement of portland cement with supplementary cementitious material is an important trend to improve the sustainability of concrete. Indeed, the consideration of these issues as well as proper and systematic design of concrete intended for highway applications is of extreme importance as concrete pavements represent up to 60% of interstate highway systems with heavier traffic loads.

The combined principles of material science and engineering can provide adequate methods and tools to facilitate improvements to concrete design and existing specifications. Critically, durability and enhancement of long-term performance must be addressed at the design stage. Concrete used in highway pavement applications already has relatively low cement content and also can be placed at low slump. However, further reduction of cement (cementitious materials) content to 280 kg/m^3 (470 lb/yd^3) vs. current WisDOT specifications which require the use of 315 - 340 kg/m^3 (530 - 570

lb/yd^3) of cementitious materials for concrete intended for pavement applications and 335 kg/m^3 (565 lb/yd^3) for bridge substructure and superstructure needs a delicate proportioning of the mixture to maintain the expected workability, overall performance, and ensure long-term durability in the field. Such design includes, but is not limited to the optimization of aggregates and supplementary cementitious materials (SCM), as well as fine-tuning of the type and dosage of chemical and air-entraining admixtures.

This research evaluated various theoretical and experimental methods for aggregate optimization which can result in the reduction of cement content. For selected mixtures, reported research investigated further reduction of cementitious materials content to 250 kg/m^3 (420 lb/yd^3), which can be attractive for the design of sustainable concrete pavements. The reported research demonstrated that aggregate packing can be used as a tool to optimize the particulate assemblies and achieve the optimal particle size distribution of aggregate blends. The SCM and air-entraining admixtures were selected to comply with existing WisDOT performance requirements, and chemical (mid-range and high range water reducing) admixtures were selected based on the optimization study. The performance of different concrete mixtures was evaluated for fresh properties, compressive and flexural strength ranging from 1 and up to 365 days and also for important durability indicators such as freeze-thaw resistance and chloride permeability. The methods and tools discussed in this research are applicable, but not limited to concrete pavement and bridge applications.

The current concrete proportioning standards such as ACI 211 or current WisDOT roadway standard specifications (Part 5: Structures, Section 501: Concrete) for concrete have limited or no recommendations, methods or guidelines on aggregate

optimization, the use of ternary aggregate blends (e.g., such as those used in asphalt), the optimization of SCM (e.g., Class F and C fly ash, slag cement, metakaolin, silica fume), the use of modern superplasticizers (such as polycarboxylate ether, PCE, based) and air-entraining admixtures. This research has demonstrated that the optimization of concrete mixture proportions can be achieved by the use and proper selection of modern superplasticizers and optimal aggregate blends. This optimization can result in up to 18% reduction of cementitious materials content and, for selected mixtures, provide the enhancement of performance. To prove the proposed concrete proportioning method, the following investigative steps were performed:

- The optimal products and dosages of chemical admixtures were selected for three types of plasticizing and superplasticizing admixtures;
- The SCM effects and compatibility with chemical admixtures were investigated to comply with current WisDOT specifications;
- The experimental packing of aggregates was investigated for northern and southern aggregates available in Wisconsin;
- The theoretical aggregate packing models were evaluated and results were compared with the experiments;
- Multiple aggregate optimization methods (e.g., optimal grading, coarseness chart) were studied and compared to aggregate packing results and the performance of experimental concrete mixtures;
- Optimal aggregate blends were defined, evaluated and used for concrete mixtures;
- The optimal dosage of air-entraining admixture was investigated based on the performance of trial concrete mixtures;

- The effect of cementitious materials content was investigated at two levels of 280 kg/m^3 (470 lb/yd^3) and 250 kg/m^3 (420 lb/yd^3);
- Optimal concrete mixtures were tested for fresh properties, compressive strength development, modulus of rupture and length change at both early (1-day) and ultimate ages (up to 365 days);
- The durability performance was tested to evaluate this resistance of concrete to rapid chloride permeability (RCP) at 30 and 90 days and also resistance to rapid freezing and thawing (up to 300 cycles).

Based on the established correlations, it was concluded that the aggregate packing can provide a good prediction for compressive strength and can be used to optimize concrete mixtures. The improved compressive strength and enhanced concrete performance can be used as a tradeoff to reduce the cementitious material content to 280 kg/m^3 (470 lb/yd^3). The optimized superplasticized concrete, with up to 30% of fly ash (Class C), and up to 50% ground granulated blast furnace slag, demonstrated very exceptional mechanical and durability performance. The proposed concrete optimization provided material with enhanced performance and durability, providing the extension of life cycle, sustainability and environmental benefits.

ACKNOWLEDGMENTS

The authors would like to thank the Wisconsin Highway Research Program for sponsoring this research. The authors would also like to thank Bloom Companies, Lafarge Cement Company, Holcim US Inc., St. Marys Cement Group, We Energies Corporation, American Materials, Zignego Ready Mix, Handy Chemicals, BASF Chemical Company, W. R. Grace Company for providing the materials required for the project.

The authors would like to convey special thanks to all students that assisted in preparation of concrete mixtures, tests and heavy work in the lab: Nathaniel Havener, Katie LeDoux, Gaven Kobes, Jason Atchison, Craig Vindedahl, Clayton Cloutier, Chris Ball, Mark Moyle, Alper Kolcu, Kristian Nygaard, Andrew Sinko, Jesus Cortes, Sunil Rao, Jayeesh Bakshi, Tyler Beinlich, Leif Stevens Jackson, Emily Ann Szamocki, Brandon Bosch, and Rahim Reshadi.

TABLE OF CONTENTS

LIST OF TABLES

LIST OF FIGURES

LIST OF ABBREVIATIONS

PCE/SP:	Polycarboxylic Ether / Superplasticizer
SNF/SP:	Sulfonated Naphthalene Formaldehyde / Superplasticizer
MR/P:	Mid-Range Plasticizer (also Water Reducing Admixture)
P/SP:	Plasticizer/Superplasticizer
WR(A):	Water Reducing Admixture (also Plasticizer)
HRWR(A):	High-Range Water Reducing Admixture (also Superplasticizer)
AE(A):	Air Entraining Admixture
L:	Cement 1 (Type I)
H:	Cement 2 (Type I)
S:	Cement 3 (Type I)
SCM:	Supplementary Cementitious Material
AF:	Class F Fly Ash
AC:	Class C Fly Ash
GGBFS/SL:	Ground Granulated Blast Furnace Slag (Slag Cement)
CPD.:	Compacted Packing Degree
LPD:	Loose Packing Degree
PSD:	Particle Size Distribution
DF:	Durability Factor
W/C:	Water to Cement Ratio
W/CM:	Water to Cementitious Materials Ratio
PC:	Power Curve

Notation Used for Concrete Mixtures: Type of Cement - Type of Aggregate - Type of WRA - Type of SCM - (R for Reduced Cement Content)

Notation Example:

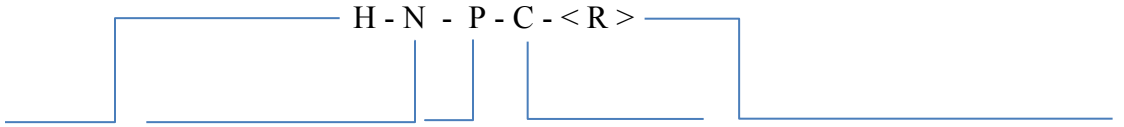

1. INTRODUCTION

In 2013, the American Society of Civil Engineers (ASCE) estimated that one-third of America's major roads are in poor or mediocre condition. The ASCE report concluded that an annual investment of $190.5 billion is needed to substantially improve the conditions of roads and bridges [1]. The pavement industry was challenged to establish advanced practices for the improvement of concrete mixtures and pavement design which can address both environmental and financial viability [2]. On the other side, the concrete and pavement industry aims to produce a sustainable concrete [3]. The contribution of portland cement to carbon dioxide (CO_2) emissions and relatively short service life of mainstream concrete are identified as the key factors that require immediate improvement to reach the sustainable concrete objective.

Traditionally, concrete pavement design is focused on determining the thickness of the slab based on the traffic loads [2]. A "recipe-based" or prescriptive concrete mixture proportioning does not necessarily respond to the performance requirements, exposure conditions and the best use of the materials available. As a result, the proportioning of concrete for highway pavement applications is hindered from further advancements and is focused on cost-effectiveness for the manufacturer rather than on technology improvement, performance requirements and efficiency for the end user. The "performance-based" design, as opposed to the "recipe-based" approach, relies mainly on the material's performance limits and determines the optimal design based on the performance, material properties and cost. However, the application of this method requires a deep knowledge of the material's properties, behaviors and time-dependent interactions.

The use of supplementary cementitious materials (SCM), including industrial by-products such as ground granulated blast furnace slag (GGBFS, also known as slag cement) and fly ash, can potentially reduce the consumption of cement by up to 50% and 30%, respectively, and these limits are already prescribed by the WisDOT standard specification for concrete. Also, the use of SCM can provide a cementitious matrix with a better density and, therefore, better durability. In blends with portland cement, slag cement is chemically activated and demonstrates excellent long-term cementitious properties. Pozzolanic by-products (especially Class F fly ash) can react with $Ca(OH)_2$ released due to cement hydration, resulting in the formation of an additional C-S-H, the main binding component of hydrating matrix. Also, fly ash can combine with cement alkalis (K_2O and Na_2O), minimizing the risk of aggregate-alkali-silica reaction. Fly ash suitable for concrete applications is defined by ASTM 618 and its classification is based on the total proportion of Si_2O, Al_2O_3, and Fe_2O_3.

Table 1. Fly ash classification (per ASTM 618) [3]

Class	Description	Requirements
F	Pozzolanic properties	$Si_2O + Al_2O_3 + Fe_2O_3 > 70\%$
C	Pozzolanic and cementitious properties	$Si_2O + Al_2O_3 + Fe_2O_3 > 50\%$

Superplasticized concrete with enhanced performance is specified for heavily reinforced elements such as floors, foundations, bridge decks, and also applicable pavement applications. Superplasticizers release excessive water from the cement paste through better dispersion of the cement particles [47]. This type of concrete is characterized by enhanced workability, flowability, as well as reduced permeability, improved durability, and reduced shrinkage. However, plasticizers (also known as water-

reducing WR admixtures) are more common in concrete pavements when low slump mixes are required, whereas superplasticizers (high - range water reducing, HRWR admixtures) are common in high workability applications, such as structures with congested reinforcements and self-consolidating concrete. Due to exceptional water-reducing properties, modern superplasticizers enable the production of very economical concrete with reduced cementitious material content. Superplasticizers can play a larger role in concrete pavement technology, enhancing the mechanical performance and fresh properties achieved due to reduced water to cement (W/C) ratio. Although superplasticizers introduce remarkable advantages in concrete, there are some limitations. For example, the compatibility of superplasticizers with other admixtures such as retarders, air-entraining agents and SCM must be considered prior to application [4].

Air-entraining (AE) admixtures are intended to provide a desired air void system in concrete. The developed air void structure can provide extra space for freezing water to expand and so, reducing the associated stresses, enhances the concrete's freezing and thawing resistance. For adequate performance in regions exposed to freezing and thawing, it is necessary to have a concrete with certain air-void structure controlled by content of entrained air (up to 8%). However, some AE admixtures may have incompatibility with SCM, specifically, in the case when fly ash with high carbon content is used. Therefore, the design of AE concrete often requires preliminary investigation to determine the dosage of AE admixture that can provide the required air content [4].

The research on concrete and the evaluation of new technologies is vital for enhancing infrastructure performance and durability, updating specification requirements, and to provide the guidelines to the industry for adoption of sustainable design methods

and the use of by-products. Optimizing concrete proportions for enhanced performance and reduced cement content is a complicated task as several components are involved, including various aggregate types, as well as air-entraining (AE) admixtures, water reducing (or high range water reducing) admixtures and supplementary cementitious materials (SCM). Optimized concrete mixtures can offer savings by reducing cementitious material content by up to 18% vs. current standards (e.g., WisDOT standard specifications, Part 5: Structures, Section 501: Concrete) [5]. The reported research uses a multi-scale approach including the optimization of individual components and phases prior to their application in concrete while also incorporating industrial by-products.

Mineral additives or supplementary cementitious materials (SCM) and chemical admixtures (such as HRWR, AE) are common components of concrete technology, but sometimes these are not effectively used due to the complexity and variability in composition, processes, and the diverse effects on concrete performance. Therefore, the individual components such as SCM, HRWR, and AE admixtures must be optimized at smaller scale in pastes and mortars prior to their use in concrete. Hence, the reported results of such optimization are accurate for the scope of the cementitious materials and chemical admixtures used and to the extent of the materials characterized. These materials, even of the same standard grade, often possess different characteristics and different behaviors due to the variation in raw materials, manufacturing technology and processing. However, the fundamental properties of characterized and optimized individual phases (paste, mortar, aggregates) can be used as input parameters for concrete mixture proportioning and so the proposed approach is valid for a wide range of components.

In the past decades, "traditional" concrete proportioning specifications were challenged with the difficulty of establishing a uniform design procedure for concrete containing SCM, HRWR, and AE admixtures. The difficulties are partially due to the use of different component materials with various behaviors, different characteristics, and potential chemical incompatibilities. For example, the ASTM C150 Type I cement products are manufactured with a wide range of properties and mechanical responses. Such variations include the physical and chemical properties affecting the cement compatibility with different SCM and chemical admixtures. To address far-reaching results, a novel optimization method focusing on aggregate and admixture optimization was proposed [7]. The approach used in reported research was previously verified by extensive experiments on high-performance concrete containing different SCM (silica fume, fly ash, slag cement) and chemical admixtures [6, 7].

The advent of ready mixed concrete and the use of large capacity pumps for transporting concrete demanded the use of improved aggregate blends tuned for mixtures with high workability, as well as imposed limitations on the maximal size of aggregates (D_{max}). Aggregates comprise 60 to 75 percent of concrete (by volume), and so concrete performance is strongly affected by the aggregate's packing, properties and proportioning [8-16]. Optimized aggregate blends can provide concrete with improved performance or can be used to design a concrete mix with reduced volumes of cementitious materials. Therefore, the optimization of aggregates is an attractive option to improve the engineering properties, reduce the cementitious materials content, reduce the materials costs, and minimize the environmental impacts associated with concrete production. Early reports on concrete technology have emphasized the performance enhancement

effects due to improved packing and grading of aggregates [12, 16-18]. Indeed, improving the main engineering properties of concrete, such as strength, modulus of elasticity, creep, and shrinkage, can be achieved by the fine-tuning of aggregate packing [9-11, 14, 15, 18-25]. It was demonstrated that the optimization of aggregate blends by packing or particle size distribution (PSD) techniques can bring significant savings due to the reduction of cementitious materials/binder [18]. Still, due to complexities in aggregate packing and irregularities in shape and texture, there is no universal approach to account for the effects of particle size distributions and packing degree on the performance of concrete in fresh and hardened states [3-11].

The importance of aggregate characteristics is widely discussed in the literature [8]. Abrams stated that "…the problem is to put together the aggregates available in order to have the best concrete mixture we can for a given cost or at a minimum cost" [8, 9]. Gilkey [8, 10] proposed the modification of Abrams' W/C to strength relationship by considering the ratio of cement to aggregate as well as grading, shape, strength of aggregate particles, and D_{max} [8, 10]. Other researchers also discussed the relevance and importance of aggregate characteristics [11-16]. The theory of aggregate particle packing has been discussed for more than a century [23-38] and includes the discrete particle packing theories, continuous theories, and discrete element models (DEM). Discrete models include the interaction effects between the particles to calculate the maximum packing density for binary, ternary or multi-component mixtures [29-32]. Continuous models are believed to represent the maximum theoretical density mixtures. It is postulated that the optimal PSD corresponds to the "best" or the densest packing of the constituent particles; however, modeling of large particulate assemblies has demonstrated

that the densest arrangements of particles corresponding to random Apollonian packings (RAP) are not practically achievable in concrete [38]. Therefore, the dense packings calculated by RAP methods for regular particles and corresponding PSD are not utilized in concrete technology [24]. The static or dynamic DEM can generate virtual packing structures from a given PSD using random distribution of spherical particles [36-38]. The packing criteria for optimizing concrete mixtures are occasionally used for various applications including high-strength concrete, self-consolidating concrete, concrete for pavement applications, and heavyweight concrete [13, 19, 20, 26, 39, 40]. The experimental packing depends on a loose or compacted condition of blends, packing energy, packing method, which must be specified prior to correlating the experiments and the models. A better understanding of packing mechanisms for aggregates of various combinations and sizes, as required for concrete applications, is needed. As a result, the PSD is a commonly known criterion towards the optimization of aggregate blends affecting the fresh and hardened properties of concrete. The effect of PSD on workability, density and compressive strength on concrete was reported in the literature [31, 41, 42].

The use of packing degree as a tool to optimize the binary and ternary aggregate blends targeting for minimal void content (or the maximal packing degree) was accomplished [13]. The problem of the best-possible aggregate packing and associated to its beneficial effects on concrete has been the subject of experimental and theoretical investigations [6, 11-20, 40, 43-45]. Other researchers have proposed a comprehensive theory utilizing scientific insight to providing a better understanding of the role of aggregates on compressive strength [7, 20, 31, 38-40, 46, 47]. To improve the aggregate mixture proportions, ACI Education Bulletin E1-07 recently recommended using an

intermediate aggregate (IA) fraction to compensate for "missing" grain sizes [17], and ACI 211 drafted a Technote document for the use of multiple criteria for aggregate optimization. In spite of several reports discussing the importance of theoretical models representing the packing of natural or artificial aggregate assemblies [40, 43, 48], the empirical approach remains a very important tool to verify the models by testing different aggregate combinations and correlating the packing degree to the strength characteristics of particular composites [39, 40, 42, 49].

The identification of the best aggregate blends for concrete and the relationship between the packing and performance still remain a challenging task for future research. To address the objective of this research, the best aggregate blend for concrete is selected using multiple criteria, and the effect of aggregate packing is investigated by simulation and experiments. These criteria include grading techniques with power curves (PC), the Shilstone coarseness factor chart, and the experimental and simulated packing. The experimental PSD and corresponding packing values are compared with associated packing simulations based on the best fit to corresponding PC. Optimizing aggregate compositions with the use of ternary aggregate blends (as commonly used in asphalt) and specified packing degree can be suggested as an experimental approach which can, therefore, reduce the volume of voids within the aggregate mix. As a result, at the same separation of aggregates (as required for flow and compaction), cement paste content can be reduced for the same unit volume of concrete. Along with the use of superplasticizers, the aggregate packing can be used as a tool to optimize concrete mixtures and improve compressive strength.

2. LITERATURE REVIEW

2.1. CONCRETE OPTIMIZATION

Concrete mixture optimization is a broad term used for fine tuning of various types of concrete targeting for several performance aspects and desirable properties. More specifically, the optimization of concrete mixture proportions deals with the selection of the most efficient quantities of aggregates, SCM, chemical admixtures, and the minimization of cementitious material content *(Figure 1)*.

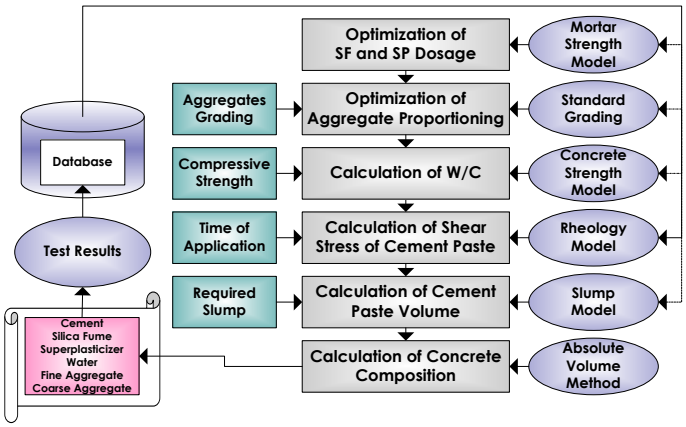

Figure 1. Proposed concrete mixture proportioning method [7]

Concrete mixture proportioning was holistically represented by many researchers [5, 7, 50-57]. The subject was further approached by performance based modeling [57], computer-aided modeling for a system of ingredient particles [46, 58, 59], sustainability concepts [2, 60, 61], chemical admixture optimization, aggregates optimization, including the effect of aggregates on concrete strength [23, 36, 40, 49, 52, 56, 62-64], and statistical design of concrete mixtures [3, 7]. Furthermore, a mix proportioning for sustainable "green" concrete was realized by using by-products [65-67] and by improving the aggregate characteristics related to packing density [68].

2.2. THE APPLICATION OF CHEMICAL ADMIXTURES

2.2.1. Modern Superplasticizers

Superplasticized concrete has been effectively used for the production of heavily reinforced elements such as floors, foundations slabs, bridges, pavements, roof decks and others [4]. This type of concrete is characterized by reduced permeability, improved surface finish, reduced shrinkage, enhanced durability, and overall cost savings. Due to exceptional water-reducing properties, modern superplasticizers (SP) enable the production of very economical concrete with reduced cementitious material content without any detrimental effects on performance. Although superplasticizers introduce remarkable advantages in concrete, there are some limitations. For example, the compatibility of SP with other admixtures such as water reducers, retarders, accelerators and air-entraining agents must be investigated prior to application of superplasticizers. The combination of SP with air-entraining agents may alter the air bubble size distribution and spacing. In addition, reduced strength due to high porosity and retardation of hydration may occur when superplasticizer is mixed with Type V cement, (*Figure 2*) [4]. Workability and setting of superplasticized cement paste may change depending on the amount and type of sulfate (i.e., anhydrite or gypsum) used for cement production. The differences can be explained by different rates of dissolution of the sulfates [69].

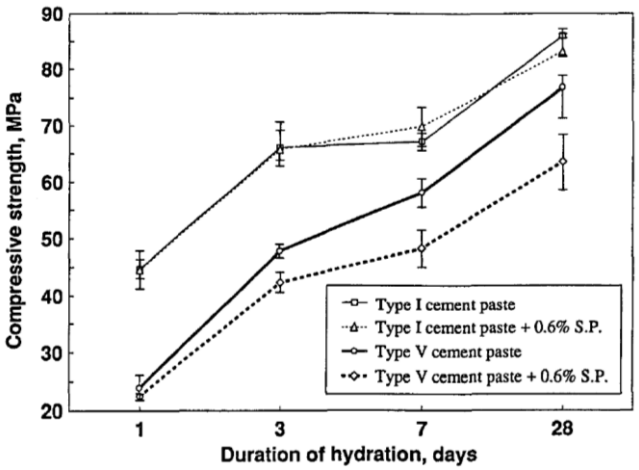

1 MPa = 145 psi

Figure 2. The Effect of Sulfonated Melamine Formaldehyde (SMF) Superplasticizer on the Compressive Strength of Type I and V Cement [4].

Admixtures of the same generic type may result in different effects in concrete because of the variations in the molecular weight, chain length, production technology, etc. Similarly, the same type of cement can be represented by a material with different fineness, mineral, alkali, and sulfate contents. In this way, each admixture combination must be evaluated before application. In addition, superplasticizers should be evaluated for side effects related to workability, setting, air content, and mechanical properties [4].

In terms of chemical structure, there are two main categories of superplasticizing polymers, also known as a surfactants, or dispersants: sulfonated ring structures and acrylic or polycarboxylate derivatives [4, 70]. There are two main dispersion mechanisms that explain the particle separation behavior: electrostatic repulsion and steric hindrance (*Figure 3*). In the electrostatic repulsion mechanism, the dispersant molecule has a localized negative ionic character at one region and a localized positive ionic character at another. The dispersant attracts to the particle surface and orients in a way that the outer layer of the film is now exclusively positive. As other particles are similarly coated, these

are all essentially positively charged and cannot agglomerate. The steric hindrance mechanism similarly relies on portions of the dispersant to be attracted to the particle surface, but the outer regions of the dispersant chains tend to be long and non-polar (or partially polar) in character rather than ionic. Entanglement or crystalline-ordering of the outlying chains of different particles is thermodynamically unfavorable, so the particles tend to stay separated [70, 71].

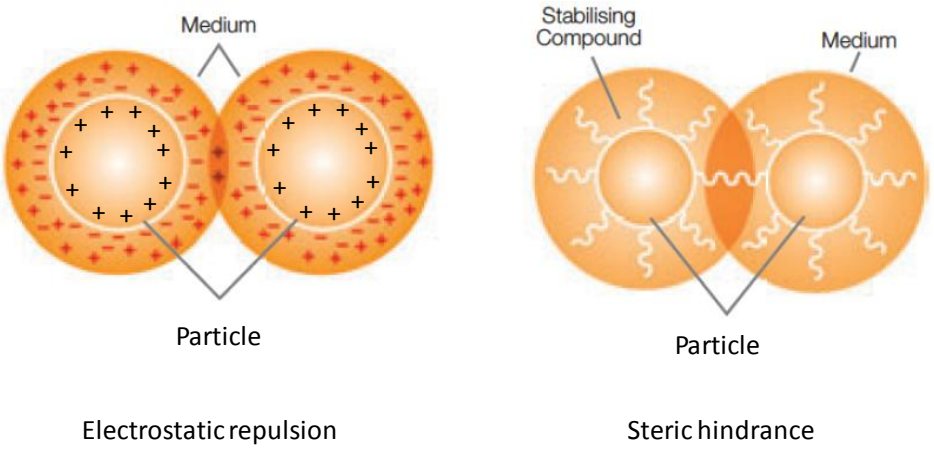

Figure 3. Particle's Dispersing Mechanisms [71].

Sulfonated ring polymers are anionic polymers with many $-SO^{3-}$ groups that attract to regions of positive charge on the cement particles, primarily Ca^{+2} (*Figure 4*). As particles are wetted with a film of polymer, these effectively become negatively charged and repel each other [70, 72]. Additionally, free water that would have been bound in particle agglomerates becomes available as a fluidizer, which reduces the viscosity of the paste or slurry [73, 74]. Selective structures for sulfonated ring polymers are displayed in *Figure 5*. The morphology of these polymers can vary. Structures with more branching and less linearity can be produced that would be candidates for superplasticizers, as long as these have a sufficient number of anionic sites.

However, there are limits to the effectiveness of an increase in molecular weight and bulk. The gains in mini slump (as measure of workability) and polymer adsorption are limited by the molecular weight (MW, as indicated by polymer solution viscosity), as demonstrated for sulfonated naphthalene SP [74]. The basic structure of a sulfonated naphthalene formaldehyde (SNF) condensate polymer is well established, and it was demonstrated that similar effectiveness can be achieved by medium to high MW polynapthatlene sulfonate SPs [75].

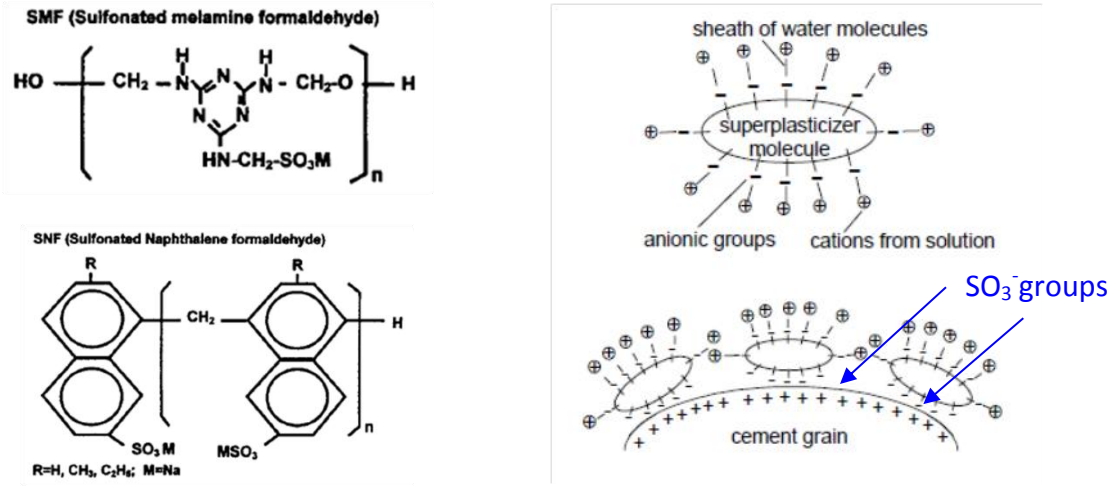

a) Sulfonated ring structures **b) Electrostatic repulsion**

Figure 4. Chemical structure and electrostatic repulsion mechanism of sulfonated ring superplasticizers [70].

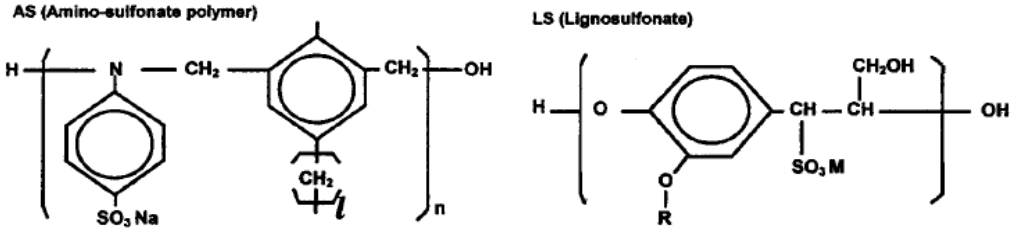

Figure 5. Selective sulfonated ring superplasticizers [70].

Polycarboxylate polymers have the main trunk of the molecule being the backbone and the ethoxy block polymer branches at the ends. The trunk contains carboxylate groups, which couple with Ca^{+2} sites on cement or hydration products. The branches, or side chains, contain ether oxygen groups (-C-O-C-), which form strong hydrogen bonds with water *(Figure 6)*.

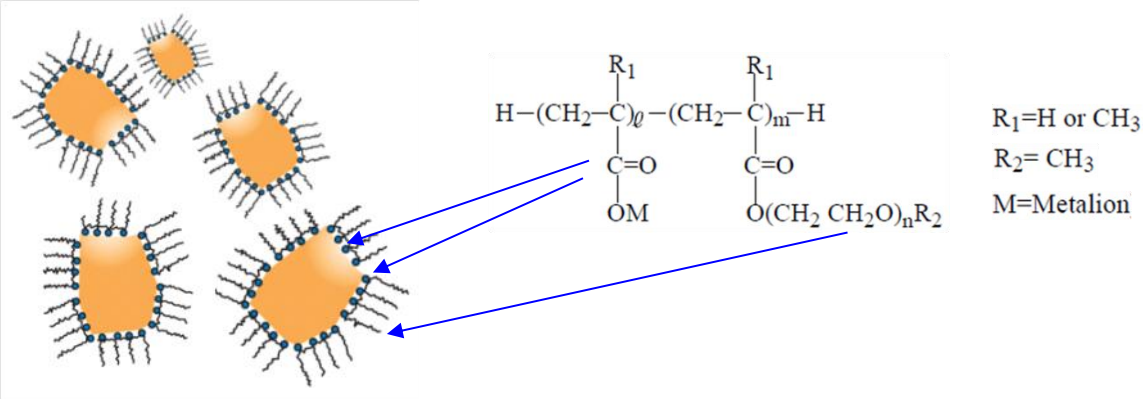

Figure 6. Polycarboxylate superplasticizers: steric hindrance mechanism, adapted from Lubrizol [71] (left) and generic structure [60] (right).

Sakai et al. [75] and Tanaka and Ohta [73] reported that the average molecular weight (MW) of the trunk polymer tailored for the best dispersion was 5,000 g/mol. For good dispersion, the maximum molecular weight for the trunk polymer was on the order of 10,000. With a 5,000 MW trunk, side chains containing twelve ethylene oxide groups (with each EtO MW = 44) gave maximum dispersion, and it was believed that these groups also imparted a strong electrostatic repulsion effect [75].

Kirby and Lewis investigated the effects of the structure morphology using 5,000 MW trunk length and polyethylene oxide corresponding to 100, 700, 1,000, 2,000, and 3,000 MW [76]. It was reported that only a few ethylene oxide groups were needed to

abate the aggregation and stiffening. The theoretical MW of developed polycarboxylate polymers ranged from 5,000 to 31,100 g/mol. Kirby and Lewis grafted the polyethylene oxide side chains to the trunk polymer with -C-N-C- bonds (imide bonding). Work by Magarotto et al. reported that polymer molecular weights of 30,000 to 50,000 or more were needed for better superplasticizer performance [75].

Generally, shorter trunk lengths and increased side chain length increase dispersibility and mini-slump retention (*Table 2*). The improved performance was believed to be due to increased SP film thicknesses. *Figure 7* demonstrates these assessments along with the approximations of polymer size.

Table 2. Structural factors affecting dispersibility and retention of dispersibility [75]

Structural factor / Dispersibility	Relative chain length of trunk polymer	Relative graft length	Relative number of grafts
Low dispersibility and short dispersibility retention	Long	Short	Large
High dispersibility	Short	Long	Small
Long dispersibility retention	Shorter	Long	Large

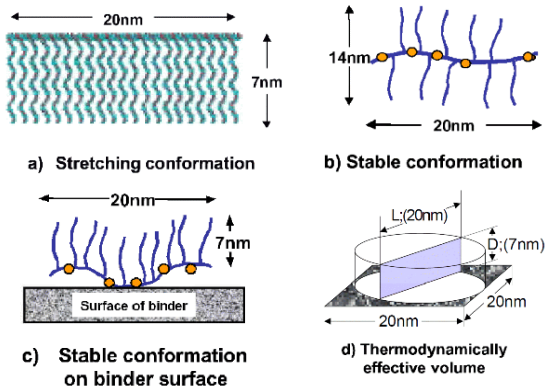

1 nm = 3.937E^{-8} in.

Figure 7. Size and morphology of polycarboxylate SP, from Sakai et al. [75].

The dosage of superplasticizers (SP) is typically less than 1% of the cement weight. A number of studies reported on the use of less than 0.5% by weight of the cement, based on the solid content [70, 75]. The effectiveness of SP can be influenced by a number of factors such as cement particle size (or surface area), cement composition, SP dosage, and time of addition. Products of hydration can interfere with SP by sequestering the SP polymer directly or by associating SP on the particle surface. As hydration takes place, the SP polymer becomes incorporated into the hydrating matrix and is completely consumed [70, 72, 75, 76].

Although the general practice to dissolve the SP in water allows easy addition and a more homogenous cement paste mix, based on the mini slump test, Collepardi [70] demonstrated that making a paste (by mixing water and cement) first, before adding SP, was a preferred method of incorporation. Sakai [75] quantified the SP dosage and response for various cement compositions. It was reported that the critical dosage, which is the minimum dosage of SP where flow begins to increase, and dispersibility, as the rate of response to additional SP, are the key parameters for effective application of SP admixtures.

2.3. AGGREGATE OPTIMIZATION

The optimization of concrete aggregates involves theories, simulation, and experimental assessment related to packing of particles, the effects of aggregate shape, compaction, and optimal gradations. Aggregate optimization is required for proportioning of a range of cement based materials including mortar, high-performance concrete (HPC), self-consolidating concrete (SCC), light-weight concrete (LWC) and structural concrete [13, 14, 16, 25-27, 29-38, 45, 52, 53, 60, 77-112]. Some researchers used the aggregate optimization methods to reduce the cementitious materials content in concrete pavements [26, 77].

The aggregate optimization is based on experimental and theoretical methods and approaches to quantify the best combination of aggregates used for particulate composites. These include, but are not limited to methods dealing with maximal packing degree, minimum void content; optimal particle size distribution (PSD) of aggregate combinations, optimal individual percentage retained (IPR), and optimal coarseness and workability factors known as a Shilstone coarseness chart [113]. Additionally, other effects such as the size, shape and geological origin of the aggregates can be taken into account for the selection of aggregates proportions. A concrete mixture is largely constituted of aggregates and so the performance of concrete strongly depends on the characteristics of aggregate blends.

2.3.1. Theories of Particle Packing

The optimization of aggregate packing is an approach for the selection of aggregate types and combinations. The main purpose of this approach is to reach the lowest void content or the maximal packing degree [13]. The packing of particles,

however, is not limited to the concrete industry and is a major field of interest to other industries such as materials design, powder metallurgy, ceramics and asphalt [13]. The packing concept is based on the use of smaller particles to fill in the voids between the larger particles and, as a result, reduce the volume of voids. Powers stated that the best aggregate mixture for concrete is not necessarily the one with lowest void content: "the production of satisfactory concrete nevertheless requires aggregates with low content of voids even if not the lowest possible, and this requires finding proper combinations of sizes within the allowable size range" [85]. In concrete, the reduction of volume of voids is equal to the reduction in the volume of cement paste that must be used to fill in the voids between the aggregates [13]. At the same time, concrete flow and workability requirements impose some limitations on the packing arrangement of aggregates, advocating the need for continuous, "loosely packed" gradings. It was reported that low to zero slump concrete is very sensitive to aggregates packing, especially, mixtures with low cement content [40].

The packing density or packing degree ϕ of a specific aggregate or aggregate combination is defined as the ratio between the bulk density of aggregate (ρ_{bulk}) and grain density (ρ_{grain}) or volume of particles V_p in a unit volume V_b [13]:

$$\phi = \frac{\rho_{bulk}}{\rho_{grain}} = \frac{V_p}{V_b} = \frac{m_p}{\rho_{grain}.V_b} \qquad (1)$$

As a result, packing is characteristic of the aggregate type and defines the minimum volume of cement paste required to fill the voids. The void content or porosity (ε) is then:

$$\varepsilon = 1 - \phi \qquad (2)$$

The design of optimal aggregate combinations can be achieved by packing simulations. The use of aggregate packing simulations to predict concrete behavior, or to design the optimal mix, has been widely discussed in literature and industrial projects since the early 1900s [77, 79-82], but the need for a realistic packing model still requires further attention. Particle packing is approached in two fundamental directions: as discrete models and continuous models. The discrete models are based on the assumption that "each class of aggregates packs to its highest density in the assigned volume" and are further classified into (a) binary (b) ternary and (c) multimodal mixture models [78].

2.3.2. Discrete Models

Discrete models are usually based on several assumptions including but not limited to the following: (a) the aggregates are perfect disks or spheres; (b) aggregates are mono-sized; and (c) fine and coarse aggregates differ in characteristic diameters. The other assumption was the use of fine particles required to fill-in between the coarse particles [78]. These assumptions can conflict with experimental packing of realistic aggregates and combinations. One of the earliest works on ideal packing of spheres was accomplished by Furnas [15, 23]. In Furnas' theory, spherical binary blends of particles are assumed to provide the ideal packings, *Figure 8*.

Two interaction effects between the aggregates, the wall effect and loosening effect, are demonstrated by *Figure 9*. Both effects reduce the packing degree, and thus, are accounted for in the model with factors representing the reduction in packing degree [53]. The wall effect occurs when the amount of fine particles is high and the presence of coarse particle increases the void in the vicinity of coarse particles (because the small particles cannot be packed at maximum bulk density).

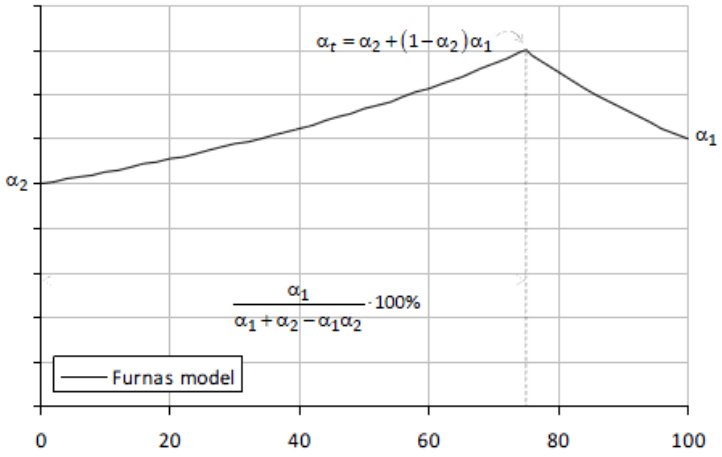

Figure 8. Packing of two mono-sized particle classes [25].

The loosening effect occurs due to the incorporation of fine (and intermediate) particles between larger grains. Here, when the fine particles are no longer able to fit in the voids between the interstices of larger particles, the packing density is disturbed.

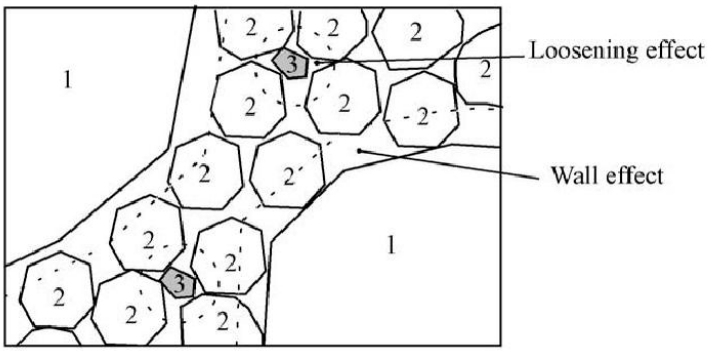

Figure 9. The interaction effects between the aggregates [53].

Westmann and Hugill [84] used a discrete particle packing theory and developed an algorithm for multiple classes of particles assuming zero interaction [60]. Aim and Goff suggested a model for calculating the packing density of a binary mixture of particles that takes into account the wall effect with a correction factor [29, 78]. This

model took into account the interaction of large particles with smaller particles based on the Furnas model [25]. The assumptions of this model are similar to other discrete models and consider two cases: fine and coarse dominant mixtures, for which there are two equations for the packing degree:

$$\phi = \frac{\phi_2}{1 - y_1} \quad \text{for} \quad y_1 < y^* \quad (3)$$

$$\phi = \frac{1}{[\frac{y_1}{\phi_1} + (1 - y_1) \times (1 + 0.9 * \frac{d_1}{d_2})]} \quad \text{for} \quad y_1 > y^* \quad (4)$$

where -- ϕ_1 and ϕ_2 are the eigenpacking degrees of fine and coarse aggregates, respectively;

- y_1 and y_2 are the grain volumes of the fine and coarse aggregates; and
- d_1 and d_2 are the characteristic diameters of fine and coarse aggregates.

Here, the packing degree of individual fine and coarse aggregates is called eigenpacking degree. The y^* parameter defines the border of two cases between the fine and coarse aggregate dominance. In the first case, the amount of coarse particles is higher, and in the second case, the amount of fine particles is higher. Therefore, the y^* is the dividing point of packing degree and is defined as:

$$y^* = p/(1 + p) \quad (5)$$

where, $$p = \frac{\phi_1}{\phi_2} - \left(1 + 0.9 * \frac{d_1}{d_2}\right) * \phi_1 \quad (6)$$

Powers reported on a void ratio of concrete aggregates [27]. The particle interactions (wall and loosening effect) were investigated and an empirical relationship to estimate the minimum void ratio of binary mixtures of particles was proposed [13].

Reschke [89] developed the model proposed by Schwanda [88] that incorporated both interactions of large and small particles. In contrast, Aim and Goff only incorporated the wall effect in their earlier model [25, 88, 89].

Toufar et al., introduced an additional group of particles to the packing density model of binary mixes [30]. Initially, the model was developed to calculate the packing density of binary blends and was updated to estimate the packing of ternary mixes [25]. This model assumed that smaller particles (at a diameter ratio of < 0.22) are too small to fit in the interstices of larger particles and, hence, the packing consists of packed areas of larger particles and packed areas of smaller particles. The larger particles were assumed to be distributed discretely throughout the matrix of smaller particles [78]. For ternary groups of particles each of two components form a binary mixture and the resulting blend was used as a binary group with a third set of particles. In this way, the proposed approach can be extended to multi-component mixtures [78]. The total packing degree is described as α_t:

$$\alpha_t = \frac{1}{\frac{r_1}{\alpha_1} + \frac{r_2}{\alpha_2} - r_2\left(\frac{1}{\alpha_2} - 1\right)k_d k_s} \qquad (7)$$

where:

- α_1 and α_2 are the eigenpacking degree of fine and coarse aggregates, respectively,
- r_1 and r_2 are the grain volume of the fine and coarse aggregates;
- and d_1 and d_2 are the characteristic diameters of fine and coarse aggregates.

Here, the k_d is a factor that considers the diameter ratio of two particles in the packing density, and the k_s is a statistical factor that considers the probability of the number of interstices between coarse particles and a fine particle surrounded by four coarse particles [25]:

$$k_d = \frac{d_2 - d_1}{d_2 + d_1} \qquad (8)$$

$$k_s = 1 - \frac{1 + 4x}{(1 + x)^4} \qquad (9)$$

where:

$$x = \frac{(\text{bulk volume of fine particles})}{(\text{void volume between the coarse aggregates})} = \frac{r_1}{r_2} \frac{\alpha_2}{\alpha_1(1 - \alpha_2)} \qquad (10)$$

Without interaction, the Toufar model uses k_d =1, which is similar to the Furnas model (at $d_1 \gg d_2$) and the corresponding packing density for two cases ($r_1 \gg r_2$ and $r_2 \gg r_1$). This model can be extended for multi-component mixes; however, it was found that such an approach tends to underestimate the packing density [25]. Europack is a software that uses the Toufar model and calculates the proportions of aggregates that produce the maximum or the desired packing degree. The software uses a stepwise method to overcome the underestimation for multi-component mixes by calculating the packing density of binary mixes with larger diameters first and blending the combined mix with the fine size material in a secondary binary models.

Aim and Goff found the best fit of the theoretical and experimental packing densities for small particle diameter ratios [29]. Goltermann et al. compared the packing values suggested by the Aim model, the Toufar model and the Modified Toufar model for the experimental packing degree of the binary mixtures [13]. The Aim model predicted a

sharp maximum, whereas the Toufar model predicted a flat maximum. Goltermann et al. favored the use of a modified Toufar and Aim model associated with Rosin-Raimmler size distribution parameters that are used to represent the characteristic diameter of aggregates [13]. The model proposed three experimental values to overcome the conflicts between the models and realistic aggregates commonly observed for discrete models. The characteristic diameter parameter was proposed to represent the non-spherical aggregates in the model. The characteristic diameter is defined as a position parameter of the Rosin-Raimmler-Sperling-Bennet size distribution curve (D') for which the cumulative probability that the diameter of the particle is less than D is 0.368. This parameter can be used to adjust the theoretical model to assemblies representing real aggregates. A minor correction factor to k_s is based on the assumption that each fine particle is placed within the space between four coarse particles:

$$k_s = \frac{0.3881x}{0.4753} \qquad for \qquad x < 0.4753 \qquad (11)$$

$$k_s = 1 - \frac{1 + 4x}{(1 + x)^4} \qquad for \qquad x > 0.4753 \qquad (12)$$

The Rosin-Rammbler distribution can be used to define the Rosin-Rambler Coefficient (D') also called the characteristic diameter of aggregates [13]. From the Rosin-Rammler (R-R) equation, D' can be calculated:

$$R(D) = 1 - F(D) = \exp\left(\frac{D}{D'}\right)^n \qquad (13)$$

where $R(D)$ is the R-R distribution, $F(D) = P(d < D)$ is the cumulative probability that the diameter d is less than D.

The parameters D and n describe the R-R distribution and can be calculated from the following transform:

$$\ln\left(\frac{1}{R}\right) = (D/D')^n \qquad (14)$$

$$\ln(\ln\frac{1}{R}) = n\ln D - n\ln D' \qquad (15)$$

On a ln-ln paper, the ln 1/R vs. D plot can provide the slope n intercepting at $-n\ln D'$ that follows the calculations of D' as:

$$\ln D' = \frac{\text{intercept}}{n} \qquad (16)$$

$$D' = \exp\left(-\frac{\text{intercept}}{n}\right) \qquad (17)$$

The Strategic Highway Research Program (SHRP) has developed a computer packing model for dry particles, based on the Toufar et al. [30, 101] and Aim and Goff work [86]. This discrete packing model was used to calculate the density of polydispersed systems of particles including cement and fine and coarse aggregates [69, 70]. The Cement and Concrete Association (CCA), Portland Cement Association (PCA), and Pennsylvania Department of Transportation (PennDOT) recommended concrete formulations based on theoretical equations [26]. The packing calculation results were usually represented by ternary diagrams with isodensity lines and in a numeric table format. It was found that the location of recommended concrete mixtures on the ternary diagram is located within the area of optimal packing [26]. The developed mixtures were designed to have the maximum dry packing density [26]. It was reported that "the

correlation between the rheology and packing of the mix has found that the workability of concrete is mainly controlled by the binary packing of coarse and fine aggregate at a fixed cement content and w/c ratio" [30]. The purpose of these studies was to provide the means to determine the optimal proportion of fine and coarse aggregates and to calculate the theoretical packing based on the aggregate's characteristics such as specific gravity and size (i.e., packing and characteristic diameter), correlate these parameters with the strength and workability, and compare the results with recommended mixtures of PCA and State DOTs [26]. As a result, the packing tables of SHRP-C-334 [26] for the volume of coarse aggregates based on the maximum packing were intended for the use in conjunction with ACI 211 (or other mix design methods) to produce a workable mix and concrete with lower permeability and improved durability.

2.3.3. Continuous Models

Continuous models, also known as optimization curves, estimate the effect of aggregates distributions on concrete performance and assume that all particle sizes are present in the distribution and there is no gap between the different size classes [78]. Optimization with particle size distribution (PSD) curve can be achieved by the analysis of the curves corresponding to the minimum void content or highest packing.

Ferret [35] demonstrated that the packing of aggregates can affect concrete properties by reducing porosity of the granular mixes maximizing the strength. In this regard, the continuous grading of the particulate component of the composite was suggested to improve the properties of concrete [35, 78]. Fuller and Thomson proposed the gradation curves for maximum density known as Fuller's "ideal" curves [16].

These curves can be plotted using the following equation, which relates each particle size to the maximum size of particles [18, 24, 38]:

$$\mathrm{CPFT} = 100\ (\mathrm{d/D})^{\mathrm{n}},\ \ \% \qquad \mathrm{n} = 0.5 \qquad (25)$$

where the CPFT is the Cumulative (volume) Percent Finer Than, and n is the power exponent. The n = 0.5 was suggested initially (as represented by *Figure 10*) and later, the exponent was changed to 0.45. Talbot and Richard described the Fuller curve in a similar equation [92]. Currently, a power 0.45 curve has been applied in grading of aggregates in the asphalt industry.

Andreassen et al. improved the Fuller curves and proposed Andreassen equations for ideal packing and suggested a range for exponent n between 0.33 - 0.5. Andreassen assumed that the smallest particle in the mix must be infinitesimally small. Andreassen's ideal packing curve for n = 0.37 is shown in *Figure 10* [100]. In that model, the exponent had to be determined experimentally and, as a result, it is affected by the properties of the aggregates [25]. Dinger [94, 95] and Funk realized [103, 104] that Andreassen equations need to have a finite lower size limit as a finite smallest particle. Therefore, an important advancement in continuous gradings was developed, in contrast to Fuller curves, by considering not only the largest particle size in the equation, but the smallest size as well. The modified Andreassen equation was proposed as following:

$$\mathrm{CPFT} = \left(\frac{(\mathrm{d} - \mathrm{d_0})}{(\mathrm{D} - \mathrm{d_0})}\right)^{\mathrm{n}} . 100, \% \qquad (26)$$

where:

d is the particle size,

d_0 is the minimum particle size of distribution,

D is the maximum particle size, and

n (also often designated as *q*) is the distribution exponent.

The exponent *n* is proposed to be 0.37 for optimal packing used for common concrete, as reported in *Figure 10*, and for high-performance concrete it was suggested to be 0.25-0.3.

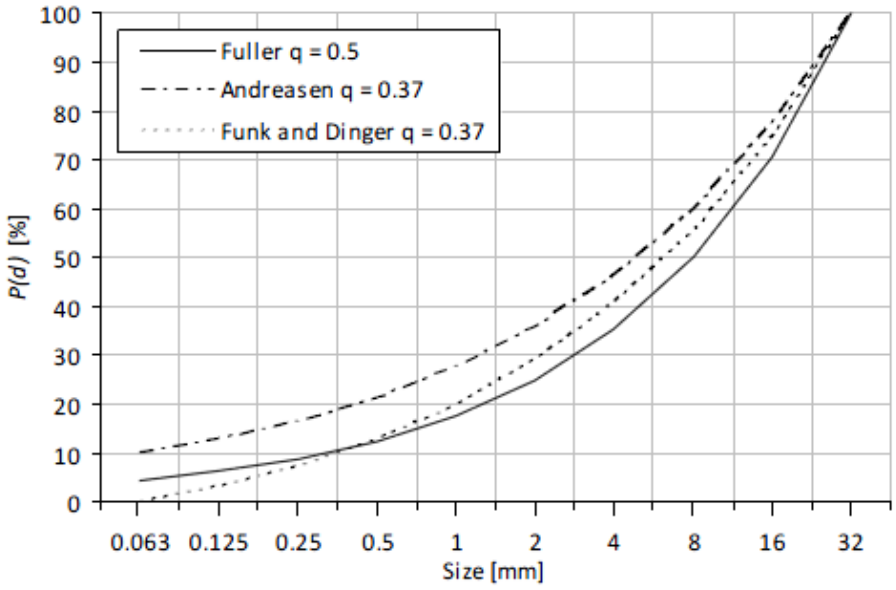

Figure 10. The distribution curves by Fuller, Andreassen, Funk and Dinger [25].

By the selection of exponent n, the effect of aggregate shape can be taken into account. For example, for angular coarse particles, the lower n can describe the ideal curve because more fines are needed to fill in the coarse particles with irregularities of the shape [25, 93]. As the target and application of the optimization curves is to reach the mixtures of the highest density, the effect of shape on packing density was considered by many researchers [93]. Zheng et al. determined q (or n) as an average of all q-values of all classes used by varying the particle shape [97]. Peronius et al. calculated the porosity

of the mixtures of particles with different shapes based on the roundness and the deviation from Fuller curves [99]. This relates the highest packing (or lowest porosity) to the shape and the deviation from a target distribution (such as Fuller curve). The Funk and Dinger model was used by other researchers for optimization of mixtures by adjusting the q-value based on the required workability and other experimental results [25, 33, 34, 93, 99, 100].

2.3.4. Comparison of Continuous Models

The optimization curves can be used to optimize different blends of particles. Three curves represented in *Figure 10* can lead to mixtures with high packing density when different particle sets are optimized to fit these curves; however, in these models, the shape of the particles is not taken into account [25]. The selection of the suitable range for the exponent *n* must consider the workability level requirements of concrete mixtures. For higher workability, smaller *n* leads to the use of higher volumes of fine particles and vice versa for zero/low slump mixtures. However, the change in packing density is not significant for slight variations in the coarse to fine ratio near the maximum packing zone.

The segregation can be very low for PSD corresponding to continuous distributions. The highest potential segregation can occur in concrete based on gap graded PSD, which can provide a very high packing density that is close to maximum possible density defined by random Apollonian packing (RAP) [31].

2.3.5. Packing Simulations

The discrete element models (DEM) are able to generate the virtual particle structure from a given size distribution or based on packing algorithm's rules. In these models particles are randomly positioned in a definite space where the packing density can be calculated [60]. The early models were static simulations with fixed positions of assigned particles. The later models evolved to dynamic simulations and, therefore, enabled the relocation, expanding and sliding of the particles under the exerted forces. A dynamic model can be used to consider the gravity and collision forces applied on the particles. Both static and dynamic models can lead to loose or compacted packings, and a dynamic model is not necessarily required to achieve the highly compacted packing assemblies.

The dynamic DEM were able to model the loose packing of particles by exerting the gravity on the polydisperse particles as described by Fu and Dekelbab [36, 102]. These models generate a loose packing structure and then reduce the volume of the container to reach a compacted state, as proposed by Stroeven et al. [45]. Other approaches enable the particles to overlap initially and then enlarge the container by rearranging the particles until no overlap occurs, as proposed by Kolonko et al. [37].

Sobolev et al. solved the computational resource problems related to both dynamic and static DEM in the sequential packing algorithm (SPA) by assigning several factors that can generate different packing assemblies, including loose packing, compacted packing, and packing of particles with defined distributions [7, 31, 38, 47]. In addition, spacing between the particles was introduced; such spacing can be adjusted starting with an initial separation coefficient and the reduction rate as the particles are

positioned. The diameter of the particles can be reduced at a constant range starting with the maximal size D_{max} of aggregates to allow the smaller particles to pack between the larger particles. Another factor, the number of trials, was introduced as a parameter to allow the desired packing efforts to fit a particle at a certain diameter range with certain spacing [7]. *Figure 11* demonstrates the application and 2D/3D visualization of the algorithm.

The sequential packing algorithm developed by Sobolev and Amirjanov [38, 47] assumes that the particles are spherical (or circular in a 2D educational model) [45]. Spherical particles with radii in the range of $r_{min} < r \leq r_{max}$ are sequentially placed into the cube with the centers glued to the node of a very fine lattice grid [38]. The D_{max} is defined depending on the container size and is fixed at the beginning of simulation, but minimal diameter d_{min} is decreased gradually by a controllable procedure, thus allowing larger spheres to be placed prior to the placement of smaller ones [38]. To realize the packing routine, a set of parameters including the reduction rate of the minimal size of the particle (K_{red}), the initial separation between the particles (K_{del}), the step of separation (S), and the number of packing trials are defined as inputs. Before locating the sphere with d_i, the various conditions are examined: the center of a new sphere cannot be located inside of any already packed spheres; a new sphere cannot cross any already packed sphere; so the minimum distance to the surface of any already packed sphere is evaluated [38]. The cube can be pre-packed with initial objects including intersecting spheres enabling the combinations of different packing rules to assemble the "real world" particulate composite.

For example, the simulation of aggregates packing established by Sobolev et al. [38] was used for the optimization of concrete mixtures. The performance of the proposed algorithm is illustrated by a 2D packing achieved with a limited number of objects (500 disks) and a relatively low reduction coefficient (K_{red}=1.001) as represented in *Figure 11a*. This 2D packing resulted in a packing degree of 86.2%, *Figure 11a*. Higher initial separation coefficient value *(*K_{del}) leads to larger initial separation between the particles [38]. The separation is introduced to provide the spacing between the larger objects, but allows for smaller separation between the midsize and small particles and achieved by the use of separation with a reduction coefficient (*S*=1.001) proportional to the grain size. For the reported example, the initial separation (K_{del}) of 1.5 was used.

Furthermore, the 3D simulations of particulate composites with a large number of particles, up to 20 millions, can provide a very realistic aggregate packing arrangement in respect to size distribution and degree of packing used in "real world" concrete. In reported research, a simulation experiment with 5 million particles was compared with ASTM 33 limits and with a 0.55 power curve as coarse and combined aggregate benchmarks, respectively. Preliminary exploration of the simulation with 5 million spheres was used for the virtual experiment. The error from each of these curves was minimized by selection of suitable packing parameters. To achieve two different compositions corresponding to 0.7 and 0.55 power curves, the 3D packing simulation experiment was conducted for the combination of a reduction coefficient of K_{red}=1.01 and a relatively low number of packing trials, 10 corresponding to a low packing energy (i.e., defined as Loose Initial Packing, LIP) at a relatively large separation with $K_{del} = 5$ and 10 and a step of separation of *S*=1.025 (as demonstrated in *Figure 11b*).

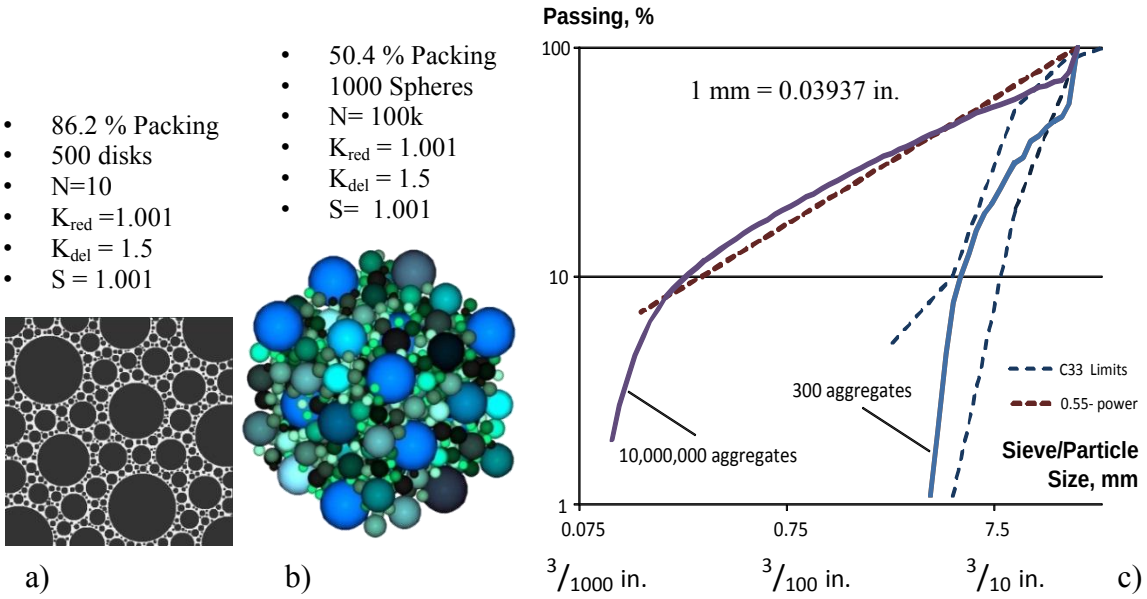

Figure 11. The output of SPA algorithm: a) 2D representation of Apollonian Random Packing with LIP separation b) 3D visualization and c) the PSD based on the output of packing algorithm [40].

The packing simulations offer a great potential for the modeling of other properties of concrete that may not be possible with discrete or continuous models. The particle structure reveals the particle size distribution, packing degree, size, shape (if not assumed spherical), the location of particles, and the contact points. The model can also be used as a basis for estimating the stress transmission by aggregates and matrix, flow properties, response to loads resistance and permanent deformation capacity [103-105]. These models can help to predict the volumes of cementitious materials, water and admixtures by calculating the spacing or the paste thickness between the particles for a certain viscosity of paste in order to achieve a certain workability or strength needed. This can minimize the need for extensive experiments required to specify the optimized mixtures [44].

The most important feature of these models is the capability to find the best particle size distribution (i.e., aggregate blends) corresponding to the highest packing. It should be noted that the ultimate selection of the best aggregate blends should be based on the workability requirements, segregation potential, strength and stiffness achieved at the highest packing density possible. Currently, the transfer from binary to multi particle mixtures is facilitated with development of software based on the theoretical models. The commercial particle packing software based on theoretical packing models can calculate the packing density based on various compositions using the aggregate's PSD and packing density. Each model assumes different particle interactions and packing effort (energy) implemented in the mathematical equations of the model. Numerous virtual compositions can be evaluated to determine the maximum packing density achievable based on the model used.

2.3.6. Coarseness Chart

The coarseness factor chart was proposed by Shilstone [113] and defines the Workability Factor (WF) and Coarseness Factor (CF) for various aggregate blends. The CF chart relates the aggregates grading and concrete performance by specifying Zone II as the desired well-graded zone in *Figure 12*. The empirical WF and CF parameters depend on the composition, grading and cement content of the mix:

$$\text{WF} = P_{2.36} + 0.045\ (\text{C} - 335) \qquad \text{< SI units >} \qquad (20)$$

$$\text{WF} = P_{2.36} + [2.5\ (\text{C} - 564)]/94 \qquad \text{< US customary units >}$$

$$\text{CF} = 100 * R_{9.5}\ /R_{2.36} \qquad (21)$$

where $P_{2.36}$ percent passing 2.36 mm (#8) sieve;

C cement content of the mix, kg/m^3 (lb/yd^3)

$R_{2.36}$ cumulative percent retained on 2.36 mm (#8) sieve;

$R_{9.5}$ cumulative percent retained on 9.5 mm (3/8") sieve.

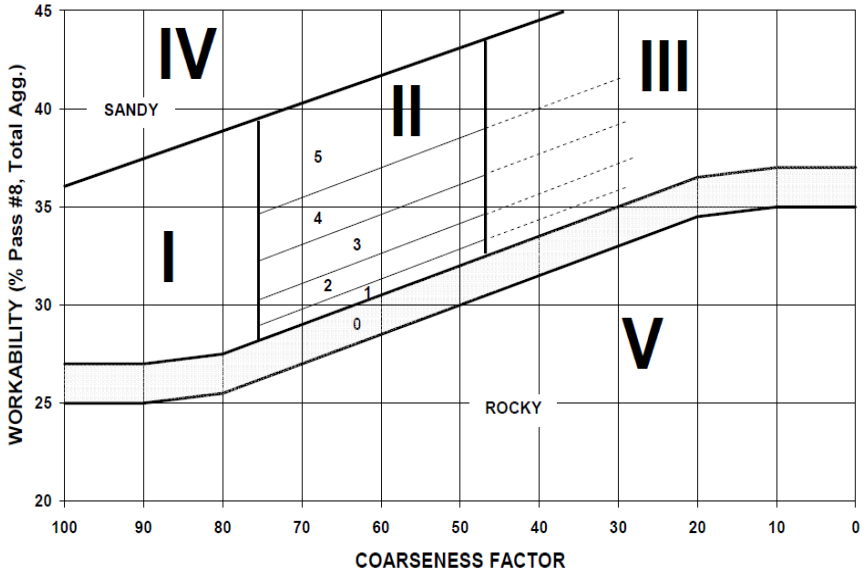

Figure 12. Coarseness chart for various concrete mixtures [23].

The coarseness chart can help to identify the level of workability and coarseness of the blends with binary, ternary or multi-class aggregates. It can also help to identify the effect of combined criteria such as grading, the location corresponding to experimental packing, and the properties of low cement concrete mixtures.

2.3.7. Other Methods

The linear packing density model (LPDM) was developed by Stovell and De Larrard [90]. The LPDM is based on the improved Furnas model and the use of multi-component blends combined with the geometrical interaction between the particles [25]. The other feature of LPDM is that it can be used to optimize the grading when multiple class sizes are used and the packing density of each class is known. The first LPDM

equation (without interaction) is actually similar to the continuous model described by Funk and Dinger in the form of an optimization curve.

In 1994, de Larrard and Sedran suggested another model, called the Solid Suspension Model (SSM), which was used for packing density calculations of small particles and cementitious materials reaching high packing densities [14, 78]. Furthermore, de Larrard introduced a new model for compaction of the mixture via virtual compaction as the Compressible Packing Model (CPM) [31]. This model included the as compaction effort and can be considered as an extension of LPDM [25]. CPM used a virtual packing density (β) and index K *(Table 3*) to calculate the actual packing density (α_t).

Table 3. The K value for different compaction methods [31]

Packing method		K value
Dry	Pouring	4.1
	Sticking with rod	4.5
	Vibration	4.75
	Vibration + compression at10 kPa	9
Wet	Smooth thick paste (Sedran and Larrard, 2000)	6.7
	Proctor test	12
Virtual	-	∞

Another feature of CPM model is the capability to evaluate the "filling diagram" of different mixtures, which indicate the filling ratio of the *i*-th fraction in the void left by the coarser fractions [52]. The commercial software packages BETONLABPRO and RENE LCPC use this model to predict the optimal mixture composition and maximum of packing density, respectively [25]. Given the experimentally determined packing degree and a joint K index for each class, the model can calculate the packing degree of any particulate mixture and combination. The CPM was the first model that used the experimental compaction method. De Larrard suggested using vibration plus pressure (10 kPa) for measuring the dry packing density as an input for the compressible packing model (CMP).

Therefore, for experimental dry packing, Dewar suggested loose packing density, de Larrard suggested vibrated and pressure packing, and Andersen suggested dry rodded packing density; the latter was adopted by ASTM C 29 [49].

3. MATERIALS AND METHODS

3.1. MATERIALS

3.1.1. Portland Cements

Four ASTM Type I portland cements from three different suppliers were used for the research. The chemical composition and physical properties of cements are presented in *Table 4* and *Table 5*, respectively, along with the requirements of ASTM C150 Standard Specification for Portland cement. The chemical composition of cements was tested using the X-Ray Fluorescence (XRF) technique and reported by the cement manufacturer.

Table 4. Chemical composition of portland cement

Parameter	ASTM C150 Limits	Test Result L1	L2	H1	S1
SiO_2, %	-	19.8	19.1	19.4	18.6
Al_2O_3, %	-	4.9	5.1	5.3	5.5
Fe_2O_3, %	-	2.8	2.5	3.0	2.6
CaO, %	-	63.2	63.3	63.2	61.1
MgO, %	6.0 max	2.3	2.7	2.9	4.3
SO_3, %	3.0 max	2.9	3.3	3.3	3.9
Na_2O, %	-	0.2	0.3	0.3	0.3
K_2O, %	-	0.5	0.6	0.7	0.6
Others, %	-	0.6	0.9	0.9	1.5
Ignition loss, %	3.0 max	2.8	2.5	1.1	1.5
Potential Composition					
Al_2O_3 / Fe_2O_3		1.8	2.1	1.8	2.1
C_4AF, %	-	8.5	7.5	9.1	8.0
C_3A, %	-	8.2	9.3	8.9	10.1
C_2S, %	-	10.3	4.9	9.9	11.3
C_3S, %	-	61.6	65.8	60.7	55.8
Na_2O_{equi}, %	0.6 max	0.5	0.7	0.8	0.7

Table 5. Physical properties of portland cement

Parameter	ASTM C150 Limit	Test Results L1	L2	H1	S1
Specific Gravity	-	3.13	3.17	3.08	3.07
Time of setting, min					
Initial	45 min	103	74	88	93
Final	375 max	264	231	222	228
Compressive strength, MPa (psi) at the age of:					
1 day	-	12.1 (1731)	17.2 (2460)	18.1 (2589)	21.2 (3032)
3 days	12 (1716)	21.7 (3104)	28.5 (4077)	28.7 (4105)	26.2 (3748)
7 days	19 (2718)	28.3 (4048)	32.6 (4663)	34.3 (4906)	29.4 (4205)
28 days	28 (4005)	36.5 (5221)	40.4 (5779)	40.1 (5735)	34.6 (4949)

3.1.2. Fly Ash

ASTM Class C and F fly ash from Wisconsin power Stations were used in this research. The chemical composition and physical properties of two types of fly ash are summarized in *Table 6* and *Table 7*, respectively, along with the requirements of ASTM C618, "Standard Specification for Coal Fly Ash and Raw or Calcined Natural Pozzolan for Use in Concrete".

Table 6. Chemical composition of fly ash

Component	Chemical Composition %			
	Class F (AF)	Class C (AC)	ASTM C618 limits Class F	Class C
SiO_2	46.9	32.7	-	-
Al_2O_3	22.9	17.6	-	-
Fe_2O_3	19.2	5.9	-	-
Total, SiO_2+Al_2O_3+Fe_2O_3	89.0	56.2	70 min	50 min
SO_3	0.3	2.0	5.0 max	5.0 max
CaO	3.8	27.3	-	-
MgO	0.8	6.6	-	-
K_2O	1.7	0.4	-	-
Na_2O	0.6	2.2	-	-
Moisture Content, %	0.1	0.8	3.0 max	3.0 max
Loss on Ignition, %	2.3	0.3	6.0 max	6.0 max

Table 7. Physical properties of fly ash

Parameter	Class F (AF)	Class C (AC)	ASTM C618 limits: Class F	ASTM C618 limits: Class C
Specific Gravity	2.50	2.83	-	-
7-day Strength Activity Index, %	77.5	82.9	75 min	75 min
Water Requirement, %	102	91	105 max	105 max

3.1.3. Blast Furnace Slag

ASTM Grade 100 ground granulated blast furnace slag (GGBFS) or slag cement (SL) was used in this research. The chemical composition and physical properties of SL are presented in *Table 8*, along with the requirements of ASTM C989, "Standard Specification for Ground Granulated Blast Furnace Slag for Use in Concrete and Mortars."

Table 8. Chemical composition and physical properties of blast furnace slag

Chemical Composition

Component	Composition, %	
	ASTM C989 Limit	Test Result
SiO_2	-	33.4
Al_2O_3	-	10.1
Fe_2O_3	-	0.7
SO_3	4.0 max	2.5
CaO	-	42.8
MgO	-	10.0
K_2O	-	0.4
Na_2O	-	0.3
Loss on Ignition	-	1.0

Physical Properties

Performance characteristics	ASTM C989 Limit	Test Result
Specific Gravity	-	3.01
7-day Strength Index,%	75 min	88.1

3.1.4. Chemical Admixtures

Locally available air-entraining, mid-range and high-range water-reducing (superplasticizing) admixtures were used in this study. After preliminary evaluation and screening, one plasticizing (mid-range) and four superplasticizing products combined with AE admixture (AMA) were selected for the research program as summarized by *Table 9.*

Table 9. Properties of chemical admixtures

Designation	Admixture Type	Composition	Specific gravity	Solid Content, %	Manufacturer recommended dosage *
AMA	Air-Entraining	Tall Oil, Fatty acids, Polyethylene Glycol	1.007	12.3	8-98 mL (0.13-1.5 fl oz)
RP8	Water-Reducing Admixture	4-chloro-3-methyl phenol	1.200	40.3	195-650 mL (3-10 fl oz)
HG7	High Range Water-Reducing	Polycarboxylate Ether	1.062	34.0	325-520 mL (5-8 fl oz)
HR1		Naphthalene Sulphonate	1.193	40.3	650-1,600 mL (10-25 fl oz)
HAC		Polyacrylate Aqueous Solution	1.072	36.7	650-1040 mL (10-16 fl oz)
HD1		Naphthalenesulfonic acid, polymer with formaldehyde, calcium	1.193	39.8	650-1040 mL (10-16 fl oz)

* *The dosage of chemical admixtures is expressed by 100 kg (100 lbs) of cementitious material*

3.1.5. Aggregates

Coarse, intermediate and fine (natural sand) aggregates from two different locations (Northern and Southern WI) were used in this project. *Table 10* provides a summary of the aggregate types and sources. Physical characteristics of aggregates are summarized in *Table 11*. Bulk density and void content for loose and compacted

aggregates are listed in *Tables 12-15*. The sieve analysis of aggregates is provided by *Tables 13 - 15* and *Figures 13-14*.

Table 10. Designation and sources of aggregates

Designation	Type	Location
C1	1"Limestone	Sussex Pit - Sussex, WI
C2	1"Glacial	Northern WI
I1	5/8"Limestone	Lannon Quarry - Lannon, WI
I2	5/8" Glacial	Northern WI
F1	Torpedo Sand	Sussex Pit - Sussex, WI
F2	Glacial Sand	Northern WI

Table 11. Physical characteristics of aggregates in oven dry (OD) and saturated surface dry (SSD) conditions

Aggregate Type	Specific Gravity			Water Absorption, %	Fines <75µm (#200), %
	OD	SSD	Apparent		
C1	2.730	2.765	2.829	1.29	0.78
C2	2.706	2.741	2.803	1.27	0.81
I1	2.684	2.734	2.824	1.84	0.79
I2	2.659	2.715	2.816	2.09	0.94
F1	2.566	2.637	2.762	2.77	1.19
F2	2.563	2.620	2.720	2.20	0.78

Table 12. Bulk density and void content of aggregates in loose and compacted state

Aggregate Type	Bulk Density kg/m^3 (lb/ft^3)								Void Content, %	
	Loose				Compacted					
	OD		SSD		OD		SSD		Loose	Compacted
C1	1562	(98)	1582	(99)	1638	(102)	1659	(104)	42.7	39.9
C2	1549	(97)	1569	(98)	1675	(105)	1696	(106)	42.7	38
I1	1466	(92)	1493	(93)	1605	(100)	1635	(102)	45.3	40.1
I2	1508	(94)	1540	(96)	1610	(101)	1644	(103)	43.2	39.3
F1	1782	(111)	1831	(114)	1868	(117)	1920	(120)	30.4	27
F2	1681	(105)	1718	(107)	1797	(112)	1837	(115)	34.3	29.7

It can be observed that the aggregate grading's were within the limits set by ASTM C33. Slight access of 300 μm fraction in sand F1 can be considered acceptable.

Table 13. Grading of coarse aggregates

Aggregate Types	Amount Finer than Sieve (mass %)				
	25 mm (1 in)	19 mm (3/4 in)	9.5 mm (3/8 in)	4.75 mm (No. 4)	2.36 mm (No. 8)
No. 67: 3/4 - No.4 (ASTM C33)	100	90-100	40-70	0-15	0-5
C1	100	97.4	23.4	1.1	0.2
C2	100	97.9	34.1	3.6	0.7

Table 14. Grading of intermediate aggregates

Aggregate Types	Amount finer than Sieve (mass %)						
	19 mm (3/4 in)	12.5 mm (1/2 in)	9.5 mm (3/8 in)	4.75 mm (N. 4)	2.4 mm (N. 8)	1.2 mm (N. 16)	0.3 mm (N.50)
No. 7: 1/2 - No.4 (ASTM C33)	100	90-100	40-70	0-15	0-5	-	-
I1	100.0	87.6	58.5	12.8	2.5	-	-
No. 89: 3/8 - No.16 (ASTM C33)	-	100	90-100	20-55	5-30	0-10	0-5
I2	-	100.0	99.8	29.3	7.8	5.5	2.1

Table 15. Grading of fine aggregates (sand)

Aggregate Types	Fineness Modulus	Amount Finer than Sieve (mass %)						
		9.5 mm (3/8 in)	4.7 mm (N. 4)	2.4 mm (N. 8)	1.2 mm (N. 16)	0.6 mm (N. 30)	0.3 mm (N. 50)	0.15 mm (N. 100)
Sand (ASTM 33)	2.3-3.1	100	95-100	80-100	50-85	25-60	3-50	0-10
F1	2.43	100	99	83	70	58	35	13
F2	2.64	100	99	89	74	47	23	5

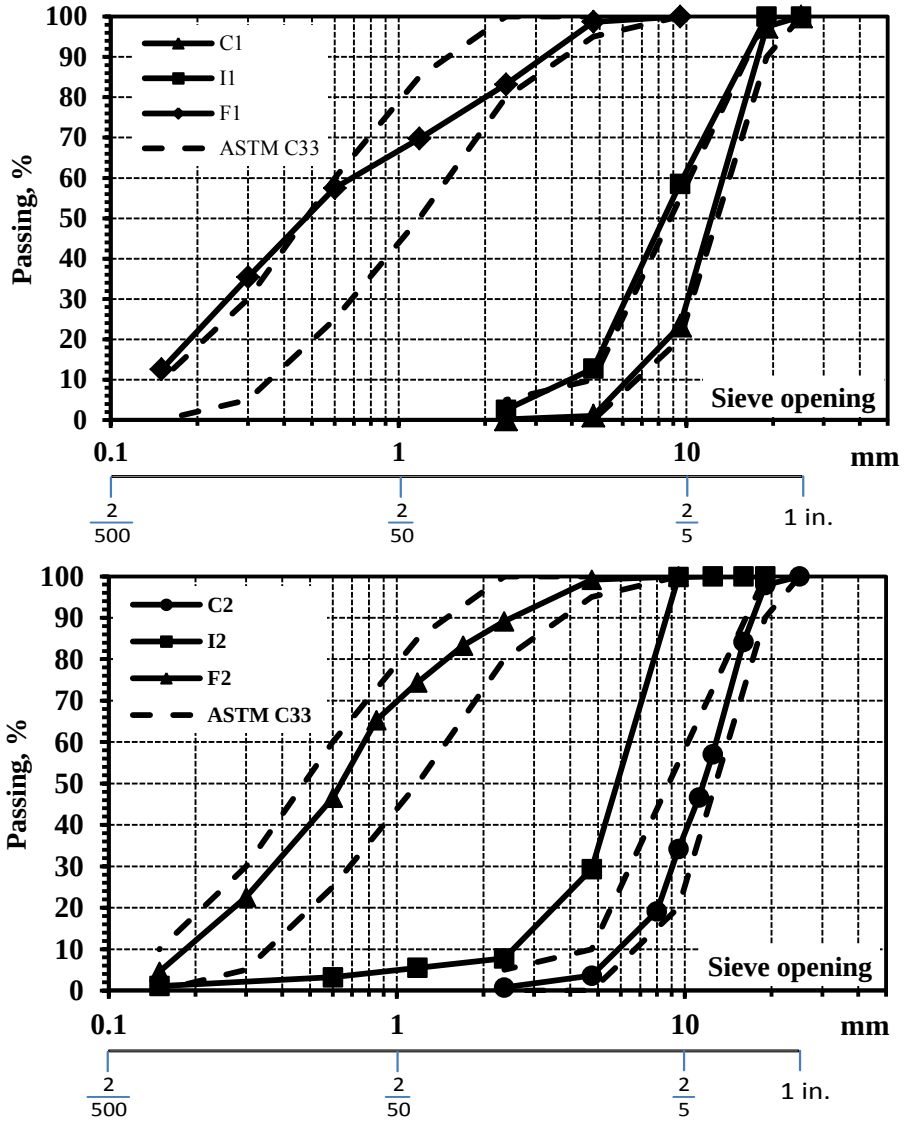

Figure 13. Particle size analysis of southern aggregates C1, F1, I1 (top); and *northern aggregates C2, F2, I2* (bottom).

Visual observations of northern aggregate C2 and I2 revealed the presence of ultrafine dust fraction on the surface *(Figure 14)*. The dust appeared to be of the same genesis as the rock material, and further evaluation of dust was not conducted. It can be expected that such fine impurities can affect the water demand of concrete mixture as well as can compromise the structure of aggregate and cementitious matrix interface transitional zone (ITZ) and, therefore, strength of the concrete. These effects as well as contribution of fines on durability were outside the scope of reported investigation.

Figure 14. Fine material collected from coarse aggregate C2 by washing and drying

3.2. EXPERIMENTAL PROGRAM

Principal factors affecting the mechanical properties and durability of superplasticized low-slump concrete are the W/CM ratio, cementitious material content, the HRWR admixture type, the type and dosage of SCM.

The experimental matrix for the design of concrete mixes was developed based on the vast experience and database gathered by the University of Wisconsin collaborative team over the past decade. A "smart" experimental matrix based on multi-scale concrete design and optimization was proposed.

3.2.1. Express evaluation of admixtures and cementitious materials

The performance of combinations of supplementary cementitious materials (SCMs) and superplasticizers can be used to evaluate concrete using express methods and computer models *(Figure 1)*. The properties of supplementary cementitious materials such as slag cement and fly ash are tested according to corresponding ASTM standards [114, 115], and, therefore, such information is readily available at the stage of concrete mixture design. The results of a mortar test (ASTM C109) can be effectively used for predicting the behavior of concrete manufactured with supplementary cementitious materials (e.g., slag cement, fly ash, silica fume) and chemical admixtures [25, 60]. A similar method was postulated by DIN and effectively used for concrete mixture proportioning in the case of blended cements or cements with different compressive strength. It was proved that the strength of mortars with different quantities of SCMs is proportional to the strength of concrete based on the same binder [25]. This approach was also used by P. Tikalsky et al. for evaluating the performance of ternary cementitious mixes [116, 117]. The main idea of this method is to use the specific performance

characteristics (i.e., compressive/flexural strength) of binder material rather than testing each particular source (since each particular source can demonstrate the variability in the performance over the time) and combination in concrete. This method can be effectively used in practice as SCM and chemical admixtures quality control or acceptance tool.

The advantage of such multi-scale method is that it can effectively accommodate the contribution of virtually any cementitious material, mineral additive, and chemical admixture and, with sufficient accuracy, predict the performance of concrete (including strength development, flexural/splitting tensile strength, and the effect of admixtures).

3.2.2. Optimization of aggregates

The variability of concrete experiments is normally much higher compared with tests on standard mortars due to higher fluctuations in the properties of coarse aggregates, which affect the aggregate-cementitious matrix bond and overall composite behavior. The importance of aggregate optimization was emphasized by L. Sutter in his report to WHRP (08-08 study); and this is especially true when different aggregates with different particle size distributions are used [118]. It was demonstrated that the analytical optimization of aggregate proportions to meet the “optimal” combined 0.45-power aggregate grading can greatly improve the performance of concrete and significantly reduce materials costs.

To reduce the variability among the experiments on different aggregates, the comparison of different aggregates proportioned for the same “target” grading is required. The range of aggregate gradings that can meet WisDOT requirements combined at 40% of sand is located between 0.45- and 0.7- power curves. Based on experimental

work and packing models [11, 14], the best (resulting in optimal fresh and hardened concrete properties) aggregates particle size distribution (or target curve) lies between these two limits. The research plan was designed to optimize the proportion of sand, intermediate and coarse aggregates to meet the target curves with a minimal deviation and providing high packing density.

Following the approach described above, the experimental program was realized. The final investigation involved the comprehensive testing of 36 optimized concrete mixtures containing 280 kg/m^3 (470 lb/yd^3) of cementitious materials and two combinations of aggregates, including:

- Reference concrete based on Type I portland cement with plasticizer and two types of HRWR admixture (18 combinations);
- Concrete with Class C and F fly ash SCM, plasticizer and two types of HRWR admixtures (12 combinations);
- Concrete with slag cement, plasticizer and two types of HRWR admixtures (6 combinations).

In addition to these, 18 concrete mixtures with reduced cementitious materials content of 250 kg/m^3 (420 lb/yd^3) were evaluated. Each investigated combination is technically advantageous, economical, and represents a potential concrete mixture to use in the field.

The performance of four different superplasticizers and two air-entraining admixtures was evaluated prior to application in this research, enabling to select the best

product in respect to compatibility, optimal dosages (applicable to all combinations of concrete mixtures according to experimental matrix). The performance of selected superplasticizers was compared to conventional plasticizer (water reducer) approved for DOT projects using standard mortar tests. Such comprehensive material investigation was vital in helping to interpret the variability in the measured properties between the compositions with different cement brands, combinations of cementitious materials and chemical admixtures.

Six types of aggregates were characterized by packing density, grading, Shilstone coarseness chart and performance in concrete.

All concrete mixtures were proportioned according to the ACI 211 concrete specification. The extensive experimental program testing 123 concrete mixtures (with 54 mixtures tested for complete set of properties and 69 “preliminary” mixtures subjected to express testing) and 38 standard mortar compositions was realized.

3.3. TEST METHODS

Concrete mixtures were batched, mixed, and the concrete specimens were cast, cured, and tested according to the corresponding ASTM and AASTHO standards. The experimental data were obtained using the required number of specimens for various tests: for each testing age and each test, the reported results are based on testing of: 3 specimens for compressive strength, 2 specimens for modulus of rupture, 3 specimens for length change, 2 specimens for rapid chloride permeability, and 3 specimens for freezing and thawing resistance. The errors and standard deviations for all results of final batches were calculated and the outliners were eliminated from the results, according to the requirements imposed by associated standards for compressive strength, modulus of rupture, and durability tests.

3.3.1. Mini-Slump of Cement Pastes

For the cement paste study, the water to cementitious material (W/C) ratio of 0.45 was selected. Lower W/C ratio vs. that specified by the ASTM Standard for mortars (W/C=0.485, ASTM C109) was used for the evaluation of water-reducing admixtures. In addition, similar W/C was used in concrete tests. The mixing procedure for pastes was performed as specified by ASTM C305.

A mini-slump cone (with a bottom diameter of 38 mm, a top diameter of 19 mm, and a height of 57 mm) was used in this research to determine the effect of supplementary cementitious materials and chemical admixtures. To determine the mini slump, the cone was filled with paste, lifted, and, when the cement paste stopped spreading, four flow diameters were recorded and the average value was reported.

3.3.2. Mortars Tests

For mortar specimens, the water to cementitious material (W/C) ratio of 0.45 was selected, and the sand to cement (S/C) ratio was set to 2.75. The W/C ratio was reduced from that specified by the ASTM Standard (W/C=0.485, ASTM C109) due to the use of water-reducing admixtures in the mix. Also, the W/C is selected to provide a reasonable workability for all tested compositions and enabling to compare the effects of WR and HRWR admixtures at different dosages without poor compaction or segregation. The mixing of mortars was performed as specified by ASTM C109 and ASTM C305. The workability and density of fresh mortars was evaluated as specified by ASTM C 1437 and ASTM C 138, respectively.

For the compressive strength investigation, cube mortar specimens with the dimensions of 50 × 50 × 50 mm (2 × 2 × 2 in.) were cast and cured in accordance with ASTM C 109. Test samples were removed from the molds after 24 hours of curing, immersed in a lime water, cured at a temperature of 23±2C^{o}, and then tested at the age of 3, 7 and 28 days. The compressive strength of the mortar specimens was determined using a pace rate of 1.4 kN (315 lb). The reported values represent a mean of at least two specimens tested for each age.

3.3.3. Heat of Hydration

An isothermal calorimeter measures the rate of heat release from hydrating mixture due to ongoing chemical reactions. In this study, an isothermal calorimeter TAM Air (TA Instruments) was used to evaluate the hydration kinetics at a constant temperature of 25 °C during the early 48-hour period. The output of the calorimeter was evaluated by graphical and mathematical means to evaluate the effect of different

material combinations. The isothermal curves or hydration profiles indicate setting characteristics, compatibility of different materials, early strength development, and the effect of chemical admixtures on the cement hydration.

3.3.4. Experimental Testing Methods for Packing Density

The VB apparatus *(Figure 15)* was initially developed for zero slump concrete and is currently used to measure the consistency and density of roller-compacted concrete. In this research, the VB vibro-compacting apparatus was adopted (from the ASTM C1170, method A) to test the packing of aggregate combinations. Different aggregate blends (with a total weight of 5.0 kg) were selected and tested for density and packing degree in loose and compacted conditions. Aggregates were thoroughly mixed before the entire sample was placed into the cylindrical mold of the VB consistometer to form a conical pile. The conical pile was carefully flattened to a uniform thickness by spreading the aggregates with a scoop. An aluminum disk attached to the base was placed into the cylinder on the top of the aggregate sample. The distance between the bottom of the mold and the bottom of the disk for loose and compacted aggregates was then determined using four different points. For compacted samples, trials with different combinations of aggregates were performed to determine the time required for compaction. A time period of 45 seconds was used as an appropriate time for compaction. At least five tests were performed for each aggregate combination, and bulk packing density (BPD) was determined using the following equation:

$$\gamma = BPD = 4000\left(\frac{W}{(H-\Delta h)\pi D^2}\right), \quad \text{kg/m}^3 \qquad (22)$$

where: γ: bulk packing density of aggregates in loose or compacted conditions, kg/m^3;

W: mass of combined aggregates, kg;

H: height the container, mm;

D: diameter of the cylindrical container, mm;

Δh: height reduction of the compacted materials in cylindrical container, mm.

Loose and compacted densities of aggregates and aggregate blends were determined by the following equation:

$$\varphi = \gamma . \sum_{i=1}^{n} \frac{A_i}{\rho_i} \text{ , \%} \quad (23)$$

where: γ: packing density of aggregate blend, kg/m^3;

ρ_i: grain density of *i*- aggregate fraction, kg/m^3;

A_i: proportion of *i*- aggregate fraction;

n: total number of aggregate fractions.

Figure 15. The VB apparatus used for experimental packing test

3.3.5. Preparation, Mixing, and Curing of Concrete

Concrete batching, mixing, casting and curing procedures were conducted according to ASTM C192 "Standard Practice for Making and Curing Concrete Test Specimens in the Laboratory". The mixing procedure included mixing of aggregates with 20% of total water for 30 seconds using a drum mixer suitable for the volume of the batch. Next, cement was added to the mix, and then SCM (if any component) was added. The rest of the water with chemical admixtures was added upon the addition of cementitious materials. Finally, sand was added to the mixer. The mixing was resumed for an additional 3 minutes. The mix was left in the drum mixer at rest for a period of 3 minutes and was then mixed for another 2 minutes.

3.3.6. Slump

A concrete slump test was performed according to ASTM C143 to measure the workability of fresh concrete. This test is widely used in the field to determine the suitability of concrete pavement mixtures for slip-forming; however, there may be other characteristics such as finishability that are not accounted for by this test. The test was repeated at the time corresponding to 30 minutes after the initial contact of water and cement to measure the slump loss.

3.3.7. Density of Fresh Concrete

The density of fresh concrete was tested per ASTM C34. All the mixtures, regardless of the slump, were consolidated using rodding and tapping the side of the container with a rubber mallet repeated for 3 layers. The top of the container was leveled off and the weight was measured using a scale per ASTM C34.

3.3.8. Air Content of Fresh Concrete

Concrete air content was tested in the fresh state using an air meter as per as ASTM C231. Optimized mixtures were designed to reach air content of 6±1.5%; however, some changes occurred due to the variation in type of HRWRA and SCM.

3.3.9. Temperature

Fresh concrete temperature was tested according to ASTM C164 to monitor the potential effect of temperature. The temperature can be used to track any potential variation in different batches due to moisture loss, as well as heat of hydration.

3.3.10. Compressive Strength

Compressive strength tests were performed on cylinders with a diameter of 102 mm (4-in.) and height of 203 mm (8-in) according to ASTM C39. These specimens were tested with an ADR-Auto ELE compression machine at a loading rate of 2.4 kN/s (540 lb/s). The maximum load and maximum compressive stress were recorded. The test was performed at different ages including 1, 3, 7, 28, 90, and 360 days of normal curing.

3.3.11. Flexural Strength (Modulus of Rupture)

Flexural tests were performed on 102 x 102 x 356 mm (4 x 4 x 14-in.) beams according to ASTM C293. These specimens were tested using an ADR-Auto ELE machine, suitable for a center-point loading method at a loading rate of 1.4 kN/s (315 lb/s). The width and height of the sample at two cross sections were measured prior to testing, and the maximum load was then recorded upon testing.

The modulus of rupture at 3, 7, 28, and 90 days was calculated as follows:

$$R = \frac{3PL}{2bd^2} \quad (24)$$

where: R: modulus of rupture, MPa (psi)

P : maximum load, N (lb)

L: length of the span, mm (in.)

b : width of the specimen, mm (in.)

d: height of the specimen, mm (in.)

3.3.12. Length Change

The length change of investigated concrete due to drying was measured according to ASTM C157 "Standard Test Method for Length Change of Hardened Hydraulic-Cement Mortar and Concrete." The specimens were cured in the molds for 24 hours. Following this initial curing the specimens were removed from the molds and were cured in a lime-saturated water for additional 48 hours. At the age of 3 days the specimens were removed from water, wiped with damp cloth and measured for the initial length. The specimens were then placed in an air storage chamber with controlled humidity (50%) and temperature of 70 F. The length comparator readings were measured and the relative length change was recorded for each specimen at the age of 4, 5, 6, 7, 14, 28, 60, 90, and 360 days using 3-day reading as a reference.

3.3.13. Air Void Analysis

For air void analysis, concrete samples were prepared by cutting 102 x 102 mm (4 x 4-in.) cross-section blocks from the beams to approximately 20 mm (0.8 in.) in length using an oil-cooled diamond-edged rotary saw to provide an adequate surface to be lapped or polished. The surface was then lapped with an automated grinding, lapping and

polishing machine at 300 rpm using No.80 grit until irregularities on the surface were removed (typically 3 minutes of lapping time). This process was repeated using No. 120 grit, No. 220 grit, No. 500 grit, and, finally, No. 1200 grit polishing disks. Between lapping the sample on each grit size, a hardening solution was used to strengthen the surface of the concrete and ensure that the rims of the air voids maintain their true shape. The solution was created by mixing a 10 part acetone to 1 part oil-based lacquer. After each lapping sequence, the samples were cleaned using a soft brush and allowed to dry. The hardening solution was then painted onto the surface of the sample and again allowed to dry before starting the next lapping sequence. The specimens were lapped using the 80 grit disk twice with a coating of hardener between the sequences to preserve the void structure. After the final lapping, using a No. 1200 grit disk, the samples were briefly (3-5 minutes) placed in acetone to remove any leftover hardener. The samples were then cleaned and dried.

To prepare the polished and lapped sections for air void analysis, the surface was colored black using a broad tip marker pen by marking parallel lines with slightly overlapping strokes. This layer was allowed to dry and a second coat of marker was applied with strokes oriented at 90 degrees from the first direction. After the second coat was allowed to dry, a layer of white 99% pure barium sulfate, with a typical particle size of 0.7 μm, was placed on the surface of the sample. The barium sulfate was then pressed into the voids using a rubber stamper with sufficient force to ensure that all the voids had been filled. Excess powder was then brushed away until a sharp contrast was achieved between the black paste and aggregate zone and the white voids. The sample was viewed under a stereomicroscope to ensure an adequate contrast. At this stage, careful attention

was paid to blacken any voids within the aggregate using a fine point marker. The sample was then tested using a Rapid Air C 457 machine to calculate air void properties using ASTM C 457 Procedure A - Linear Transverse Method. A threshold of 174 was used to distinguish white and black portions of the sample. The paste content of the samples was estimated based on concrete mix design.

3.3.14. Chloride Permeability

Preparation and testing for Rapid Chloride Permeability followed the procedures described in the Standard Test Method for Electrical Indication of Concrete's Ability to Resist Chloride Ion Penetration ASTM C1202 (equivalent AASHTO T259). From each batch of concrete, there were two 102 x 203 mm (4 x 8-in) cylinders, one for 30-day testing and the other for 90-day testing. The cylinders were moist-cured in a wet room under temperature of 70 F until two days prior to their testing dates.

Two days prior to the testing date, two 50 mm (2-in.) thick slides were cut from the cylinder. Before this, a slide with thickness of approximately 12.5 mm (½ in.) was removed from the end of the cylinder so that the testing surfaces of both specimens had similar conditions. The slides were dried for about one hour before epoxy was applied to the side surface. Two-part marine grade epoxy PC-11 was used. All holes on the side were covered in this process. Attempts were made to avoid any epoxy on the testing surfaces of the specimens. After the epoxy cured for about 12 hours the specimens were ready for the vacuum saturation process.

The two slides were kept in a container inside a desiccator under vacuum, in dry condition, for 3 hours. Then tap water vigorously boiled for 20 minutes and cooled to

room temperature was poured into the container through a pipe attached to the side of the desiccator. The vacuum pump was kept running for an additional hour. Then the vacuum was released and the specimens were kept under water, usually overnight, for 18±2 hours.

The specimens were removed from water and mounted between the two test cells. Four bolts were used to secure the specimen to the cells. Silicone caulk was applied to seal the gap between the specimen and the cells, after which the caulk was allowed to dry for about one hour. One cell, which would be connected to the negative terminal of the power supply, was filled with 3% NaCl solution and the other, which would be connected to the positive terminal, was filled with 0.3N NaOH solution. The power was turned on and maintained at 60±0.1 V. Current and voltage readings were automatically recorded every 30 (or 60) seconds by a software. The test was run for 6 hours. The charge passing through the specimen was calculated by integration of the current with time and then adjusted to account for the diameter of the specimen, as specified by the ASTM C1202 equation (25) and analyzed using the *Table 16*:

$$Q = 900\ (I_0+2I_{30}+2I_{60}+\ldots+2I_{300}+2I_{330}+I_{360}) \qquad (25)$$

where:

- Q - charge passed (Coulombs);
- I_t - current passed (Amperes) at time t after the voltage was applied.

Table 16. Classification of Concrete Based on Chloride Ion Penetrability

Chloride Ion Penetrability	Charge Passed (Coulombs)
High	>4,000
Moderate	2,000-4,000
Low	1,000-2,000
Very Low	100-1,000
Negligible	<100

3.3.15. Resistance to Freezing and Thawing

From each batch of concrete, three 76 x 102 x 406 mm (3 x 4 x 16 in.) beams were produced. The testing for freeze-thaw durability followed the procedure of the Standard Test Method for Resistance of Concrete to Rapid Freezing and Thawing (ASTM C 666, equivalent to AASHTO T161), Procedure A and Standard Test Method for Fundamental Transverse, Longitudinal, and Torsional Resonant Frequencies of Concrete Specimens ASTM C 215 with the following exceptions:

- 3% NaCl solution (by weight) was used instead of water;
- The specimens were moist-cured for 28 days and then conditioned in a lab environment at a relative humidity of 50% and temperature of 70 °F.

At the age of 56 days, each specimen was saturated in the 3% NaCl solution for 48 hours. The purpose of this saturation process was to make the initial measurements comparable to later conditions of the specimen. This follows the instructions for conditioning beams cut from hardened concrete stated in provision 8.1 of ASTM C666.

Immediately after the conditioning period (at the age of 56 days), the fundamental traverse frequency of the specimens was measured according to the ASTM C215. Mass, average length and cross-section dimensions were measured within the tolerance required in Test Method C215.

Freezing and thawing tests were started by placing the specimens in 3% NaCl solution at the beginning of the thawing phase of the cycle. The specimens were removed from the apparatus at intervals between 30 and 36 freezing cycles and tested for fundamental traverse frequency and mass change. The specimens were then returned to

the apparatus and further subjected to freeze-thaw cycling. Each specimen was tested for 300 cycles or until the relative dynamic modulus of elasticity reached 60 % of the initial modulus, whichever occurred first. The relative dynamic modulus of elasticity of was calculated as follows:

$$Pc = (n_C/n_0)^2 \times (M_C/M_0) \times 100, \% \quad (26)$$

where:

- n_0 and M_0 are fundamental transverse frequency and mass, respectively, after 0 cycle of freezing and thawing, and
- n_C and M_C are fundamental transverse frequency and mass, respectively, before freezing and thawing.
- The above equation was modified from equation (1) in the ASTM C 666 standard to account for mass change as mentioned in Note 9 of the same document.

The durability factor of each specimen was calculated as follows:

$$DF = PN/M \quad (27)$$

where:

- P is the relative dynamic modulus of elasticity at N cycles, %,
- N is the number of cycles at which P reaches the specified minimum value for discontinuing the test or the specified number of cycles at which the exposure is to be terminated, whichever is less, and
- M is the specified number of cycles.

4. CONCRETE OPTIMIZATION

This chapter discusses the preliminary optimization of HRWR, WR, and air-entraining admixtures, the optimization of aggregates, selection (and adjustment) of water to cement (cementitious material) ratio in concrete, and the development and fine-tuning of the "final" optimized concrete mixtures for strength and durability assessment.

4.1. CEMENT PASTES: THE EFFECT OF ADMXITURES

The mini-slump of paste specimens corresponding to several water-to-cement ratios (W/C) was tested and reported in *Table 17*. The W/C of 0.45 resulting in a flow of ≈ 60 mm was selected for subsequent admixture testing. The selected W/C provides a good balance to compare plain pastes with different dosages of chemical admixtures with the range of 50 – 200 mm (2 – 8 in.).

Different portland cements (L1, L2, H1 and S1) combined with supplementary cementitious materials such as slag (SL), Class F fly ash (AF) and Class C fly ash (AC), and selected chemical admixtures were tested in pastes to determine the mini-slump at a specific dosage (RP8-0.15%, HR1-0.4% and HG7-0.15%). Other admixtures were evaluated and screened out; and, because of the best performance, HG7 was selected to investigate the effect of SCM. The results of these tests are reported in *Figure 16* and *Figure 17*.

Table 17. Mini-Slump of Cement Pastes Based on L1 at Different W/C Ratios

W/C	0.4	0.45	0.5	0.6	0.8	1.0
Flow, mm (in.)	38 (1.5)	59 (2.3)	65 (2.6)	98 (3.8)	138 (5.4)	189 (7.4)

Mini-slump tests had demonstrated that L1 and H1 cements are perfectly compatible with SNF (HR1) and PCE (HG7) superplasticizers; however, L2 and S1 cements designed for rapid strength development had a reduced compatibility with superplasticizers (*Figure 16*). The H1 cement had an excellent compatibility with all tested admixtures and demonstrated the best flow properties. The S1 cement had the worst compatibility with admixtures tested. The mini slump test of pastes with SCM demonstrated that the addition of SCM (especially Class C fly ash and slag cement) was beneficial to improving the workability of cement pastes and portland cement systems with SCM (*Figure 17*).

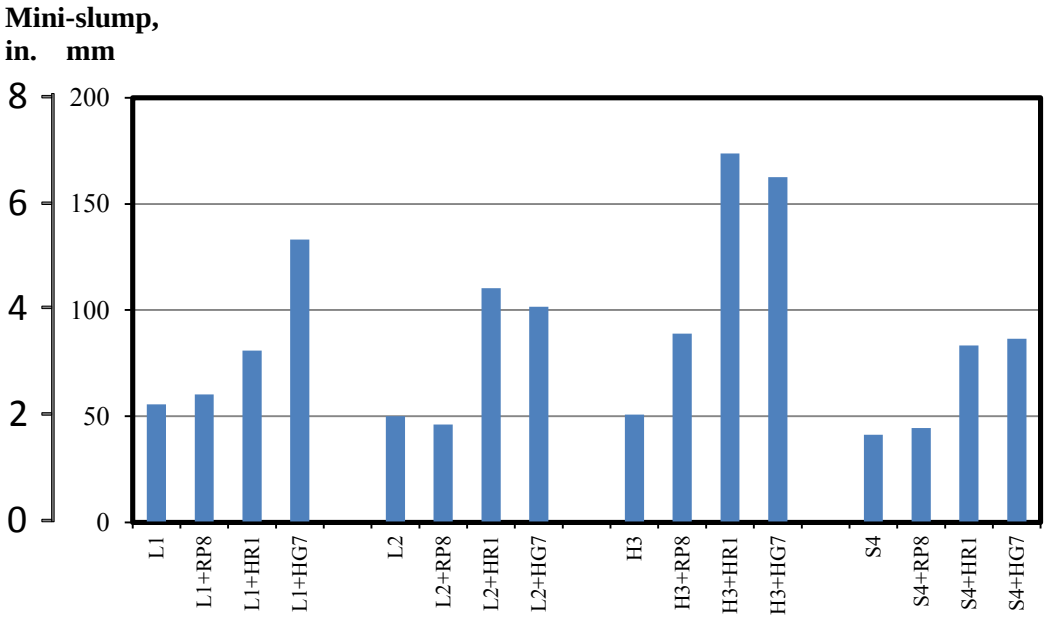

Figure 16. The effect of portland cement and admixture type on

It can be observed that the addition of SCM improves the flow of blended cement pastes as demonstrated by *Figure 17*. Class C fly ash based mixtures had excellent flow properties in systems with plasticizing or superplasticizing admixtures. Slag cement had the best compatibility with PCE superplasticizer.

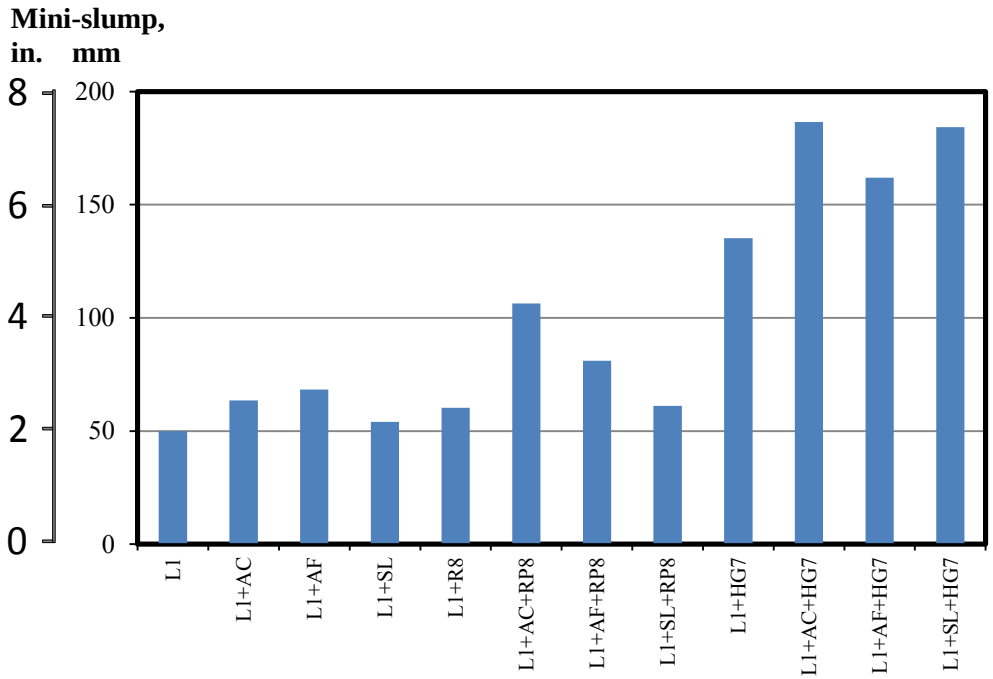

(a)

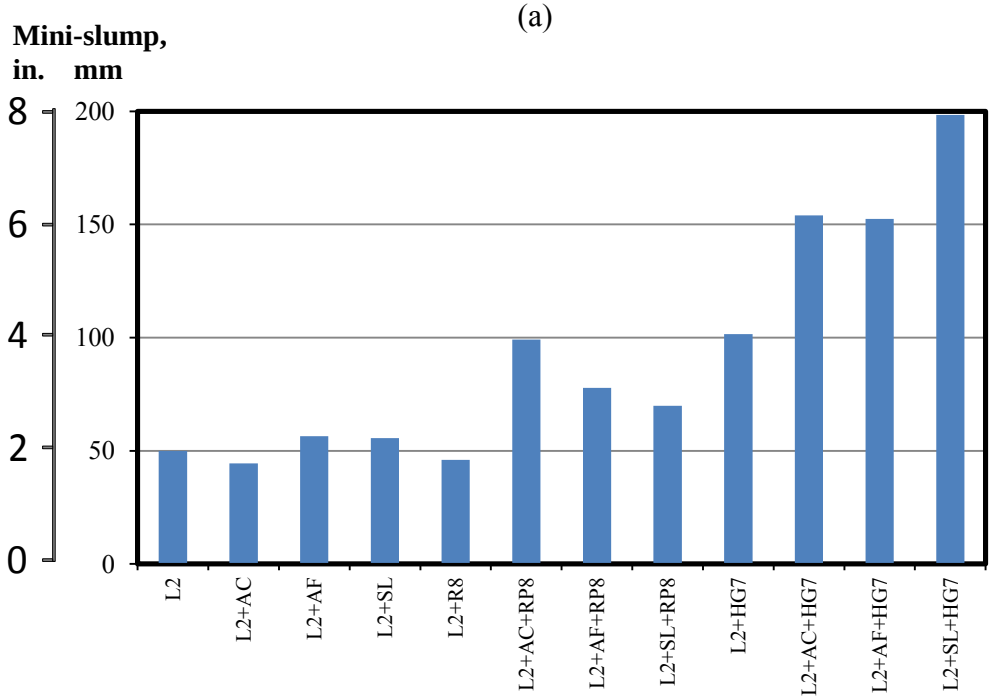

(b)

Figure 17. The effect of SCM and type of admixture on mini-slump of pastes based on cements L1 (a) and L2 (b)

4.2. MORTARS: THE EFFECT OF ADMIXTURES

4.2.1. The Effect of Chemical Admixtures on Fresh Properties of Mortars

Tests for flow and fresh density of mortars were used to determine the optimal dosage of chemical admixtures (expressed as a solid or "active" content, by the weight of the binder). The performance of chemical admixtures was compared with the properties of a reference mortar (Ref L1). Relevant ASTM standards were used for the evaluation of mortar flow (ASTM C 1437) and fresh density (ASTM C 138). The research results are reported in *Table 18* and *Table 19* and plotted in *Figure 18* and *Figure 19*. The superplasticizers were selected and recommended based on their flow and density performance in pastes and mortars. The HG7 (SNF) and HR1 (PCE) superplasticizers were selected for the use in concrete due to their higher flow at lower dosage levels. The effect of reference RP8 plasticizer was similar to the performance of the superplasticizers, but, due to excessive air entrainment, at higher dosages the addition of RP8 drastically reduces the density of the mortar (*Table 19*)

Table 18. Effect of admixtures on flow of mortars

Chemical Admixtures	Flow, % at Admixture Dosage, %							
	0	0.05	0.1	0.15	0.2	0.3	0.4	0.5
Ref L1	26.5	-	-	-	-	-	-	-
HD1		-	-	45.5	54.0	57.4	61.8	62.9
HAC		-	52.4	60.4	66.3	71.0	-	-
HG7		56.1	68.9	73.4	-	-	-	-
HR1		-	-	49.6	55.8	65.9	70.5	-
RP8		-	38.2	60.6	76.7	-	-	-

Table 19. Effect of admixtures on fresh specific gravity of mortars

Chemical Admixtures	Fresh Specific Gravity at Admixture Dosage, %							
	0	0.05	0.1	0.15	0.2	0.3	0.4	0.5
Ref L1	2.297	-	-	-	-	-	-	-
HD1		-	-	2.202	2.129	2.076	2.071	2.061
HAC		-	2.153	2.142	2.121	2.070	-	-
HG7		2.155	2.128	2.092	-	-	-	-
HR1		-	-	2.202	2.160	2.129	2.106	-
RP8		-	1.990	1.974	1.971	-	-	-

Therefore, mortar tests can be effectively used to select the optimal dosage of superplasticizers (e.g., 0.15% and 0.4% for HG7 and HR1, respectively). The dosage of mid-range plasticizing admixture must be limited to 0.15%, as a higher dosage may result in excessive air entrainment and reduction in strength.

For the range of investigated compositions, there is a good correlation between the flow properties of pastes (mini-slump) and the flow of mortars (*Figure 20*). Using the mini slump test, the flow of mortars based on different cements and compatibility with admixtures can be predicted.

Mortars based on cements L1, L2 and H1 had similar flow, and the use of cement S1 induced a reduced flow (possibly to higher fineness and higher C_3A content), as demonstrated by *Figure 21,* similar to mini-slump performance, flow of mortars was improved with the addition of SCM as reported in *Figure 22*.

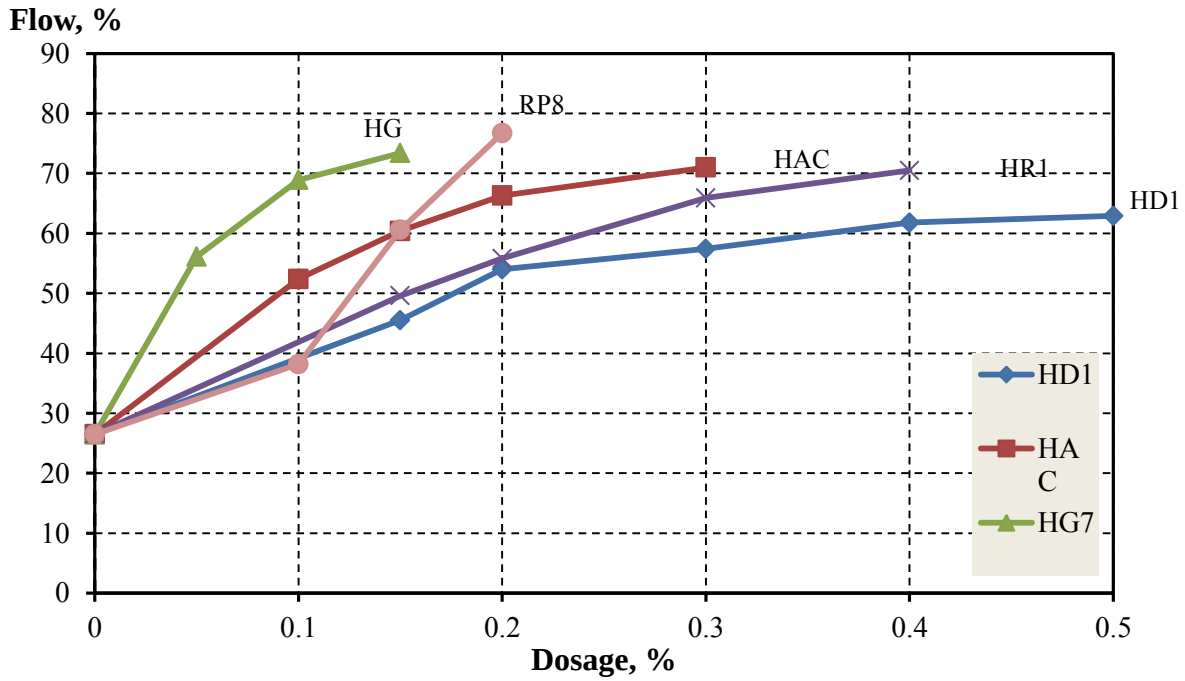

Figure 18. The effect of SNF (HR1 / HD1) and PCE (HAC / HG7) superplasticizers and mid-range water-reducer (RP8) on the flow of mortars

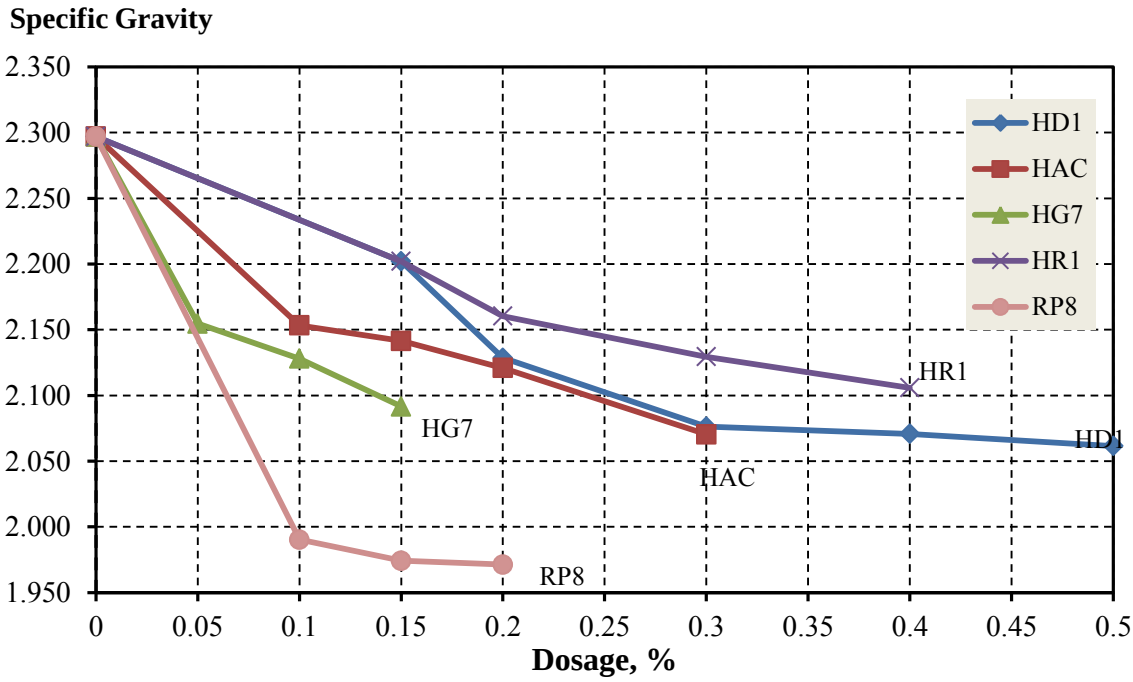

Figure 19. The effect of SNF (HR1 / HD1) and PCE (HAC / HG7) superplasticizers on the fresh density of mortars vs. mid-range water-reducer (RP8)

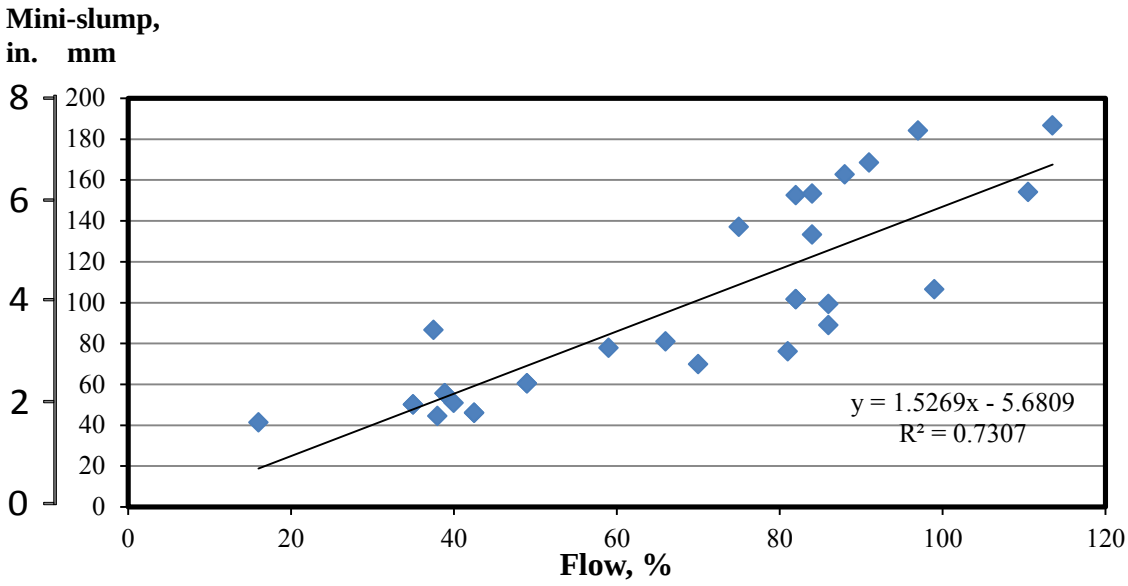

Figure 20. The correlation between the mini-slump of pastes and mortar flow

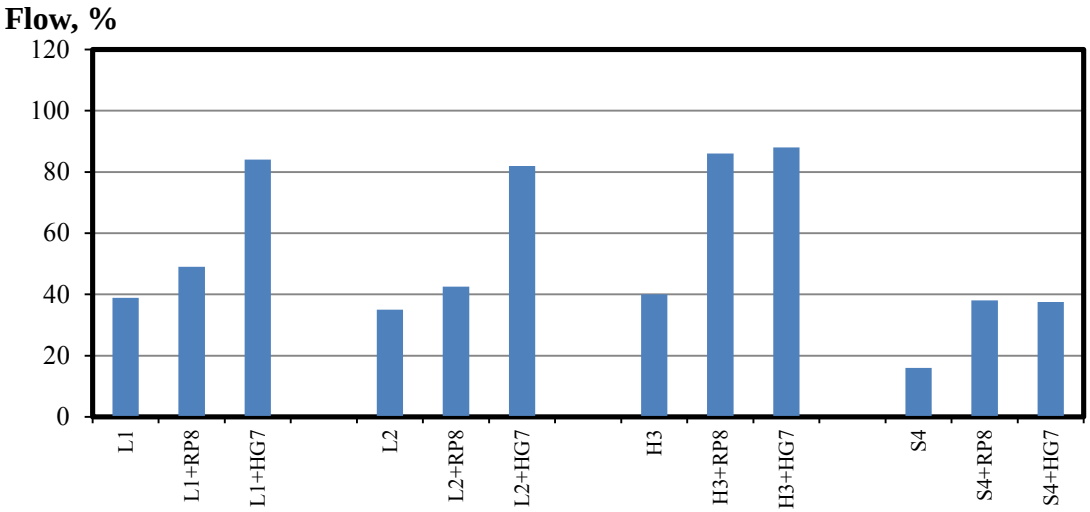

Figure 21. The effect of chemical admixtures on mortar flow

The best improvement was achieved in the systems with Class C fly ash, especially combined with PCE (HG7) superplasticizers. The response of portland cement mortars with slag cement was very similar to reference portland cement systems modified with the corresponding admixture.

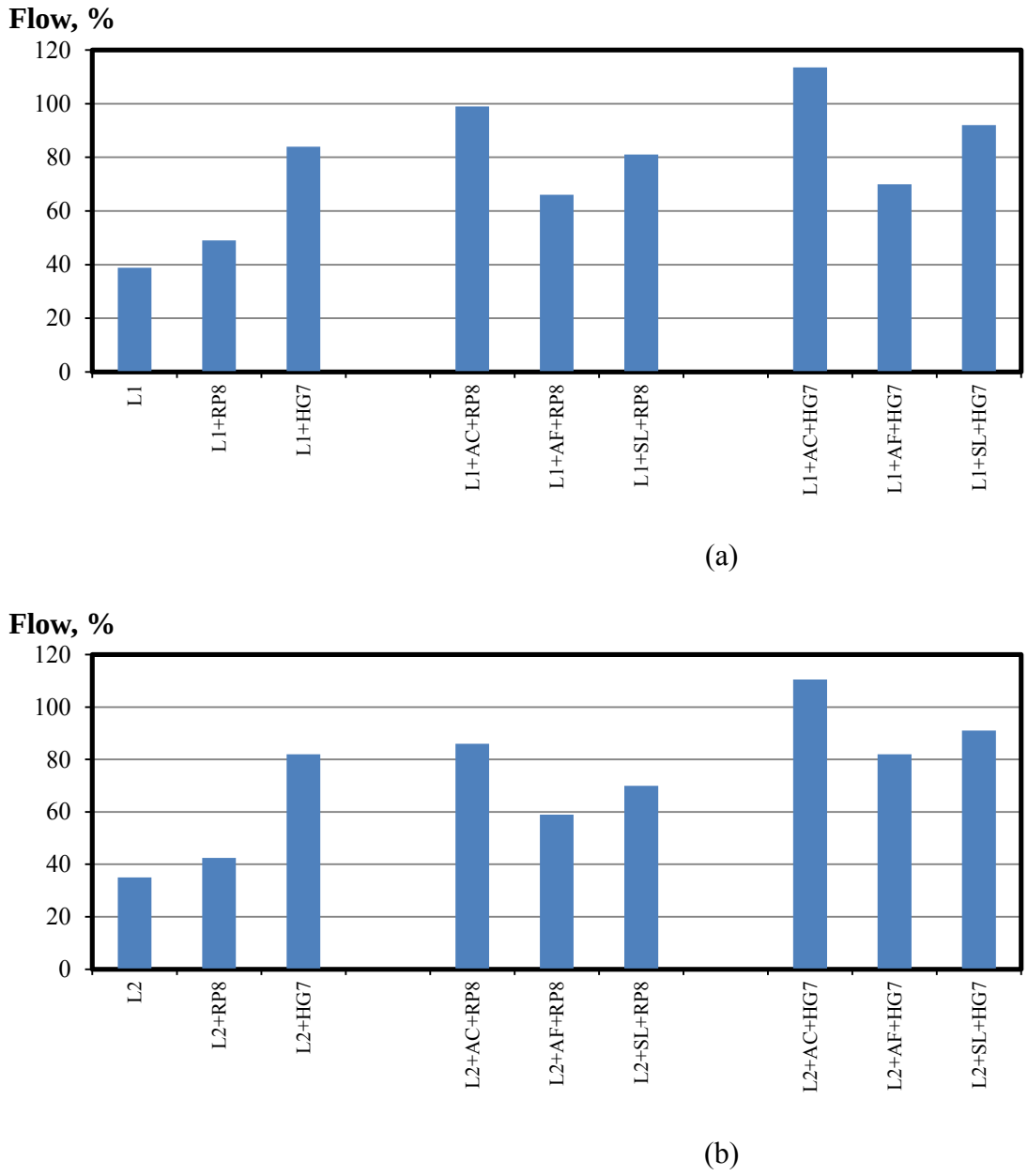

Figure 22. The effect of admixtures and SCMs on flow of mortars (based on cement L1 (a) and L2 (b)

The relative flow enhancement was more significant in the systems with mid-range plasticizers. This can be explained by different absorption capacities of the cements and SCM; therefore, cement replacement with SCM, which absorbs lower quantities of surfactants is equal to a relative increase in admixture dosage. In respect to this, in the

systems with SCM, the dosage of admixture can be reduced to avoid the overdose and potential delay in strength development (especially in the case of WR).

At the same time, in the case of synergy between the superplasticizer and SCM, no delay in strength development is observed; and so, improved workability can be used to boost the strength of concrete (by reducing w/cm ratio) or to reduce the cementitious material content (at a constant w/cm ratio).

4.2.2. Effect of Chemical Admixtures on Heat of Hydration

The performance of selected plasticizing (RP8) and superplasticizing (HR1/ HG7) admixtures was investigated and compared to a reference mortar using the parameters of the hydration process detected by isothermal calorimeter. For this study, mortars based on portland cement L1 were monitored for the early hydration period of 48 hours. The observed effects are represented by *Figure 23*, *Figure 24* and *Figure 25* reporting on the of RP8, HR1 and HG7 admixtures, respectively.

It can be observed that all admixtures slightly delay the hydration as demonstrated by the 3- to 3.5- hour shift of the C_3S hydration peak and about 2- hour extension of the dormant period. These minor delays can be considered as positive, enabling to preserve the workability while in transit to the jobsite. With the addition of admixtures, the intensity of the main exothermal peak was reduced, possibly because of selective action of the admixtures, delaying the hydration of C_3A by about 7.5 hours, so the 2^{nd} peak (corresponding to C_3A) appears at the heat flow curves.

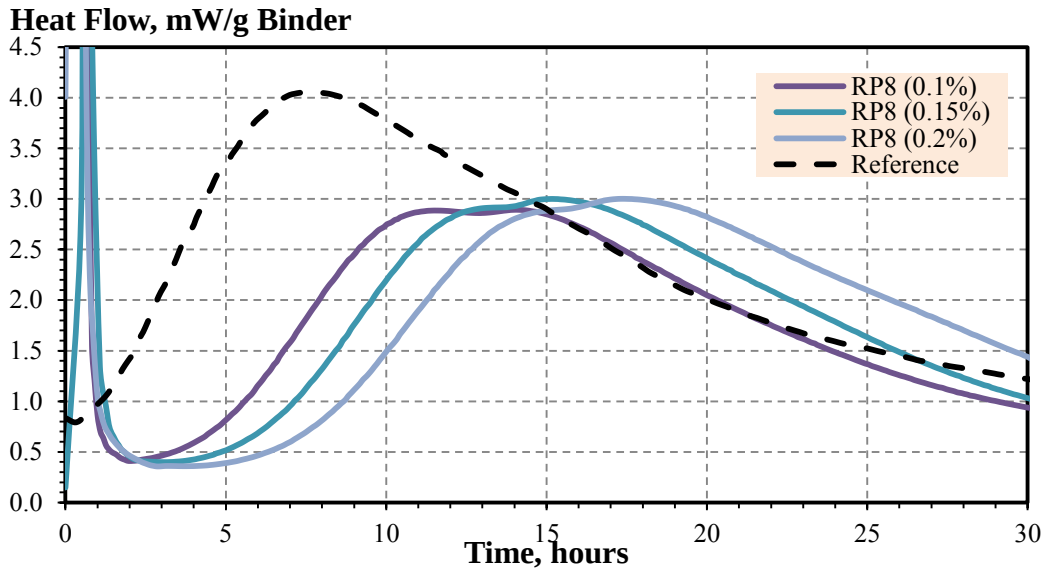

Figure 23. The effect of mid-range water-reducing admixture (RP8) on cement hydration

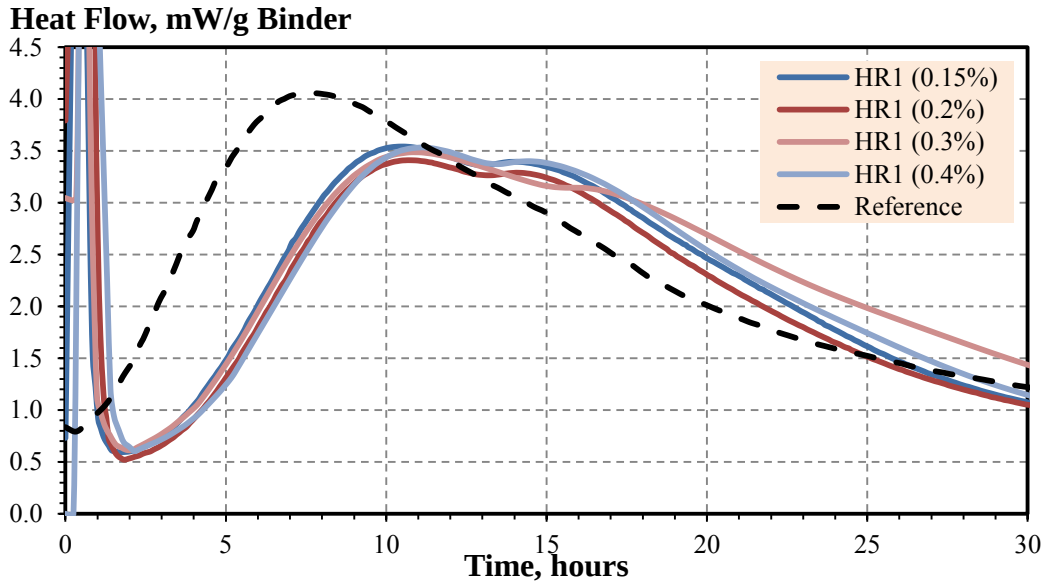

Figure 24. The effect of SNF (HR1) admixture on cement hydration

The heat flow curves can be used to confirm the optimal dosage of admixture. It can be observed that an increment of RP8 as small as 0.05% (by weight of cement), e.g., from 0.1% to 0.15%, can result in a significant delay of cement hydration and a potential reduction of strength, especially, at the early age of 1 to 3 days.

It can be confirmed that the addition of SNF superplasticizer (HR1) at the dosage from 0.15% to 0.4% has no significant effect on the heat of hydration. Therefore, this admixture can be used within this tested range.

The addition of PCE superplasticizer (HG7) at a dosage of 0.15% of cement weight results in a considerable increase of the heat responses associated with C_3A and C_3S, suggesting that 0.15% dosage intensifies the hydration. However, a further increase of SP to 0.2% results in a reduction of the heat flow, suggesting a delay in hydration (due to overdose). Therefore, 0.15% was suggested to be the optimal (maximal) dosage of HG7 in cement systems based on L1 cement. These observations are commonly verified by strength testing.

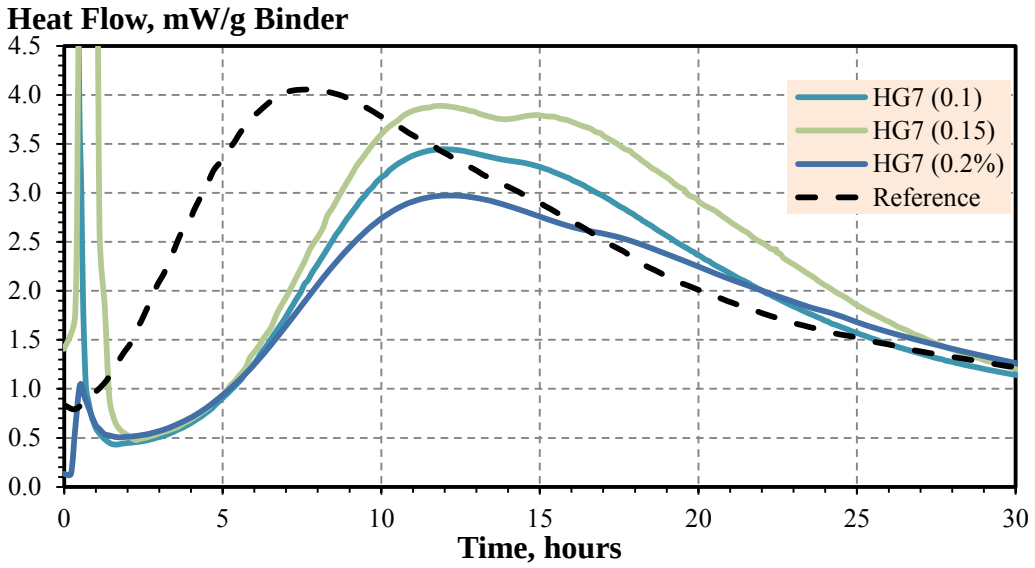

Figure 25. The effect of PCE (HG7) admixture on cement hydration

4.2.3. Effect of Chemical Admixtures on Mechanical Performance of Mortars

The effect of chemical admixtures was evaluated by testing the compressive strength of mortars at different stages of hardening. The performance of selected

admixtures are summarized in *Table 20* and further demonstrated by *Figure 26, Figure 27* and *Figure 28*.

Table 20. The effect of admixtures on the compressive strength of mortars (w/c=0.45)

Mix ID	Dosage, %	Compressive Strength, MPa (psi) at the Age of		
		3 days	7 days	28 days
Ref (L1)	-	18.4 (2669)	32.9 (4772)	36.8 (5337)
RP8 (0.1%)	0.1	18.0 (2611)	22.3 (3234)	26.7 (3873)
RP8 (0.15%)	0.15	18.9 (2741)	25.7 (3727)	30.6 (4438)
RP8 (0.2%)	0.2	14.8 (2147)	22.9 (3321)	31.7 (4598)
HR1 (0.15%)	0.15	28.5 (4134)	31.1 (4511)	39.5 (5729)
HR1 (0.2%)	0.2	24.0 (3481)	29.3 (4250)	34.9 (5062)
HR1 (0.3%)	0.3	20.7 (3002)	29.9 (4337)	39.5 (5729)
HR1 (0.4%)	0.4	20.8 (3017)	29.6 (4293)	38.3 (5555)
HG7 (0.05%)	0.05	20.8 (3017)	29.3 (4250)	38.7 (5613)
HG7 (0.1%)	0.1	27.0 (3916)	37.8 (5482)	44.8 (6498)
HG7 (0.15%)	0.15	33.1 (4801)	37.1 (5381)	41.2 (5976)
HG7 (0.2%)	0.2	23.6 (3423)	30.4 (4409)	36.2 (5221)

It can be observed that the use of plasticizing admixture RP8 results in a reduction of strength at 7 and 28 days of hardening. Surprisingly, the 3-day strength of these mortars was very similar to the strength of the reference L1, as reported by *Figure 26*. The plasticizing effect of RP8 was very impressive, especially at increased dosages; however, due to early-age strength reduction, the effective dosage of RP8 must be kept to the lowest tested. The 28-day strength of mortars with RP8 was 20% lower than reference (*Table 20*).

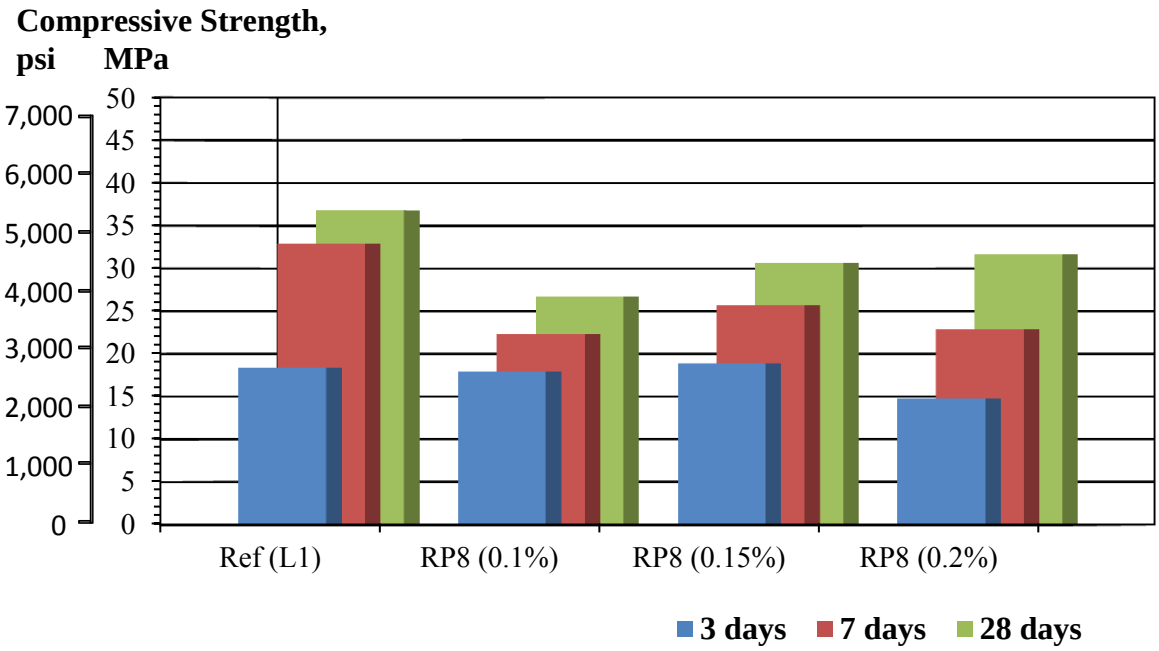

Figure 26. Compressive strength of mortars with mid-range water-reducer (RP8)

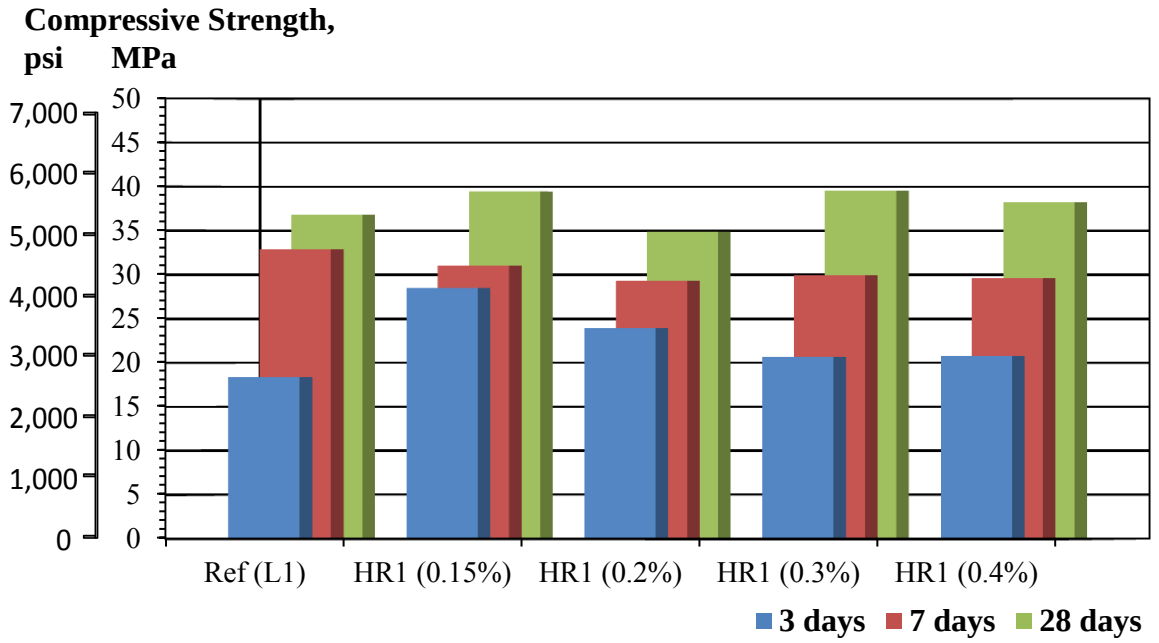

Figure 27. Compressive strength of mortars with SNF superplasticizer (HR1)

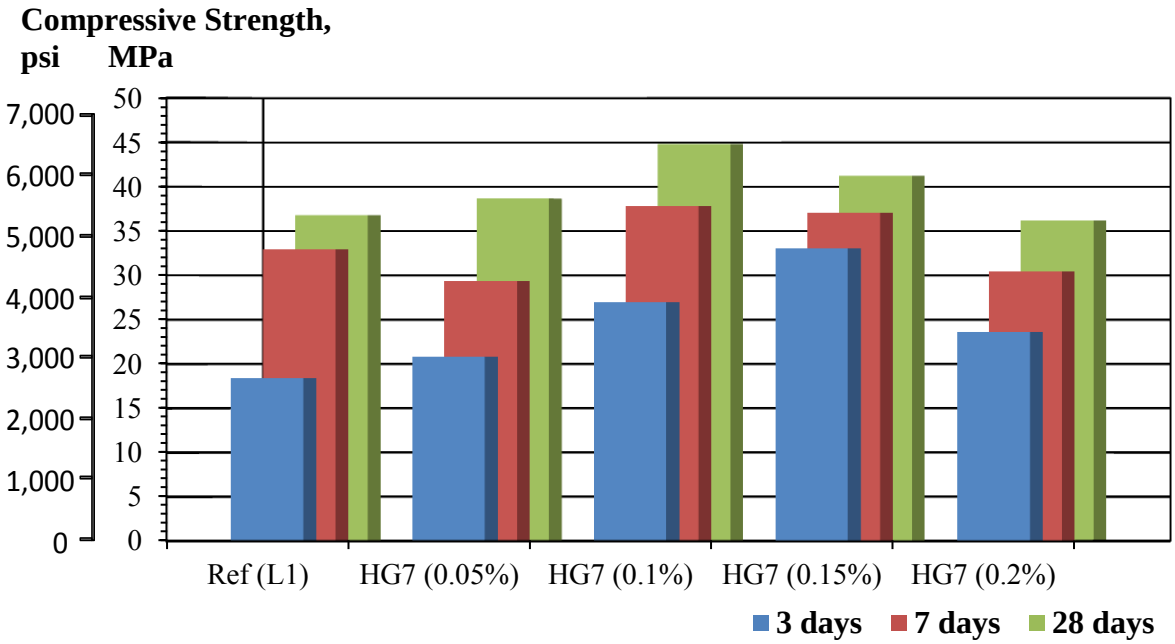

Figure 28. Compressive strength of mortars with PCE superplasticizer (HG7)

At the age of 7 and 28 days, the strength of SNF modified mortars was similar to that of reference mortars, suggesting that the tested dosage range of 0.15% to 0.4% was robust and applicable for investigated binding systems. A significant increase of 3-day strength was observed at the SNF dosage of 0.15%: 28.5 MPa vs. 18.4 MPa for reference plain mortar. This effect diminished at higher SNF dosages (up to 0.4%). In this way, SP can be used in the portland cement systems to achieve the desired response. Practically, a higher SP dosage can be used for significant reduction of W/C and, therefore, to boost the strength at all ages.

The PCE superplasticizer demonstrated exceptional performance in mortars based on L1 cement (*Figure 28*): at the same W/C ratio, the mortars with HG7 had 28-day compressive strength of 44.8 MPa vs. 36.8 MPa for reference plain mortar. The 3-day compressive strength of mortars with 0.15% of HG7 was 33.1 MPa vs. 18.4 MPa of

reference plain mortar. This response can be correlated to observations on accelerated hydration and released heat (*Figure 25*).

4.2.4. The Effect of SCM on Mechanical Performance of Mortars

The test results related to the effect of SCM on strength of mortars based on L1 and L2 cements are reported in *Table 21* and *Figure 29*. It can be observed that the use of SCM results in a reduction of 3- and 7- day compressive strength, which was considerable in the Class F fly ash and slag cement mortars produced with plasticizer RP8 and cement L1. However, L2 cement provided a better compatibility with SCM and chemical admixtures.

Table 21. Compressive strength of mortars with different SCM

Mortar Mix ID	Flow, %	Compressive Strength, MPa (psi) at the Age of		
		3 days	7 days	28 days
L1	39	19.1 (2770)	21.9 (3176)	25.9 (3756)
L1+RP8	49	20.3 (2944)	23.9 (3466)	28.4 (4119)
L1+HG7	84	26.3 (3814)	32.9 (4772)	38.7 (5613)
L1+AC+RP8	99	10.3 (1494)	21.2 (3075)	27.9 (4308)
L1+AF+RP8	66	10.4 (1508)	15.6 (2263)	24.7 (3582)
L1+SL+RP8	81	7.5 (1088)	12.7 (1842)	19.1 (2770)
L1+AC+HG7	114	14.5 (2103)	20.4 (2959)	31.5 (4569)
L1+AF+HG7	70	13.5 (1958)	15.4 (2234)	25.4 (3684)
L1+SL+HG7	92	15.2 (2205)	24.0 (3481)	32.6 (4728)
L2	35	20.6 (2988)	26.2 (3800)	28.1 (4075)
L2+RP8	47	23.2 (3365)	31.2 (4525)	34.4 (4989)
L2+HG7	81	27.9 (4046)	32.1 (4656)	42.3 (6135)
L2+AC+RP8	86	17.2 (2495)	23.3 (3379)	37.7 (5468)
L2+AF+RP8	59	16.0 (2321)	18.4 (2669)	30.4 (4409)
L2+SL+RP8	70	13.9 (2016)	24.9 (3611)	38.2 (5540)
L2+AC+HG7	111	20.4 (2959)	26.3 (3814)	35.9 (5207)
L2+AF+HG7	82	18.3 (2654)	22.2 (3219)	29.6 (4293)
L2+SL+HG7	91	24.1 (3495)	23.5 (3408)	39.0 (5656)

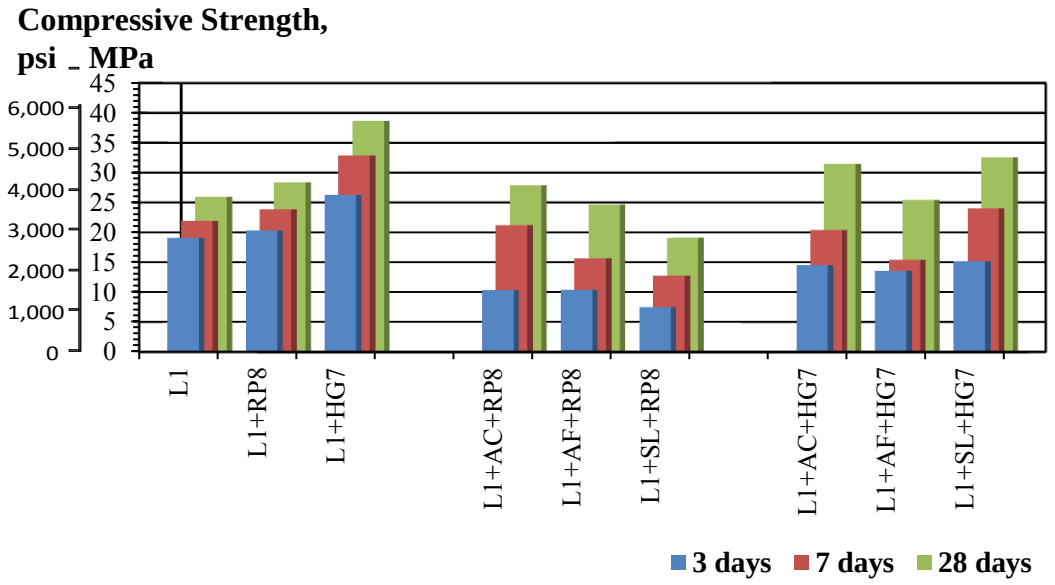

(a)

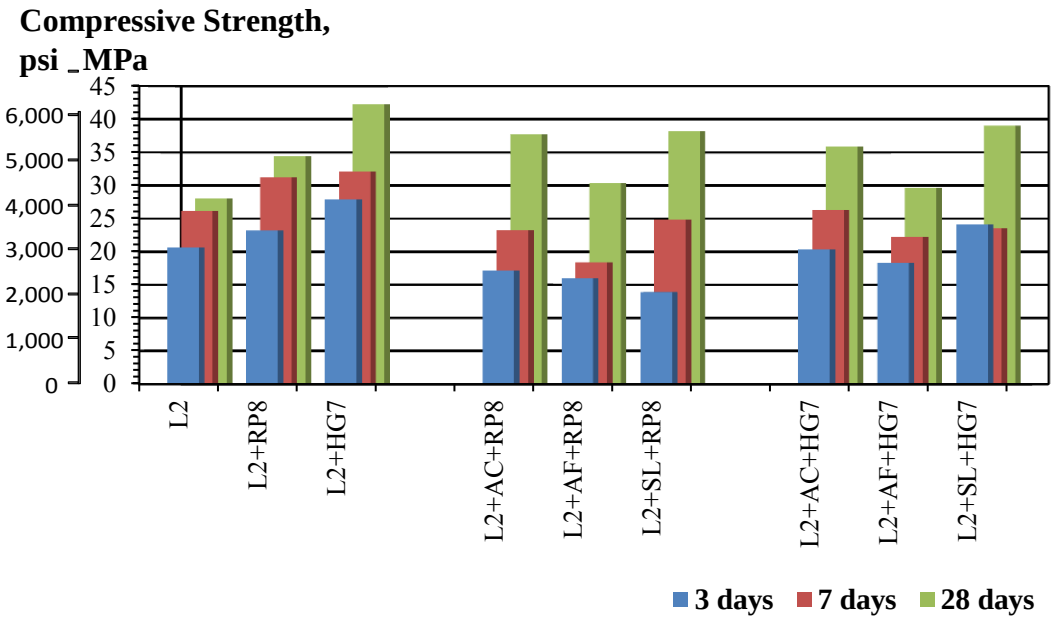

(b)

Figure 29. The effect of SCM on strength of mortars based on cement L1 (a) and L2 (b)

At the age of 28 days, the compressive strength of investigated mortars with SCM was comparable to the properties of plain portland cement mortar. However, considerable reduction in 28-day strength was observed for L1-SCM based mortars combined with plasticizer RP8; in this group, only Class C fly ash demonstrated strength comparable to portland cement systems. The performance of RP8 in L2-SCM based mortars was better (vs. L1-SCM mortars), resulting in a 28-day strength comparable to that of the reference portland cement mortars with RP8 (*Figure 29*).

The use of Class C fly ash and slag cement in mortars with plasticizing or superplasticizing admixtures was very effective, as supported by the 28-day strength results. Class F fly ash resulted in a reduction of strength and reduced strength at all ages of up to 28 days. Due to ongoing pozzolanic reactions, the strength of mortars with Class F fly ash can potentially be improved at later stages of hardening.

4.3. OPTIMIZATION OF AGGREGATES

This section reports on the application of theoretical models, simulation, and experimental results related to aggregate optimization, characteristics of aggregate blends, applicability of gradation techniques, and a coarseness chart. The aggregates were also evaluated in concrete mixtures in order to make a comparison between the aggregates structure and the performance of corresponding blends.

4.3.1. Experimental Packing of Aggregates

The experimental bulk density and void content for loose and compacted aggregates are summarized in *Table 22* and *Table 23*. Higher densities of aggregate blends correspond to the lower void content of the material. As demonstrated by *Figure 30* and *Figure 31*, loose and compacted density of 40 different southern aggregate blends and 40 different northern aggregate blends were used to determine the experimental packing degree. Selective combinations of aggregates and the corresponding densities before and after compaction are summarized in Table 22 and Table 23. As illustrated by *Figure 30* and *Figure 31*, in southern aggregates, the packing degree tends to increase at fine aggregates content of 50% to 70% (top of ternary diagram) and for northern aggregates the best packings were achieved at fine aggregate content of 40% to 60% and different levels of intermediate aggregates (IA).

The ternary diagrams *Figure 30* and *Figure 31* demonstrate that the use of 10% of IA tends to increase the packing degree of all mixtures based on both northern and southern aggregates.

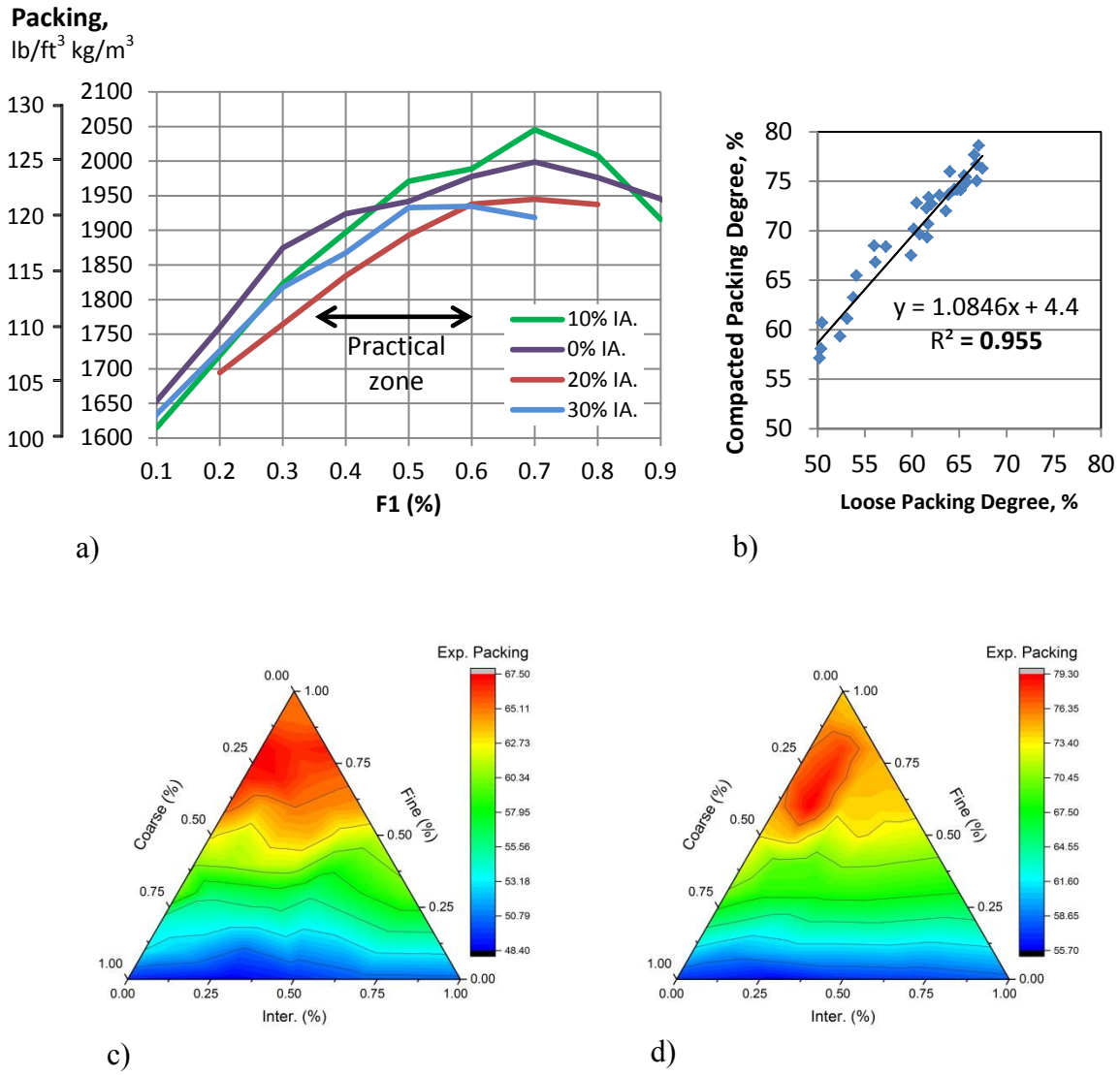

Figure 30. The experimental packing degree of southern aggregate blends a) the effect of fine aggregates (F1); b) compacted vs. loose relationship; c) ternary diagrams for loose and d) compacted packing

For both types of aggregates, the impractical zone of the diagram corresponds to mixtures with less than 40% of coarse aggregates. An experimental packing degree as high as 79% for compacted, and 68% for loose conditions, were achieved as illustrated in *Figure 30* for southern aggregates. Similarly, packing was 78% for compacted and 68% for loose states as illustrated in *Figure 31* of northern aggregates.

For northern aggregates, the packing test indicates that the intermediate aggregates have a high compatibility with other aggregate fractions; therefore, the use of these can contribute to dense packing and better aggregate blends.

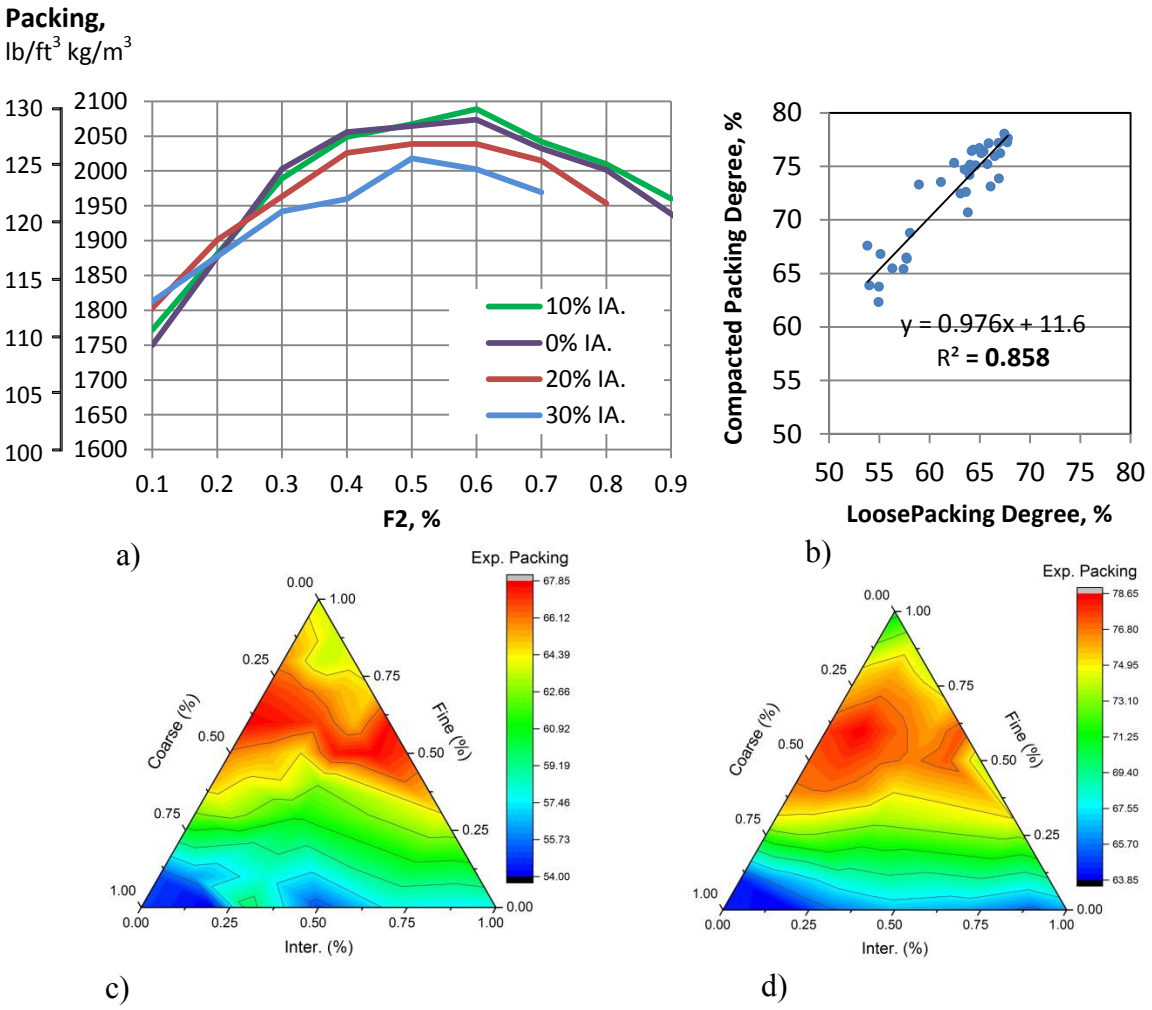

Figure 31. The experimental packing degree of northern aggregate blends: a) the effect of fine aggregates (F2); b) compacted vs. loose relationship; c) ternary diagrams for loose and d) compacted packing

Table 22. Performance of concrete mixtures based on southern aggregate blends

Mix ID	Packing Degree, %		Aggregate Combinations, %			Experimental Results					Power Distribution of Aggregate Blends					
						Slump, mm (in)	Bulk density, kg/m^3 (lb/ft^3)	Air (Pressure) %	Compressive Strength, MPa (psi)		Power	Statistical Parameters				
	Loose	Comp.	CA	IA	FA				7 days	28 days	n	Square Error	MSE	Root MSE	NRMSE %	Std. Dev.
S1	60.4	71.5	65	0	35	76 (2.99)	2480 (155)	1.0	15.6 (2263)	22.8 (3307)	0.70	943	67.4	8.2	73.0	53.7
Fit 2	-	**78.8**	-			-	-	-	-	-	-	-	-			**14.8**
S2	60.5	72.8	60	0	40	70 (2.76)	2477 (155)	0.8	20.2 (2930)	25.5 (3698)	0.59	893	63.8	8.0	65.2	55.4
S3	61.7	73.2	55	0	45	191 (7.52)	2463 (154)	1.0	20.4 (2959)	25.8 (3742)	0.51	796	56.9	7.5	65.5	53.7
S4	62.9	73.6	50	0	50	191 (7.52)	2435 (152)	1.3	21.2 (3075)	25.7 (3727)	0.46	676	48.3	6.9	68.6	42.8
S5	65.7	75.4	40	0	60	165 (6.50)	2406 (150)	2.2	23 (3336)	27.8 (4032)	0.36	471	33.6	5.8	64.7	31.3
S6	58.5	68.2	55	10	35	205 (8.07)	2480 (155)	0.9	16.5 (2393)	23.6 (3423)	0.64	649	46.4	6.8	61.9	39.7
S7	61.3	71.5	45	10	45	191 (7.52)	2449 (153)	1.2	20.3 (2944)	27.6 (4003)	0.49	497	35.5	6.0	60.0	32.8
S8	61.8	73.4	40	10	50	191 (7.52)	2435 (152)	1.2	22.4 (3249)	28 (4061)	0.43	405	28.9	5.4	59.6	27.2
S9	62.4	74.0	37.5	10	52.5	191 (7.52)	2446 (153)	1.3	23 (3336)	31.3 (4540)	0.40	372	26.6	5.2	59.0	26.5
S10	62.9	74.7	35	10	55	171 (6.73)	2446 (153)	1.8	22.5 (3263)	30.8 (4467)	0.39	326	23.3	4.8	60.3	21.4
S11	59.7	67.8	45	20	35	181 (7.13)	2469 (154)	0.9	17.7 (2567)	20.9 (3031)	0.60	427	30.1	5.5	64.8	27.8
S12	61.6	69.3	40	20	40	175 (6.89)	2460 (154)	0.9	17.9 (2596)	24.9 (3611)	0.53	360	25.7	5.1	64.3	24.0
S13	63.6	72.0	30	20	50	156 (6.14)	2463 (154)	1.2	23.5 (3408)	30.2 (4380)	0.42	227	16.2	4.0	66.8	15.2
Fit 1	-	**78.8**	-			-	-	-	-	-	-	-	-			**53.7**
S14	59.5	69.5	35	30	35	166 (6.54)	2483 (155)	0.9	17.7 2567)	22.4 (3249)	0.57	268	19.1	4.4	64.3	18.6
S15	61.7	70.7	30	30	40	146 (5.75)	2457 (153)	1.1	22.9 (3321)	30.1 (4366)	0.51	218	15.6	3.9	65.4	14.5
S16	63.8	73.6	20	30	50	165 (6.50)	2443 (153)	1.3	21.6 (3133)	30.4 (4409)	0.40	151	10.8	3.3	45.2	14.0

Table 23. Performance of concrete mixtures based on northern aggregate blends

Mix ID	Packing Degree, %		Aggregate Combinations, %			Experimental Results					Power Distribution of Aggregate Blends					
						Slump, mm (in.)	Bulk density, kg/m^3 (lb/ft^3)	Air (Pressure) %	Compressive Strength, MPa (psi)		Power n	Statistical Parameters				
	Loose	Comp.	CA	IA	FA				7 days	28 days		Square Error	MSE	Root MSE	NRMSE %	Std. Dev.
N1	63.7	76.0	65	0	35	32 (1.26)	2544 (159)	0.8	19.4 (2814)	29.5 (4279)	0.62	521	37.2	6.1	32.4	33.9
N2	64.9	76.0	60	0	40	93 (3.66)	2525 (158)	0.8	21.7 (3147)	28.0 (4061)	0.55	513	36.6	6.1	39.0	31.9
N3	65.9	77.1	50	0	50	70 (2.75)	2473 (154)	2.2	21.5 (3118)	33.1 (4801)	0.44	495	35.4	5.9	65.7	28.8
N4	67.8	77.6	40	0	60	20 (0.79)	2410 (150)	2.8	17.4 (2524)	27.7 (4017)	0.36	587	41.9	6.5	38.5	51.9
N5	65.5	76.9	55	10	35	36 (1.41)	2502 (156)	1.0	20.2 (2930)	31.6 (4583)	0.58	305	21.8	4.7	29.0	25.7
N6	64.0	75.1	50	10	40	43 (1.69)	2524 (157)	1.3	24.8 (3600)	32.4 (4699)	0.52	301	21.5	4.6	37.1	23.3
N7	64.7	75.8	45	10	45	70 (2.75)	2486 (155)	0.8	23.8 (3452)	30.2 (4380)	0.46	308	22.0	4.7	56.5	24.2
N8	64.2	76.4	40	20	40	33 (1.3)	2477 (154)	1.6	21.9 (3176)	30.9 (4482)	0.49	229	16.4	4.0	42.5	18.8
N9	64.3	76.5	30	20	50	30 (1.18)	2476 (154)	3.0	21.1 (3060)	26.7 (3872)	0.40	520	37.1	6.1	48.4	35.7
N10	66.1	73.1	30	30	40	44 (1.73)	2490 (155)	1.8	20.9 (3031)	29.0 (4206)	0.40	520	37.1	6.1	69.2	22.4

4.3.2. Modeling vs. Experimental Packing

The aggregate packing results obtained from VB packing experiments were compared to output predicted by theoretical discrete models. The purpose of this study was to verify the experimental packing results and associated best blends (in terms of maximum packing) with the models. The models can evaluate the separate effects of the fine, coarse and intermediate aggregates on packing degree. The Aim model [83] was used as a classical model to describe the packing degree of binary blends, and a modified Toufar model [30] was used to describe the packing degree for binary and ternary blends. The Aim model takes into account the wall effect to calculate the packing degree. The Toufar model takes into account the diameter ratio of the particles, probability of the number of interstices between the coarse particles and also uses the characteristic diameter, eigenpacking degree, and grain density of each individual class of particles to calculate the packing degree.

These properties are aggregate specific and were measured for each class and type of aggregate. The properties of the aggregates used for the Toufar model are summarized in *Table 24.* and *Table 25*. Grain density of the aggregates was obtained from the specific gravity test. The compacted packing degree of each type of aggregate used in the model was taken from the VB packing experiments. The characteristic diameter was determined as position on the particle size distribution curve at the cumulative probability of less than 0.368.

Table 24. Properties of southern aggregates used in packing models

Aggregate Type	Specific Density	Eigenpacking degree		Characteristic diameter, mm (in.)
		compact	loose	
C1	2.730	0.57	0.49	14.1 (0.55)
I1	2.684	0.58	0.50	10.0 (0.39)
F1	2.566	0.74	0.65	0.87 (0.03)

Table 25. Properties of northern aggregates used in packing models

Aggregate Type	Specific Density	Eigenpacking degree		Characteristic diameter, mm (in.)
		compact	loose	
C2	2.706	0.6231	0.5498	13.3 (0.52)
I2	2.659	0.6636	0.5777	8.4 (0.33)
F2	2.563	0.7068	0.6385	0.83 (0.03)

Figure 32 to *Figure 34* demonstrate a binary representation for packing degree of the southern aggregates, and *Figure 35* to *Figure 37* demonstrate the binary representation for northern aggregates, based on Aim and Toufar models.

Figure 38 demonstrates the ternary packing degree based on the Toufar model for both southern and northern aggregates.

As demonstrated for binary blends C1-F1, I1-F1, C2-F2, and I2-F2 (*Figure 32* to *Figure 34)* the maximum packing based on the Aim model occurs at a slightly higher fine material content than the maximum packing determined by the Toufar model. The maximum experimental packing, however, occurs in coarser blends as predicted by both models for C1-F1, I1-F1, C2-F2, and I2-F2 binary blends.

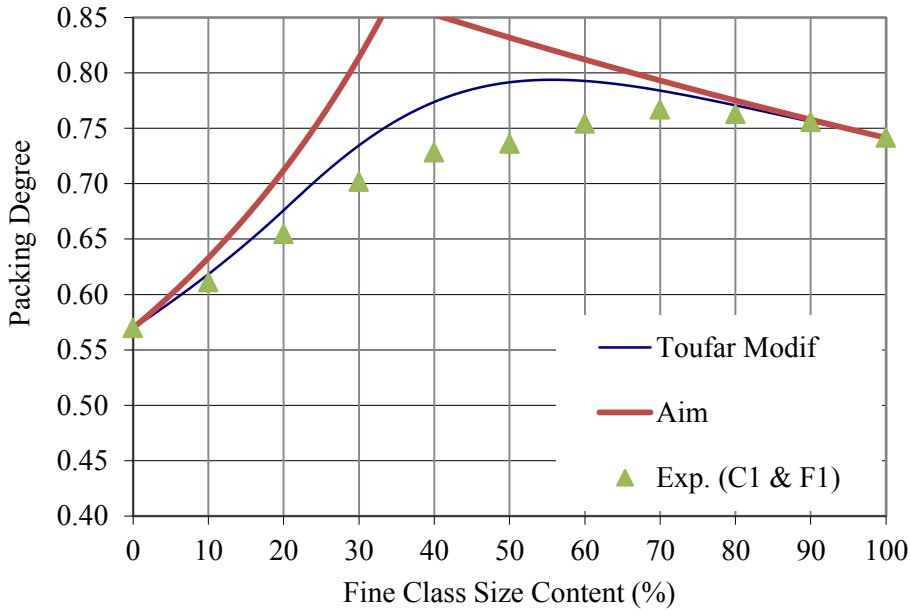

Figure 32. The Packing degree based on Toufar and Aim model vs. experimental results for binary blends of C1 and F1

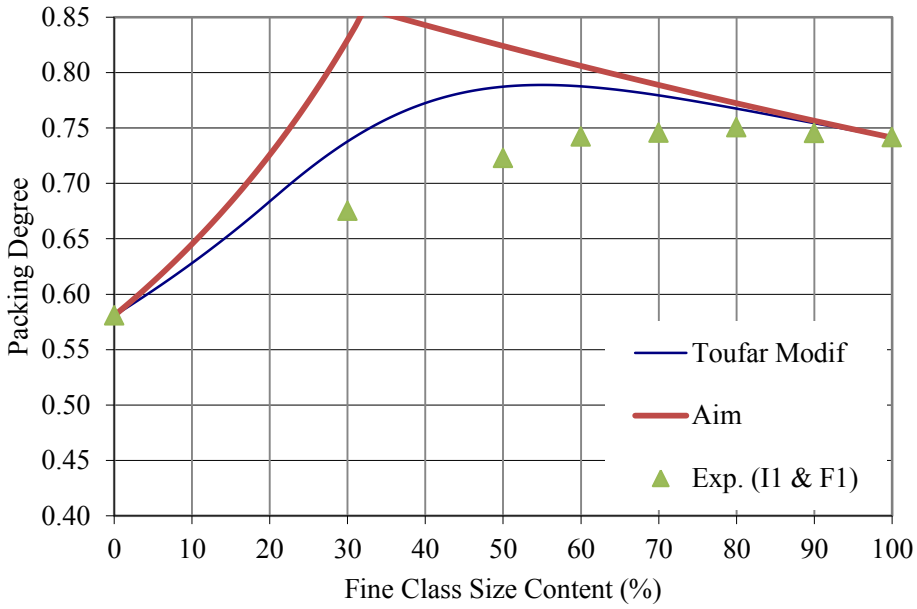

Figure 33. The performance of Toufar and Aim model vs. packing degree of binary blends of I1 and F1

In comparison to experimental packing, the Aim model overestimates the packing degree by about 10% at the vicinity of maximum packing for C1-F1, I1-F1, C2-F2, and I2-F2 binary blends. The Toufar model, on the other hand, closely follows the experimental trend observed for both southern and northern aggregates.

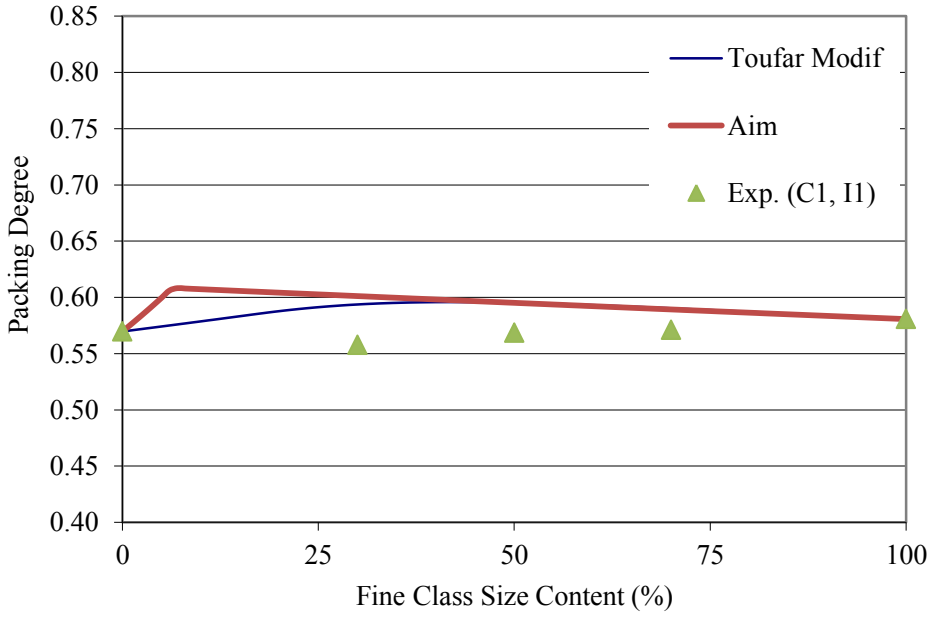

Figure 34. The performance of Toufar and Aim models vs. packing degree of binary blends of C1 and I1

The maximum packing prediction from the Toufar model is about 5% different from the experimental results for southern aggregate blends C1-F1 and I1-F1 (as illustrated by *Figure 32* and *Figure 33*). For northern aggregate blends C2-F2 and I2-F2 the Toufar model prediction of maximum packing, 80%, is only 3% different from the experimental packing results (*Figure 35* and *Figure 36*).

The packing degree for the binary blends of fine and coarse southern aggregates tends to increase with an increase in fine content up to 70%, where the Toufar model

predicts the maximum packing degree at 55% (*Figure 33*). A similar trend can be observed for the binary blends of intermediate and fine southern aggregates as illustrated in *Figure 34*. *Figure 35*. illustrates that the packing degree for binary blends of fine and coarse northern aggregates tends to increase with the increase in fine material content up to 60%, where the Toufar model predicts the maximum packing degree at 45%. A similar trend was observed for binary blends of intermediate and fine northern aggregates as illustrated in *Figure 36*.

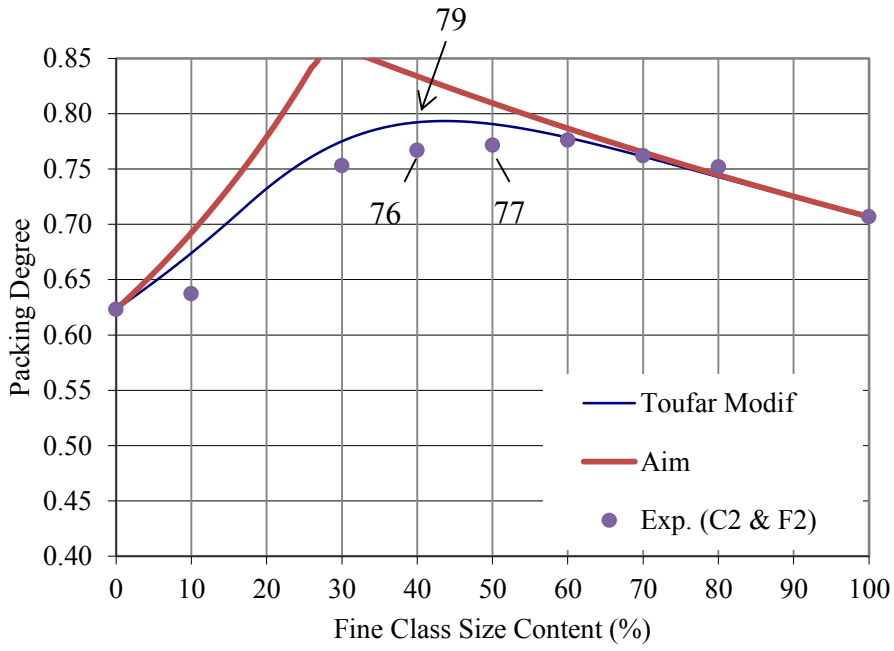

Figure 35. The performance of Toufar and Aim model vs. packing degree of binary blends of C2 and F2

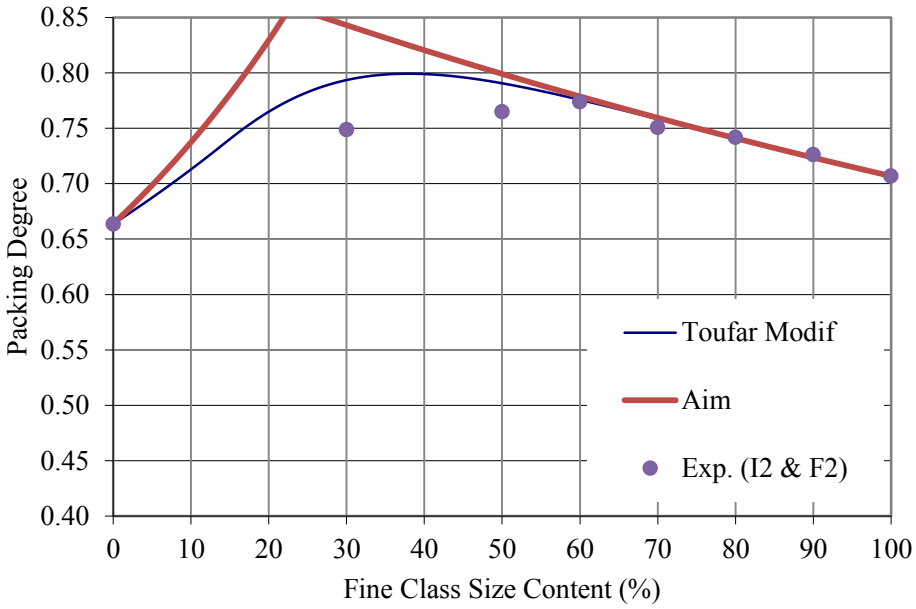

Figure 36. The performance of Toufar and Aim model vs. packing degree of binary blends of I2 and F2

Figure 37 reports on the packing degree for ternary blends of fine, coarse and intermediate aggregates for southern and northern aggregates based on the Toufar model. Comparing *Figure 37* with *Figure 30* and *Figure 31* demonstrates the difference between the locations of blends with maximum packing for both types of aggregates. For southern blends the maximum experimental packing degree of about 75% to 76% occurs at 55% to 60% of fine aggregates and 0 % to 10% of intermediate aggregates. The Toufar model predicted the maximum packing degree of 79% at 55% fine aggregates and 20% intermediate aggregates.

For northern aggregate blends, the maximum packing degree of about 78% was realized for blends with a range of fine aggregates from 40% to 60% and intermediate aggregates from 0% to 20%; these observations are close to the maximum packing degree

by Toufar model of 81% for blends with 40% fine aggregates and 20% intermediate aggregates. As a result, Toufar model provides an excellent estimate for the optimized aggregate blends in terms of compositions and packing degree.

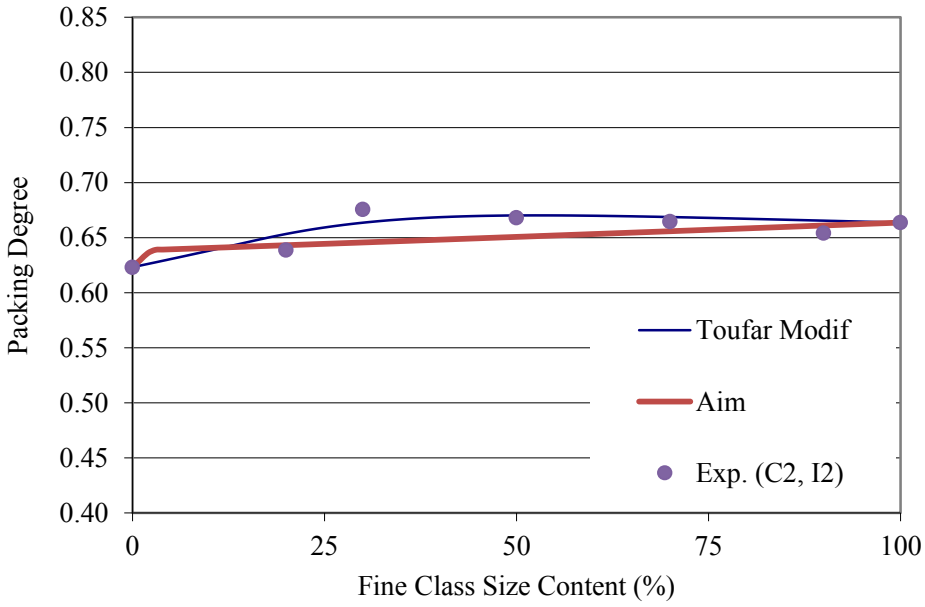

Figure 37. The performance of Toufar and Aim model vs. packing degree of binary blends of C2 and I2

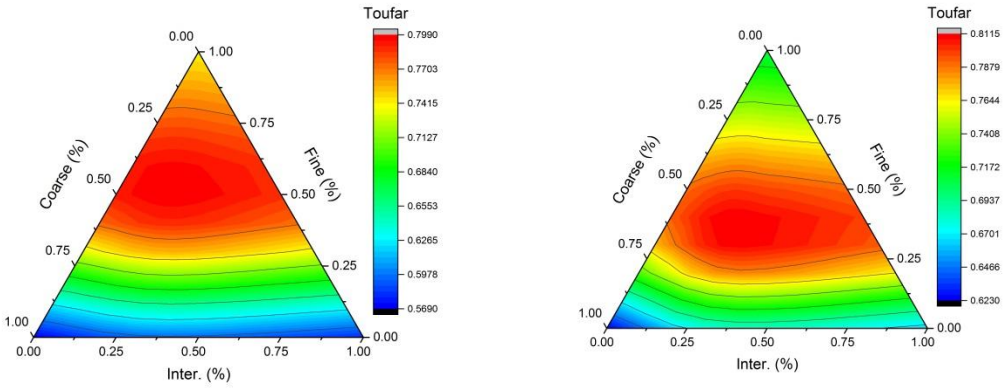

a) *b)*

Figure 38. Toufar models for a) southern aggregates and b) northern aggregates

For southern blends, the experimental packing test suggested using 55% fine aggregates with 0% to 20% intermediate aggregates (*Table 22*). The mechanical performance, on the other hand, supports the use of the blend with 52.5% of fine and 10% of intermediate aggregates. The workability of concrete mixtures was similar for the compositions with 50% to 55% of fine aggregates and up to 10% of intermediate aggregates; the mixtures with intermediate aggregates had a better cohesiveness compared to binary mixtures, which had some segregation. As a result, the optimal blends proposed for the southern aggregate concrete contained 50% of fine, 10% of intermediate, and 40% of coarse aggregates.

For northern aggregates the packing experiment suggested the use of 40% to 60% fine and 0% to 20% intermediate aggregates (*Table 22*). The mechanical performance suggests the use of the blend with 40% fine and 10% intermediate aggregates. The workability of concrete was similar for mixtures with 35% to 40% of fine and up to 10% of intermediate aggregates. The mixtures with intermediate aggregates had a better cohesiveness compared to binary mixtures. As a result, the blends selected for northern aggregate based concrete contained 40% of fine, 10% of intermediate, and 50% of coarse aggregates.

4.3.3. The Application of Packing Simulation Model

Two combinations were selected for 3D packing simulation with an initial separation coefficient of 5 and 10 *(Figure 39b),* corresponding to realistic packing arrangements of compacted aggregates. These compositions were developed to achieve the best PSD fit to 0.7 (Fit 1) and 0.45 (Fit 2) power curves. This was realized by the

selection of input variable parameters of simulation: a reduction coefficient, K_{red} of 1.01, initial separation, K_{del} of 5 and 10, and step of separation, S of 1.025 which provided target particle size distributions as illustrated by *Figure 39b*. The resulting packing degree of 74.5% and 78.8% for 0.7 and 0.45 power curves, respectively, and the corresponding square errors are given in *Table 22*. In the 3D models, realistic packing can be achieved with a step of separation higher than the reduction coefficient. The experimental blends of southern aggregates corresponding to the best fit to 0.7 and 0.45 power curves and the associated aggregate combinations are presented in *Figure 39b* and *Table 22*, which compares the packing degrees and other parameters obtained by the simulation and experiment. Furthermore, *Table 23* represents the experimental results corresponding to northern aggregates.

Among 16 concrete mixtures based on southern aggregates and 10 mixtures with northern aggregates, the experimental mixtures with the best fit to 0.7 and 0.45 power curves were selected. In southern (S) mixtures, the binary mixture S1 has the best fit to the 0.7 power curve and mixture S13 produced with 50% fine aggregates corresponds to the 0.45 power curve. Other mixtures, such as S8, can be considered to be close to the 0.45 power curve, but have a slightly higher deviation compared to mixture S13. For northern (N) mixtures, the binary mixture N1 has the best fit to the 0.7 power curve, and mixture N7 with 45% fine aggregates can be described by the 0.45 power curve. The real world aggregate combinations would fall in between 0.7 and 0.45 power distributions as boundary limits. Other mixtures such as N3 and N9 are also close to the 0.45 power distribution, but these have a slightly higher deviation when compared to N7.

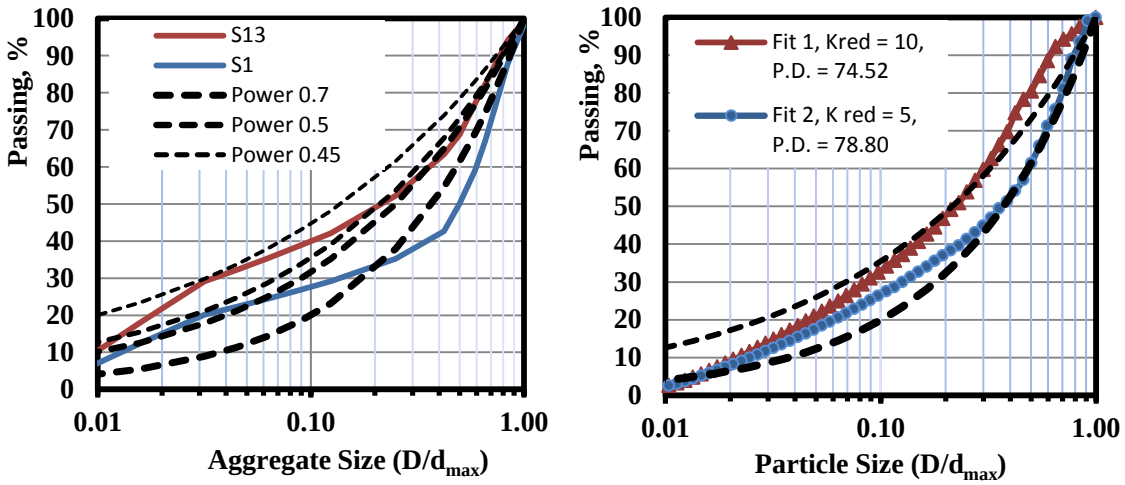

Figure 39. The normalized PSD corresponding to a) the best fit to experimental blends and b) the output of 3D packing simulation

The use of simulation algorithm provides the PSD suitable for the desired power curve which can be correlated to the particular type of concrete. The simulation with realistic parameters such as number of particles, packing trials and reduction coefficients can then be used for the spatial representation of various aggregate blends. *Table 22* and *Table 23* provide the difference between the errors and standard deviation for simulated and experimental compositions. As it appears from *Figure 39 b*, "Fit 1" (corresponding to mixtures S13, N7, and the 0.45 power distribution) has a higher error and standard deviation than "Fit 2", corresponding to mixtures S1, N1, and a 0.7 power distribution. Simulated compositions have an S shape PSD converging to a 0.7 power curve at diameters smaller than $0.02D_{max}$, mainly due to the limited number of small particles, whereas the experimental mixtures have a reverse S shape imposed by the PSD of individual components.

The use of lower initial spacing results in the fitting of particles with larger diameters (Fit 2). The packing degrees obtained by the simulation are higher than those corresponding to experimental blends. This can be explained by the irregularities in the real aggregates including the shape vs. the use of idealized spheres as well as a better particle positioning achieved by simulation.

4.3.4. Gradation Techniques: the use of Particle Size Distribution

The selection of the best power curve for the optimized aggregate blends was performed using the least standard deviation. The exponent n that generates the least square error from the aggregate's combined PSD is reported in *Table 22* for southern aggregates and *Table 23* for northern aggregates. The square error from the suggested power curve (PC) is an important parameter to evaluate the best fit distribution. As expected, the blends with finer PSD can find a better fit to the smaller exponents in a range that varies from 0.36 to 0.7 for both types of aggregates. In addition to square error, other statistical parameters including standard deviations were calculated and reported in *Table 22* and *Table 23*. Furthermore, the normalized root of mean square error (NRMSE) is calculated as follows:

$$NRMSE\ (\%) = \frac{RMSE}{e_{max} - e_{min}} * 100 \qquad (42)$$

where, e_{max} and e_{min} are the maximum and minimum errors (deviations) from the associated power curve, respectively.

The NRMSE takes into account the maximum and minimum deviations from the PC as well as the root mean square error. The correlation between the NRMSE and both loose and compacted packing degree indicates the relationship between the deviation

from the power curves and the experimental packing degree. For a given composition, the best fit can be associated with either lower RMSE from the curve or a lower difference between the maximal and minimal errors. The best fit blend, therefore demonstrates the lowest errors and highest NRMSE.

Figure 40 and *Figure 41* illustrate the PSD for coarsest and finest mixtures obtained at different levels of IA and provide the range for practical mixtures. The use of IA assists in shifting the coarsest and finest mixtures to the middle zone confined by the 0.45 and 0.7 power curves as observed southern and northern aggregates.

4.3.5. Performance of Concrete Mixtures

Sixteen mixtures with different combined aggregate gradations (and different packing degrees) were tested to determine the effect of aggregate proportions on fresh properties and mechanical performance of concrete as summarized in *Table 22* for southern aggregates. Similar tests were conducted on ten mixtures for northern aggregates (*Table 23*). The workability of fresh concrete is affected by many parameters, such as air content, aggregate surface area and also the volume of fines. Cement paste volume was held constant by holding the W/C ratio and cement content constant.

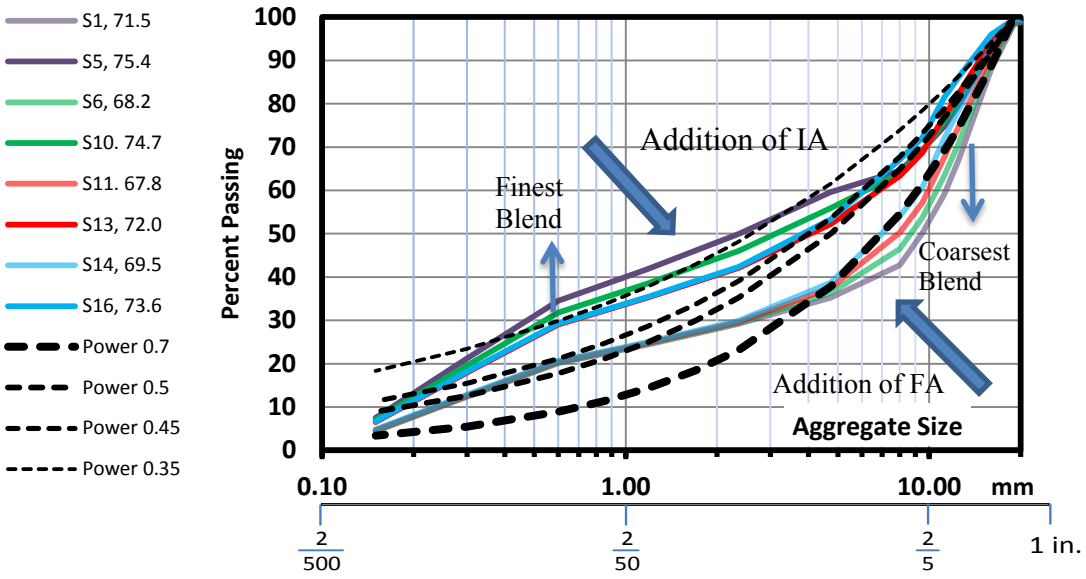

Figure 40. The PSD corresponding to investigated southern aggregate blends

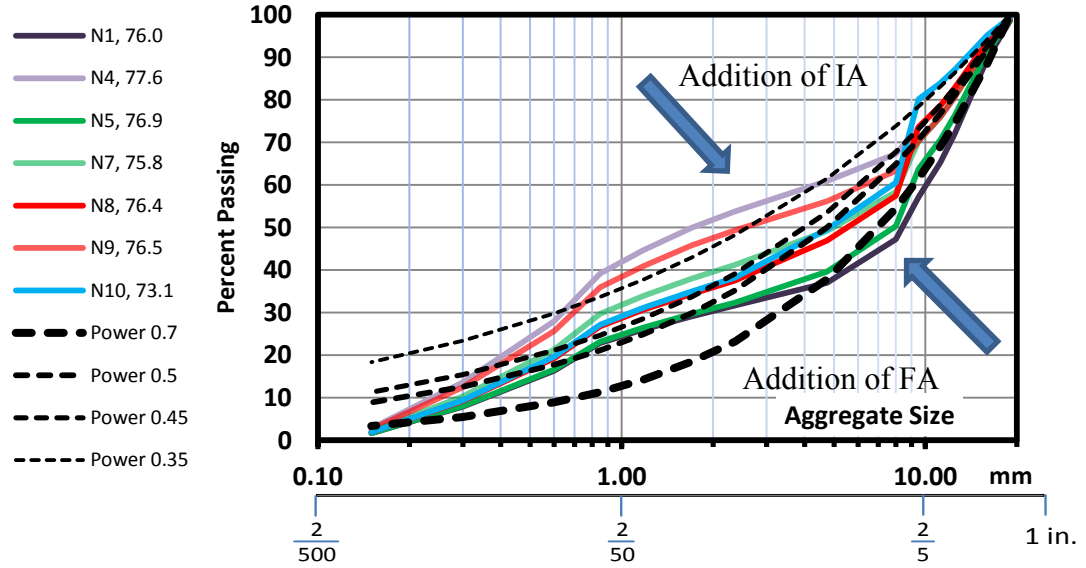

Figure 41. The PSD corresponding to investigated northern aggregate blends

All mixtures were produced without air entraining admixture in order to minimize the contribution of air. Therefore, all the mixtures listed in the *Table 22* and *Table 23* had the same aggregate volume, W/C ratio, and cement content, but different combined aggregate gradings. The mixtures were produced at a relatively high water to cement ratio of 0.6 for southern aggregate and 0.53 for northern aggregate blends in order to provide sufficient workability, which is important for the detection of differences in performance.

4.3.6. Coarseness Chart

The coarseness factor (CF) and workability factor (WF) were defined by Shilstone [113]. The Shilstone chart *(Figure 43)* correlates the individual and cumulative passing of certain aggregate sets and cement content. The WF is controlled mainly by the fine aggregate content and the CF is controlled by the ratio of fine aggregates to combined fine and intermediate aggregate groups. The effect of intermediate and fine aggregates on CF and WF is illustrated by *Figure 42* and *Figure 43.* A sharp increase in WF and a gradual decrease in CF, due to the replacement of coarse aggregates with sand at different levels of IA, can be observed in *Figure 42* for a range of mixtures, including mixture sequences S1...S5, S6...S10, S11...S13, and S14...S16. This is due to the increase in percent passing the 2.36 mm (#8) sieve, which is mostly controlled by the volume of fine aggregates.

The addition of intermediate aggregates leads to the improvement of CF in some blends, but has a negligible effect on the WF. The improvement of CF is more pronounced at a higher fine aggregate content. As cumulative percent retained on the 9.5 mm (3/8") sieve is decreasing at a higher rate with the addition of sand (for example, S4, S8, S13, S16 mixture sequence), the cumulative percent retained on the 2.36 mm sieve (#8) does not change throughout the IA replacement. The cumulative percent passing on the 9.5 mm (3/8") sieve increases faster and the cumulative percent retained on the 9.5 (3/8") mm sieve decreases faster when there are more fine aggregates in the mix. This effect is observed in mixes with similar sand content such as represented by the sequences from S1 to S14, S2 to S15, and S4 to S16 observed on the row of the Shilstone chart, *Figure 42*.

All the mixtures with up to 50% sand were able to reach Zone II-5, which is desirable for concrete with low cement content such as those used for typical pavement operations. However, from the workability standpoint, Zones II-2 and II-3 can be more desirable for slip-form concrete; those mixtures (e.g., S2) prone to low cement content and reduced paste volume can provide the robust performance required in the field. The replacement of coarse aggregates with intermediate aggregates provides a horizontal shift of the mixtures to lower CF and higher WF value, enabling the concrete mix to pass the cautious workability "0" band towards a sandy subzone of Zone II. In this way, the chart can be used to verify and tune the performance of low cement concrete with different aggregate blends.

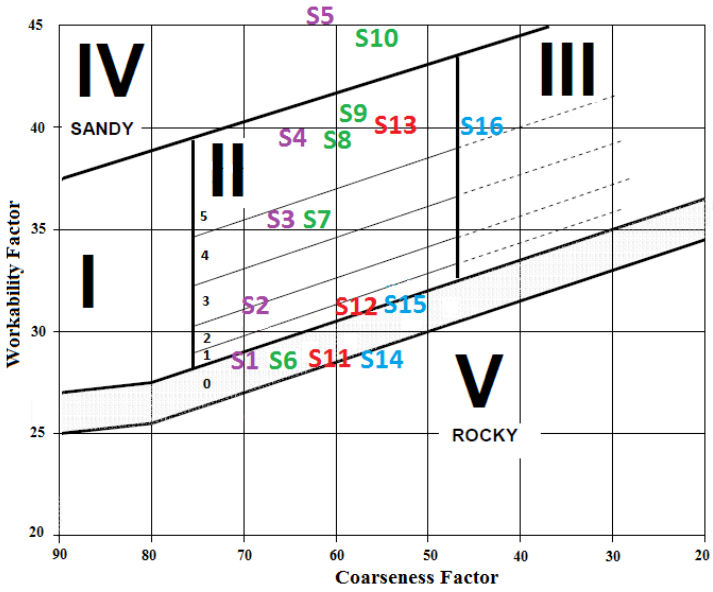

Figure 42. Coarseness chart for southern aggregate mixtures, based on [23, 113]

The use of 40% to 50% fine aggregates improves the particle to particle contacts in the mixtures and reduces the coarseness factor compared to mixes with 35% of FA (e.g., for southern aggregate mixtures S1, S6, S11, and S14). The mixes that appear

between the Subzone 2 and 5 of Zone II are considered ideal for slip-form paving, but may require the use of higher quantities of fine aggregates. The mixtures in this zone such as S8 and N7 can be beneficial for application in low cement concrete pavements.

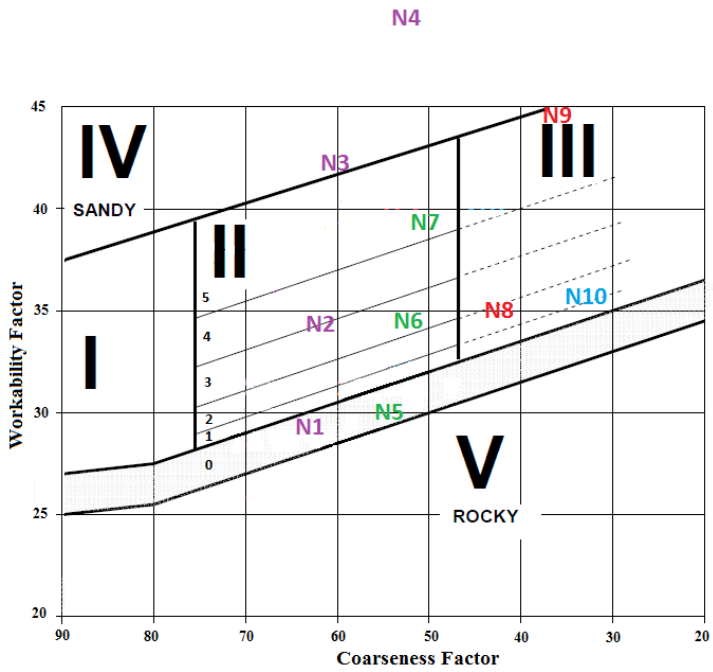

Figure 43. Coarseness chart for northern aggregate mixtures, based on [23, 113]

4.3.7. The Evaluation of Concrete Mixtures

Table 22 and *Table 23* demonstrate the results related to experimental packing of aggregate blends, the statistical deviation from the corresponding power curve for the mixtures, concrete strength, and other performance characteristics for southern and northern aggregate based concrete. The entrapped air content was less than 2% for almost all mixtures, providing little interference with the relationships observed. As demonstrated for each level of IA, the mixtures with minimal square error from power curve result in the highest strength as demonstrated for both types of southern and northern aggregates. As it was demonstrated by the experimental packing of aggregate

blends, a lower deviation from the power curve represents better packing degrees. This verifies that high density mixtures are achievable with different power curves.

The correlation between the 7-day and 28-day compressive strength and aggregate packing degree is demonstrated by Figure 44 for southern aggregate concrete. The highest correlation was found to be between the loose packing degree and 7-day compressive strength for southern aggregates. In addition, the correlation with R^2 of 0.95 between the loose and compacted packing was demonstrated for southern aggregates (*Figure 30b*). The correlation between 7-day and 28-day compressive strength and aggregate packing was not established for northern aggregate concrete. One reason for this may be that with the use of a relatively narrow range of blends (between 30% to 60% of fine aggregates and 0% to 20% of intermediate aggregates) such correlation may be difficult to establish. In this way the most of the investigated aggregate blends have already reached a very high packing degree.

For concrete based on southern aggregates the experimental results demonstrate that a mixture with 50% fine aggregates had a higher compressive strength than concrete with lower sand content (except for the ternary mixes with 10% IA). At a relatively low cement content of 280 kg/m^3 (470 lb/yd^3), higher volumes of fine aggregates are required for better packing (Table 22) and the requirement for an additional volume of fine materials to fill the voids in coarse aggregates is better addressed.

For concrete based on northern aggregates, the experimental results demonstrate that a mixture with 40% of fine aggregates had a higher compressive strength than concrete with other contents of sand. For optimal performance at a relatively low cement

content of 280 kg/m^3 (470 lb/yd^3) the blends with at least of 40% of fine aggregates are required, *Table 23*.

Figure 44 demonstrates that southern aggregate mixtures with the highest strength are located in Zone II-5. For the level of cement content of 280 kg/m^3 (470 lb/yd^3), this zone seems to be a suitable area; however, zones II-2 and II-3 are known to be excellent for concrete with low cement content (in the range of 310 to 350 kg/m^3) intended for application in the pavements. The improvement in strength observed for the S1 to S5 mixture sequence, and similarly, for other concrete mixtures with different contents of IA, is directly proportional to the improvement of coarseness and workability factors as demonstrated by *Figure 45* and *Table 22*.

Figure 45 demonstrates that concrete based on northern aggregates with the highest strength are mostly located in Zone II. For the level of cement content of 280 kg/m3 (470 lb/yd3), there is a lower need for sand proportion (~40%) when northern aggregates are specified.

Binary southern aggregate blends had a better packing vs. mixtures with 20% and 30% of IA; however, concrete based on ternary blends achieved higher compressive strength as presented in *Table 22*. The highest compressive strength was achieved in composition with 10% of IA matching the experimental packing tests. Some binary northern aggregate blends had a better packing vs. mixtures with IA. The concrete based on binary blends had a higher compressive strength at 50% of sand and for the highest ternary blends compressive strength was achieved at 40% of sand (*Table 23*).

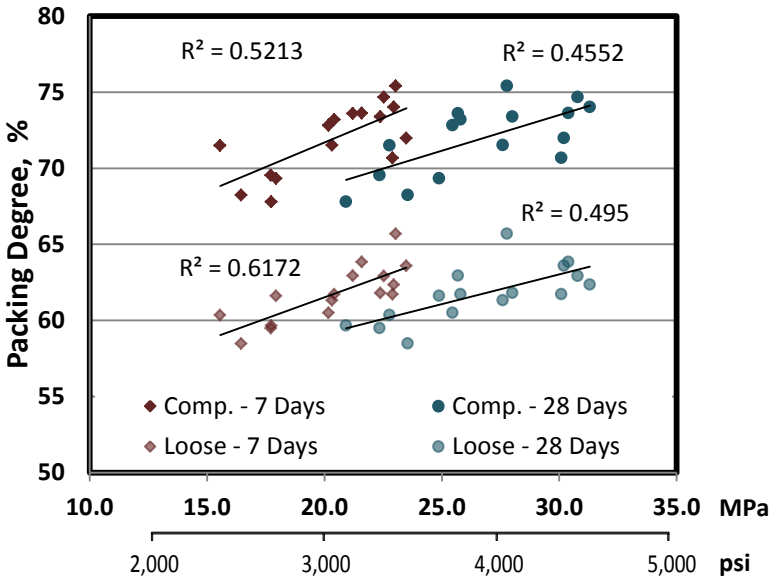

Figure 44. The correlation between the concrete compressive strength and packing degree for southern aggregate compositions

For both types of aggregates, the density of fresh mixtures was decreased due to the addition of sand. Concrete mixtures with sand content ranging between 45% to 50% for southern- and 40% to 50% for northern- aggregate blends had better workability than achieved by other mixtures outside these limits. Concrete mixtures with 45% and 50% of FA are located in the middle of Zone II of the coarseness chart (S3-S4, S7-S8, S13-14, S15-16), and the mixtures with 40% to 45% of FA (N2, N6-N7, N8) are all located in the middle of the Zone II and the edge of rocky side of Zone III. All the southern aggregate mixtures with 50% FA had the same WF, but the slump of the mixtures with 20% and 30% IA was lower. The same trend was observed at 45% of FA (*Figure 44* and *Table 22*). For northern aggregates, all the mixtures with 40% FA had the same WF (N2, N6, N8, N10); however, the workability was lower for concrete based on ternary aggregate blends. Further research is required to explore the effect of WF and aggregate proportions on workability parameters, including slump.

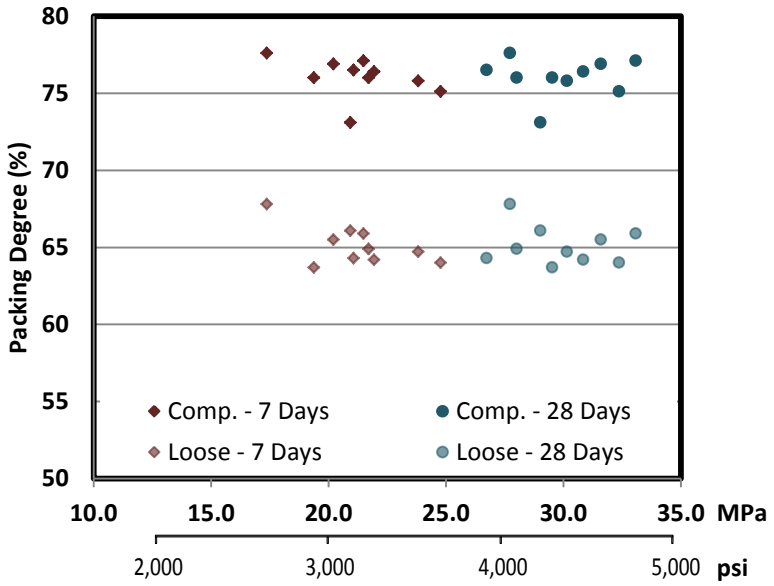

Figure 45. The correlation between the concrete compressive strength and packing degree for northern aggregate concrete compositions

4.4. OPTIMIZATION OF CONCRETE MIXTURES

Concrete mixtures were designed based on a multi-scale procedure using the steps corresponding to evaluation of admixtures and optimization of aggregates. The concrete mixtures, therefore, were designed with the best admixture and aggregate combinations selected using the results of preliminary investigation considering the admixture compatibility, effect of SCM, the desired PSD of aggregates, packing degree, coarseness factor and performance in concrete (best strength and workability). Specifically, the benefit of aggregate optimization was to obtain an optimal structure resulting in improved strength, overall performance and potential reduction of cementitious materials.

4.4.1. The Optimization of AE Admixtures

The purpose of preliminary concrete investigation was to identify the dosage of AE admixture required to achieve suitable air content and required workability. All preliminary mixtures based on southern aggregates were tested for compressive strength at 7 and 28 days to ensure that the required strength levels are achieved. For this research, the effects of plasticizer, superplasticizer, and AE admixture to achieve the required levels of workability were investigated. To optimize the dosage of admixtures, the lowest desirable W/CM ratio that meets the specification requirements for slump of 50 - 100 mm (2 - 4 in.) was selected. Other target parameters were: 7 ±1.5% air content, and early (7 day) compressive strength of 20 MPa (3,000 psi). In this research, the cement content was varied at two levels of 280 kg/m^3 (470 lb/yd^3) and 250 kg/m^3 (420 lb/yd^3). However, the AE admixture optimization study was performed on preliminary mixtures with 280 kg/m^3 (470 lb/yd^3) and southern aggregates.

The design of concrete mixtures was based on the best aggregate blends. The cement content of 280 kg/m^3 (470 lb/yd^3) was determined as 18% reduction from current WisDOT specifications (570 lb/yd^3 as required for general use in concrete pavements and structures). The W/CM ratio was then defined based on the results of preliminary study and admixtures optimization. For most of the mixtures, the lowest possible W/CM ratio was adjusted in 0.05 increments. This approach provided ranking of admixtures and helped to identify the beneficial combinations. The volumes of the cement paste (cementitious materials and water), admixtures, and tentative air content of 6% were subtracted from the total volume of the mix based on the absolute volume method. Based on the optimal proportions, the remaining volume of aggregates was then split between the coarse, intermediate, and fine aggregates. Four sets of experiments were conducted for concrete mixtures based on optimal proportion of southern aggregates including plain concrete mixtures (without any SCM), with Class F fly ash, Class C fly ash, and slag cement as reflected by *Table 26*, *Table 28*, *Table 30* and *Table 32*.

The fresh and hardened properties of preliminary study mixtures including reference mixtures, with Class F fly ash, Class C fly ash, and slag cement are presented in *Table 29*, *Table 31* and *Table 33*, accordingly. All the mixtures were compared with the plain reference mixture CM 64 (L-S-M) produced without mid-range plasticizer (WR) and without any air-entraining admixture. For each set of mixtures, three different water-reducing products were used. These three admixtures were mid-range plasticizer, SNF, and PCE type admixtures *(Table 9).* The SP admixtures were used to achieve the required air and slump parameters at the lowest W/CM ratio with the goal of obtaining optimal mechanical performance. Here, the higher compressive strength can be achieved at lower

W/CM ratio; however, low W/CM ratio may result in impractical workability levels and poor compaction.

For reference mixtures with plasticizer (mid-range water reducing admixture) SCM, the mixture CM69 obtained the required performance in terms of air content of 8.2% and slump of 45 mm (1.8 in) as demonstrated by *Table 26* and *Table 27*. The compressive strength of CM69 was lower than that of the reference CM64 because of the incorporation of an additional air. The use of a mid-range plasticizing admixture can assist in the reduction of W/C ratio and provide the slump at almost the same levels as demonstrated by plain mixtures. For compositions with PCE admixtures, CM79 achieved the optimal performance with 4.4% air content and 44 mm (1.8 in.) slump. The compressive strength was similar to the reference concrete (CM64), especially at early ages. Even at 10% reduction of W/CM ratio (0.48 vs. 0.38), the slump of CM79 was almost equal to the reference, indicating the superior qualities of PCE admixtures in terms of workability enhancement and W/C ratio reduction. For concrete with SNF admixtures, the mixture CM101 achieved the optimal performance at 5.8% air content and 65 mm (2.6 in.) slump. Even with the reduction of W/C ratio to 0.44, the slump of this concrete is equal to the reference mix, indicating desirable performance. At early ages the compressive strength of CM101 concrete was reduced, but at 28 days, it was very similar to the strength of the reference. Compared to the reference mixture CM64, concrete with PCE (CM79) had very similar strength at early ages, and concrete with SNF (CM101) reached the reference strength benchmark at 28 days, *Table 27*.

Table 28 and *Table 29* represent the mix designs and the test results for concrete mixtures with Class F fly ash used at 30% of portland cement replacement level. For

concrete mixtures with mid-range admixture, CM72 obtained the required performance in terms of air content of 4.5%. The slump of 10 mm (0.4 in.) was lower than required and, therefore, higher W/CM must be used for the design of the final mixture. The compressive strength of this concrete was reduced versus the reference mixture CM64 (without AE), mainly because of the effect of Class F fly ash. The concrete mixture CM108 achieved the optimal performance with 5.8% air content and 130 mm (5 in.) slump at a reduced W/C ratio of 0.38. Even at a reduced W/CM ratio, the slump of CM108 is double that of the reference, indicating the desirable benefits of PCE admixtures in terms of providing a better workability and reduction of W/CM ratio. The increase in slump from 40 mm (1.6 in.) for mixture (CM79) with no SCM to 130 mm (5.1 in.) for CM108 concrete with Class F fly ash can be explained by the ball bearing effect of fly ash and also the incorporation of an additional air. The compressive strength was lower at all tested ages due to the addition of Class F fly ash and slowed pozzolanic reaction. Concrete with SNF admixtures, CM71 achieved the optimal performance demonstrating 6.5% air content and 90 mm (3.5 in.) slump. Still, the compressive strength of CM71 was lower than that of the reference. Compared to reference CM64, the concrete mixture with PCE (CM108) had a very similar performance at 7-day and 28-day ages. This proves that the effective use of Class F fly ash requires the application of PCE and adjustment of air content to reduce the W/CM and to achieve the desirable strength development.

Table 30 and *Table 31* demonstrate the mix designs and test results for concrete with Class C fly ash used at 30% portland cement replacement level. These mixtures demonstrated superior performance. Concrete compositions with mid-range plasticizer

CM84 obtained the required performance in terms of air content of 7.5% and slump 50 mm (2 in.). Even at higher air content, the compressive strength of CM84 was very similar to the reference CM64 at 7-day age and exceeded that of the reference at later ages. The beneficial properties of Class C fly ash can be used to enhance the workability of concrete. For concrete mixtures with PCE admixtures, CM103 achieved the optimal performance at air content of 7% and slump of 95 mm (3.7 in.) which were realized at a reduced W/CM ratio of 0.33. The increase in slump, from 40 mm (1.6 in.) to 95 mm (3.7 in.) compared to plain mixture with PCE (CM79), can be explained by incorporation of additional air (2.6% extra) and by the beneficial effects of Class C fly ash. Also, the improved performance can be correlated to the synergic effect of PCE admixture and Class C fly ash demonstrating perfect compatibility between these components. In spite of higher air content and due to extreme reduction of W/CM ratio, the 7-day and 28-day compressive strength of this concrete was very high compared to the reference (*Table 27*). For Class C fly ash concrete with SNF admixtures, CM85 achieved the optimal performance at a reduced W/CM ratio resulting in an air content of 7.5% and slump of 70 mm (2.8 in.). The compressive strength of CM85 concrete was similar to the reference and the workability was higher. Compared to the reference CM64, the PCE based concrete (CM83) has achieved up to 20% higher compressive strength at all ages. This proves that the use of PCE admixtures with Class C fly ash can provide superior performance in terms of workability and strength development. *Table 32* and *Table 33* represent the mix design and the test results for concrete mixtures with slag cement used at 50% level replacement. These mixtures had a superior performance. For mixtures with mid-range admixture, the CM86 concrete obtained the required fresh properties in terms

of air content of 6% and slump of 59 mm (2.3 in.). The compressive strength of slag concrete was slightly reduced vs. the reference at both ages due to the relatively high portland cement replacement level of 50%. The compressive strength of CM86 was slightly higher than the reference CM64. Chemical composition and compatibility of slag and portland cement had a great contribution to mechanical performance enabling the reduction of W/CM ratio to 0.38. The PCE based concrete CM89 achieved the optimal performance with slightly reduced air content of 3.5% and slump of 50 mm (2 in.). Due to the similarity between the portland cement and slag in terms of superplasticizer absorption, the slump values remain close to the reference portland cement mixtures produced with corresponding admixture. The slag cement is activated in an alkali environment, which is the case for the slag blends with portland cement. As a result, CM89 concrete with slag had even higher 28-day strength vs. reference concrete CM64. For SNF concrete, CM77 achieved the optimal performance with air content of 6% and slump of 68 mm (2.7 in.). The workability of this concrete was very similar to the reference, but was achieved at a lower W/C ratio of 0.43. This type of concrete had a compressive strength similar to the reference.

Table 26. Mixture proportions used for preliminary concrete mixtures based on portland cement

a) SI Units

Type		**Dosage of Chemical Admixtures, %**				**Mixture Proportioning, kg/m^3**								W/CM	Yield
		PCE	SNF	MR	AE	Cement	Aggregates (SSD), CA	IA	FA	Total AGG	SP	Air Entraining Admixtures	Total W		
L-S-M	CM64			0.15	0.000	280	801	198	955	1954	1.038	0.000	133	0.48	0.98
L-S-M	CM81			0.20	0.010	280	749	185	893	1828	1.384	0.227	122	0.44	1.04
L-S-M	CM65			0.15	0.008	280	816	202	973	1991	1.038	0.181	118	0.42	1.03
L-S-M	CM57			0.20	0.015	280	816	202	972	1990	1.384	0.340	119	0.43	1.08
L-S-M	CM69			0.15	0.010	280	816	202	973	1991	1.038	0.227	118	0.42	1.03
L-S-P	CM66	0.15			0.010	280	816	202	973	1991	1.230	0.227	119	0.43	1.02
L-S-P	CM100	0.15			0.020	280	765	189	912	1866	1.230	0.453	107	0.38	0.97
L-S-P	CM96	0.20			0.020	280	765	189	911	1865	1.641	0.453	107	0.38	0.94
L-S-P	CM79	0.15			0.0150	280	765	189	912	1866	1.230	0.340	107	0.38	0.94
L-S-N	CM68		0.40		0.020	280	814	201	970	1985	2.768	0.453	120	0.43	1.01
L-S-N	CM80		0.50		0.02	280	746	184	890	1821	3.460	0.453	123	0.44	0.99
L-S-N	CM83		0.40		0.015	280	763	189	909	1861	2.768	0.340	108	0.39	0.95
L-S-N	CM91		0.50		0.015	280	762	188	908	1859	3.460	0.340	108	0.39	0.96
L-S-N	CM97		0.60		0.015	280	761	188	907	1856	4.152	0.340	109	0.39	0.94
L-S-N	CM101		0.40		0.015	280	747	185	891	1823	2.768	0.340	123	0.44	0.94

b) US Customary Units

Type		Dosage of Chemical Admixtures, %				Mixture Proportioning, lb/yd^3								W/CM	Yield
						Cement	Aggregates (SSD)			Total AGG	SP	Air Entraining Admixtures	Total W		
		PCE	SNF	MR	AE		CA	IA	FA						
L-S-M	CM64			0.15	0.000	470	1762	436	2101	4299	2.28	0.00	293	0.48	0.98
L-S-M	CM81			0.20	0.010	470	1648	407	1965	4022	3.04	0.50	268	0.44	1.04
L-S-M	CM65			0.15	0.008	470	1795	444	2141	4380	2.28	0.40	260	0.42	1.03
L-S-M	CM57			0.20	0.015	470	1795	444	2138	4378	3.04	0.75	262	0.43	1.08
L-S-M	CM69			0.15	0.010	470	1795	444	2141	4380	2.28	0.50	260	0.42	1.03
L-S-P	CM66	0.15			0.010	470	1795	444	2141	4380	2.71	0.50	262	0.43	1.02
L-S-P	CM100	0.15			0.020	470	1683	416	2006	4105	2.71	1.00	235	0.38	0.97
L-S-P	CM96	0.20			0.020	470	1683	416	2004	4103	3.61	1.00	235	0.38	0.94
L-S-P	CM79	0.15			0.0150	470	1683	416	2006	4105	2.71	0.75	235	0.38	0.94
L-S-N	CM68		0.40		0.020	470	1791	442	2134	4367	6.09	1.00	264	0.43	1.01
L-S-N	CM80		0.50		0.02	470	1641	405	1958	4006	7.61	1.00	271	0.44	0.99
L-S-N	CM83		0.40		0.015	470	1679	416	2000	4094	6.09	0.75	238	0.39	0.95
L-S-N	CM91		0.50		0.015	470	1676	414	1998	4090	7.61	0.75	238	0.39	0.96
L-S-N	CM97		0.60		0.015	470	1674	414	1995	4083	9.13	0.75	240	0.39	0.94
L-S-N	CM101		0.40		0.015	470	1643	407	1960	4011	6.09	0.75	271	0.44	0.94

Table 27. Fresh and hardened properties of concrete mixtures based on portland cement

Type		Slump, mm	Slump, in	Air, %	Fresh Density, kg/m^3	Fresh Density, lb/ft^3	Temp., °F	AGG Vol Ratio	Compressive Strength, MPa		Compressive Strength, psi	
									7 days	28 days	7 days	28 days
L-S-M	CM64	63	2.5	4.0	2440	152	65	0.724	29.5	38.4	4273	5570
L-S-M	CM81	95	3.7	15.0	2180	136	66	0.678	17.6	20.4	2555	2966
L-S-M	CM65	26	1.0	7.0	2350	147	66	0.738	27.5	34.4	3988	4993
L-S-M	CM57	68	2.7	12.0	2231	139	69	0.737	20.3	25.1	2940	3640
L-S-M	CM69	45	1.8	8.2	2338	146	66	0.738	25.1	31.4	3635	4551
L-S-P	CM66	150	5.9	5.4	2375	148	68	0.738	27.0	32.0	3919	4638
L-S-P	CM100	95	3.7	6.5	2341	146	68	0.692	32.8	37.5	4755	5434
L-S-P	CM96	30	1.2	5.0	2415	151	69	0.691	20.9	25.4	3033	3685
L-S-P	CM79	40	1.6	4.4	2432	152	70	0.692	29.1	34.7	4224	5032
L-S-N	CM68	29	1.1	6.2	2392	149	65	0.736	28.8	35.3	4173	5127
L-S-N	CM80	100	3.9	10.0	2271	142	67	0.675	21.2	26.4	3073	3825
L-S-N	CM83	10	0.4	4.8	2404	150	70	0.690	32.5	40.0	4719	5806
L-S-N	CM91	11	0.4	5.5	2375	148	72	0.689	31.9	41.3	4633	5996
L-S-N	CM97	25	1.0	4.7	2415	151	68	0.688	31.3	37.0	4537	5363
L-S-N	CM101	65	2.6	5.8	2406	150	67	0.676	21.7	36.1	3144	5237

** immediately after mixing*

Table 28. Mix design for preliminary concrete mixtures with Class F fly ash

a) SI Units

Type		**Dosage of Chemical Admixtures, %**				**Mixture Proportioning, kg/m^3**									W/CM	Yield
		PCE	SNF	Mid-Range	AE	Cement	AF	Aggregates (SSD)			Total AGG	SP	Air Entraining Admixture	Total W		
								CA	IA	FA						
L-S-M	CM64			0.15	0	280	0	801	198	955	1954	1.038	0.000	133	0.48	0.98
L-S-M-F	CM88			0.15	0.02	195	84	742	183	884	1809	1.038	0.453	122	0.44	0.98
L-S-M-F	CM72			0.15	0.01	195	84	808	200	963	1971	1.038	0.227	119	0.43	1.00
L-S-P-F	CM70	0.15			0.015	195	84	808	200	963	1971	1.230	0.340	119	0.43	1.04
L-S-P-F	CM87	0.15			0.015	195	84	757	187	902	1847	1.230	0.340	107	0.38	0.95
L-S-P-F	CM92	0.15			0.015	195	84	772	191	921	1884	1.230	0.340	93	0.33	1.05
L-S-P-F	CM98	0.20			0.015	195	84	772	191	920	1883	1.641	0.340	93	0.33	0.95
L-S-P-F	CM102	0.10			0.02	195	84	757	187	903	1847	0.820	0.453	107	0.38	0.95
L-S-P-F	CM107	0.10			0.015	195	84	758	187	903	1848	0.820	0.340	107	0.38	0.94
L-S-P-F	CM108	0.15			0.015	195	84	757	187	902	1847	1.230	0.340	107	0.38	0.98
L-S-N-F	CM71		0.4		0.025	195	84	806	199	960	1965	2.768	0.567	120	0.43	1.01

b) US Customary Units

Type		Dosage of Chemical Admixtures, %				Mixture Proportioning, lb/yd^3									W/CM	Yield
		PCE	SNF	Mid-Range	AE	Cement	AF	Aggregates (SSD) CA	IA	FA	Total AGG	SP	Air Entraining Admixture	Total W		
L-S-M	CM64			0.15	0	470	0	1762	436	2101	4299	2.28	0.00	293	0.48	0.98
L-S-M-F	CM88			0.15	0.02	329	184	1632	403	1945	3980	2.28	1.00	268	0.44	0.98
L-S-M-F	CM72			0.15	0.01	329	184	1778	440	2119	4336	2.28	0.50	262	0.43	1.00
L-S-P-F	CM70	0.15			0.015	329	184	1778	440	2119	4336	2.71	0.75	262	0.43	1.04
L-S-P-F	CM87	0.15			0.015	329	184	1665	411	1984	4063	2.71	0.75	235	0.38	0.95
L-S-P-F	CM92	0.15			0.015	329	184	1698	420	2026	4145	2.71	0.75	205	0.33	1.05
L-S-P-F	CM98	0.20			0.015	329	184	1698	420	2024	4143	3.61	0.75	205	0.33	0.95
L-S-P-F	CM102	0.10			0.02	329	184	1665	411	1987	4063	1.80	1.00	235	0.38	0.95
L-S-P-F	CM107	0.10			0.015	329	184	1668	411	1987	4066	1.80	0.75	235	0.38	0.94
L-S-P-F	CM108	0.15			0.015	329	184	1665	411	1984	4063	2.71	0.75	235	0.38	0.98
L-S-N-F	CM71		0.4		0.025	329	184	1773	438	2112	4323	6.09	1.25	264	0.43	1.01

Table 29. Fresh and hardened properties of concrete mixtures with Class F fly ash

Type		Slump, mm	Slump, in	Air, %	Fresh Density, kg/m^3	Fresh Density, lb/ft^3	Temp., °F	AGG Vol Ratio	Compressive Strength, MPa		Compressive Strength, psi	
									7 days	28 days	7 days	28 days
L-S-M	CM64	63	2.5	4.0	2440	152	65	0.724	29.5	38.4	4273	5570
L-S-M-F	CM88	88	3.5	9.5	2293	143	73	0.670	12.9	18.3	1869	2661
L-S-M-F	CM72	10	0.4	4.5	2395	150	66	0.731	18.3	25.9	2651	3754
L-S-P-F	CM70	175	6.9	8.0	2299	144	68	0.730	14.6	20.4	2113	2958
L-S-P-F	CM87	164	6.5	5.0	2389	149	67	0.684	21.7	20.7	3153	2998
L-S-P-F	CM92	0	0.0	7.2	2169	135	69	0.698	14.9	17.9	2159	2591
L-S-P-F	CM98	12	0.5	1.5	2401	150	69	0.698	11.6	14.8	1677	2142
L-S-P-F	CM102	15	0.6	5.6	2378	148	69	0.685	19.1	26.4	2766	3832
L-S-P-F	CM107	10	0.4	4.5	2398	150	71	0.685	20.7	28.7	3002	4159
L-S-P-F	CM108	130	5.1	5.8	2313	144	69	0.684	20.0	27.1	2894	3927
L-S-N-F	CM71	90	3.5	6.5	2367	148	65	0.728	16.6	24.0	2406	3474

** immediately after mixing*

Table 30. Mix design for preliminary concrete mixtures with Class C fly ash

a) SI Units

Type		**Dosage of Chemical Admixtures, %**				**Mixture proportioning, kg/m^3**									W/CM	Yield
		PCE	SNF	Mid-Range	AE	Cement Content	AC	Aggregates (SSD)			Total AGG	SP	Air Entraining Admixtures	Total W		
								CA	IA	FA						
L-S-M	CM64			0.15	0.00	280	0	801	198	955	1954	1.038	0.000	133	0.48	0.98
L-S-M-C	CM93			0.15	0.005	195	84	762	188	908	1858	1.038	0.113	107	0.38	1.08
L-S-M-C	CM84			0.15	0.005	195	84	762	188	908	1858	1.038	0.113	107	0.38	0.97
L-S-M-C	CM99			0.20	0.005	195	84	761	188	907	1857	1.384	0.113	107	0.38	0.97
L-S-M-C	CM75			0.15	0.01	195	84	812	201	969	1982	1.038	0.227	119	0.43	1.05
L-S-P-C	CM73	0.15			0.015	195	84	812	201	968	1981	1.230	0.340	119	0.43	1.07
L-S-P-C	CM82	0.15			0.015	195	84	761	188	908	1857	1.230	0.340	107	0.38	0.98
L-S-P-C	CM103	0.15			0.015	195	84	777	192	926	1895	1.230	0.340	93	0.33	0.96
L-S-N-C	CM74		0.4		0.025	195	84	810	200	965	1975	2.768	0.567	120	0.43	1.05
L-S-N-C	CM85		0.4		0.015	195	84	759	188	905	1852	2.768	0.340	108	0.39	0.97

b) US Customary Units

Type		Dosage of Chemical Admixtures, %				Mixture proportioning, lb/yd^3									W/CM	Yield
		PCE	SNF	Mid-Range	AE	Cement Content	AC	Aggregates (SSD)			Total AGG	SP	Air Entraining Admixtures	Total W		
								CA	IA	FA						
L-S-M	CM64			0.15	0.000	470	0	1762	436	2101	4299	2.28	0.00	293	0.48	0.98
L-S-M-C	CM93			0.15	0.005	329	184	1676	414	1998	4088	2.28	0.25	235	0.38	1.08
L-S-M-C	CM84			0.15	0.005	329	184	1676	414	1998	4088	2.28	0.25	235	0.38	0.97
L-S-M-C	CM99			0.20	0.005	329	184	1674	414	1995	4085	3.04	0.25	235	0.38	0.97
L-S-M-C	CM75			0.15	0.010	329	184	1786	442	2132	4360	2.28	0.50	262	0.43	1.05
L-S-P-C	CM73	0.15			0.015	329	184	1786	442	2130	4358	2.71	0.75	262	0.43	1.07
L-S-P-C	CM82	0.15			0.015	329	184	1674	414	1998	4085	2.71	0.75	235	0.38	0.98
L-S-P-C	CM103	0.15			0.015	329	184	1709	422	2037	4169	2.71	0.75	205	0.33	0.96
L-S-N-C	CM74		0.4		0.025	329	184	1782	440	2123	4345	6.09	1.25	264	0.43	1.05
L-S-N-C	CM85		0.4		0.015	329	184	1670	414	1991	4074	6.09	0.75	238	0.39	0.97

Table 31. Fresh and hardened properties of concrete mixtures with Class C fly ash

Type		Slump, mm	Slump, in	Air, %	Fresh Density, kg/m^3	Fresh Density, lb/ft^3	Temp., °F	AGG Vol	Compressive Strength, MPa		Compressive Strength, psi	
									7 days	28 days	7 days	28 days
L-S-M	CM64	63	2.5	4.0	2440	152	65	0.724	29.5	38.4	4273	5570
L-S-M-C	CM93	0	0.0	5.4	2107	132	67	0.689	11.1	13.3	1610	1933
L-S-M-C	CM84	50	2.0	7.5	2338	146	68	0.689	28.8	38.8	4182	5632
L-S-M-C	CM99	50	2.0	7.0	2338	146	70	0.688	27.8	37.3	4027	5406
L-S-M-C	CM75	110	4.3	12.0	2293	143	70	0.735	18.2	26.4	2642	3823
L-S-P-C	CM73	180	7.1	12.0	2248	140	67	0.734	19.8	26.7	2868	3868
L-S-P-C	CM82	215	8.5	9.0	2313	144	68	0.688	27.2	36.4	3941	5282
L-S-P-C	CM103	95	3.7	7.0	2387	149	69	0.702	35.5	46.7	5154	6772
L-S-N-C	CM74	120	4.7	12.0	2293	143	68	0.732	17.8	24.4	2580	3535
L-S-N-C	CM85	70	2.8	7.5	2350	147	69	0.686	28.3	38.2	4099	5535

** immediately after mixing*

Table 32. Mix design for preliminary concrete mixtures with slag

a) SI Units

Type		Dosage of Chemical Admixtures, %				Mixture Proportioning, kg/m^3									W/CM	Yield
		PCE	SNF	Mid-Range	AE	Cement	Slag	Aggregates (SSD)			Total AG	SP	Air Entraining Admixture	Total W		
								CA	IA	FA						
L-S-M	CM64			0.15	0.00	280	0	801	198	955	1954	1.038	0.000	133	0.48	0.98
L-S-M-S	CM86			0.15	0.01	140	140	747	185	890	1822	1.038	0.227	121	0.44	0.95
L-S-P-S	CM76	0.15			0.015	140	140	813	201	969	1983	1.230	0.340	119	0.43	0.99
L-S-P-S	CM104	0.15			0.035	140	140	762	188	908	1858	1.230	0.794	108	0.39	0.94
L-S-P-S	CM89	0.15			0.025	140	140	762	188	908	1858	1.230	0.567	107	0.38	0.94
L-S-N-S	CM94		0.5		0.025	140	140	759	187	904	1851	3.460	0.567	109	0.39	0.97
L-S-N-S	CM77		0.4		0.025	140	140	811	200	966	1977	2.768	0.567	120	0.43	0.99

b) US Customary Units

Type		Dosage of Chemical Admixtures, %				Mixture Proportioning, lb/yd^3									W/CM	Yield
		PCE	SNF	Mid-Range	AE	Cement	Slag	Aggregates (SSD)			Total AG	SP	Air Entraining Admixture	Total W		
								CA	IA	FA						
L-S-M	CM64			0.15	0.00	470	0	1762	436	2101	4299	2.28	0.00	293	0.48	0.98
L-S-M-S	CM86			0.15	0.01	236	307	1643	407	1958	4008	2.28	0.50	266	0.44	0.95
L-S-P-S	CM76	0.15			0.015	236	307	1789	442	2132	4363	2.71	0.75	262	0.43	0.99
L-S-P-S	CM104	0.15			0.035	236	307	1676	414	1998	4088	2.71	1.75	238	0.39	0.94
L-S-P-S	CM89	0.15			0.025	236	307	1676	414	1998	4088	2.71	1.25	235	0.38	0.94
L-S-N-S	CM94		0.5		0.025	236	307	1670	411	1989	4072	7.61	1.25	240	0.39	0.97
L-S-N-S	CM77		0.4		0.025	236	307	1784	440	2125	4349	6.09	1.25	264	0.43	0.99

Table 33. Fresh and hardened properties of preliminary concrete mixtures with slag

Type		**Slump, mm**	**Slump, in**	**Air, %**	**Fresh Density,** kg/m^3	**Fresh Density,** lb/ft^3	**Temp.,** °F	**AGG Vol Ratio**	**Compressive Strength, MPa**		**Compressive Strength, psi**	
									7 days	28 days	7 days	28 days
L-S-M	CM64	63	2.5	4.0	2440	152	65	0.724	29.5	38.4	4273	5570
L-S-M-S	CM86	59	2.3	6.0	2364	148	71	0.675	30.0	23.7	4346	3441
L-S-P-S	CM76	140	5.5	3.2	2429	152	70	0.735	21.8	29.9	3163	4336
L-S-P-S	CM104	200	7.9	5.0	2418	151	69	0.689	23.1	31.6	3349	4588
L-S-P-S	CM89	50	2.0	3.5	2432	152	72	0.689	28.3	36.8	4106	5336
L-S-N-S	CM94	71	2.8	8.5	2327	145	66	0.686	25.6	33.4	3711	4838
L-S-N-S	CM77	68	2.7	6.0	2437	152	66	0.733	26.4	40.1	3827	5811

** immediately after mixing*

Based on the preliminary study, it was confirmed that fresh density, air content, and compressive strength have a strong relationship and, therefore, the mixtures with various air contents (including the reference), can be represented by the fresh density-air content graph as illustrated by *Figure 32*. To meet the WisDOT specifications, some of the optimized mixtures based on the preliminary study required further minor adjustments of the dosage of AE admixture before the use in the final (large volume) batches required for extended performance and durability testing. In this respect, fresh density and air content relationship was very useful for the adjustment of air content in fresh concrete and fine-tuning the dosage of AE admixture.

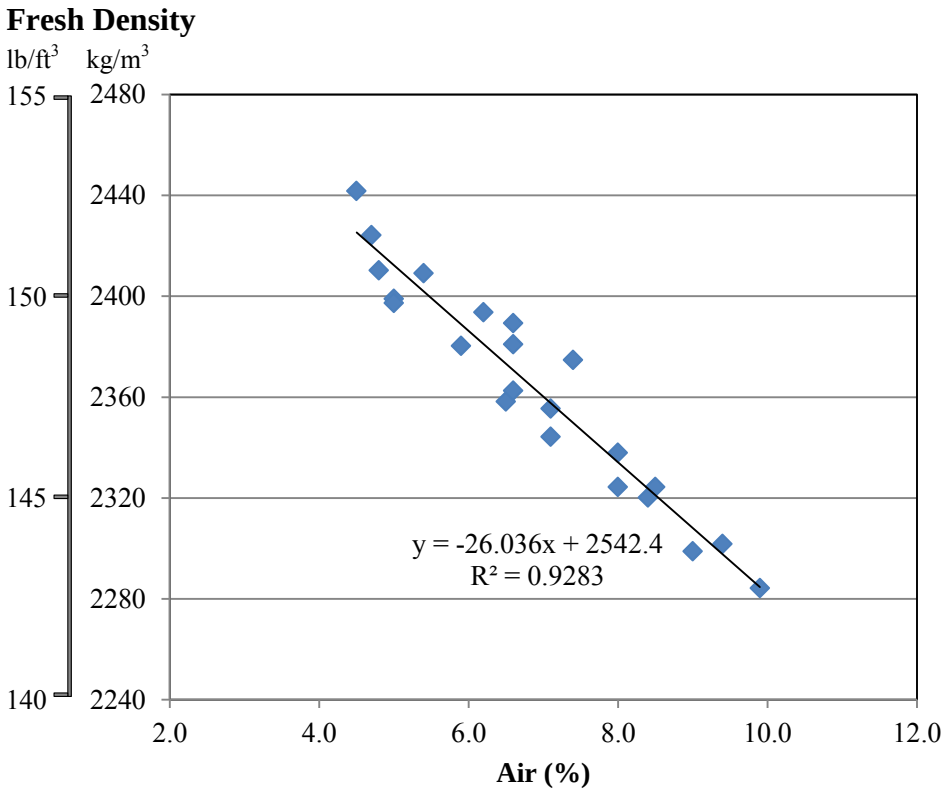

Figure 46. The relationship between the air content and fresh density of concrete mixtures

4.4.2. The Evaluation of Optimized Concrete

The optimized concrete mixtures were produced based on the results of aggregate and admixture optimization, using different SCMs and two different cementitious material contents of 280 kg/m^3 (470 lb/yd^3) and 250 kg/m^3 (420 lb/yd^3). The mix design for the optimized concrete was based on the adjustment of preliminary mixtures (mainly for AE admixture dosage and the W/CM ratio). The mixture proportions of concrete based on southern aggregates are reported in *Table 34*, *Table 35, Table 38* and *Table 39* for concrete with cementitious material content of 280 kg/m^3 (470 lb/yd^3) and 250 kg/m^3 (420 lb/yd^3), respectively. The mix designs based on northern aggregates are reported in *Table 42* and *Table 45* for concrete with cementitious material content of 280 kg/m^3 (470 lb/yd^3) and 250 kg/m^3 (420 lb/yd^3), respectively. The concrete mixtures with southern aggregates are reported in *Table 34* to *Table 41* and arranged based on the cement content level, the type of SCM used, and the admixture type. The concrete mixtures with northern aggregates are reported in *Table 42* to *Table 47*. To evaluate the fresh properties, the slump, air content, bulk density, and temperature tests were performed. To evaluate the hardened properties the compressive strength at 1, 3, 7, 28, 90, and 360 days and flexural strength (modulus of rupture) at 3, 7, 28, and 90 days were tested.

Length change due to drying (temperature of 70ºF and RH of 50%) was tested for up to 1 year period. The durability of concrete was evaluated using the freeze-thaw test (using specimens cured for 56 days) and the rapid chloride permeability test (using specimens cured for 30 days and 90 days); the durability tests were performed at UW-Madison.

4.4.3. Concrete Mixtures Based on Southern Aggregates: Fresh Properties

The workability of concrete mixtures was evaluated using the slump test. Concrete slump depends on various parameters, including W/CM ratio, water and cement content (the volume of cement paste) the type of admixtures (WR vs. HRWR), and the volume of air. In this study, the proportioning of aggregates was held constant for each level of cement content; therefore, this parameter did not affect the slump results. The workability of fresh concrete was evaluated right after the mixing and also after 30 minutes measured from contact of cement with water (in the mixer) as reported by *Table 36, Table 40, Table 43 Table 46* and Appendix 1.

Comparing concrete mixtures based on L1 cement produced at the same W/CM ratio with reference BB04 reveals that, at the same W/CM ratio of 0.42, the mixtures containing slag (BB02, BB08) and Class F fly ash (BB05, BB03) had better workability about 50 mm higher (2 in.) than plain mixtures without SCM. Such behavior was observed for both concrete types with the SNF admixture (BB04) and the reference mid-range plasticizing admixture (BB09). In the case of a W/CM ratio of 0.38, mixtures with slag (BB11) and PCE admixture had a better workability than the plain concrete mixture (BB13) and concrete with Class C fly ash and mid-range admixture (BB06). Only two mixtures with PCE containing Class C and Class F fly ash (BB10, BB12) were able to reach a high level of water reduction and were produced at a W/CM ratio of 0.33. It must be noted that the effect of air content on slump is very significant and so all compared mixtures were assumed to have a similar level of air content.

Comparing the concrete mixtures based on H1 cement produced at the same W/CM ratio of 0.37 (BB19, BB18, BB17) demonstrates the superior effect of PCE admixture on slump and

slump retention (tested after 30 minutes). Comparing the concrete mixtures based on S1 cement produced at the W/CM ratio of 0.42-0.43 (BB16, BB15) demonstrates that with this cement SNF performs better than the mid-range plasticizing admixture in terms of workability. The mixture with PCE admixture (BB14) was produced at W/CM of 0.37 assuring a superior long-term performance.

Comparing concrete mixtures BB13, BB17, and BB14 with the same type of admixtures reveals that some cements require higher water content to achieve the same workability; however, the air content (which can make a significant contribution to slump) in these three mixtures varies only by about 2% (Appendix 1).

For concrete with southern aggregates and reduced cement content level of 250 kg/m^3 (420 lb/yd^3), the workability was evaluated right after mixing and after a 30-minute period (upon mixing water and cement), *Table 40*. This experimental matrix was realized with one type of WR and one type of HRWR (PCE) admixtures. Comparing concrete mixtures based on portland cement and tested at about the same W/CM ratio of 0.45 proves that the mixtures with the PCE admixture (BB21) provide higher slump by 100 mm (4 in.) than the mixture with the mid-range admixture (BB20). An increase in W/CM ratio or air content may be required for the design of concrete mixtures with mid-range plasticizer and reduced cement content of 250 kg/m^3 (420 lb/yd^3), such as BB20, to achieve the required workability (Appendix 1).

For concrete with SCM and reduced cementitious materials content of 250 kg/m^3 (420 lb/yd^3) and SCM produced at about the same W/CM ratio of 0.4 (BB22, BB23, BB24), the mixture containing slag cement provided improved slump, even at slightly lower air content

(versus the other two mixtures and the reference mixture BB04). In the case of concrete mixtures based on H1 (BB29, BB27) and S1 (BB28, BB26) cements, at the same W/CM ratio of about 0.40, the mixtures had the same fresh performance with small deviations depending on the air content (Appendix 1). It must be noted that the incorporation of an additional (over specification limit) air into mixtures with reduced cement content is essential to maintain the required volume of cement paste and compensate for the reduced amount of cementitious materials.

4.4.4. Concrete Mixtures Based on Northern Aggregates: Fresh Properties

In this study, the concrete mixture proportioning used gradual increments of W/CM ratio from 0.35 to 0.50, with an increment of 0.05 for compositions with cementitious materials content of 280 kg/m^3 (470 lb/yd^3) and an increment of 0.025 for 250 kg/m^3 (420 lb/yd^3). This approach enabled the grouping of concrete types based on the effectiveness of superplasticizer and also the type of contribution SCM. However, some of the mixtures, especially those based on the mid-range water reducing admixture, had a slump of less than 50 mm (2 in). Nevertheless, due to optimal aggregate combination, the workability of all tested concrete mixtures was satisfactory. Furthermore, the air content of some mixtures produced at cementitious content of 280 kg/m^3 (470 lb/yd^3) was less than 5%. The produced at a slump of less than 50 mm (2-in) were mainly compositions with mid-range plasticizer and SNF. It can be expected that in the case of higher slump these mixtures would entrain higher volumes of air. Still, some of the designs resulted in an air content of more than 7% (Table 36). In the case of concrete mixtures with low cementitious content of 250 kg/m^3 (420 lb/yd^3), air content was intentionally kept at the level of more than 5% and, in some mixtures, reached up to 8.5%.The fresh properties of concrete with a reduced cement content level of 250 kg/m^3 (420 lb/yd^3) were evaluated right

after mixing and after 30 minutes. This experimental matrix included one type of WR (mid-range) and one type of HRWR (PCE). Comparing the concrete mixtures based on L1 cement reveals that, at about the same W/CM ratio of 0.45, the PCE admixture (BB21) can provide about 100 mm (4 in.) higher slump and higher air content vs. achievable by the concrete with the mid-range admixture (BB20). Higher W/CM ratios or elevated air content can be required for concrete mixtures with low cement content to achieve the same workability as reference concrete (BB04) with a cement content of 280 kg/m^3 (470 lb/yd^3).

For concrete mixtures with reduced cementitious materials content and SCM produced at about the same W/CM ratio 0.40 (BB22, BB23, BB24), the mixture containing slag cement provided enhanced slump vs. the other two mixtures and the reference mixture, (BB04). Concrete produced at the same W/CM ratio of about 0.40 based on H1 (BB29, BB27) and S1 (BB28, BB26) cements had similar performance with little variation depending on the air content, demonstrating lower slump vs. reference BB04 (and BB20). It must be noted that entrainment of some additional air is essential for maintaining workability in the case of low cement content concrete in order to compensate for the reduced volume of cement paste.

4.4.5. Concrete with on Southern Aggregates: Strength Development

Table 37 and *Table 41* report on the hardened properties, including the compressive strength and modulus of rupture, for concrete based on southern aggregates with cementitious material content of 280 kg/m^3 (470 lb/yd^3) and 250 kg/m^3 (420 lb/yd^3), respectively. The mechanical performance was evaluated for early (1-7 days) and long-term (up to 1 year) periods. Similarly to fresh properties, the effect of W/CM and air content on mechanical performance was

found to be essential. As reported by *Table 37,* at the W/CM ratio of 0.43, concrete based on portland cement and southern aggregates (BB09) demonstrated better strength at the ages of 1, 3, and 7 days vs. mixtures with SCM (BB02, BB08, BB05, BB03). At the 28-day age and afterwards, concrete containing slag (BB02, BB08) exceeded the strength of portland cement concrete. However, the compressive strength (including 1-year strength) of Class F fly ash concrete (BB05, BB03) was lower than the corresponding reference.

At early ages, portland cement based concrete (BB13) with a W/CM ratio of 0.38 performed better than the slag concrete with PCE (BB11) and also Class C fly ash concrete with mid-range and SNF admixtures (BB06, BB07); however, after 7 days, Class C fly ash concrete exceeded the strength of reference concrete (BB13), and, after 28 days, slag concrete (BB11) reached the same strength as the reference (BB13). At such W/CM ratio, all tested concrete types based on southern aggregates achieved early and long-term strength higher than that of the reference (BB04) as reported in *Table 37*. At the age of 1 year, concrete containing Class C fly ash reached the highest compressive strength of 63.2 MPa (9,166 psi). However, the PCE concrete had the highest strength when compared to concrete with other admixtures, mainly due to the use of lower W/CM ratio and also very good compatibility between the PCE and cementitious materials.

In the case of a W/CM ratio of 0.32, for southern aggregates concrete containing the PCE admixture and Class C and F fly ash (BB10 and BB12) had improved early and long-term strength compared to the reference, *Table 37*. Concrete based on H1 cement produced at the same W/CM ratio of 0.37 (BB19, BB18, BB17) achieved extremely high early strength (about

three times higher than the reference) and had the minimum specified compressive strength of 20 MPa (3,000 psi) as required for traffic opening at the age of 1 day, as demonstrated by *Table 37*. The long-term strength of this concrete was similar to the performance of concrete based on L1 cement and Class C fly ash. The concrete with PCE admixtures was the best up to 28 days and concrete with the SNF type admixture had a very best performance at later ages.

At all ages, concrete based on southern aggregates and S1 cement (BB16, BB15, BB14) performed slightly better or at the same level as the reference concrete (BB04), as demonstrated by *Table 37*. Comparing the reference concrete based on S1 cement to concrete based on H1 and L1 cements revealed that the use of S1 cement performed better than L1 cement in terms of 1-day strength. The H1 cement performed better than L1 at all the ages, for all types of admixtures, and the most of the SCMs (except for the Class C and PCE admixture combination). However, in combination with slag, all investigated cements were comparable, especially, in terms of long-term behavior.

Table 34. Optimized concrete mixture proportions based on southern aggregates and total cementitious materials of 280 kg/m³ (470 lb/yd³); SI Units

Cement Factor	Mix ID		Dosage of Chemical Admixture (%)				Mixture Proportioning, kg/m³								
							Cement Content	SCM	Aggregates (SSD)			Total AGG	WR HRWR	Air Entraining Admixtures	Total Water
			PCE	SNF	Mid-Range	AE			CA	IA	FA				
280 kg/ m³ (470 lb/yd³)	**L-S-M**	BB04			0.15	0.010	280	0	750	185	894	1829	1.038	0.227	118
	L-S-N	BB09		0.4		0.015	280	0	747	185	891	1823	2.768	0.340	119
	L-S-P	BB13	0.15			0.020	280	0	765	189	912	1866	1.230	0.453	104
	L-S-M-S	BB02			0.15	0.005	140	140	747	185	890	1822	1.038	0.227	118
	L-S-N-S	BB08		0.4		0.015	140	140	744	184	887	1816	2.768	0.340	119
	L-S-P-S	BB11	0.15			0.025	140	140	762	188	908	1858	1.230	0.567	104
	L-S-M-C	BB06			0.15	0.005	195	84	761	188	907	1857	1.038	0.567	104
	L-S-N-C	BB07		0.4		0.010	195	84	759	188	905	1852	2.768	0.227	105
	L-S-P-C	BB10	0.15			0.010	195	84	777	192	926	1895	1.230	0.227	89
	L-S-M-F	BB05			0.15	0.020	195	84	742	183	884	1809	1.038	0.340	119
	L-S-N-F	BB03		0.4		0.025	195	84	739	183	881	1803	2.768	0.567	120
	L-S-P-F	BB12	0.15			0.015	195	84	772	191	921	1884	1.230	0.340	89
	H-S-M	BB19			0.15	0.005	280	0	765	189	912	1867	1.038	0.113	103
	H-S-N	BB18		0.4		0.015	280	0	763	189	909	1861	2.768	0.340	105
	H-S-P	BB17	0.15			0.020	280	0	765	189	912	1866	1.230	0.453	104
	S-S-M	BB16			0.15	0.010	280	0	750	185	894	1829	1.038	0.227	118
	S-S-N	BB15		0.4		0.025	280	0	747	185	891	1823	2.768	0.567	120
	S-S-P	BB14	0.15			0.045	280	0	764	189	911	1864	1.230	1.020	104

Table 35. Optimized concrete mixture proportions based on southern aggregates and total cementitious materials of 280 kg/m³(470 lb/yd³); US Customary Units

Cement Factor	Mix ID		Dosage of Chemical Admixtures, %				Mixture Proportions, lb/yd³								
							Cement	SCM	Aggregates (SSD)				Admixtures		Total Water
			PCE	SNF	MR	AE			CA	IA	FA	Total	WR HRWR	Air Entraining	
280 kg/m³ (470 lb/yd³)	**L-S-M**	BB04			0.15	0.010	470	0	1691	335	1283	3310	1.750	0.382	212
	L-S-N	BB09		0.40		0.015	470	0	1686	334	1280	3300	4.666	0.573	212
	L-S-P	BB13	0.15			0.0125	470	0	1724	342	1308	3373	2.074	0.478	188
	L-S-M-S	BB02			0.15	0.010	235	235	1685	334	1279	3298	1.750	0.191	212
	L-S-N-S	BB08		0.40		0.010	235	235	1680	333	1275	3288	4.666	0.382	212
	L-S-P-S	BB11	0.15			0.020	235	235	1717	340	1303	3360	2.074	0.764	188
	L-S-M-C	BB06			0.15	0.005	329	141	1716	340	1302	3358	1.750	0.191	188
	L-S-N-C	BB07		0.40		0.010	329	141	1711	339	1299	3349	4.666	0.382	188
	L-S-P-C	BB10	0.15			0.005	329	141	1748	347	1327	3422	2.074	0.191	165
	L-S-M-F	BB05			0.15	0.010	329	141	1674	332	1270	3277	1.750	0.382	212
	L-S-N-F	BB03		0.40		0.010	329	141	1674	332	1270	3277	1.750	0.382	212
	L-S-P-F	BB12	0.15			0.150	329	141	1739	345	1319	3403	2.074	0.573	165
	H-S-M	BB19			0.15	0.005	470	0	1724	342	1308	3374	1.750	0.191	188
	H-S-N	BB18		0.40		0.015	470	0	1719	341	1304	3367	4.666	0.573	188
	H-S-P	BB17	0.15			0.015	470	0	1723	342	1308	3373	2.074	0.573	188
	S-S-M	BB16			0.15	0.005	470	0	1677	331	1289	3298	1.750	0.191	212
	S-S-N	BB15		0.40		0.025	470	0	1671	331	1278	3280	4.666	0.955	212
	S-S-P	BB14	0.15			0.050	470	0	1722	341	1306	3369	2.074	1.911	188

Table 36. The fresh properties of optimized concrete mixtures based on southern aggregates and total cementitious materials of 280 kg/m^3 (470 lb/yd^3)

Cement Factor	Mix ID		W/CM	Vol. of AGG Ratio	Yield	Air, %	Concrete Temp., F	Bulk Density		Slump, mm		Slump, in	
								kg/m^3	lb/ft^3	0 min	30 mins	0 min	30 mins
280 kg/m^3 (470 lb/yd^3)	**L-S-M**	BB04	0.42	0.678	0.944	6.5	71	2358	147	49	30	1.9	1.2
	L-S-N	BB09	0.43	0.676	0.926	5.0	69	2399	150	51	20	2.0	0.8
	L-S-P	BB13	0.37	0.692	0.959	7.1	69	2344	146	43	30	1.7	1.2
	L-S-M-S	BB02	0.42	0.675	0.954	8.0	68	2324	145	100	55	3.9	2.2
	L-S-N-S	BB08	0.43	0.673	0.940	7.1	69	2355	147	100	50	3.9	2.0
	L-S-P-S	BB11	0.37	0.689	0.924	4.7	68	2424	151	188	160	7.4	6.3
	L-S-M-C	BB06	0.37	0.689	0.929	5.4	73	2409	150	30	15	1.2	0.6
	L-S-N-C	BB07	0.38	0.686	0.921	5.9	69	2429	152	65	35	2.6	1.4
	L-S-P-C	BB10	0.32	0.702	0.939	4.8	69	2410	150	45	10	1.8	0.4
	L-S-M-F	BB05	0.42	0.671	0.960	9.0	69	2299	144	95	65	3.7	2.6
	L-S-N-F	BB03	0.43	0.668	0.972	9.5	69	2265	141	130	92	5.1	3.6
	L-S-P-F	BB12	0.32	0.698	1.013	6.9	71	2224	139	32	25	1.3	1.0
	H-S-M	BB19	0.37	0.692	0.921	4.5	69	2442	152	7	0	0.3	0.0
	H-S-N	BB18	0.38	0.690	0.910	4.0	67	2467	154	10	8	0.4	0.3
	H-S-P	BB17	0.37	0.692	0.967	8.5	74	2324	145	92	39	3.6	1.5
	S-S-M	BB16	0.42	0.678	0.935	6.6	68	2381	149	35	20	1.4	0.8
	S-S-N	BB15	0.43	0.676	0.940	6.6	72	2363	148	56	42	2.2	1.7
	S-S-P	BB14	0.37	0.691	0.939	6.2	71	2394	149	30	20	1.2	0.8

Table 37. The mechanical performance of optimized concrete based on southern aggregates and cementitious materials of 280kg/m^3 (470 lb/yd^3)

a) SI Units

Cement Factor	Mix ID		W/CM	Compressive Strength, MPa at the Age of						Modulus of Rupture, MPa at the Age of			
				1 day	3 days	7 days	28 days	90 days	360 days	3 days	7 days	28 days	90 days
280 kg/ m^3 (470 lb/yd^3)	**L-S-M**	BB04	0.42	6.8	17.7	25.2	31.7	35.0	38.8	6.6	7.3	8.8	8.6
	L-S-N	BB09	0.43	13.9	22.6	27.2	33.6	39.2	40.9	6.4	7.2	8.6	9.5
	L-S-P	BB13	0.37	13.6	27.7	32.5	38.1	43.6	47.4	7.1	7.7	9.3	7.3
	L-S-M-S	BB02	0.42	2.9	13.2	19.8	33.3	41.6	45.1	0.0	6.7	8.9	9.6
	L-S-N-S	BB08	0.43	4.9	14.7	24.2	35.2	41.0	43.5	5.2	7.5	9.9	9.7
	L-S-P-S	BB11	0.37	8.9	20.2	30.3	38.0	40.3	48.0	5.9	7.3	9.2	8.4
	L-S-M-C	BB06	0.37	6.0	23.3	35.0	48.3	56.4	59.4	6.1	8.1	9.6	11.4
	L-S-N-C	BB07	0.38	5.1	22.0	30.0	41.9	50.4	50.7	6.6	6.6	9.1	10.9
	L-S-P-C	BB10	0.32	10.1	25.7	38.1	49.3	56.6	63.2	7.0	8.6	10.4	11.6
	L-S-M-F	BB05	0.42	3.5	9.6	13.3	19.1	27.0	31.3	3.7	4.6	5.9	7.5
	L-S-N-F	BB03	0.43	4.0	8.8	12.6	18.6	25.2	29.4	3.8	4.7	6.0	7.5
	L-S-P-F	BB12	0.32	10.0	20.3	25.0	32.7	42.6	48.4	6.2	6.3	8.0	7.5
	H-S-M	BB19	0.37	20.4	31.0	34.9	41.7	49.2	46.6	5.8	6.7	7.3	8.3
	H-S-N	BB18	0.38	22.8	33.4	40.2	43.8	51.0	55.3	6.2	6.9	7.3	8.8
	H-S-P	BB17	0.37	25.1	25.6	29.3	32.9	38.0	43.4	5.5	5.6	6.1	8.8
	S-S-M	BB16	0.42	11.1	17.7	22.8	29.9	35.6	38.7	6.4	6.1	7.0	8.2
	S-S-N	BB15	0.43	13.0	18.8	23.1	28.2	34.0	37.3	6.3	7.3	6.6	6.8
	S-S-P	BB14	0.37	16.3	24.0	27.4	34.6	42.8	48.1	6.8	7.6	7.1	7.8

b) US Customary Units

Cement Factor	Mix ID		W/CM	Compressive Strength, psi at the Age of						Modulus of Rupture, psi at the Age of			
				1 day	3 days	7 days	28 days	90 days	360 days	3 days	7 days	28 days	90 days
280 kg/ m^3 (470 lb/yd^3)	**L-S-M**	BB04	0.42	986	2567	3654	4597	5075	5626	957	1059	1276	1247
	L-S-N	BB09	0.43	2016	3277	3944	4872	5684	5931	928	1044	1247	1378
	L-S-P	BB13	0.37	1972	4017	4713	5525	6322	6873	1030	1117	1349	1059
	L-S-M-S	BB02	0.42	421	1914	2871	4829	6032	6540	0	972	1291	1392
	L-S-N-S	BB08	0.43	711	2132	3509	5104	5945	6308	754	1088	1436	1407
	L-S-P-S	BB11	0.37	1291	2929	4394	5510	5844	6960	856	1059	1334	1218
	L-S-M-C	BB06	0.37	870	3379	5075	7004	8178	8613	885	1175	1392	1653
	L-S-N-C	BB07	0.38	740	3190	4350	6076	7308	7352	957	957	1320	1581
	L-S-P-C	BB10	0.32	1465	3727	5525	7149	8207	9164	1015	1247	1508	1682
	L-S-M-F	BB05	0.42	508	1392	1929	2770	3915	4539	537	667	856	1088
	L-S-N-F	BB03	0.43	580	1276	1827	2697	3654	4263	551	682	870	1088
	L-S-P-F	BB12	0.32	1450	2944	3625	4742	6177	7018	899	914	1160	1088
	H-S-M	BB19	0.37	2958	4495	5061	6047	7134	6757	841	972	1059	1204
	H-S-N	BB18	0.38	3306	4843	5829	6351	7395	8019	899	1001	1059	1276
	H-S-P	BB17	0.37	3640	3712	4249	4771	5510	6293	798	812	885	1276
	S-S-M	BB16	0.42	1610	2567	3306	4336	5162	5612	928	885	1015	1189
	S-S-N	BB15	0.43	1885	2726	3350	4089	4930	5409	914	1059	957	986
	S-S-P	BB14	0.37	2364	3480	3973	5017	6206	6975	986	1102	1030	1131

Table 38. Optimized concrete mixture proportions based on southern aggregates and total cementitious materials of 250 kg/m^3 (420 lb/yd^3); SI Units

Cement Factor	Mix ID		Dosage of Chemical Admixtures, %				Mixture Proportions, kg/m^3								
							Cement	SCM	Aggregates (SSD)				Admixtures		Total Water
			PCE	SNF	MR	AE			CA	IA	FA	Total	WR HRWR	Air Entraining	
250 kg/ m^3 (420 lb/yd^3)	**L-S-M-R**	BB20	-	-	0.15	0.010	249	-	750	185	929	1864	0.928	0.203	113
	L-S-P-R	BB21	0.15	-	-	0.030	249	-	776	192	914	1881	1.099	0.608	108
	L-S-P-C-R	BB22	0.15	-	-	0.015	174	75	780	193	934	1907	1.099	0.304	94
	L-S-P-S-R	BB23	0.15	-	-	0.030	125	125	762	188	940	1890	1.099	0.608	101
	L-S-P-F-R	BB24	0.15	-	-	0.050	174	75	757	187	934	1878	1.099	1.013	101
	H-S-M-R	BB29	-	-	0.15	0.015	249	-	771	191	920	1882	0.928	0.304	103
	H-S-P-R	BB27	0.15	-	-	0.020	249	-	778	192	928	1898	1.099	0.405	96
	S-S-M-R	BB28	-	-	0.15	0.005	249	-	772	191	920	1882	0.928	0.101	104
	S-S-P-R	BB26	0.15	-	-	0.025	249	-	771	191	919	1881	1.099	0.507	102

Table 39. Optimized concrete mixture proportions based on southern aggregates and total cementitious materials of 250 kg/m^3 (420 lb/yd^3); US Customary Units

Cement Factor	Mix ID		Dosage of Chemical Admixtures, %				Mixture Proportions, lb/yd^3								
							Cement	SCM	Aggregates (SSD)				Admixtures		Total Water
			PCE	SNF	MR	AE			CA	IA	FA	Total	WR HRWR	Air Entraining	
250 kg/ m^3 (420 lb/yd^3)	**L-S-M-R**	BB20	-	-	0.15	0.010	420	-	1716	340	1302	3358	1.563	0.171	210
	L-S-P-R	BB21	0.15	-	-	0.030	420	-	1730	343	1313	3385	1.853	0.341	200
	L-S-P-C-R	BB22	0.15	-	-	0.015	294	126	1752	347	1329	3429	1.853	0.171	179
	L-S-P-S-R	BB23	0.15	-	-	0.030	210	210	1738	345	1319	3402	1.853	0.512	189
	L-S-P-F-R	BB24	0.15	-	-	0.050	294	126	1729	343	1312	3384	1.853	0.171	189
	H-S-M-R	BB29	-	-	0.15	0.015	420	-	1729	343	1312	3384	1.563	0.854	200
	H-S-P-R	BB27	0.15	-	-	0.020	420	-	1744	346	1324	3414	1.853	0.341	189
	S-S-M-R	BB28	-	-	0.15	0.005	420	-	1715	339	1319	3373	1.563	0.085	200
	S-S-P-R	BB26	0.15	-	-	0.025	420	-	1730	343	1312	3385	1.853	0.512	200

Table 40. The fresh properties of optimized concrete mixtures based on southern aggregates and total cementitious materials of 250 kg/m^3 (420 lb/yd^3)

Cement Factor	Mix ID		W/CM	Vol. of AGG	Yield	Air, %	Concrete Temp., F	Bulk Density		Slump, mm		Slump, in	
								kg/m^3	lb/ft^3	0 min	30 mins	0 min	30 mins
250 kg/ m^3 (420 lb/yd^3)	**L-S-M-R**	BB20	0.45	0.691	0.960	8.4	74	2320	145	35	11	1.4	0.4
	L-S-P-R	BB21	0.43	0.697	0.972	9.4	68	2302	144	133	113	5.2	4.4
	L-S-P-C-R	BB22	0.38	0.707	0.941	6.6	71	2389	149	37	30	1.5	1.2
	L-S-P-S-R	BB23	0.40	0.701	0.941	5.9	71	2380	149	110	45	4.3	1.8
	L-S-P-F-R	BB24	0.41	0.696	1.005	9.8	68	2218	138	68	30	2.7	1.2
	H-S-M-R	BB29	0.41	0.697	0.933	5.0	67	2397	150	13	0	0.5	0.0
	H-S-P-R	BB27	0.41	0.703	0.961	8.0	72	2338	146	40	7	1.6	0.3
	S-S-M-R	BB28	0.42	0.698	0.942	7.4	67	2375	148	22	12	0.9	0.5
	S-S-P-R	BB26	0.41	0.697	0.979	9.9	72	2284	143	38	28	1.5	1.1

Table 41. The mechanical performance of optimized concrete based on southern aggregates and cementitious materials of 250 kg/m^3 (420 lb/yd^3)

Cement Factor	Mix ID		W/CM	Compressive Strength, MPa at the Age of						Modulus of Rupture, MPa at the Age of			
				1 day	3 days	7 days	28 days	90 days	360 days	3 days	7 days	28 days	90 days
250 kg/ m^3 (420 lb/yd^3)	L-S-M-R	BB20	0.45	3.9	14.0	19.5	23.4	28.7	29.8	3.8	4.3	5.3	5.5
	L-S-P-R	BB21	0.43	8.4	18.3	21.1	26.6	29.3	30.9	4.3	5.2	5.4	5.6
	L-S-P-C-R	BB22	0.38	7.1	19.6	28.2	39.7	44.1	49.8	4.5	5.5	7.1	8.3
	L-S-P-S-R	BB23	0.40	7.8	18.5	28.3	38.0	39.8	44.3	4.7	5.9	7.8	8.1
	L-S-P-F-R	BB24	0.41	6.1	10.0	12.5	16.9	22.7	26.7	3.1	3.2	4.0	4.4
	H-S-M-R	BB29	0.41	12.3	20.7	23.1	30.1	37.2	38.6	4.2	5.7	6.9	7.1
	H-S-P-R	BB27	0.41	17.9	23.9	26.6	32.1	35.2	37.2	5.2	5.2	6.1	6.9
	S-S-M-R	BB28	0.42	14.1	22.6	26.4	31.2	35.3	37.5	5.2	5.7	6.3	7.2
	S-S-P-R	BB26	0.41	11.1	15.7	18.8	25.1	29.0	31.9	3.9	4.3	5.7	5.7

Cement Factor	Mix ID		W/CM	Compressive Strength, psi at the Age of						Modulus of Rupture, psi at the Age of			
				1 day	3 days	7 days	28 days	90 days	360 days	3 days	7 days	28 days	90 days
250 kg/ m^3 (420 lb/yd^3)	L-S-M-R	BB20	0.45	566	2031	2828	3394	4163	4322	551	624	769	798
	L-S-P-R	BB21	0.43	1218	2654	3060	3858	4250	4482	624	754	783	812
	L-S-P-C-R	BB22	0.38	1030	2843	4090	5758	6396	7223	653	798	1030	1204
	L-S-P-S-R	BB23	0.40	1131	2683	4105	5511	5773	6425	682	856	1131	1175
	L-S-P-F-R	BB24	0.41	885	1450	1813	2451	3292	3873	450	464	580	638
	H-S-M-R	BB29	0.41	1784	3002	3350	4366	5395	5598	609	827	1001	1030
	H-S-P-R	BB27	0.41	2596	3466	3858	4656	5105	5395	754	754	885	1001
	S-S-M-R	BB28	0.42	2045	3278	3829	4525	5120	5439	754	827	914	1044
	S-S-P-R	BB26	0.41	1610	2277	2727	3640	4206	4627	566	624	827	827

The modulus of rupture (MOR) obtained from the flexural center-point (3-point) loading of the beams has a good correlation with the corresponding compressive strength for various mixtures and ages. The relationship between the modulus of rupture and compressive strength is represented in *Figure 47* for all test ages. The slight variation depends on the type of SCM, W/CM ratio, and cement type. Therefore, the modulus of rupture can be evaluated and predicted based on the reported equation using the compressive strength as an input parameter (*Figure 47* and Appendix 2).

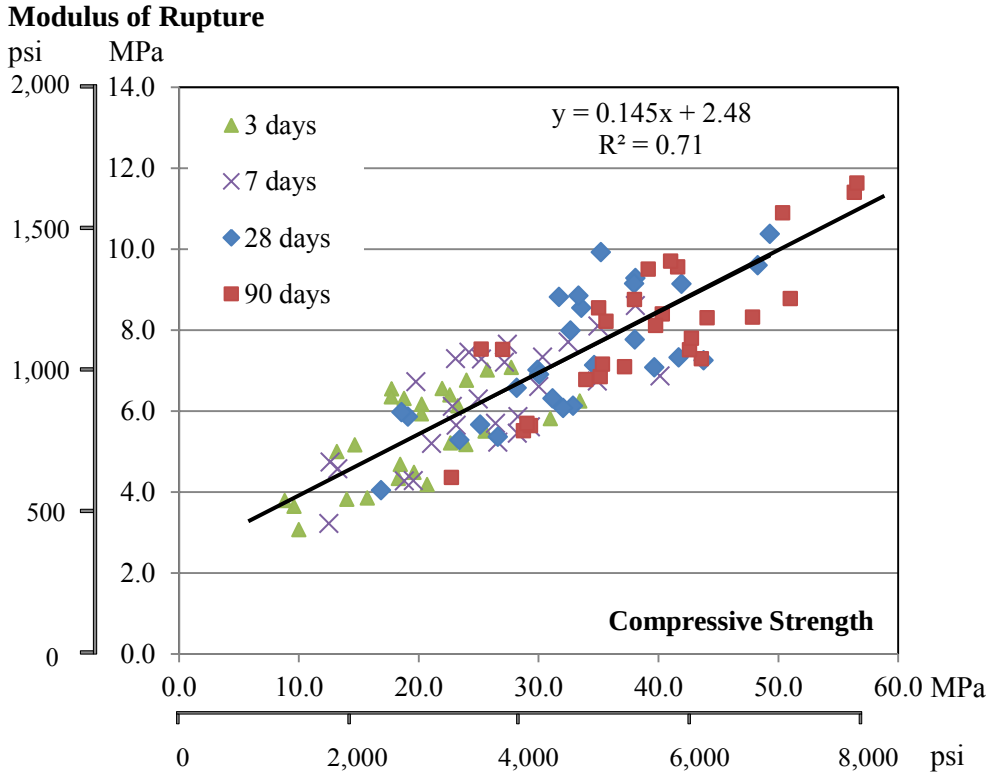

Figure 47. The relationship between the compressive strength and modulus of rupture

As discussed, depending on the type of SCM, chemical admixtures (WR/HRWR), W/CM ratio, and cement type, various concrete compositions demonstrate very different kinetic of strength development. *Table 37* and *Table 41* represent the strength development of investigated concrete for the period of up to 1 year and compare such

performance to the reference concrete (L-S-M, BB04) based on L1 cement, southern aggregates and mid-range admixture.

At W/CM ratio of 0.42, concrete containing slag and mid-range or SNF admixture gains strength at a higher rate than the other compositions, especially at later stages of hardening. At a W/CM ratio of 0.42, concrete with mid-range or SNF admixtures based on L1 cement also achieved better strength vs. S1 cement based concrete. Considering the long-term performance, up to 1 year, the strength gain for concrete containing Class F fly ash (BB03 and BB05) was not sufficient to match the performance of reference composition.

Furthermore, at a W/CM ratio of 0.37, concrete based on L1 cement and Class C fly ash with mid-range or SNF admixtures developed strength at a higher rate compared to other concrete types. Similar behavior was observed for concrete containing slag and PCE admixtures. The concrete with H1 cement had the same strength gain as the reference, but with enhanced 1-day compressive strength, by up to 8 MPa (1160 psi) depending on the admixture type. Concrete based on S1 cement and PCE admixtures provided higher strength vs. the reference (BB04); however, it was comparable to the reference at later stages of hardening.

At a very low W/CM ratio of 0.32, concrete with L1 cement, fly ash (Class C and F) and PCE admixtures provided very advanced performance. Compared to the reference concrete, these compositions developed strength at accelerated rates, especially, for concrete with Class C fly ash. While concrete with Class F fly ash and other admixtures was not able to achieve the satisfactory performance in terms of strength development, concrete with PCE had developed compressive strength of 20 MPa (3,000 psi) in 3 days,

out-performing the reference. The water-reducing effect of PCE resulted in an excellent strength gain, especially in compositions with Class C fly ash (BB10), enabling to reach an outstanding 1-year compressive strength of 63 MPa (9,140 psi).

Table 41 represents the strength development of concrete with low cementitious content of 250 kg/m^3 (420 lb/yd^3) and compares the performance to reference concrete (BB04) with cement content of 280 kg/m^3 (470 lb/yd^3). Only mid-range and PCE admixtures were tested at this cement content. The most of the concrete types was produced at a target W/CM ratio of 0.41, except for BB22 and BB20 compositions, which were produced at 0.38 and 0.45, respectively. Depending on the type of SCM and chemical admixtures, the strength development of low cement concrete appeared to have the same trends as observed for concrete with cement factor of 280 kg/m^3 (470 lb/yd^3). Concrete containing slag and Class C fly ash had higher strength vs. concrete with Class F fly ash. The concrete based on H1 and L1 cements had very similar performance. However, due to the significant reduction of cement content, concrete based on S1, L1 cement and L1 combinations with Class F fly ash did not achieve the strength level of the reference concrete, even at later ages of hardening, up to 1 year.

It must be noted that the strength development rates of concrete based on various cements was different for early and later ages. Concrete based on L1 had a lower strength at early ages compared to compositions with cements H1 and S1, but developed strength at a higher rate after 3 days. The rate of strength development also depends on the type of admixture and SCM combination, and becomes very similar for different concrete compositions after 28 days.

4.4.6. Concrete with Northern Aggregates: Strength Development

The strength of concrete based on northern aggregates was dependent on the W/CM ratio, the type and source of cement, the type of SCM, and also overall content of cementitious materials (affecting W/CM) as reported in *Table 43* to *Table 47*. It can be observed that in portland cement based compositions without SCM, H1 cement provided the best 1-day compressive strength when combined with a mid-range plasticizer and an SNF superplasticizer; the corresponding L2 and S1 based concrete had comparable, but slightly lower strength levels. The highest 1-day strength of 21.6 MPa (3,133 psi) was achieved by concrete based on with L2 cement combined with the PCE superplasticizer.

The most of the investigated concrete with portland cement content of 280 kg/m^3 (470 lb/yd^3) reached the 20 MPa (3,000 psi) benchmark at the age of 3 days; however, longer curing, up to 7 days, was necessary for S1 based concrete produced with mid-range plasticizer or SNF admixture.

The performance of concrete with Class C fly ash was outstanding. All Class C fly ash concrete based on L2 cement demonstrated 3-day compressive strength of more than 20 MPa (3,000 psi) and 28-day strength of more than 40 MPa (6,000 psi), out-performing the reference L2 (and H1, S1) portland cement based concrete. The 90-day compressive strength of Class C fly ash based concrete with PCE reached the highest compressive strength of 49.0 MPa (7,107 psi). Most of concrete with SCM had a 1-day compressive strength of less than 10 MPa (1,500 psi). After the 7-day age, the strength development and overall performance of concrete with slag cement was similar to the corresponding reference concrete.

Concrete with Class F fly ash had a slow strength development and only the use of PCE admixture enabled to produce concrete with performance comparable to the reference. Actual 90-day strength of this concrete was 48.1 MPa (6,976 psi), which is similar to the corresponding Class C concrete with PCE.

In the case of concrete with a low cement content of 250 kg/m^3 (420 lb/yd^3), the use of the PCE admixture enabled to achieve a 1-day compressive strength of more than 10 MPa (1,450 psi), *Table 47*. Concrete with mid-range plasticizer reached the compressive strength benchmark only at the age of 7 days and even only at the age of 28 days for H1 cement based concrete.

For the most of the low cement concrete of the 90-day strength was around the 30 MPa (4,500 psi) benchmark; only concrete based on the H1 cement, mid-range plasticizer and L2 cement-Class F fly ash combination had 90-day strength of 23.3 MPa (3,379 psi) and 28.8 MPa (4,177 psi), respectively.

The best performance in this group was achieved by Class C fly ash concrete with PCE admixture, which reached 35.5 MPa (5,150 psi) at the age of 90 days. The 1-year strength achieved by Class C fly ash concrete with PCE admixture was 37.4 MPa (5,424 psi).

The modulus of rupture response followed the compressive strength trends and had a relationship similar to that established for southern aggregates (Appendix 2).

Table 42. Optimized concrete mixture proportions based on northern aggregates and total cementitious materials of 280 kg/m^3 (470 lb/yd^3)

a) SI units

Cement Factor	Mix ID		Dosage of Chemical Admixtures, %				Mixture Proportions, kg/m^3								
							Cement	SCM	Aggregates (SSD)				Admixtures		Total Water
			PCE	SNF	MR	AE			CA	IA	FA	Total	WR HRWR	Air Entraining	
280 kg/m^3 (470 lb/yd^3)	**L-N-M**	B14	-	-	0.15	0.010	280	0	1003	199	761	1964	1.038	0.227	126
	L-N-N	B13	-	0.40	-	0.015	280	0	1000	198	759	1958	2.768	0.340	126
	L-N-P	B12	0.15	-	-	0.0125	280	0	1023	203	776	2001	1.230	0.283	112
	L-N-M-S	B23		-	0.15	0.010	140	140	1000	198	759	1957	1.038	0.113	126
	L-N-N-S	B22		0.40	-	0.010	140	140	997	198	756	1951	2.768	0.227	126
	L-N-P-S	B18	0.15	-	-	0.020	140	140	1018	202	773	1993	1.230	0.453	112
	L-N-M-C	B17	-	-	0.15	0.005	195	84	1018	202	773	1992	1.038	0.113	112
	L-N-N-C	B16	-	0.40	-	0.010	195	84	1015	201	770	1987	2.768	0.227	112
	L-N-P-C	B15	0.15	-	-	0.005	195	84	1037	206	787	2030	1.230	0.113	98
	L-N-M-F	B20	-	-	0.15	0.010	195	84	993	197	754	1944	1.038	0.227	126
	L-N-N-F	B21	-	0.40	-	0.010	195	84	993	197	754	1944	1.038	0.227	126
	L-N-P-F	B19	0.15	-	-	0.150	195	84	1032	204	783	2019	1.230	0.340	98
	H-N-M	B3	-	-	0.15	0.005	280	0	1023	203	776	2002	1.038	0.113	112
	H-N-N	B2	-	0.40	-	0.015	280	0	1020	202	774	1996	2.768	0.340	112
	H-N-P	B1	0.15	-	-	0.015	280	0	1022	203	776	2001	1.230	0.340	112
	S-N-M	B6	-	-	0.15	0.005	280	0	995	197	765	1956	1.038	0.113	126
	S- N-N	B5	-	0.40	-	0.025	280	0	991	196	758	1946	2.768	0.567	126
	S-N-P	B4	0.15	-	-	0.050	280	0	1021	202	775	1999	1.230	1.134	112

b) US Customary Units

Cement Factor	Mix ID		Dosage of Chemical Admixtures, %				Mixture Proportions, lb/yd^3								
							Cement	SCM	Aggregates (SSD)				Admixtures		Total Water
			PCE	SNF	MR	AE			CA	IA	FA	Total	WR HRWR	Air Entraining	
280 kg/m^3 (470 lb/yd^3)	**L-N-M**	B14	-	-	0.15	0.010	470	0	1691	335	1283	3310	1.750	0.382	212
	L-N-N	B13	-	0.40	-	0.015	470	0	1686	334	1280	3300	4.666	0.573	212
	L-N-P	B12	0.15	-	-	0.0125	470	0	1724	342	1308	3373	2.074	0.478	188
	L-N-M-S	B23		-	0.15	0.01	235	235	1685	334	1279	3298	1.750	0.191	212
	L-N-N-S	B22		0.40	-	0.010	235	235	1680	333	1275	3288	4.666	0.382	212
	L-N-P-S	B18	0.15	-	-	0.020	235	235	1717	340	1303	3360	2.074	0.764	188
	L-N-M-C	B17	-	-	0.15	0.005	329	141	1716	340	1302	3358	1.750	0.191	188
	L-N-N-C	B16	-	0.40	-	0.010	329	141	1711	339	1298	3349	4.666	0.382	188
	L-N-P-C	B15	0.15	-	-	0.005	329	141	1748	347	1327	3422	2.074	0.191	165
	L-N-M-F	B20	-	-	0.15	0.010	329	141	1674	332	1270	3277	1.750	0.382	212
	L-N-N-F	B21	-	0.40	-	0.010	329	141	1674	332	1270	3277	1.750	0.382	212
	L-N-P-F	B19	0.15	-	-	0.150	329	141	1739	345	1319	3403	2.074	0.573	165
	H-N-M	B3	-	-	0.15	0.005	470	0	1724	342	1308	3374	1.750	0.191	188
	H-N-N	B2	-	0.40	-	0.015	470	0	1719	341	1304	3364	4.666	0.573	188
	H-N-P	B1	0.15	-	-	0.015	470	0	1723	342	1308	3373	2.074	0.573	188
	S-N-M	B6	-	-	0.15	0.005	470	0	1677	331	1289	3298	1.750	0.191	212
	S- N-N	B5	-	0.40	-	0.025	470	0	1671	331	1278	3280	4.666	0.955	212
	S-N-P	B4	0.15	-	-	0.050	470	0	1722	341	1306	3369	2.074	1.911	188

Table 43. The fresh properties of concrete mixtures based on northern aggregates and total cementitious materials of 280 kg/m^3 (470 lb/yd^3)

Cement Factor	Mix ID		W/CM	Vol. of AGG Ratio	Yield	Air, %	Concrete Temp., F	Bulk Density		Slump, mm		Slump, in	
								kg/m^3	lb/ft^3	0 min	30 mins	0 min	30 mins
280 kg/m^3 (470 lb/yd^3)	**L-N-M**	B14	0.45	0.726	0.946	4.0	67	2369	148	16	12	0.6	0.5
	L-N-N	B13	0.45	0.724	0.945	4.4	69	2363	147	29	24	1.1	0.9
	L-N-P	B12	0.40	0.740	0.973	7.0	70	2392	149	158	53	6.2	2.1
	L-N-M-S	B23	0.45	0.723	0.953	4.1	71	2361	147	25	0	1.0	0.0
	L-N-N-S	B22	0.45	0.721	0.945	4.0	69	2356	147	66	38	2.6	0.2
	L-N-P-S	B18	0.40	0.737	0.975	6.1	69	2384	149	133	20	5.2	0.8
	L-N-M-C	B17	0.40	0.737	0.970	6.0	71	2383	149	27	16	1.0	0.6
	L-N-N-C	B16	0.40	0.734	0.945	4.0	70	2378	148	31	24	1.2	0.9
	L-N-P-C	B15	0.35	0.750	0.970	5.7	70	2407	150	75	35	2.9	1.4
	L-N-M-F	B20	0.45	0.719	0.991	8.0	71	2349	147	90	50	3.5	1.9
	L-N-N-F	B21	0.45	0.719	0.948	4.3	71	2349	147	41	31	1.6	1.2
	L-N-P-F	B19	0.35	0.743	0.959	5.4	67	2388	149	25	10	1.0	0.4
	H-N-M	B3	0.40	0.740	1.009	7.6	65	2339	146	54	20	2.1	0.8
	H-N-N	B2	0.40	0.738	0.963	5.0	65	2445	153	163	45	6.4	1.8
	H-N-P	B1	0.40	0.740	0.981	5.2	63	2405	150	163	45	6.4	1.8
	S-N-M	B6	0.45	0.726	0.992	8.1	67	2361	147	68	30	2.7	1.2
	S- N-N	B5	0.45	0.723	0.974	7.0	67	2351	147	48	25	1.9	1.0
	S-N-P	B4	0.40	0.739	1.014	5.6	67	2390	149	16	10	0.6	0.4

Table 44. The mechanical performance of concrete based on northern aggregates and cementitious materials of 280 kg/m^3 (470 lb/yd^3)

a) SI Units

Cement Factor	Mix ID		W/CM	Compressive Strength, MPa at the Age of						Modulus of Rupture, MPa at the Age of			
				1 day	3 days	7 days	28 days	90 days	360 days	3 days	7 days	28 days	90 days
279 kg/m^3 (470 lb/yd^3)	**L-N-M**	B14	0.45	10.6	25.0	28.1	34.9	36.1	42.0	5.0	5.6	5.9	5.9
	L-N-N	B13	0.45	12.6	25.2	32.2	39.6	42.1	47.6	4.9	6.0	6.1	5.7
	L-N-P	B12	0.40	21.6	29.6	33.0	39.2	40.8	44.5	4.9	5.3	5.9	5.8
	L-N-M-N	B23	0.45	5.6	17.9	22.5	38.0	45.4	46.9	3.9	5.8	6.7	7.3
	L-N-N-S	B22	0.45	4.9	15.9	25.7	40.2	44.3	52.0	4.1	5.3	6.5	6.7
	L-N-P-S	B18	0.40	7.1	18.8	23.7	29.7	34.8	35.1	4.1	4.6	6.0	6.0
	L-N-M-C	B17	0.40	6.4	22.2	32.4	41.8	42.7	49.9	4.3	5.2	5.6	6.0
	L-N-N-C	B16	0.40	6.7	22.2	32.8	40.8	45.3	49.1	4.3	5.8	5.6	8.8
	L-N-P-C	B15	0.35	11.5	28.1	38.3	45.7	49.0	58.5	5.5	5.6	6.5	7.1
	L-N-M-F	B20	0.45	4.0	10.1	16.3	18.7	29.2	34.5	2.7	3.6	4.4	5.0
	L-N-N-F	B21	0.45	3.8	12.2	17.5	25.3	32.6	41.7	2.5	3.8	5.2	6.5
	L-N-P-F	B19	0.35	9.9	25.8	32.8	40.4	48.1	-	4.4	4.5	7.7	6.7
	H-N-M	B3	0.40	13.3	21.7	27.1	32.7	33.8	36.5	4.2	4.8	5.4	6.9
	H-N-N	B2	0.40	15.1	27.1	31.0	37.4	39.5	47.6	5.1	5.4	5.6	5.9
	H-N-P	B1	0.40	17.1	25.2	30.4	35.6	38.3	43.5	4.6	5.7	5.8	6.0
	S-N-M	B6	0.45	11.0	17.3	21.1	33.0	30.7	32.9	4.0	4.6	5.1	5.2
	S- N-N	B5	0.45	12.0	19.0	29.5	30.5	31.9	35.6	4.5	4.6	5.4	4.9
	S-N-P	B4	0.40	17.2	26.2	29.8	37.4	41.4	49.9	5.2	5.9	6.7	6.7

b) US Customary Units

Cement Factor	Mix ID		W/CM	Compressive Strength, psi at the Age of						Modulus of Rupture, psi at the Age of			
				1 day	3 days	7 days	28 days	90 days	360 days	3 days	7 days	28 days	90 days
279 kg/m^3 (470 lb/yd^3)	**L-N-M**	B14	0.45	1537	3626	4076	5062	5236	6092	725	812	856	856
	L-N-N	B13	0.45	1827	3655	4670	5743	6106	6904	711	870	885	827
	L-N-P	B12	0.40	3133	4293	4786	5685	5918	6454	711	769	856	841
	L-N-M-N	B23	0.45	812	2596	3263	5511	6585	6802	566	841	972	1059
	L-N-N-S	B22	0.45	711	2306	3727	5831	6425	7542	595	769	943	972
	L-N-P-S	B18	0.40	1030	2727	3437	4308	5047	5091	595	667	870	870
	L-N-M-C	B17	0.40	928	3220	4699	6063	6193	7237	624	754	812	870
	L-N-N-C	B16	0.40	972	3220	4757	5918	6570	7121	624	841	812	1276
	L-N-P-C	B15	0.35	1668	4076	5555	6628	7107	8485	798	812	943	1030
	L-N-M-F	B20	0.45	580	1465	2364	2712	4235	5004	392	522	638	725
	L-N-N-F	B21	0.45	551	1769	2538	3669	4728	6048	363	551	754	943
	L-N-P-F	B19	0.35	1436	3742	4757	5860	6976	-	638	653	1117	972
	H-N-M	B3	0.40	1929	3147	3931	4743	4902	5294	609	696	783	1001
	H-N-N	B2	0.40	2190	3931	4496	5424	5729	6904	740	783	812	856
	H-N-P	B1	0.40	2480	3655	4409	5163	5555	6309	667	827	841	870
	S-N-M	B6	0.45	1595	2509	3060	4786	4453	4772	580	667	740	754
	S- N-N	B5	0.45	1740	2756	4279	4424	4627	5163	653	667	783	711
	S-N-P	B4	0.40	2495	3800	4322	5424	6005	7237	754	856	972	972

Table 45. Optimized concrete mixture proportions based on northern aggregates and total cementitious materials of 250 kg/m^3 (420 lb/yd^3)

a) SI units

Cement Factor	Mix ID		Dosage of Chemical Admixtures, %				Mixture Proportions, kg/m^3								
							Cement	SCM	Aggregates (SSD)				Admixtures		Total Water
			PCE	SNF	MR	AE			CA	IA	FA	Total	WR HRWR	Air Entraining	
250 kg/ m^3 (420 lb/yd^3)	**L-N-M-R**	B27	-	-	0.15	0.005	250	0	1018	202	772	1992	0.928	0.101	125
	L-N-P-R	B28	0.15	-	-	0.010	250	0	1026	203	779	2008	1.099	0.203	118
	L-N-P-C-R	B25	0.15	-	-	0.005	174	75	1039	206	789	2034	1.099	0.101	106
	L-N-P-S-R	B26	0.15	-	-	0.015	125	125	1031	204	783	2018	1.099	0.304	112
	L-N-P-F-R	B24	0.15	-	-	0.005	175	75	1026	203	779	2008	1.099	0.101	112
	H-N-M-R	B10	-	-	0.15	0.025	250	0	1026	203	778	2008	0.928	0.507	118
	H-N-P-R	B9	0.15	-	-	0.010	250	0	1035	205	785	2025	1.099	0.203	112
	S-N-M-R	B8	-	-	0.15	0.003	250	0	1018	201	782	2001	0.928	0.051	118
	S-N-P-R	B7	0.15	-	-	0.015	250	0	1026	203	779	2008	1.099	0.304	118

b) US Customary Units

Cement Factor	Mix ID		Dosage of Chemical Admixtures, %				Mixture Proportions, lb/yd^3								
							Cement	SCM	Aggregates (SSD)				Admixtures		Total Water
			PCE	SNF	MR	AE			CA	IA	FA	Total	WR HRWR	Air Entraining	
250 kg/ m^3 (420 lb/yd^3)	**L-N-M-R**	B27	-	-	0.15	0.005	420	0	1716	340	1302	3358	1.563	0.171	210
	L-N-P-R	B28	0.15	-	-	0.010	420	0	1730	343	1313	3385	1.853	0.341	200
	L-N-P-C-R	B25	0.15	-	-	0.005	294	126	1752	347	1329	3429	1.853	0.171	179
	L-N-P-S-R	B26	0.15	-	-	0.015	210	210	1738	345	1319	3402	1.853	0.512	189
	L-N-P-F-R	B24	0.15	-	-	0.005	294	126	1729	343	1312	3384	1.853	0.171	189
	H-N-M-R	B10	-	-	0.15	0.025	420	0	1729	343	1312	3384	1.563	0.854	200
	H-N-P-R	B9	0.15	-	-	0.010	420	0	1744	346	1324	3414	1.853	0.341	189
	S-N-M-R	B8	-	-	0.15	0.003	420	0	1715	339	1319	3373	1.563	0.085	200
	S-N-P-R	B7	0.15	-	-	0.015	420	0	1730	343	1312	3385	1.853	0.512	200

Table 46. The fresh properties of concrete mixtures based on northern aggregates and total cementitious materials of 250 kg/m^3 (420 lb/yd^3)

Cement Factor	Mix ID		W/CM	Vol. of AGG Ratio	Yield	Air, %	Concrete Temp., F	Bulk Density		Slump, mm		Slump, in	
								kg/m^3	lb/ft^3	0 min	30 mins	0 min	30 mins
250 kg/m^3 (420 lb/yd^3)	**L-N-M-R**	B27	0.500	0.736	0.971	5.6	71	2366	148	35	5	1.4	0.2
	L-N-P-R	B28	0.475	0.742	1.010	8.2	75	2376	148	70	45	2.8	1.8
	L-N-P-C-R	B25	0.425	0.752	0.977	5.1	71	2390	149	80	25	3.1	1.0
	L-N-P-S-R	B26	0.450	0.746	0.992	7.6	72	2380	149	200	100	7.9	3.9
	L-N-P-F-R	B24	0.450	0.742	0.979	6.1	71	2370	148	175	95	6.9	3.7
	H-N-M-R	B10	0.475	0.742	1.013	8.5	67	2376	148	136	70	5.4	2.8
	H-N-P-R	B9	0.450	0.749	0.993	6.6	68	2387	149	104	57	4.1	2.2
	S-N-M-R	B8	0.475	0.743	0.974	6.6	66	2369	148	56	25	2.2	1.0
	S-N-P-R	B7	0.475	0.742	0.991	6.6	68	2376	148	35	30	1.4	1.2

Table 47. The mechanical performance of concrete based on northern aggregates and cementitious materials of 250 kg/m^3 (420 lb/yd^3)

a) SI Units

Cement Factor	Mix ID		W/CM	Compressive Strength, MPa at the Age of						Modulus of Rupture, MPa at the Age of			
				1 day	3 days	7 days	28 days	90 days	360 days	3 days	7 days	28 days	90 days
250 kg/m^3 (420 lb/yd^3)	**L-N-M-R**	B27	0.500	6.8	16.9	23.9	28.6	31.8	33.8	4.1	5.1	5.4	5.3
	L-N-P-R	B28	0.475	10.4	21.4	25.5	26.4	30.0	38.2	4.5	6.8	7.3	4.9
	L-N-P-C-R	B25	0.425	5.5	18.5	24.2	31.5	35.5	37.4	4.4	4.9	4.9	5.6
	L-N-P-S-R	B26	0.450	4.2	11.8	18.5	25.5	29.9	30.6	2.9	4.1	5.4	6.5
	L-N-P-F-R	B24	0.450	4.4	10.9	15.9	19.9	28.8	34.9	3.4	4.6	4.6	5.2
	H-N-M-R	B10	0.475	7.0	14.6	17.6	21.7	23.3	23.8	3.1	4.0	3.8	4.6
	H-N-P-R	B9	0.450	15.7	26.0	26.9	30.6	32.3	36.1	4.8	4.7	5.1	5.4
	S-N-M-R	B8	0.475	11.6	19.0	23.0	30.0	33.9	37.0	4.1	5.0	5.9	6.0
	S-N-P-R	B7	0.475	10.3	16.8	20.5	27.1	30.9	32.9	3.8	4.7	5.6	5.7

b) US Customary Units

Cement Factor	Mix ID		W/CM	Compressive Strength, psi at the Age of						Modulus of Rupture, psi at the Age of			
				1 day	3 days	7 days	28 days	90 days	360 days	3 days	7 days	28 days	90 days
250 kg/m^3 (420 lb/yd^3)	**L-N-M-R**	B27	0.500	986	2451	3466	4148	4612	4902	595	740	783	769
	L-N-P-R	B28	0.475	1508	3104	3698	3829	4351	5540	653	986	1059	711
	L-N-P-C-R	B25	0.425	798	2683	3510	4569	5149	5424	638	711	711	812
	L-N-P-S-R	B26	0.450	609	1711	2683	3698	4337	4438	421	595	783	943
	L-N-P-F-R	B24	0.450	638	1581	2306	2886	4177	5062	493	667	667	754
	H-N-M-R	B10	0.475	1015	2118	2553	3147	3379	3452	450	580	551	667
	H-N-P-R	B9	0.450	2277	3771	3902	4438	4685	5236	696	682	740	783
	S-N-M-R	B8	0.475	1682	2756	3336	4351	4917	5366	595	725	856	870
	S-N-P-R	B7	0.475	1494	2437	2973	3931	4482	4772	551	682	812	827

4.4.7. Concrete with Southern Aggregates: Length Change

The length change data for concrete based on southern aggregate are reported in *Table 48* to *Table 51*. It can be observed that the most of the length change due to drying shrinkage is within the range of $2.0x10^{-4}$ mm/mm (in/in) to $6.0x10^{-4}$ mm/mm (in/in), *Figure 53a*. Some of the concrete types produced at lower W/CM of 0.4 and less can be characterized by lower 28-day shrinkage of less than $3.4x10^{-4}$ mm/mm. However, slag cement based concrete with SNF admixture, even at relatively high W/CM of 0.43, demonstrated very low shrinkage of $2.1x10^{-4}$ mm/mm.

Most of the concrete with SNF and mid-range plasticizing admixtures had higher length reduction due to drying; these concrete types were often produced at higher W/CM ratio vs. PCE based concrete. The highest ultimate (360- day) shrinkage was achieved by concrete based on S2 cement.

Generally, the addition of SCM such as slag cement or Class F fly ash resulted in concrete with reduced shrinkage vs. portland cement concrete. Actually, some of these concrete types started to expand slightly after 90- day period, adding up to 25% expansion after drying at the age of 360 days (vs. 90- day values). The addition of Class C fly ash increases the shrinkage of concrete which keeps increasing over 90- day period (similarly to the reference BB04).

Due to a relatively high W/CM > 0.40, concrete produced at low cementitious material content of 250 kg/m^3 (420 lb/yd^3) had a high value of length change, often more than $3.5x10^{-4}$ mm/mm at the age of 28 days, over $4.5x10^{-4}$ mm/mm at the age of 90 days, and reaching up to $6.0x10^{-4}$ mm/mm at the age of 360 days.

Table 48. The length change of concrete based on southern aggregates and cementitious materials of 280 kg/m^3 (470 lb/yd^3)

Cement Factor	Mix ID		W/C	Vol. of AGG	Length Change due to Drying, mm/mm (in/in), at the Age, days								
					4	5	6	7	14	28	60	90	360
280 kg/m^3 (470 lb/yd^3)	**L-S-M**	BB04	0.42	0.678	-	-	-	-9.0E-05	-3.4E-04	-3.8E-04	0.0E+00	-4.1E-04	-5.0E-04
	L-S-N	BB09	0.43	0.676	-	-	-	-1.3E-04	-2.1E-04	-3.0E-04	0.0E+00	-3.8E-04	-4.1E-04
	L-S-P	BB13	0.37	0.692	-	-	-	-1.2E-04	-2.7E-04	-3.1E-04	0.0E+00	-3.0E-04	-3.2E-04
	L-S-M-S	BB02	0.42	0.675	-	-	-	-1.6E-04	-3.9E-04	-4.4E-04	0.0E+00	-4.8E-04	-4.1E-04
	L-S-N-S	BB08	0.43	0.673	-	-	-	-8.0E-05	-1.8E-04	-2.1E-04	0.0E+00	-2.1E-04	-3.8E-04
	L-S-P-S	BB11	0.37	0.689	-	-	-	-1.4E-04	-1.9E-04	-2.7E-04	0.0E+00	-3.4E-04	-1.5E-04
	L-S-M-C	BB06	0.37	0.689	-	-	-	-3.0E-04		-3.9E-04	0.0E+00	-4.1E-04	-5.6E-04
	L-S-N-C	BB07	0.38	0.686	-	-	-	-1.3E-04	-1.9E-04	-2.3E-04	0.0E+00	-2.8E-04	-4.4E-04
	L-S-P-C	BB10	0.32	0.702	-	-	-	-1.7E-04	-2.8E-04	-3.7E-04	0.0E+00	-3.6E-04	-3.4E-04
	L-S-M-F	BB05	0.42	0.671	-	-	-	-1.4E-04	-2.9E-04	-3.5E-04	0.0E+00	-3.4E-04	-3.4E-04
	L-S-N-F	BB03	0.43	0.668	-	-	-	-2.2E-04	-1.9E-04	-4.3E-04	0.0E+00	-4.8E-04	-3.1E-04
	L-S-P-F	BB12	0.32	0.698	-	-	-	-1.4E-04	-2.1E-04	-2.1E-04	0.0E+00	-2.6E-04	-2.2E-04
	H-S-M	BB19	0.37	0.692	-2.0E-03	-	-1.0E-04	-1.4E-04	-1.8E-04	-3.3E-04	-4.0E-04	-4.8E-04	-3.7E-04
	H-S-N	BB18	0.38	0.690	-1.4E-04	-	-1.6E-04	-	-2.5E-04	-3.6E-04	-4.8E-04	-5.0E-04	-5.6E-04
	H-S-P	BB17	0.37	0.692	-2.0E-05	-7.5E-05	-1.4E-04	-	-2.5E-04	-3.0E-04	-4.3E-04	-4.6E-04	-3.7E-04
	S-S-M	BB16	0.42	0.678	-4.5E-05	-5.7E-05	-2.5E-04	-1.3E-04	-2.7E-04	-3.8E-04	-5.0E-04	-5.7E-04	-5.2E-04
	S-S-N	BB15	0.43	0.676	-4.5E-05	-1.8E-04	0.0E+00	-2.6E-04	-2.8E-04	-4.2E-04	-5.6E-04	-6.6E-04	-6.2E-04
	S-S-P	BB14	0.37	0.691	-	-	-1.8E-04	-	-3.4E-04	-3.9E-04	0.0E+00	-6.2E-04	-5.5E-04

Table 49. The length change of concrete based on southern aggregates and cementitious materials of 250 kg/m^3 (420 lb/yd^3)

Cement Factor	Mix ID		W/C	Vol. of AGG	Length Change due to Drying, mm/mm (in/in), at the Age, days								
					4	5	6	7	14	28	60	90	360
250 kg/m^3 (420 lb/yd^3)	**L-S-M-R**	BB20	0.45	0.691	-	-1.0E-04	-1.3E-04	-1.7E-04	-2.6E-04	-4.2E-04	-5.2E-04	-5.9E-04	-6.0E-04
	L-S-P-R	BB21	0.43	0.697	-1.1E-04	-	-1.5E-04	-1.8E-04	-2.7E-04	-3.5E-04	-	-4.6E-04	-4.9E-04
	L-S-P-C-R	BB22	0.38	0.707	-1.3E-04	-1.8E-04	-2.0E-04	-2.3E-04	-2.8E-04	-4.2E-04	-5.3E-04	-5.2E-04	-5.2E-04
	L-S-P-S-R	BB23	0.40	0.701	-1.2E-04	-1.4E-04	-1.6E-04	-2.1E-04	-2.3E-04	-3.6E-04	-4.5E-04	-4.7E-04	-4.8E-04
	L-S-P-F-R	BB24	0.41	0.696	-5.0E-05	-6.0E-05	-1.1E-04	-2.2E-04	-2.5E-04	-3.1E-04	-4.8E-04	-4.5E-04	-4.9E-04
	H-S-M-R	BB29	0.41	0.697	-	-	-0.9E-04	-1.9E-04	-2.7E-04	-4.3E-04	-5.2E-04	-5.8E-04	-6.0E-04
	H-S-P-R	BB27	0.41	0.703	-6.3E-05	-1.0E-04	-1.4E-04	-2.4E-04	-3.2E-04	-3.3E-04	-5.0E-04	-5.3E-04	-5.5E-04
	S-S-M-R	BB28	0.42	0.698	-7.0E-05	-1.3E-04	0.0E+00	-1.7E-04	-3.0E-04	-4.3E-04	-4.6E-04	-5.4E-04	-5.8E-04
	S-S-P-R	BB26	0.41	0.697	-2.0E-05	-6.7E-05	-1.2E-04	-1.4E-04	-1.9E-04	-3.5E-04	-5.5E-04	-5.6E-04	-5.7E-04

4.4.8. Concrete with Northern Aggregates: Length Change

The length change due to drying shrinkage of concrete based on northern aggregates is reported in *Table 50* and *Table 51*. It can be observed that at the 28-day age, the most of the investigated concrete had a length change of around 4.0×10^{-4} mm/mm, *Figure 48*. Obviously, the W/CM ratio and cementitious materials content were the most influential factors affecting the shrinkage. Generally, concrete with SCM based on L2 cement had lower shrinkage. However, these compositions also had a reduced water-to-cement ratio. The use of slag cement, especially in combination with mid-range plasticizers and PCE, resulted in very low shrinkage strains of 3.0×10^{-4} mm/mm. The use of H1 and L2 cements and mid-range plasticizer resulted in 90-day shrinkage of up to 3.5×10^{-4} mm/mm and 4.3×10^{-4} mm/mm, respectively. The length change was sensitive to the type of cement used, as S1 cement had considerably higher shrinkage, especially after 90- day age, reaching the 360- day strains of up to 7.9×10^{-4} mm/mm. After exposure to drying, at the age of 360 days concrete with mid-range plasticizers and SNF resulted in a higher shrinkage strain (often more than 5.0×10^{-4} mm/mm) likely due to the higher W/CM ratio used in these concrete types. The shrinkage of other concrete types based on northern aggregates and low cementitious material content of 250 kg/m3 (420 lb/yd3) followed similar trends. The key parameters affecting the length change were the same: W/CM ratio, cement type and the type of SCM (*Table 42* and *Table 45*).

Due to lower W/CM used, the concrete based on southern aggregates had lower ultimate shrinkage vs. concrete based on northern aggregates, *Figure 48*. However, the observed values were slightly exceeding the limits predicted by ACI 224R.

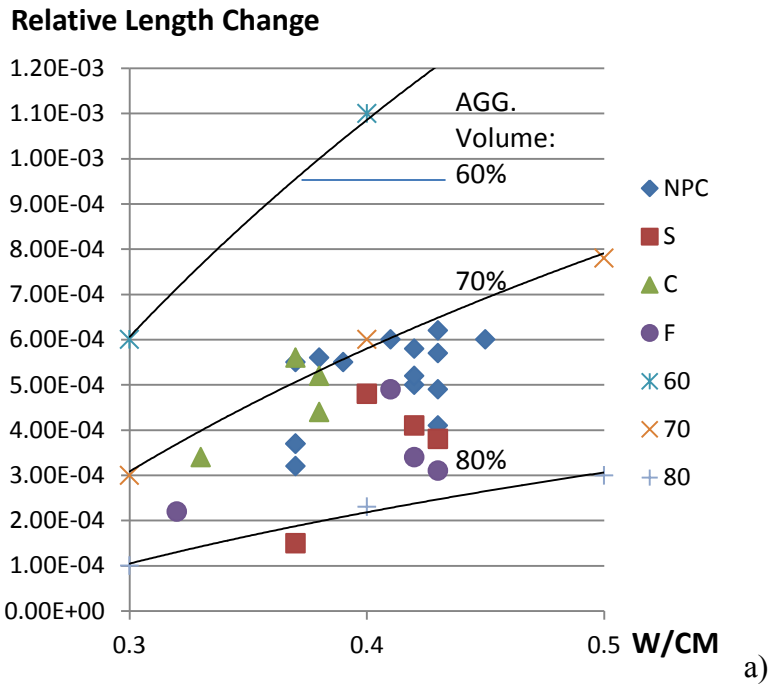

a)

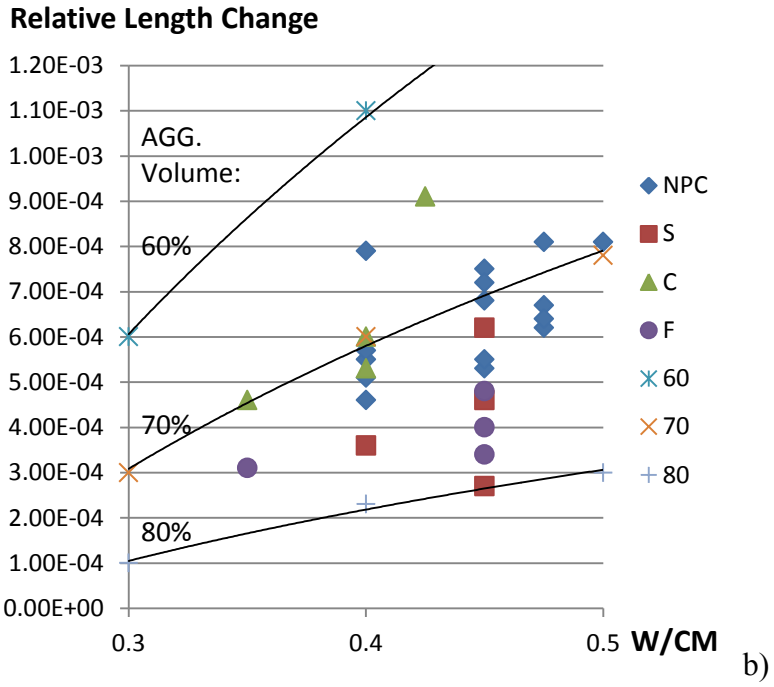

b)

Figure 48. The length change of investigated concrete at the age of 360 days: a) southern aggregates; b) northern aggregates, after ACI 224R and [119]

Table 50. The length change of concrete based on northern aggregates and cementitious materials of 280 kg/m³ (470 lb/yd³)

Cement Factor	Mix ID		W/C	Vol. of AGG	Length Change due to Drying, mm/mm (in/in), at the Age, days								
					4	5	6	7	14	28	60	90	360
280 kg/m³ (470 lb/yd³)	**L-N-M**	B14	0.45	0.726	-4.0E-05	-7.7E-05	-1.8E-04	-2.6E-04	-2.7E-04	-3.8E-04	-	-4.3E-04	-5.3E-04
	L-N-N	B13	0.45	0.724	-	-	-1.1E-04	-2.5E-04	-3.5E-04	-4.3E-04	-	-5.2E-04	-6.8E-04
	L-N-P	B12	0.40	0.740	-7.5E-05	-1.1E-04	-	-1.9E-04	-2.9E-04	-3.5E-04	-	-4.4E-04	-5.5E-04
	L-N-M-S	B23	0.45	0.723	-	-2.0E-04	-	-3.5E-04	-3.9E-04	-4.3E-04	-	-5.2E-04	-4.6E-04
	L-N-N-S	B22	0.45	0.721	-1.8E-04	-2.3E-04	-2.6E-04	-3.8E-04	-5.1E-04	-5.7E-04	-	-5.5E-04	-6.2E-04
	L-N-P-S	B18	0.40	0.737	-9.0E-05	6.7E-05	-	-1.5E-04	-2.2E-04	-3.0E-04	-	-2.6E-04	3.6E-03
	L-N-M-C	B17	0.40	0.737	-	-	-	-2.0E-04	-3.1E-04	-4.4E-04	-	-5.2E-04	-6.0E-04
	L-N-N-C	B16	0.40	0.734	-7.0E-05	-	-1.5E-04	-2.5E-04	-3.3E-04	-4.0E-04	-	-4.0E-04	-5.3E-04
	L-N-P-C	B15	0.35	0.750	-	-8.5E-05	0.0E+00	-2.3E-04	-2.8E-04	-3.3E-04	-	-3.3E-04	-4.6E-04
	L-N-M-F	B20	0.45	0.719	-	-	-1.2E-04	-1.7E-04	-3.4E-04	-	-	-4.7E-04	-4.8E-04
	L-N-N-F	B21	0.45	0.719	-7.0E-05	-	-	-1.2E-04	-3.2E-04	-	-	-3.9E-04	-4.0E-04
	L-N-P-F	B19	0.35	0.746	-	-8.5E-05	-9.5E-05	-	-2.6E-04	-	-	-3.5E-04	-3.1E-04
	H-N-M	B3	0.40	0.740	-4.7E-05	-	-	-2.2E-04	-2.9E-04	-3.5E-04	-	-3.5E-04	-5.1E-04
	H-N-N	B2	0.40	0.738	-1.0E-04	-1.1E-04	-1.2E-04	-2.3E-04	-3.7E-04	-3.9E-04	-	-4.1E-04	-5.7E-04
	H-N-P	B1	0.40	0.740	-7.1E-05	-7.3E-05	-8.7E-05	-1.8E-04	-2.8E-04	-4.1E-04	-	-4.3E-04	-4.6E-04
	S-N-M	B6	0.45	0.726	-1.7E-04	-1.9E-04	-2.3E-04	-3.5E-04	-5.0E-04	-5.3E-04	-	-5.9E-04	-7.5E-04
	S- N-N	B5	0.45	0.723	-1.8E-04	-	-1.9E-04	-4.5E-04	-	-4.6E-04	-	-5.4E-04	-7.2E-04
	S-N-P	B4	0.40	0.739	-1.0E-04	-1.1E-04	-1.7E-04	-3.0E-04	-3.6E-04	-3.9E-04	-	-4.4E-04	-7.9E-04

Table 51. The length change of concrete based on northern aggregates and cementitious materials of 250 kg/m^3 (420 lb/yd^3)

Cement Factor	Mix ID		W/C	Vol. of AGG	Length Change due to Drying, mm/mm (in/in), at the Age, days								
					4	5	6	7	14	28	60	90	360
250 kg/m^3 (420 lb/yd^3)	**L-N-M-R**	B27	0.500	0.736	-	-1.0E-05	-4.0E-05	-4.5E-05	-7.0E-05	-2.0E-04	-3.0E-04	-3.0E-04	-8.1E-04
	L-N-P-R	B28	0.475	0.742	-	-	-7.0E-05	-8.0E-05	-1.5E-04	-2.4E-04	-4.6E-04	-5.1E-04	-8.1E-03
	L-N-P-C-R	B25	0.425	0.752	-	-2.0E-05	-6.5E-05	-9.0E-05	-2.0E-04	-2.2E-04	-4.2E-04	-3.1E-04	-9.1E-04
	L-N-P-S-R	B26	0.450	0.746	-	-7.7E-05	-8.5E-05	-9.0E-05	-2.0E-04	-2.6E-04	-4.7E-04	-3.5E-04	-2.7E-04
	L-N-P-F-R	B24	0.450	0.742	-	-2.0E-05	-8.0E-05	-1.3E-04	-1.9E-04	-2.8E-04	-3.8E-04	-3.6E-04	-3.4E-04
	H-N-M-R	B10	0.475	0.742	-9.5E-05	-	-1.4E-04	-1.4E-04	-1.7E-04	-4.8E-04	-5.1E-04	-5.9E-04	-6.2E-04
	H-N-P-R	B9	0.450	0.749	-	-	-6.0E-05	-1.1E-04	-1.7E-04	-2.7E-04	-3.9E-04	-3.8E-04	-5.5E-04
	S-N-M-R	B8	0.475	0.743	-1.4E-04	-1.8E-04	-	-1.9E-04	-3.3E-04	-4.5E-04	-6.6E-04	-6.6E-04	-6.7E-04
	S-N-P-R	B7	0.475	0.742	-6.0E-05	-7.0E-05	-1.3E-04	-1.4E-04	-2.6E-04	-3.1E-04	-	-4.8E-04	-6.4E-04

5. DURABILITY PERFORMANCE

5.1. Air-Void Analysis

The volume of air tested for fresh and hardened concrete of selected mixtures is reported in *Figure 49*. The spacing factor values for investigated concrete are reported in *Figure 50*.

It can be observed that hardened air content is 2-4% higher than reported by the pressure method for fresh concrete based on southern aggregates (BB series). Considerable difference was observed for concrete based on northern aggregates (B series). With only few exceptions, for most of concrete tested, the air content was within the 6 to 10% range. Only a few concrete types had less than 6% of air when tested in fresh state. Concrete with reduced cementitious content (*-R series) was designed for higher air content as supported by the experiment.

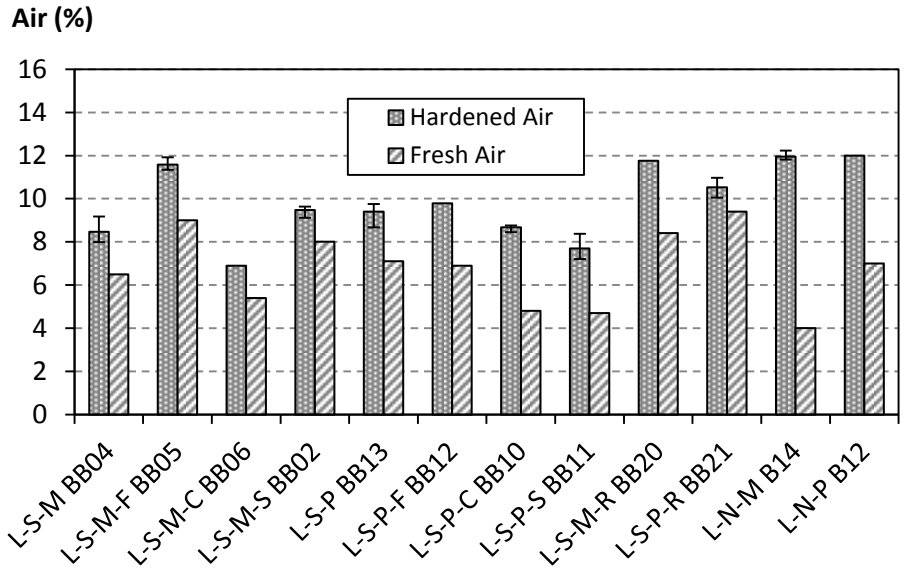

Figure 49. The comparison of air content for fresh and hardened concrete

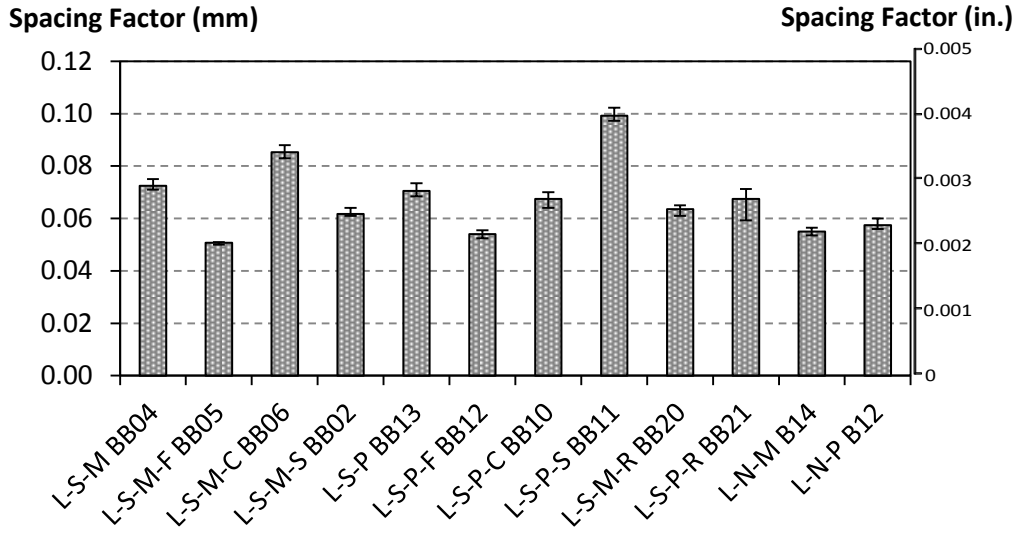

Figure 50. Spacing factor of investigated concrete

For durability performance, ASTM C666 requires the spacing factor to be less than 200 μm (0.008 in.). It can be observed that due to high air content, the spacing factor was within the limits of 50 to 120 μm (0.002 to 0.005 in.), which is significantly less than the standard limit ensuring very exceptional freeze-thaw resistance of developed concrete.

5.2. Concrete with Southern Aggregates: Durability Study

Almost all the concrete types with cementitious materials content of 280 kg/m3 (470 lb/yd^3) obtained lower chloride permeability (RCP) vs. the reference mixture (L-S-M) at the age 30 days and 90 days, *Figure 51*. These were characterized by "low" to "moderate" RCP values from 1,000 to 3,000 Coulombs (*Table 16*). Concrete based on H1 and S1 cements performed better than L1 concrete in terms of RCP with the charge reduced by up to 1000 Coulombs. At 90 days, concrete based on L1 cements with SCM had almost 50% lower permeability than the portland cement concrete (around or less

than 1000 Coulombs) and, due to pozzolanic effect, the Class F fly ash concrete obtained very significant reduction of permeability at 90 days as compared to the other concrete types.

The concrete based on Class F fly ash and slag cement had "very low" permeability of less than 1,000 Coulombs and so performed better than Class C concrete. For most of the cases, due to significant water reduction, the use of PCE admixture resulted in lower permeability vs. concrete produced with SNF and mid-range plasticizing admixtures.

Table 52. The durability of concrete based on southern aggregates and cementitious materials content of 280 kg/m^3 (470 lb/yd^3)

Cement Factor	Mix ID		W/CM	Fresh Air, %	RCP Charge Passed, Coulombs at the age of		Drop of RCP Charge, %	F/T Durability Factor, %	F/T Mass Loss, %
					30 days	90 days			
280 kg/ m^3 (470 lb/yd^3)	**L-S-M**	BB04	0.42	6.5	3220	2299	29	99	-0.10
	L-S-N	BB09	0.43	5.0	3416	2192	36	95	1.19
	L-S-P	BB13	0.37	7.1	2446	1897	22	100	-0.54
	L-S-M-S	BB02	0.42	8.0	1165	731	37	94	3.68
	L-S-N-S	BB08	0.43	7.1	1368	706	48	94	3.54
	L-S-P-S	BB11	0.37	4.7	1278	900	30	92	4.49
	L-S-M-C	BB06	0.37	5.4	1988	1045	47	93	3.82
	L-S-N-C	BB07	0.38	5.9	2263	1110	51	94	4.10
	L-S-P-C	BB10	0.32	4.8	1653	695	58	98	0.61
	L-S-M-F	BB05	0.42	9.0	3321	944	72	99	1.05
	L-S-N-F	BB03	0.43	9.5	2306	853	63	99	1.05
	L-S-P-F	BB12	0.32	6.9	1606	670	58	100	0.08
	H-S-M	BB19	0.37	4.5	2058	1333	35	97	0.99
	H-S-N	BB18	0.38	4.0	1939	1409	27	95	2.06
	H-S-P	BB17	0.37	8.5	2151	1647	23	100	-0.73
	S-S-M	BB16	0.42	6.6	2416	1503	38	100	0.22
	S-S-N	BB15	0.43	6.6	2344	1474	37	98	0.36
	S-S-P	BB14	0.37	6.2	1775	1308	26	98	0.64

Table 53. The durability of concrete based on southern aggregates and cementitious materials content of 250 kg/m^3 (420 lb/yd^3)

Cement Factor	Mix ID		W/CM	Fresh Air, %	RCP Charge Passed, Coulombs at the age of		Drop of RCP Charge, %	F/T Durability Factor, %	F/T Mass Loss, %
					30 days	90 days			
250 kg/ m^3 (420 lb/yd^3)	**L-S-M-R**	BB20	0.45	8.4	3058	2126	30	100	-0.07
	L-S-P-R	BB21	0.43	9.4	2768	2129	23	99	-0.53
	L-S-P-C-R	BB22	0.38	6.6	2119	1035	51	100	1.2
	L-S-P-S-R	BB23	0.40	5.9	934	577	38	98	1.76
	L-S-P-F-R	BB24	0.41	9.8	1964	949	52	97	1.54
	H-S-M-R	BB29	0.41	5.0	2050	1244	39	100	0.24
	H-S-P-R	BB27	0.41	8.0	2283	1936	15	100	-0.99
	S-S-M-R	BB28	0.42	7.4	2569	1768	31	100	-0.35
	S-S-P-R	BB26	0.41	9.9	1997	1107	45	100	0.11

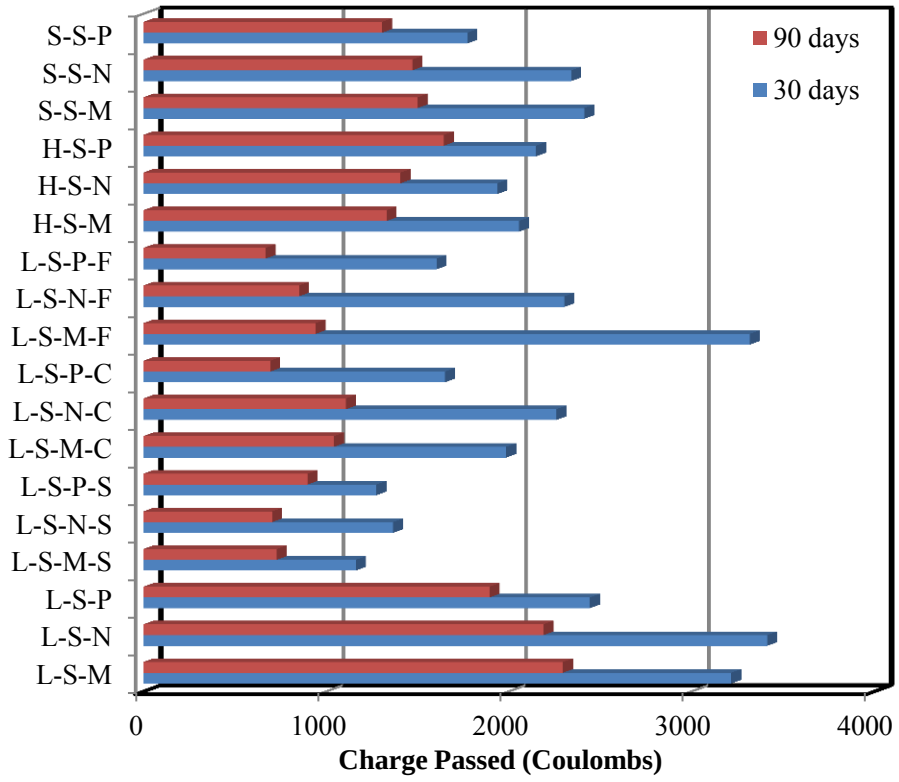

Figure 51. The RCP of concrete with cementitious materials content of 280 kg/m^3 (470 lb/yd^3)

Almost all the concrete types with cementitious materials contents of 250 kg/m^3 (420 lb/yd^3), obtained lower permeability than the reference (L-S-M) at both 30-day and 90-day ages (*Figure 52*). Concrete based on H1 and S1 cements performed better than L1 in terms of RCP. At 90 days, concrete with SCM had up to 50% lower permeability vs. reference portland cement based concrete (less than 1000 Coulombs), and concrete with Class F and C fly ash had the highest drop at 90 days when compared to other types of concrete. Concrete with slag performed better than Class F and C fly ash concrete at both testing ages and achieved the lowest permeability as compared to all other mixtures at any cement content.

Except for H1 cement reference concrete, at low cement content, the compositions with PCE achieved the lowest permeability vs. the corresponding concrete with SNF and mid-range plasticizing admixtures. The RCP of concrete with slag cement was the lowest, which may be due to a significant densification of the hardened matrix.

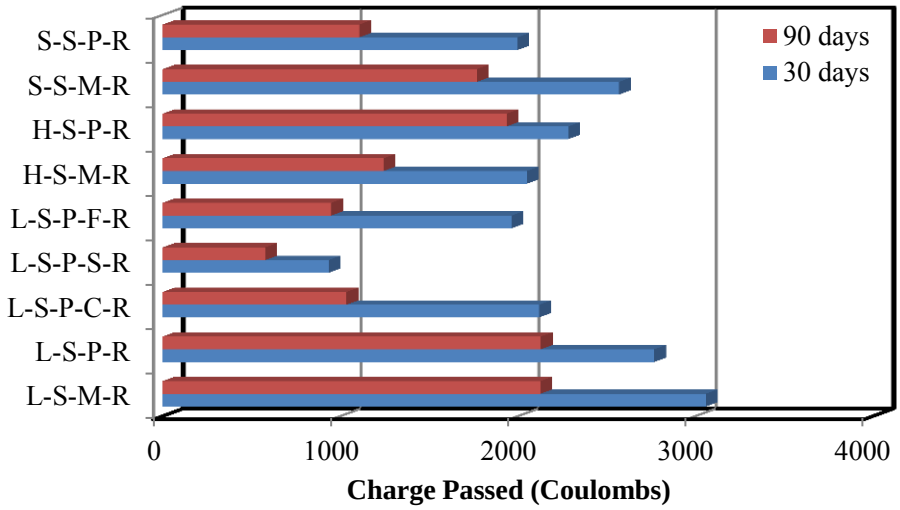

Figure 52. The RCP of concrete with cementitious materials content of 250 kg/m^3 (420 lb/yd^3)

This behavior can be explained by the use of reduced volumes of cementitious phase and lower permeability of aggregates. The higher porosity of the cementitious matrix associated with higher W/CM causes higher transport properties of the matrix; however, reduced volumes of the cementitious phase in the concrete can offset the effect of the W/CM ratio. Therefore, for the range of W/CM used, the permeability reduction is attributed to higher aggregate content. This indicates that the effect of the relative volumes of cementitious phase and aggregates in the mix is more significant than the permeability of the cementitious phase with higher transport properties.

The freezing and thawing resistance of investigated concrete is summarized in *Table 52* and *Table 53*. After 300 cycles, all tested concrete types (at both cement content levels) achieved a durability factor of more than 90% or higher and so passed the ASTM C666 benchmark of 60%.

However, maintaining DF of 60% does not necessarily represent extremely durable concrete. Northern American states can typically have up to 50 cycles per year, therefore, the benchmark of 300 cycles can guarantee adequate performance for only 6 years. Concrete containing slag (BB02, BB08, B11), Class C fly ash (BB06, BB07), concrete based on H1 cement (BB18, BB19) and reference mixture (BB09) demonstrated slightly lower durability compared to other types. Therefore, when tested for a large number of cycles (e.g., 1000), it can be anticipated that these concrete types can fail earlier than others. It can be observed that the mass loss of investigated concrete was less than 5%. As reported in *Figure 53* and *Figure 54*, after 300 cycles of freeze-thaw, a few concrete types had a small (about 1%) mass gain. This can be explained by densification of structure due to ongoing hydration of cement or crystallization of salt in the pores.

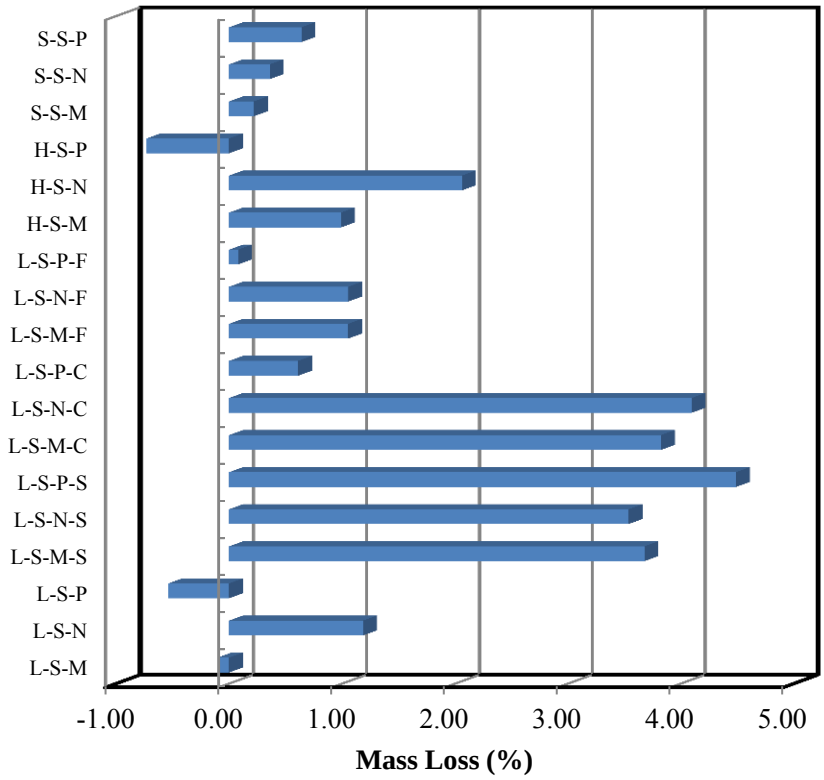

Figure 53. The mass loss of concrete with cementitious material content of 280 kg/m^3 (470 lb/yd^3) due to freezing and thawing exposure

5.3. Concrete with Northern Aggregates: Durability Study

The RCP of investigated concrete based on northern aggregates was at the level of about 2,000 Coulombs higher than that of the corresponding concrete based on southern aggregates (*Table 54* and *Table 55*). Higher permeability can be correlated to the conditions of the aggregates contact zone. For natural aggregates with smooth texture, lower surface area, and surface contamination, the formation of a weak interfacial transition zone (ITZ) is expected. Further research may be necessary to investigate this matter, especially the effects of aggregate surface contamination (see *Figure 14)*.

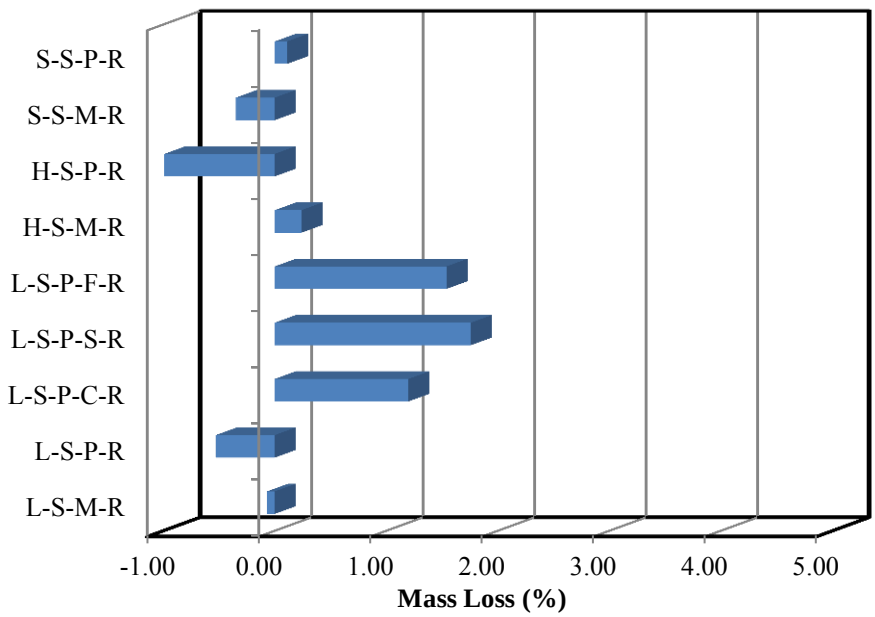

Figure 54. The mass loss of concrete with cementitious material content of 250 kg/m^3 (420 lb/yd^3) due to freezing and thawing exposure

Still, all investigated concrete types based on northern aggregates were characterized by "low" to "moderate" RCP values from 1,000 to 3,000 Coulombs *(Table 16)*. With portland cement based concrete (based on L2, H1, S1) used at cement factor 280 kg/m^3 (470 lb/yd^3), there was little to no change in RCP values with the extension of curing time from 30 to 90 days. The reduction of cementitious material to 250 kg/m^3 (420 lb/yd^3) resulted in a concrete with similar RCP performance. These observations confirm the hypothesis that the aggregate's ITZ plays a significant role in chloride transport.

The effects of W/CM ratio observed for concrete based on southern aggregates were also valid for northern aggregate concrete; however, due to the higher overall W/CM ratio used, there are only a few concrete types (e.g., with fly ash and PCE) that had a W/CM ratio of 0.35. The use of SCM contributed to the formation of concrete with

low permeability. The *best results, characterized by very low RCP of less than 1,000 Coulombs, were demonstrated by concrete based on slag cement and Class F fly ash used in combination with PCE superplasticizers*.

Table 54. The durability of concrete based on northern aggregates and cementitious materials content of 280 kg/m^3 (470 lb/yd^3)

Cement Factor	Mix ID		W/CM	Fresh Air, %	RCP Charge Passed, Coulombs at the age of		Drop of RCP Charge, %	F/T Durability Factor, %	F/T Mass Loss, %
					30 days	90 days			
280 kg/m^3 (470 lb/yd^3)	**L-N-M**	B14	0.45	4.1	3253	2737	16	99	0.3
	L-N-N	B13	0.45	4.4	3208	3031	5	95	1.5
	L-N-P	B12	0.40	6.5	2251	2138	5	99	-0.48
	L-N-M-S	B23	0.45	4.1	1894	910	52	95	4.2
	L-N-N-S	B22	0.45	4	1485	927	38	93	4.2
	L-N-P-S	B18	0.40	6.1	1522	1274	16	93	3.8
	L-N-M-C	B17	0.40	6	3836	1898	51	101	0.4
	L-N-N-C	B16	0.40	4	4512	2366	48	98	3.1
	L-N-P-C	B15	0.35	5.7	2704	1566	42	102	0.2
	L-N-M-F	B20	0.45	8	2661	1391	48	101	1.2
	L-N-N-F	B21	0.45	4.3	2949	1328	55	93	4.0
	L-N-P-F	B19	0.35	5.4	1544	757	51	95	3.3
	H-N-M	B3	0.40	7.6	2392	2005	16	101	-0.45
	H-N-N	B2	0.40	5	2280	2176	5	99	-0.14
	H-N-P	B1	0.40	5.2	2259	1988	12	98	0.14
	S-N-M	B6	0.45	8.1	2929	2562	13	100	-0.40
	S- N-N	B5	0.45	7	2956	2351	20	101	-0.41
	S-N-P	B4	0.40	5.6	1860	1491	20	100	-0.06

Most of the concrete types had air content greater than 5%, with a few exceeding 8%. Some concrete mixtures with SNF and mid-range plasticizer had an air volume within the range of 4-5%. The freeze-thaw tests demonstrated excellent performance of developed concrete types based on northern aggregates when tested up to 300 cycles. Still, some concrete types, mainly based on slag cement and with lower content of air, had lower performance (the DF of less than 95% and mass loss of more than 4%) vs. the

bulk of the investigated compositions. These concrete types meet the specifications; however, it can be expected that such materials can deteriorate at a faster rate and can fail after longer exposures. Potentially, some additional air entrainment over existing limits may help to improve the long-term freeze-thaw response; however, reduced performance can also be dictated by the type of cement hydrates formed in the presence of slag cement. Additional investigation may be necessary to address this matter.

Table 55. The durability of northern aggregates concrete with cementitious materials content of 250 kg/m^3 (420 lb/yd^3)

Cement Factor	Mix ID		W/CM	Fresh Air, %	RCP Charge Passed, Coulombs at the age of		Drop of RCP Charge, %	F/T Durability Factor, %	F/T Mass Loss, %
					30 days	90 days			
250 kg/m3 (420 lb/yd3)	**L-N-M-R**	B27	0.500	5.6	2907	2801	4	99	0.4
	L-N-P-R	B28	0.475	8.2	2606	2470	5	101	-0.5
	L-N-P-C-R	B25	0.425	5.1	3497	2194	37	102	0.1
	L-N-P-S-R	B26	0.450	7.6	1662	1095	34	83	5.1
	L-N-P-F-R	B24	0.450	6.1	3492	1792	49	100	1.4
	H-N-M-R	B10	0.475	8.5	3851	2769	28	101	0.17
	H-N-P-R	B9	0.450	6.6	2549	2358	7	100	-0.04
	S-N-M-R	B8	0.475	6.6	2930	2277	22	100	0.27
	S-N-P-R	B7	0.475	6.6	2916	2758	5	99	-0.10

6. CONCLUSIONS

Concrete mixtures can be effectively designed by optimizing two essential phases comprising the material: the aggregates and cement paste. For this project, the theoretical and experimental optimization of aggregates and cement paste was realized and validated by extensive concrete testing. As a result of optimization, the cement content was reduced by up to 18% vs. current WisDOT specifications for concrete mixtures that satisfy all other requirements.

6.1. Aggregate Optimization

Aggregate optimization can be realized by identification of the best blend through multiple criteria. The reported research included the evaluation of the effect of packing density on concrete performance. It is demonstrated that the aggregate packing alone can be used as an effective tool to optimize the aggregate blends for concrete designed for different applications.

It was proved that the power curves (PC) can be used as an effective tool for aggregate optimization. The mixtures with higher fine aggregate content can be fitted to smaller PC exponents such as 0.35 - 0.45, while binary mixtures and mixtures with a lower volume of fine aggregates are closer to power 0.5 - 0.7 gradings. The combined aggregate power grading optimized for the 0.45- power curve can serve as another criterion for optimal blends. The optimized combined grading curves can provide better packing arrangements achievable in concrete; and recommended optimal grading must fit within the range defined by 0.40- to 0.60- power curve limits. The ACI 211.1-95 or ACI

211.6T-14 concrete mixture proportioning methods can be used with optimized combined aggregates as demonstrated in Appendix 3 and 4.

The experimental results on packing degree and performance of concrete mixtures provided useful relationships for the selection of the best aggregate blends. High density mixtures are achievable using power curves as proved by the simulation and experimental packings. As demonstrated by experiment and simulations, the 0.45-power curve can provide a better packing vs. a 0.7-power distribution for the concrete mixtures with maximum aggregate size (D_{max}) used in the construction industry.

The 3D packing models which simulate the particulate packing and correlate the packing with particle size distribution provide quick feedback on the optimal blends and 3D visualization of aggregate distributions. The reported research demonstrated that the results of 3D simulation can be used as reference distributions to match with the experimental blends using available aggregates.

The Shilstone coarseness chart can assist in elaborating the level of workability of concrete and coarseness of the blends with binary, ternary or multi-class aggregates. It was proved that all mixtures located within Zone II, subzones 2 to 5 had excellent workability. The use of the Shilstone coarseness chart is recommended as an acceptance tool to tune the aggregate blends for the mixtures with various cement contents and aggregate combinations.

Based on the results of this study, in concrete with cementitious material content of less than 300 kg/m^3 (500 lb/yd^3), the aggregate optimization may require up to 50% proportion of sand in the aggregates blend. Due to improved grading and packing, the use

of intermediate aggregate fraction is beneficial for concrete performance. In this way, depending on the type and PSD of the individual aggregate fractions, the intermediate aggregates can be used in the blends, replacing up to 30% of the coarse aggregates.

The compressive strength of concrete can be correlated with the degree of packing of the aggregates. As a result of aggregate optimization, the concrete compressive strength can be increased up to 15% and, consequently, enhanced performance can be used to reduce the proportion of cementitious materials. The implementation of improved grading with ternary aggregates can greatly assist in this process.

6.2. Cement Paste and Mortar

The heat of hydration is useful for the optimization of dosage of chemical admixtures prior to application in concrete. An optimization process including the investigation of mechanical performance of cement paste and mortars is essential when various cements, SCM, and chemical admixtures are used.

6.3. Concrete Optimization

The use of PCE admixtures can enable up to 10 % reduction of W/C ratio and water content vs. commonly used with water-reducing admixtures. The PCE admixtures had demonstrated an excellent compatibility with AE agents and various SCM. As a result, the cementitious content in concrete with PCE can be reduced by up to 18%, reaching 280 kg/m^3 (470 lb/yd^3) and, in some cases (when PCE superplasticizer was used), up to 250 kg/m^3 (420 lb/yd^3) vs. current WisDOT specification requirements.

The use of effective PCE admixture and Class C fly ash combination enables the reduction of the W/CM ratio and, at the same time, enhances work demonstrated performance ability. The combination of the two components works synergistically to enhance mechanical performance resulting in compressive strength as high as 40 MPa (5,800 psi) at 28 days and above 60 MPa (8,700 psi) at 90 days.

The effective use of Class F fly ash requires the application of PCE superplasticizer and also adjustment of air content; this enables the reduction of W/CM ratio and achievement of acceptable strength levels. However, even at a cementitious material content of 280 kg/m^3 (470 lb/yd^3) the performance of Class F fly ash when used in concrete with other admixtures yielded unsatisfactory mechanical properties. This finding may require future investigation to explain the observed behavior and new approaches to improve the activity of Class F fly ash in concrete.

The use of aggregate optimization and the incorporation of additional air (by using a higher dosage of AE admixture) beyond the conventional specifications is essential in the design of low cement mixtures with 250 kg/m^3 (420 lb/yd^3) of cementitious materials.

The modulus of rupture (MOR) obtained from the flexural center-point (3-point) loading of the beams has a good correlation with the corresponding compressive strength as demonstrated for various mixtures and testing ages (as demonstrated in Appendix 2).

6.4. Durability

Due to lower W/CM used, the concrete based on southern crushed limestone aggregates had lower ultimate shrinkage vs. concrete based on northern aggregates.

However, the observed length change values were slightly exceeding the limits predicted by ACI 224R.

In durability tests, various concrete compositions had different RCP performance, but had a very similar response to freezing and thawing exposure. All investigated concrete mixtures had a relatively high air content (achieved by the application of AE admixture) and, therefore, excellent spacing factors and freeze-thaw resistance.

The RCP of investigated concrete based on northern igneous gravel aggregates was higher than that of the corresponding concrete based on southern aggregates; still, the most of investigated concrete types without SCM were characterized by “low” to “moderate” RCP values from 1,000 to 3,000 Coulombs. The best results, characterized by “very low” RCP of less than 1,000 Coulombs, were demonstrated by concrete based on slag cement and Class F fly ash used in combination with PCE superplasticizers.

7. FUTURE RESEARCH

The various aspects of reported research can be further extended.

1. Better understanding of the effects of Class F fly ash on concrete performance and new methods for activation of fly ash must be investigated.

2. Further investigation of air void structure using different methods including rapid air and flat-bed scanner and enhanced interpretation using 3D models can be suggested to develop and recommend the concrete mixtures with excellent freezing and thawing resistance.

3. A comprehensive multi-scale model of concrete can be developed based on the reported data; and, furthermore, this model can be used to establish a new concrete mixture proportioning procedure that targets low cement contents, minimizes the experiments, and serves as an expert tool for WisDOT applications. This procedure can involve the performance characteristics of different components of paste, mortar and concrete into consistent design routine intended for concrete mixtures with required performance levels.

4. The development of a software package for aggregate optimization as a tool based on the results of packing simulations, theoretical models, and experimental data can be useful for the implementation of the reported research effort.

REFERENCES

1. *Report Card for America's Infrastructure*, 2013, ASCE.
2. Van Dam, T., et al., *Sustainable concrete pavements: A manual of practice.* 2012.
3. Simon, M.J., E.S. Lagergren, and K.A. Snyder. *Concrete mixture optimization using statistical mixture design methods*. in *Proceedings of the PCI/FHWA international symposium on high performance concrete*. 1997.
4. Ramachandran, V., M. Lowery, and V. Malhotra, *Behaviour of ASTM Type V cement hydrated in the presence of sulfonated melamine formaldehyde.* Materials and structures, 1995. **28**: p. 133-138.
5. Peterson, K., L.L. Sutter, and G. Anzalone, *Reduction of Minimum Required Weight of Cementitious Materials in WisDOT Concrete Mixes*, 2011.
6. Mostofinejad, D. and M. Reisi, *A new DEM-based method to predict packing density of coarse aggregates considering their grading and shapes.* Construction and Building Materials, 2012. **35**: p. 414-420.
7. Sobolev, K., *The development of a new method for the proportioning of high-performance concrete mixtures.* Cement and Concrete Composites, 2004. **26**(7): p. 901-907.
8. Abrams, D., *A tribute to Proportioning Concrete Mixtures.* ACI Special Publication, 2008. **249**.
9. Abrams, D., *Proportioning of concrete mixtures* Structural Materials Research Laboratory December 1918. Bulletin **No.1.**(Lewis Institute Chicago).
10. Gilkey, J.H., *Water-Cement Ratio versus Strength – Another Look* ACI Journal Proceeding April 1961. **(4)**: p. 57.
11. Neville, A.M., *Proportioning of concrete mixtures.* 1995: p. 269-272.
12. Neville, A.M., *Properties of concrete. Fourth and final edition*, 1996, Pearson, Prentice Hall. ISBN 0-582-23070-5. OCLC.
13. Goltermann, P. and V. Johansen, *Packing of aggregates: an alternative tool to determine the optimal aggregate mix.* ACI Materials Journal, 1997. **94**(5).

14. de Larrard, F. and T. Sedran, *Optimization of ultra-high-performance concrete by the use of a packing model.* Cement and Concrete Research, 1994. **24**(6): p. 997-1009.
15. Vorobiev, V., *Application of physical and mathematical methods in concrete research.* Visshaya Shkola, Moscow, 1977.
16. Fuller, W.B. and S.E. Thompson, *The laws of proportioning concrete.* Transactions of the American Society of Civil Engineers, 1906. **57**(2): p. 67-143.
17. *American Concrete Institute, Aggregates for Concrete Bulletin E1-07, First Print*, 2007.
18. Sobolev, K. and A. Amirjanov, *Application of genetic algorithm for modeling of dense packing of concrete aggregates.* Construction and Building Materials, 2010. **24**(8): p. 1449-1455.
19. de Larrard, F., *A method for proportioning high-strength concrete mixtures.* Cement, concrete and aggregates, 1990. **12**(1): p. 47-52.
20. de Larrard, F. and A. Belloc, *The influence of aggregate on the compressive strength of normal and high-strength concrete.* ACI Materials Journal, 1997. **94**(5).
21. Hansen, T.C. *Influence of aggregate and voids on modulus of elasticity of concrete, cement mortar, and cement paste*. in *ACI Journal Proceedings*. 1965. ACI.
22. Li, S.-t.i. *Proposed Synthesis of Gap-Graded Shrinkage-Compensating Concrete*. in *ACI Journal Proceedings*. 1967. ACI.
23. Richardson, D.N., *Aggregate gradation optimization: literature search.* 2005.
24. Sobolev, K., et al. *Packing of aggregates as an approach to optimizing the proportioning of concrete mixtures aggregates: asphalt concrete, portland cement concrete, bases, and fines, presented at*. 2004. ICAR/AFTRE/NSSGA Symp.
25. Fennis, S., *Design of ecological concrete by particle packing optimization*2011: TU Delft, Delft University of Technology.
26. Roy, D., et al., *Concrete components packing handbook*, 1993.
27. Powers, T., *Properties of Fresh Concrete, John Wiley and Sons.* Inc., New York, 1968: p. 301.

28. Andersen P.J., J.V., *Particle packing and concrete properties.* Material Science of Concrete, The American Ceramic Society, Inc., 1991(II).
29. Aim, R.B. and P. Le Goff, *Effet de paroi dans les empilements désordonnés de sphères et application à la porosité de mélanges binaires.* Powder Technology, 1968. **1**(5): p. 281-290.
30. Toufar, W., M. Born, and E. Klose, *Beitrag zur Optimierung der Packungsdichte polydisperser körniger Systeme.* Freiberger Forschungsheft, 1976. **558**(29-44): p. 201.
31. de Larrard, F., *Concrete mixture proportioning: a scientific approach*1999: CRC Press.
32. Dewar, J., *Computer modelling of concrete mixtures*2002: CRC Press.
33. Brouwers, H. and H. Radix, *Self-compacting concrete: theoretical and experimental study.* Cement and Concrete Research, 2005. **35**(11): p. 2116-2136.
34. Vogt, C. *Ultrafine particles to save cement and improve concrete properties*. in *Nordic Concrete Research, Sandefjord, Norway, June 13-15, 2005*. 2005. The Nordic Concrete Federation.
35. Feret, R., *Sur la compactie des mortiershyrdauliques, Ann.Ponts Chaussée, mé.moires etdocuments.* Série 7, 1892. **No. IV**: p. 5-164.
36. Fu, G. and W. Dekelbab, *3-D random packing of polydisperse particles and concrete aggregate grading.* Powder Technology, 2003. **133**(1): p. 147-155.
37. Kolonko, M., S. Raschdorf, and D. Wäsch, *A hierarchical approach to estimate the space filling of particle mixtures with broad size distributions.* submitted to Powder Technology, 2008.
38. Sobolev, K. and A. Amirjanov, *The development of a simulation model of the dense packing of large particulate assemblies.* Powder Technology, 2004. **141**(1): p. 155-160.
39. Zhao, H., et al., *The effect of coarse aggregate gradation on the properties of self-compacting concrete.* Materials & Design, 2012. **40**: p. 109-116.
40. Moini, M., et al., *Aggregate Optimization for Concrete Mixtures with Low Cement Factor, 2014*

41. Yurdakul, E., et al., *A paper to be submitted to Journal of Materials in Civil Engineering (ASCE).* Proportioning for performance-based concrete pavement mixtures, 2013: p. 65.
42. Ashraf, W. and M. Noor, *Performance-evaluation of concrete properties for different combined aggregate gradation approaches.* Procedia engineering, 2011. **14**: p. 2627-2634.
43. Torquato, S., T.M. Truskett, and P.G. Debenedetti, *Is random close packing of spheres well defined?* Physical review letters, 2000. **84**(10): p. 2064.
44. Kwan, A. and C. Mora, *Effects of various, shape parameters on packing of aggregate particles.* Magazine of concrete Research, 2002. **53**(2): p. 91-100.
45. Stroeven, P. and M. Stroeven, *Assessment of packing characteristics by computer simulation.* Cement and Concrete Research, 1999. **29**(8): p. 1201-1206.
46. Moini, M. and A. Lakizadeh, *Concrete Workability: An Investigation on Temperature effects Using Artificial Neural Networks*2011: AuthorHouse.
47. Sobolev, K. and A. Amirjanov, *A simulation model of the dense packing of particulate materials.* Advanced Powder Technology, 2004. **15**(3): p. 365-376.
48. Papadakis, V.G., *Effect of fly ash on Portland cement systems: Part II. High-calcium fly ash.* Cement and Concrete Research, 2000. **30**(10): p. 1647-1654.
49. Moini, M., A. Lakizadeh, and M. Mohaqeqi, *Effect of mixture temperature on slump flow prediction of conventional concretes using artificial neural networks.* Australian Journal of Civil Engineering, 2012. **10**(1).
50. Ramseyer, C.C. and R. Kiamanesh, *Optimizing Concrete Mix Designs to Produce Cost Effective Paving Mixes*, 2009, Civil Engineering and Environmental Science, University of Oklahoma.
51. Rached, M., M. De Moya, and D.W. Fowler, *Utilizing aggregates characteristics to minimize cement content in portland cement concrete.* International Center for Aggregates Research (ICAR 401), University of Texas, Austin, USA, 2009.
52. Quiroga, P.N. and D.W. Fowler, *The effects of aggregates characteristics on the performance of Portland cement concrete*, 2004, International Center for Aggregates Research, University of Texas at Austin.

53. de Larrard, F. and T. Sedran, *Mixture-proportioning of high-performance concrete.* Cement and Concrete Research, 2002. **32**(11): p. 1699-1704.
54. Sobolev, K. and S. Soboleva, *High-Performance Concrete Mixture Proportioning.* ACI Special Publication, 1998. **179**.
55. Ji, T., et al., *A mix proportion design method of manufactured sand concrete based on minimum paste theory.* Construction and Building Materials, 2013. **44**: p. 422-426.
56. Moini M., F.V.I., Amirjanov A., Sobolev K., *The Optimization of Aggregate Blends for Sustainable Low Cement Concrete, Construction and Building Materials 93 (2015): 627-634.* 2015.
57. Noguchi, T., I. Maruyama, and M. Kanematsu. *Performance based design system for concrete mixture with multi-optimizing genetic algorithm*. in *Proceedings of the 11th International Congress on the Chemistry of Cement "Cements Contribution to the Development in the 21st Century", Durban*. 2003.
58. Yeh, I.-C., *Computer-aided design for optimum concrete mixtures.* Cement and Concrete Composites, 2007. **29**(3): p. 193-202.
59. Cheng, M.-Y., D. Prayogo, and Y.-W. Wu, *Novel Genetic Algorithm-Based Evolutionary Support Vector Machine for Optimizing High-Performance Concrete Mixture.* Journal of Computing in Civil Engineering, 2013. **28**(4).
60. Fennis, S.A. and J.C. Walraven, *Using particle packing technology for sustainable concrete mixture design.* Heron, 57 (2012) 2, 2012.
61. Liu, R., et al., *Optimization of cementitious material content for sustainable concrete mixtures.* Journal of Materials in Civil Engineering, 2011. **24**(6): p. 745-753.
62. Easa, S.M. and E.K. Can, *Optimization model for aggregate blending.* Journal of construction engineering and management, 1985. **111**(3): p. 216-230.
63. Cordon, W.A. and H.A. Gillespie. *Variables in concrete aggregates and Portland cement paste which influence the strength of concrete*. in *ACI Journal Proceedings*. 1963. ACI.
64. Koehler, E.P., *Aggregates in self-consolidating concrete,* 2007: ProQuest.

65. Kwan, A. and H. Wong, *Packing density of cementitious materials: part 2—packing and flow of OPC+ PFA+ CSF.* Materials and structures, 2008. **41**(4): p. 773-784.
66. Bergman, L.A. *Optimization of Portland-Pozzolan Concrete, Airport Runways*. in *Construction and Materials Issues 2001*. 1962. ASCE.
67. Aydın, S., *A ternary optimisation of mineral additives of alkali activated cement mortars.* Construction and Building Materials, 2013. **43**: p. 131-138.
68. *Aggregate suspension mixture proportioning method.* TechNote, ACI 211.6T-14. 68.
69. Lange, A. and Plank, J., *Formation of Nano-Sized Ettringite Crystals Identified as Root Cause for Cement Incompatibility of PCE Superplasticizers*. in *Nanotechnology in Construction, NICOM 5*. 2015.
70. Collepardi, S., et al., *Mechanisms of Actions of Different Superplasticizers for High Performance Concrete.* ACI Special Publication, 1999. **186**.
71. Shin, J.-Y., et al., *Effects of polycarboxylate-type superplasticizer on fluidity and hydration behavior of cement paste.* Korean Journal of Chemical Engineering, 2008. **25**(6): p. 1553-1561.
72. Yamada, K., et al., *Effects of the chemical structure on the properties of polycarboxylate-type superplasticizer.* Cement and Concrete Research, 2000. **30**(2): p. 197-207.
73. Bassioni, G., *The influence of cement composition on superplasticizers' efficiency.* International Journal of Engineering (IJE), 2010. **3**(6): p. 577.
74. Mikanovic, N. and C. Jolicoeur, *Influence of superplasticizers on the rheology and stability of limestone and cement pastes.* Cement and Concrete Research, 2008. **38**(7): p. 907-919.
75. Sakai, E., K. Yamada, and A. Ohta, *Molecular structure and dispersion-adsorption mechanisms of comb-type superplasticizers used in Japan.* Journal of Advanced Concrete Technology, 2003. **1**(1): p. 16-25.
76. Kim, B.-G., et al., *The adsorption behavior of PNS superplasticizer and its relation to fluidity of cement paste.* Cement and Concrete Research, 2000. **30**(6): p. 887-893.

77. Andersen, P.J. and V. Johansen, *A guide to determining the optimal gradation of concrete aggregates.* Contract, 1993. **100**: p. 206.
78. Mangulkar, M. and S. Jamkar, *Review of Particle Packing Theories Used For Concrete Mix Proportioning.* International Journal of Scientific and Engineering Research, 2013. **4**(5): p. 143-148.
79. Andersen, P.J., *Control and Monitoring of Concrete Production: A Study of Particle Packing and Rheology: a Thesis in Concrete Technology,*1990: Danish Academy of Technical Sciences.
80. Andersen, P.J. and V. Johansen, *Particle packing and concrete properties*1993.
81. Joisel, A., *Composition des Betons Hydrauliques, Ann. l'ITBTP,58,992-1065, .* 1952.
82. Poulsen, A., *Cement in seawater: report on the trials, commenced in 1896 on the reco mmendation of the society of Scaninavian Portland cement manufacturers.* 1909.
83. Furnas, C.C., *Flow of gases through beds of broken solids*. Vol. 300. 1929: US Govt. print. off.
84. Westman, A.R. and H. Hugill, *The Packing of Particles.* Journal of the American Ceramic Society, 1930. **13**(10): p. 767-779.
85. Petersen, I.F., *Report on Packing Models, F. L. Schmidt & Co.* 1981.
86. Toufar, W., E. Klose, and M. Born, *Berechnung der packungsdichte von korngemischen.* Aufbereitung-Technik, 1977. **11**: p. 603-608.
87. Furnas, C., *Grading aggregates-I.-Mathematical relations for beds of broken solids of maximum density.* Industrial & Engineering Chemistry, 1931. **23**(9): p. 1052-1058.
88. Schwanda, F., *Das rechnerische Verfahren zur Bestimmung des Hohlraumes und Zementleimanspruches von Zuschlägen und seine Bedeutung für den Spannbetonbau.* Zement und Beton, 1966. **37**(8-17): p. 13.
89. Reschke, T., *Der Einfluss der Granulometrie der Feinstoffe auf die Gefügeentwicklung und die Festigkeit von Beton*2001.
90. Stovall, T., F. De Larrard, and M. Buil, *Linear packing density model of grain mixtures.* Powder Technology, 1986. **48**(1): p. 1-12.

91. Yu, A. and N. Standish, *Porosity calculations of multi-component mixtures of spherical particles.* Powder Technology, 1987. **52**(3): p. 233-241.
92. Talbot, A.N. and F.E. Richart, *The Strength of Concrete-Its relation to the Cement, Aggregates and Water.* Illinois Univ Eng Exp Sta Bulletin, 1923.
93. Kumar, S. and M. Santhanam, *Particle packing theories and their application in concrete mixture proportioning: A review.* Indian concrete journal, 2003. **77**(9): p. 1324-1331.
94. Funk, J., D. Dinger, and J. Funk Jr, *Coal Grinding and Particle Size Distribution Studies for Coal-Water Slurries at High Solids Content.* Final Report, Empire State Electric Energy Research Corporation (ESEERCO), New York, NY, 1980.
95. Funk, J.E. and D. Dinger, *Predictive process control of crowded particulate suspensions: applied to ceramic manufacturing*1994: Springer Science & Business Media.
96. Walker, W., *Persistence of Granular Structure during Compaction Processes.* Kona, 2003. **21**: p. 133-142.
97. Zheng, J., P.F. Johnson, and J.S. Reed, *Improved equation of the continuous particle size distribution for dense packing.* Journal of the American Ceramic Society, 1990. **73**(5): p. 1392-1398.
98. Peronius, N. and T. Sweeting, *On the correlation of minimum porosity with particle size distribution.* Powder Technology, 1985. **42**(2): p. 113-121.
99. Garas, V. and K. Kurtis, *Assessment of methods for optimising ternary blended concrete containing metakaolin.* Magazine of concrete Research, 2008. **60**(7): p. 499-510.
100. Hunger, M., *An integral design concept for ecological self-compacting concrete*, 2010, Technische Universiteit Eindhoven.
101. Toufar, W., M. Born, and E. Klose, *Freiberger Forschungsheft A 559.* VEB Deutscher Verlag Fuer Grundstoffindustrie, 1967.
102. Zheng, J. and P. Stroeven. *Computer Simulation of Particle Section Patterns from Sieve Curves for Spherical Aggregate*. in *Modern concrete materials: binders, additions and admixtures: proceedings of the international Conference held at the University of Dundee, Scotland, UK on*. 1999.

103. Snoeijer, J.H., et al., *Packing geometry and statistics of force networks in granular media.* Physical Review E, 2004. **70**(1): p. 011301.
104. Gram, A. and J. Silfwerbrand, *Computer simulation of SCC flow.* Betonwerk und Fertigteil-Technik, 2007. **73**(8).
105. Roussel, N., et al., *Computational modeling of concrete flow: General overview.* Cement and Concrete Research, 2007. **37**(9): p. 1298-1307.
106. Stroeven, P., J. Hu, and Z. Guo, *Shape assessment of particles in concrete technology: 2D image analysis and 3D stereological extrapolation.* Cement and Concrete Composites, 2009. **31**(1): p. 84-91.
107. Kwan, A., C. Mora, and H. Chan, *Particle shape analysis of coarse aggregate using digital image processing.* Cement and Concrete Research, 1999. **29**(9): p. 1403-1410.
108. Mora, C. and A. Kwan, *Sphericity, shape factor, and convexity measurement of coarse aggregate for concrete using digital image processing.* Cement and Concrete Research, 2000. **30**(3): p. 351-358.
109. Kwan, A. and W. Fung, *Packing density measurement and modelling of fine aggregate and mortar.* Cement and Concrete Composites, 2009. **31**(6): p. 349-357.
110. Flores-Vivian, I., et al., *The use of Nanoparticles to improve the performance of concrete.*
111. *Laboratory study of optimized concrete pavement mixtures. WisDOT ID No. 0092-13-04.* 2015.
112. Moini, M., *The optimization of concrete mixtures for use in highway applications*, in *Civil and Environmental Engineering,* 2015, University of Wisconsin-Milwaukee.
113. Shilstone Sr, J.M., *Concrete mixture optimization.* Concrete International, 1990. **12**(6).
114. ASTM C989, *Standard Specification for Slag Cement for Use in Concrete and Mortars.*
115. American Society for Testing and Materials, A.C.-. *Standard Specification for Coal Fly Ash and Raw or Calcined Natural Pozzolan for Use in Concrete*, 2003.

116. Paul J. Tikalsky, A.J.S., David G. Tepke, *Potential Concrete Mixture Designs for the I-99 Corridor Final Report, Issues 2003-2029*, P.T. Institute and R.P.T. Institute).

117. P. Tikalsky, V.S., K. Wang, B. Scheetz, T. Rupnow, A. St. Clair, M. Siddiqi, and S. Marquez, , *Development of Performance Properties of Ternary Mixes: Phase I Final Report. FHWA Pooled Fund Study TPF-5 (117)*2007.

118. Sutter, L., *Reduction of Minimum Required Weight of Cementitious Materials in WisDOT Concrete Mixes*, in *Research Progress Report,* 2008.

119. Odman, S.T.A., *Effects of Variations in Volume, Surface Area Exposed to Drying, and Composition of Concrete on Shrinkage*, in *Manual of Concrete Practice International Colloquium on the Shrinkage of Hydraulic Concrete*, Rilem/Cembureau, 1968: Madrid.

Appendix 1: Visual Appearance of Investigated Concrete

In spite of reduced cementitious content of 420-470 lb/yd^3, the investigated concrete had excellent workability and a very low number of surface and internal imperfections (see A1.1…A1.7).

A1.1: Southern aggregate concrete with cementitious content of 470 lb/yd^3 (L1 cement):

L-S-M (BB04)

L-S-P (BB13)

A1.2: Southern aggregate concrete with cementitious content of 420 lb/yd^3 (L1 cement):

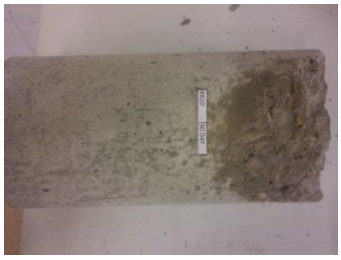

L-S-M-R (BB20)

L-S-P-R (BB21)

A1.3: Northern aggregate concrete with cementitious content of 470 lb/yd^3 (L2 cement):

L-N-M (B14)

L-N-P (B12)

A1.4: Southern aggregate concrete with cementitious content of 470 lb/yd^3 (H cement):

H-S-M (BB19)

H-S-P (BB17)

A1.5: Southern aggregate concrete with cementitious content of 470 lb/yd^3 (S cement):

S-S-M (BB16)

S-S-P (BB14)

A1.6: Northern aggregate concrete with cementitious content of 470 lb/yd^3 (H cement):

H-N-M (B3)

H-N-P (B1)

A1.7: Northern aggregate concrete with cementitious content of 470 lb/yd^3 (S cement):

S-N-M (B6)

S-N-P (B4)

Appendix 2: The Estimate for Modulus of Rupture (MOR)

Based on the extensive tests, the functional relationship for MOR vs. compressive strength of normal weight concrete is governed by ACI 318 building code:

$$f_r = 7.5 * SQRT(f_c') \text{ , psi} \qquad \text{(A1)}$$

However, ACI 318 equation provides a very conservative estimate for MOR of concrete with compressive strength of more than 3,000 psi as reported by ACI 363 "High-Strength Concrete." To address this issue for concrete with 3,000 psi < fc ′ < 12,000 psi, ACI 363 recommends an equation adopted from Carrasquillo et al. (1982):

$$f_r = 11.7 * SQRT(f_c') \text{ , psi} \qquad \text{(A2)}$$

The MOR data for all tested concrete types are summarized by Figures A2.1 and A2.2.

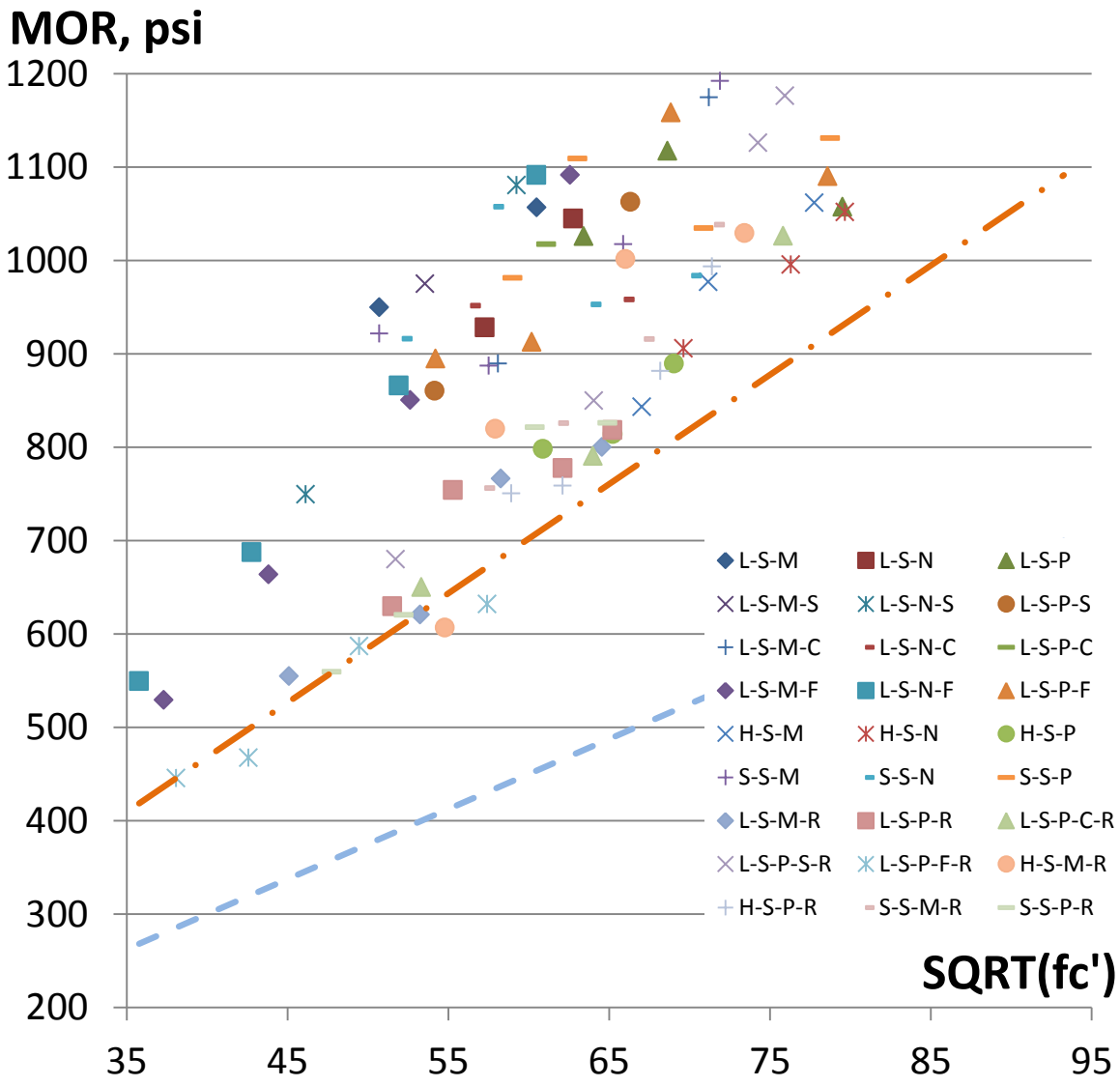

Figure A2.1. The relationship for MOR vs. compressive strength for Southern aggregate concrete

Southern aggregate concrete consistently demonstrated higher values for MOR vs. prescribed by ACI 363 equation, especially for the zone with higher compressive strength, Figure A2.1. The following equation can be derived for MOR of concrete based on Southern aggregates:

$$f_r = 15.341 * SQRT(f_c'), \text{ psi} \qquad R^2 = 0.6889 \qquad \text{(A3)}$$

Higher values of MOR and splitting tensile strength were reported for high quality crushed-rock aggregates (Dewar, 1964). Such beneficial performance can be also explained by the improved bond between the cement matrix and aggregates and enhanced interfacial transition zone (ITZ), possibly due to the effects of internal curing. Optimized gradation of aggregates can be also responsible for improved performance. Furthermore, two different cases can be considered for Southern aggregate concrete depending on the total cementitious material content:

Case 1: for cementitious content of 470 lb/yd^3 the MOR is defined by:

$$f_r = 16.213 * SQRT(f_c'), \text{ psi} \qquad R^2 = 0.6974 \qquad \text{(A4a)}$$

Case 2: for cementitious content of 420 lb/yd^3 the MOR is defined by:

$$f_r = 13.253 * SQRT(f_c'), \text{ psi} \qquad R^2 = 0.8472 \qquad \text{(A4b)}$$

In this way, for the same f_c' concrete with higher cementitious material content (Case 1) had about 22.7% higher MOR vs. concrete defined by the Case 2. The MOR bottom boundary condition for Case 2 concrete can be defined by the equation of ACI 363, especially for the zone with lower compressive strength, Figure A2.1. For the Case 1, concrete based on cement "H" had demonstrated lower MOR vs. predicted by Equation A4, Figure A2.1. Relatively high scatter for the MOR experimental values vs. predicted by the ACI equations is typical for 3-point bending test, especially when concrete with different supplementary cementitious materials and chemical admixtures is investigated.

The ACI 363 equation also provided a better fit for the MOR experimental data for Northern aggregate concrete. Indeed, the following equation derived from the experimental data is very similar to Equation A2, Figure A2.2:

$$f_r = 11.829 * SQRT(f_c'), \text{ psi} \qquad R^2 = 0.7529 \qquad \text{(A5)}$$

The Northern aggregate concrete has demonstrated considerably lower values of MOR when compared with Southern aggregate concrete, especially, for Case 1 (cementitious content of 470 lb/yd^3). This is very common difference for the aggregates with lower angularity, but also can be caused by aggregates surface contamination reported for Northern aggregates. The scatter of the experimental data for MOR values was acceptable as caused by few compositions with Class F fly ash which deviated from the mainstream trend.

The ACI 318 equation (A1) underestimates the MOR of investigated concrete and, therefore, when accuracy is required, should not be used in the design of pavements.

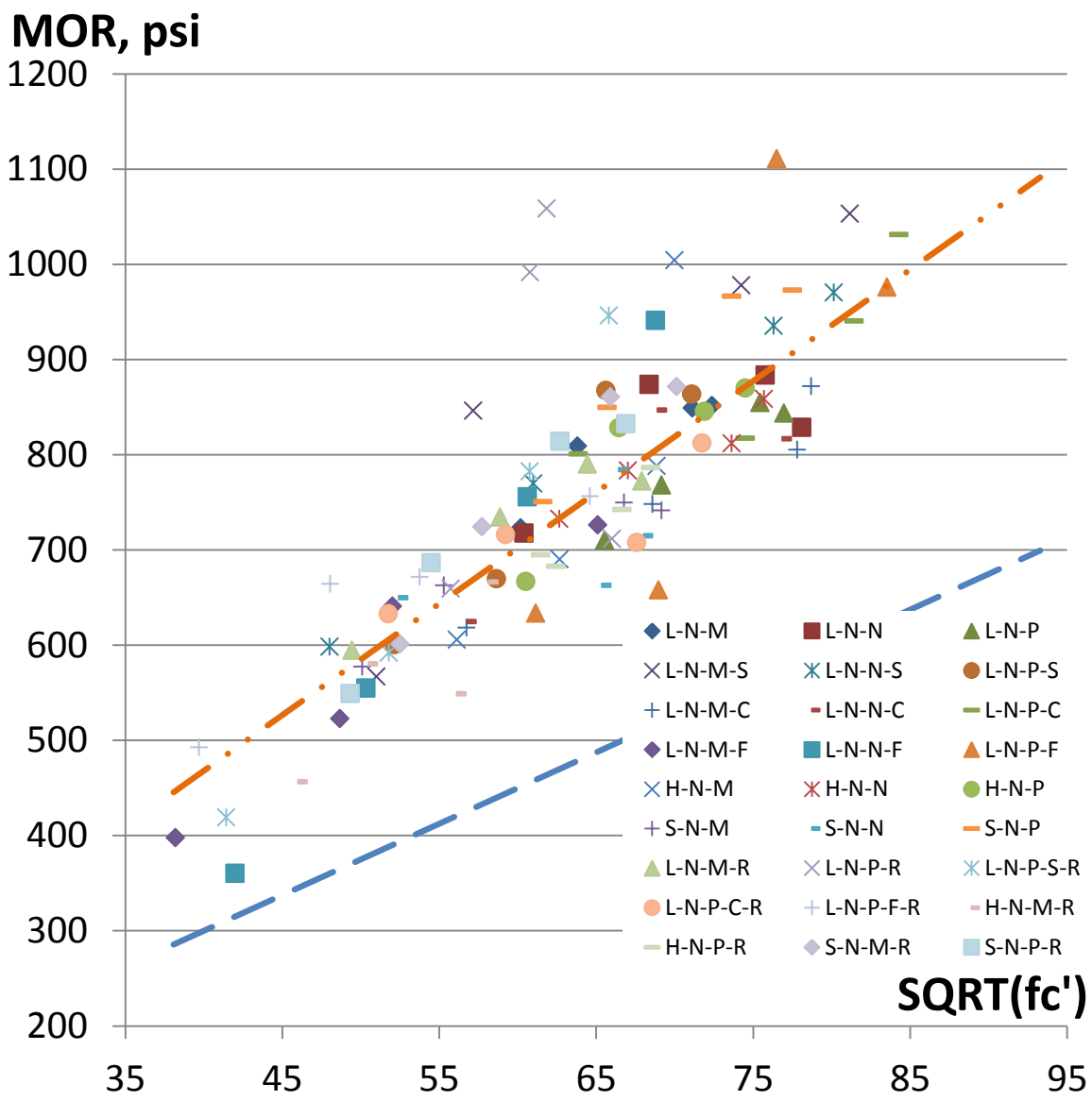

Figure A2.2. The relationship for MOR vs. compressive strength for Northern aggregate concrete

References

ACI Committee 318, 2005, "Building Code Requirements for Structural Concrete (ACI 318-05) and Commentary," American Concrete Institute, Farmington Hills, MI, 430 pp.

ACI Committee 363, 2010, "Report on High-Strength Concrete (ACI 363R-10)," American Concrete Institute, Farmington Hills, MI, 67 pp.

Carrasquillo, R. L.; Nilson, A. H.; and Slate, F. O., 1982, "Properties of High Strength Concrete Subjected to ShortTerm Loads," ACI JOURNAL, Proceedings V. 78, No. 3, May-June 1981, pp. 171-178.

Dewar, J. D., 1964, "The Indirect Tensile Strength of Concretes of High Compressive Strength," Technical Report No. 42.377, Cement and Concrete Association, Wexham Springs, 12 pp.

Appendix 3: Proposed Update of 715 QMP Concrete Pavement and Structures

715.1 Description

(1) This section describes contractor mix design and testing requirements for class I concrete used in concrete pavements, and concrete structures.

715.1.1 Quality Control Program

715.1.1.1 General

(1) Conform to the general requirements under 701 and 710 as well as the additional specific contract QMP provisions for class I concrete specified here in section 715. The department defines class I concrete as cast-in-place concrete used in pavement or structure applications where all of the following apply:

- Mix design requires review by the engineer.
- The contract defines spec limits for strength.
- The contractor may earn statistically based incentives for superior concrete strength however, HES and SHES concrete types are not eligible for 28-day strength incentives.

715.1.1.2 Small Quantities

(1) The department defines small quantities of class I concrete, subject to the reduced requirements under 710.2, as follows:

- Less than 150 cubic yards of structure concrete placed under a single bid item.
- Less than 2500 cubic yards of slip-formed pavement placed using a single mix design.
- Less than 1000 cubic yards of non-slip-formed pavement placed using a single mix design.

715.1.1.3 Pre-Pour Meetings for Structure Concrete

(1) Arrange at least two pre-pour meetings to discuss concrete placement. Discuss the placement schedule, personnel roles and responsibilities, testing and quality control, and how test results will be communicated. Schedule the first meeting before placing any concrete and the second before placing any bridge deck concrete. Ensure that representatives from all parties involved with concrete work, including contractor, sub-contractor, ready-mix supplier, testers, and the project manager, attend these meetings.

715.1.1.4 Quality Control Plan

(1) If a comprehensive quality control plan is required under 701.2.2, submit a plan conforming to 701.2.2 and include additional concrete mix information as follows:

1. Preliminary concrete mix information including proposed production facilities, sources and properties of materials as well as the name, title, and phone number of the person developing the mix design.
2. Proposed individual and combined aggregate gradation limits (including ternary aggregate blends and other information relevant to optimized gradations).
3. Proposed concrete mixture proportioning as per as ACI 211.1-91 (or 211.6T-14) and preliminary test results as outlined in ACI 211.5R-14.
4. Proposed methods for monitoring and recording batch weights.
5. Proposed sampling plan and protocols for lab and *in-situ* testing.

715.2 Materials and Concrete Mixture Proportioning

715.2.1 General

(1) Determine mixes for class I concrete used under the contract using one or more of the following methods:

- Have a HTCP-certified PCC technician II develop new concrete mixes qualified based on the results of mix development tests performed by a department-qualified laboratory.
- For new concrete mixtures provide the proportioning as per as ACI 211 (e.g., 211.1-91 or 211.6T-14) and support the design with the lab or field test records.
- Submit previously-used department-approved mixes qualified based on long-term lab reports and field performance.

(2) The contractor must provide separate laboratory mix designs for high-early strength concrete and also provide routine 1-, 3-, 7- and 28-day compressive strength test results during the placement of high early strength concrete.

(3) For lab-qualified or field-qualified mixes, in addition to the mix information required under 710.4, submit 2 copies of a concrete mix report at least 3 business days before producing concrete. For lab-qualified

mixes, include strength data, test dates, and the name and location of the laboratory that performed mix development and testing as per as ACI 211.5R-14. For field-qualified mixes, include historical data that demonstrate acceptable strength and field performance.

(4) Ensure that the concrete mix report includes a cover sheet with signature blocks for both the mix developer and the engineer. Have the mix developer sign and date each copy attesting that all information in the report is accurate. The engineer will sign and date each copy of the report. The engineer's signature verifies that the engineer had the opportunity to review the mix report, to check that it meets the concrete mix requirements, and to comment. The engineer will return a signed copy to the contractor within 3 business days of receiving the report.

715.2.2 Combined Aggregate Gradation

715.2.2 General

(1) Ensure that the combined aggregate gradation conforms to the following, expressed as weight percentages of the total aggregate:

1. One hundred percent passes the 2-inch sieve.
2. The percent passing the 1-inch sieve is less than or equal to 89. The engineer may waive this requirement for one or more of the following:
   - Clear spacing between reinforcing bars is less than 2 inches.
   - The contractor provides an engineer-approved optimized gradation analysis.
3. The percent passing the No. 4 sieve is less than or equal to 42, except if the coarse aggregate is completely composed of crushed stone, up to 47 percent may pass the No. 4 sieve. For pavement, coarse aggregate may be completely composed of recycled concrete, in which case up to 47 percent may pass the No. 4 sieve.
4. The percent passing the No. 200 sieve is less than or equal to 2.3 percent.

(2) Submit proposed combined gradation limits and target individual gradations along with the mix information required under 710.4.

715.2.2.2 Optimized Gradations for Concrete Pavement

The Contractor has the option of developing an optimized gradation under the combined aggregate gradation provisions of 715.2.2. Identify a concrete mixture design with an optimized aggregate gradation. The Engineer will use the Contractor's optimized aggregate gradation test results, as verified by Department testing, to determine eligibility for incentive.

Develop a target optimized gradation for each mix design based on normal production gradations and the relative percentages of each individual aggregate. Take samples at the belt leading to the weigh hopper or other locations close to the incorporation of the work as approved by the Engineer.

Optimized Gradation Working Range	
Sieve Sizes	Working Range, %
2 in. (50 mm)	±5
1 ½ in. (37.5 mm)	±5
1 in. (25 mm)	±5
¾ in. (19 mm)	±5
½ in. (12.5 mm)	±5
3/8 in. (9.5 mm)	±5
No. 4 (4.75 mm)	±5
No. 8 (2.36 mm)	±4
No. 16 (1.18 mm)	±4
No. 30 (600 µm)	±4
No. 50 (300 µm)	±3
No. 100 (150 µm)	±2
No. 200 (200 µm)	≤1.6

The running average of the three combined aggregate gradation tests is required to fall within the limits established by the target gradation and the working ranges listed in the table above.

Use statistical analysis of the optimized aggregate gradation samples on a lot basis representing one week's paving. The lot will represent the cumulative average of the sublot values on each sieve for the gradation band or the cumulative average of the sublot values of the coarseness factor and the workability factor for the coarseness factor chart.

An optional incentive is available to the Contractor provided concrete mixture is designed and produced with an optimized aggregate gradation that meets one of the following options listed below. The Contractor may achieve only one of the optional incentives for any single lot.

Develop optimized aggregate gradations based upon one of the following methods:

1. Individual Percent Retained Gradation Band

8-18 or 7-18 Individual Percent Retained Gradation Band		
Sieve Sizes	8-18 % Retained	7-18 % Retained
2 in. (50 mm)	0%	0%
1 ½ in. (37.5 mm)	≤9%	≤9%
1 in. (25 mm)	8-18%	7-18%
¾ in. (19 mm)	8-18%	7-18%
½ in. (12.5 mm)	8-18%	7-18%
3/8 in. (9.5 mm)	8-18%	7-18%
No. 4 (4.75 mm)	8-18%	7-18%
No. 8 (2.36 mm)	8-18%	7-18%
No. 16 (1.18 mm)	8-18%	7-18%
No. 30 (600 µm)	8-18%	7-18%
No. 50 (300 µm)	≤13%	≤13%
No. 100 (150 µm)	≤8%	≤8%
No. 200 (200 µm)	≤8%	≤8%

2. Workability vs. Coarseness Factor Analysis

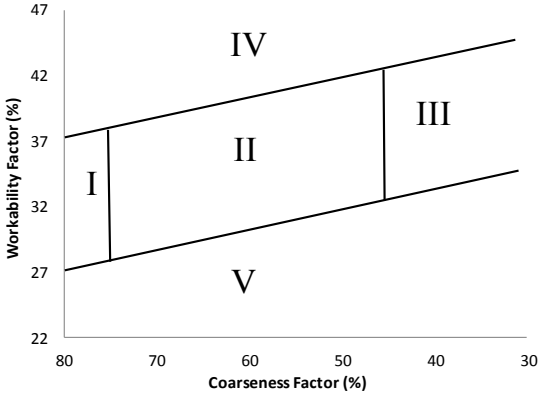

Figure 1: Coarseness and Workability (Shilstone) Chart

The coarseness and workability factors shall be calculated and plotted in a coarseness and workability (Shilstone) chart as shown in the figure above:

$$\text{Coarseness Factor} = \frac{\text{Combined Percent Passing 3/8 in. (9.5 mm) Sieve}}{\text{Combined Percent Passing No. 8 (2.36 mm) Sieve}} \times 100$$

$$\text{Workability Factor} = \text{Combined Percent Passing No. 8 (2.36 mm) Sieve} + \frac{2.5 \times (C - 564)}{94}$$

where: C is the total cementitious material content in the mix, lb/yd^3

3. Power curve optimization

Select the relative amounts of fine, intermediate, and coarse aggregates based on grading, shape, angularity, and texture as per as ACI 211.6T-14. The best grading for a mixture depends on the application and the aggregate properties. As a starting point, select a blend of fine and coarse aggregate best matching the 0.45-power curve without an excess or deficiency of material on two adjacent sieves.

The 0.45-power curve, which is shown in Figure 2a, is a plot of percent passing on the vertical axis and sieve sizes raised to the 0.45 power on the horizontal axis. A straight line is drawn from the minimum aggregate size (No. 200 sieve) to the maximum aggregate size (size with approximately 85% of the combined material passing). For better workability the gradings finer than the 0.45-power curve (achieved by reducing the exponent to less than 0.45) are usually preferred to coarser gradings because these reduce the harshness.

For paving applications the combined gradings fitting between the power curves with exponents of 0.40 and 0.60 are recommended. Up to ±5% deviation form these upper and lower limits is allowed only on two consequent sieves. In case when the maximum aggregate size differs from 1 in., the relative sieve size normalized to maximum aggregate size can be used for optimization (Figure 2b).

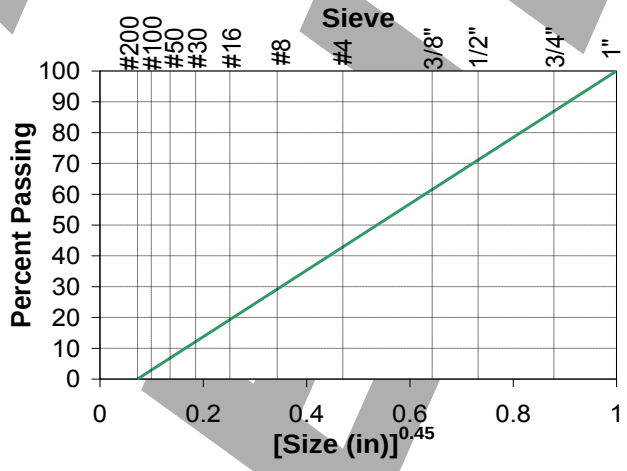

a)

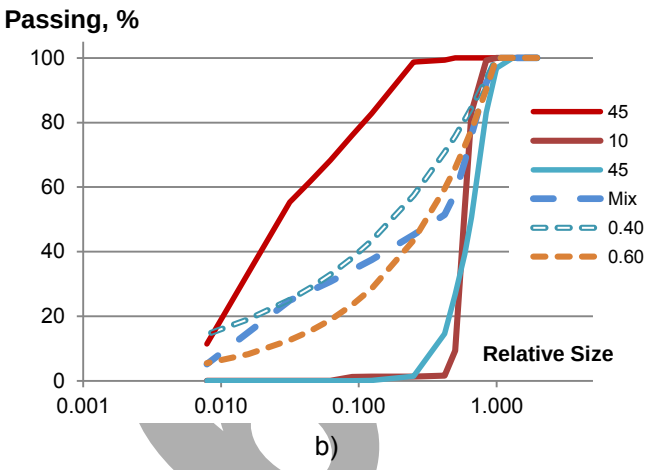

b)

Figure 2: Power Curve for Combined Aggregate from ACI 211.6T (a) and Optimization of Ternary Blend Using Normalized Particle Size Scale (b)

An incentive is available to the Contractor provided a concrete mixture is designed, produced, and meets at least one of the optimized gradation criteria defined above. The Contractor may achieve only one of the incentives for any single lot.

715.2.3 Cementitious Materials and W/CM for Class I Concrete

715.2.3.1 Pavements

(1) Use at least 5 pairs of cylinders to demonstrate the level of compressive strength of a mix design. Use either laboratory strength data for new mixes or field strength data for established mixes. Demonstrate that the 28-day compressive strength of the proposed concrete will be equal or exceed the 85 percent within limits criterion specified in 715.5.2. Report on the 90-day compressive strength for concrete with fly ash, slag cement or ternary blends.

(2) Use cement conforming ASTM C150 and C595 cements with limitations imposed by WisDOT specification 501.2.1. Provide a minimum cement content of 565 pounds per cubic yard, except if using type I, IL, or III cement in a mix where the geologic composition of the coarse aggregate is primarily igneous or metamorphic materials, provide a minimum cement content of 660 pounds per cubic yard.

(3) The contractor may use class C fly ash or slag cement of grade 100 or 120 as a partial replacement for cement. For binary mixes use up to 30% fly ash or slag cement, except for slip-formed work the contractor may use up to 50% slag. For ternary mixes use up to 30% fly ash plus slag in combination. Replacement values are in percent by weight of the total cementitious material in the mix.

(4) Ensure that the target ratio of net water to cementitious material for the submitted mix design does not exceed 0.42 by weight. Include free water on the aggregate surface but do not include water absorbed within aggregate particles (i.e., consider aggregates in Saturated-Surface Dry, SSD conditions). Record and report on the aggregate absorption, moisture content and water correction.

(5) Do not use chloride based accelerators in mixes for new construction.

715.2.3.2 Structures

(1) Qualify compressive strength according to ACI Code 318 chapter 5 subsections 5.3.1 through 5.3.3 and 5.5. Use either laboratory strength data for new mixes or field strength data for established mixes. Demonstrate that the 28-day compressive strength of the proposed concrete will be equal or exceed the 90 percent within limits criterion specified in 715.5.3. Report on the 90-day compressive strength for concrete with fly ash or slag cement.

(2) Use cement conforming ASTM C150 and C595 cements with limitations imposed by WisDOC specification 501.2.1. Provide a mix grade containing fly ash (A-FA), slag (A-S), both fly ash and slag (A-T), or blended cement (A-IP, A-IS, or A-IT) Ensure that the cementitious content equals or exceeds 565 pounds per cubic yard. Unless the engineer approves otherwise in writing, conform to one of the following:

1. Use class C fly ash, silica fume, metakaolin or grade 100 or 120 slag cement as a partial replacement for cement. For binary mixes use 15% to 30% fly ash, 20% to 30% slag, up to 5% of silica fume or metakaolin. For ternary mixes use 15% to 30% fly ash plus slag and silica fume or metakaolin in combination. Replacement values are in percent by weight of the total cementitious material in the mix.

2. Use a type IP, IS, or IT blended cement.

(3) Ensure that the target ratio of net water to cementitious material (w/cm) for the submitted mix design does not exceed 0.45 by weight. Include free water on the aggregate surface but do not include water absorbed within aggregate particles (i.e., consider aggregates in Saturated-Surface Dry, SSD conditions). Control the w/cm ratio throughout production by adjusting batch weights for changes in the aggregate moisture as required under 715.3.3.2. Record and report on the aggregate absorption, moisture content and water correction.

(4) Do not use mixes containing accelerators, except the contractor may use mixes containing non-chloride accelerators in substructure elements.

715.2.4 Chemical Admixtures

(1) In order to achieve the water to cementitious material ratios required by this specification, the use of chemical admixtures is necessary. Because strength and other important concrete qualities such as durability, shrinkage, and cracking are related to the total water content and the w/c or w/cm used, water-reducing admixtures are often used to improve concrete quality. Use chemical admixtures conforming to ASTM C494 as follows:

- Type A—Water-reducing
- Type B—Retarding
- Type C—Accelerating
- Type D—Water-reducing and retarding
- Type E—Water-reducing, and accelerating
- Type F—Water-reducing, high-range
- Type G—Water-reducing, high-range, and retarding

Type F high-range, water-reducing (HRWR) admixtures (e.g., polycarboxylate ether, PCE superplasticizers) are often used to produce flowing concrete; however these can be effectively used for the reduction of the total water content and the reduction of w/c or w/cm.

(2) Use of air-entraining (AE) agent conforming to ASTM C260 and WisDOT specification 501.2.2 in order to achieve the required air-void structure and air content specified by 501.3.2.4.2. The use of an air-entraining agent gives the concrete producer the flexibility to adjust the entrained air content and workability to compensate for the many conditions, such as: characteristics of aggregates, nature and proportions of constituents of the concrete admixtures, type and duration of mixing, consistency, temperature, cement fineness and chemistry, and the use of other cementitious materials or chemical admixtures. The combination of air-entraining agents with superplasticizers may alter the air bubble size distribution and spacing, therefore, the proof of compatibility of these admixtures is required. To ensure the adequate performance of AE agent, the provisions of WisDOT specification 501.2.2 (5) and (6) must be met.

(3) The use of accelerating ASTM C494 Type C admixtures is the subject to restriction imposed by 715.2.3.1(5) and 715.2.3.2(4) of this document.

(4) Use laboratory mix proportioning data, air content and strength results data to establish the dosages of chemical and AE admixtures. Demonstrate that the 28-day compressive strength of the concrete will be equal or exceed the requirements specified in 715.2.3.1, 715.2.3.2 and 715.5.3. For concrete with fly ash or slag cement also report on the 90-day compressive strength.

(5) An incentive is available to the Contractor provided a concrete mixture is designed, produced, and meets the reduction of water to cementitious material (w/cm) ratio from the defined above in 715.2.3.1(4) and 715.2.3.2(3). The Contractor may achieve only one of the incentives for any single lot.

715.3 Testing and Acceptance

715.3.1 Class I Concrete Testing

715.3.1.1 General

(1) Provide slump, air content, fresh unit weight, yield, concrete temperature and compressive strength test results as specified in 710.5. Provide a battery of QC tests, consisting of results for each specified property, using a single sample randomly located within each sublot. Recalculate the batch proportions to adjust for fluctuations of air content, fresh unit weight, and or yield. For each testing point/location, cast at least three cylinders for strength evaluation.

(2) If a sublot random test location falls within a mainline pavement gap, relocate the test to a different location within the sublot.

(3) From each lot collect, label and store in appropriate laboratory curing conditions at least three cylinders for strength evaluation at later ages, up to 10 years as required by the department verification testing.

715.3.1.2 Lot and Sublot Definition

715.3.1.2.1 General

(1) Designate the location and size of all lots before placing concrete. Ensure that no lot contains concrete of more than one mix design, as defined in 715.3.1, or more than one placement method, defined as either slip-formed, not slip-formed, or placed under water.

(2) Lots and sublots include ancillary concrete placed integrally with the class I concrete.

715.3.1.2.2 Lots by Lane-Feet

(1) The contractor may designate slip-formed pavement lots and sublots conforming to the following:

- Lots and sublots are one paving pass wide and may include one or more travel lanes, integrally placed shoulders, integrally placed ancillary concrete, and pavement gaps regardless of mix design and placement method.
- Sublots are 1000 feet long for single-lane and 500 feet long for two-lane paving. Align sublot limits with ride segment limits defined in the special provisions. Adjust terminal sublot lengths to match the project length or, for staged construction, the stage length. Ensure that sublot limits match for adjacent paving passes. Pavement gaps do not affect the location of sublot limits.
- Create lots by grouping 4 to 8 adjacent sublots matching lots created for adjacent paving passes.

(2) If a sublot random test location falls in a pavement gap, test at a different random location within that sublot.

715.3.1.2.3 Lots by Cubic Yard

(1) Define standard lots and sublots conforming to the following:

- Do not designate more than one sublot per truckload of concrete.
- Lots for structures are a maximum of 500 cubic yards divided into approximately equal 50-cubic-yard or smaller sublots.
- Lots for pavement are a maximum of 2000 cubic yards divided into approximately equal 250-cubic-yard or smaller sublots.

(2) The contractor may designate lots smaller than standard sized. An undersized lot is eligible for incentive payment under 715.5 if the contractor defines 4 or more sublots for that lot.

715.3.1.3 Department Verification Testing

(1) The department will perform verification testing as specified in 701.4.2 except as follows:

- Air content, slump, fresh unit weight, and temperature: a minimum of 1 verification test per lot.
- Compressive strength: a minimum of 1 verification test per lot.
- Aggregate gradation for optimized blends : collect minimum of one sample per day, test 20% of daily samples and retain the remaining samples for up to 5 years from the project close out.

715.3.2 Strength Evaluation

715.3.2.1 General

(1) The department will make pay adjustments for compressive strength on a lot-by-lot basis using the compressive strength of contractor QC cylinders. The department will accept or reject concrete on a sublot-by-sublot basis using core strength. Perform coring and testing, fill core holes with an engineer-approved non-shrink grout, and provide traffic control during coring.

(2) Randomly select 2 QC cylinders to test at 28 days for percent within limits (PWL). Compare the strengths of the 2 randomly selected QC cylinders and determine the 28-day sublot average strength as follows:

- If the lower strength divided by the higher strength is 0.9 or more, average the 2 QC cylinders.
- If the lower strength divided by the higher strength is less than 0.9, break one additional cylinder and average the 2 higher strength cylinders.

715.3.2.2 Removal and Replacement

715.3.2.2.1 Pavement

(1) If a sublot strength is less than 2,500 psi, the department may direct the contractor to core that sublot to determine its structural adequacy and whether to direct removal. Cut and test cores according to

AASHTO T24 as and where the engineer directs. Have an HTCP-certified PCC technician I perform or observe the coring.

(2) The sublot pavement is conforming if the compressive strengths of all cores from the sublot are 2,500 psi or greater or the engineer does not require coring.

(3) The sublot pavement is nonconforming if the compressive strengths of any core from the sublot is less than 2,500 psi. The department may direct removal and replacement or otherwise determine the final disposition of nonconforming material as specified in 106.5.

715.3.2.2.2 Structures

(1) The department will evaluate the sublot for possible removal and replacement if the 28-day sublot average strength is lower than f'c minus 500 psi. The value of f'c is the design stress the plans show. The department may assess further strength price reductions or require removal and replacement only after coring the sublot.

(2) The engineer may initially evaluate the sublot strength using a non-destructive method. Based on the results of non-destructive testing, the department may accept the sublot at the previously determined pay for the lot, or direct the contractor to core the sublot.

(3) If the engineer directs coring, obtain three cores from the sublot in question. Have an HTCP-certified PCC technician I perform or observe core sampling according to AASHTO T24. Determine core locations, subject to the engineer's approval, that do not interfere with structural steel.

(4) Have an independent consultant test cores according to AASHTO T24.

(5) If the 3-core average is greater than or equal to 85% of f'c, and no individual core is less than 75% of f'c, the engineer will accept the sublot at the previously determined pay for the lot. If the 3-core average is less than 85% of f'c, or an individual core is less than 75% of f'c, the engineer may require the contractor to remove and replace the sublot or assess a price reduction of $35 per cubic yard or more.

715.3.3 Aggregates

715.3.3.1 General

(1) Except as allowed for small quantities in 710.2, provide aggregate test results conforming to 710.5.6.

715.3.3.2 Structures

(1) In addition to the aggregate testing required under 710.5.6, determine the fine and coarse aggregate moisture content for each sample used to test the percent passing the No. 200 sieve.

(2) Calculate target batch weights for each mix when production of that mix begins. Whenever the moisture content of the fine or coarse aggregate changes by more than 0.5 percent, adjust the batch weights to maintain the design w/cm ratio.

715.4 Measurement

(1) The department will measure Incentive Strength Concrete Pavement and Incentive Strength Concrete Structures by the dollar, calculated as specified in 715.5.

(2) The Department will measure incentive for optimized aggregate gradations and reduced w/cm for concrete pavement by the dollar calculated as specified in 715.5.

715.5 Payment

715.5.1 General

(1) The department will pay incentive for compressive strength under the following bid items:

ITEM NUMBER	DESCRIPTION	UNIT
715.0415	Incentive Strength Concrete Pavement	DOL
715.0502	Incentive Strength Concrete Structures	DOL

(2) Incentive payment may be more or less than the amount the schedule of items shows.

(3) The department will administer disincentives for compressive strength under the Disincentive Strength Concrete Pavement and the Disincentive Strength Concrete Structures administrative items.

(4) The department will adjust pay for each lot using PWL of the 28-day sublot average strengths for that lot. The department will measure PWL relative to the lower specification limit of 3700 psi for pavements and 4000 psi for structures. The department will not pay a strength incentive for concrete that is nonconforming in another specified property, for ancillary concrete accepted based on tests of class I

concrete, or for high early strength concrete unless placed in pavement gaps as allowed under 715.3.1.2.1.

(5) Submit strength results to the department electronically using the MRS software. The department will validate contractor data before determining pay adjustments.

(6) All coring and testing costs under 715.3.2.2 including filling core holes and providing traffic control during coring are incidental to the contract.

715.5.2 Pavements

(1) The department will adjust pay for each lot using equation "QMP 3.01" as follows:

Percent within Limits (PWL)	Pay Adjustment (dollars per square yard)
≥ 95 to 100	(0.1 x PWL) - 9.5
≥ 85 to < 95	0
≥ 30 to < 85	(1.5/55 x PWL) - 127.5/55
< 30	-1.50

(2) The department will not pay incentive if the lot standard deviation is greater than 400 psi.

(3) For lots with a full battery of QC tests at less than 4 locations, there is no incentive but the department will assess a disincentive based on the individual sublot average strengths. The department will reduce pay for sublots with an average strength below 3700 psi by $1.50 per square yard.

(4) For integral shoulder pavement and pavement gaps accepted using tests from the adjacent travel lane, The department will adjust pay using strength results of the travel lane for integrally placed concrete shoulders and pavement gaps regardless of mix design and placement method, included in a lane-foot lot.

715.5.3 Structures

(1) The department will adjust pay for each lot using equation "QMP 2.01" as follows:

Percent within Limits (PWL)	Pay Adjustment (dollars per cubic yard)
≥ 99 to 100	10
≥ 90 to < 99	0
≥ 50 to < 90	(7/8 x PWL) – 78.75
< 50	-35

(2) The department will not pay incentive if the lot standard deviation is greater than 350 psi.

(3) For lots with less than 4 sublots, there is no incentive but the department will assess a disincentive based on the individual sublot average strengths. The department will reduce pay for sublots with an average strength below 4000 psi by $35 per cubic yard.

715.5.2 Optimized Gradation incentive for Concrete Pavement

The Department will pay incentive for optimized gradation under the following bid items:

ITEM NUMBER	DESCRIPTION	UNIT
715.XXXX	Incentive Optimized Gradations Concrete Pavement	Dollar

Contact:

The Department will adjust pay for each lot of concrete pavement based upon one of the following methods:

1. Incentive payment wil be calculated for coarseness and workability based on the contract unit price per square yard for concrete pavement constructed, times the percent incentive as defined in 715.2.2.2 as follows:

Gradation Zone (Workability vs. Coarseness Factor Analysis Figure)	Percent Incentive
II-A	3%
II-B	2%
II-C	1%
II-D	0%

2. Incentive payment will be calculated for Individual Percent Retained based on the contract unit price per square yard for concrete pavement constructed, times the percent incentive as defined in 715.2.2.2 as follows:

Individual Percent Reatined Incentive	
Gradation Options	Percent Incentive
8-18 Retained	2%
7-17 Retained	1%

3. Incentive payment will be calculated for Power Curve Optimization based on the contract unit price per square yard for concrete pavement constructed, times the percent incentive as defined in 715.2.2.2 as follows:

Power Curve Optimization	
Gradation Options	Percent Incentive
Combined grading fits between 0.4- and 0.6-power curves	3%
Single deviation of up to 5% from 0.4- or 0.6-power curves	2%
Double deviation of up to 5% from 0.4- or 0.6-power curves	1%

4. Incentive payment will be calculated for use of lower w/cm from specified by 715.2.3.1(4) and 715.2.3.2(3) based on the contract unit price per square yard for concrete pavement constructed, times the percent incentive as defined in 715.2.2.2 as follows:

W/CM Reduction Incentive	
W/CM Reduction	Percent Incentive
Reduction by 0.03	3%
Reduction by 0.02	2%
Reduction by 0.01	1%

Appendix 4: Example of Concrete Mix Proportioning

Given

Concrete		
Batch Volume=	10	ft3
$f'c$=	4,000	psi
Slump=	4	in
Aggregate Dmax=	0.75	in
Cement Type I		
S.G.=	3.15	
Fly Ash Class C		
S.G.=	2.40	
Coarse Aggregate		
Bulk S.G.=	2.65	
Absorption=	0.35	%
Dry-Rodded Bulk Dens.=	100	lb/ft3
Moisture=	1.5	%
SAF=	5	
Intermediate Aggregate		
Bulk S.G.=	2.65	
Absorption=	0.35	%
Dry-Rodded Bulk Dens.=	95	lb/ft3
Moisture=	1.5	%
SAF=	5	
Fine Aggregate		
Bulk S.G.=	2.60	
Absorption=	0.75	%
F.M.	2.5	
Moisture=	7.5	%
SAF=	1	
Exposure:	F/T and Deicing Salts	

Design

Concrete mix with AE agent		
Concrete mix with plasticizer	10	%
Concrete mix with superplasticizer	15	%

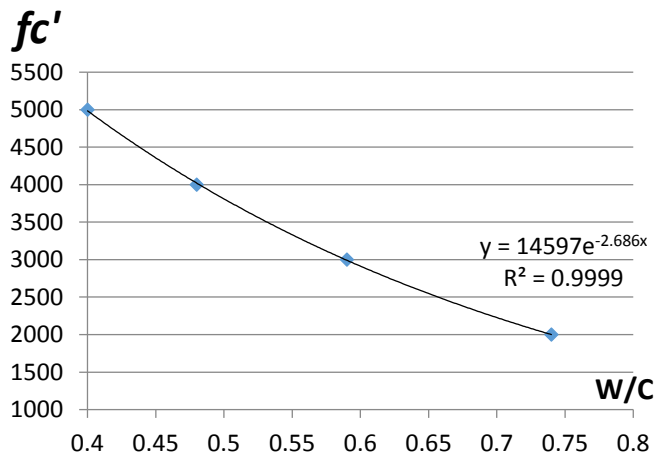

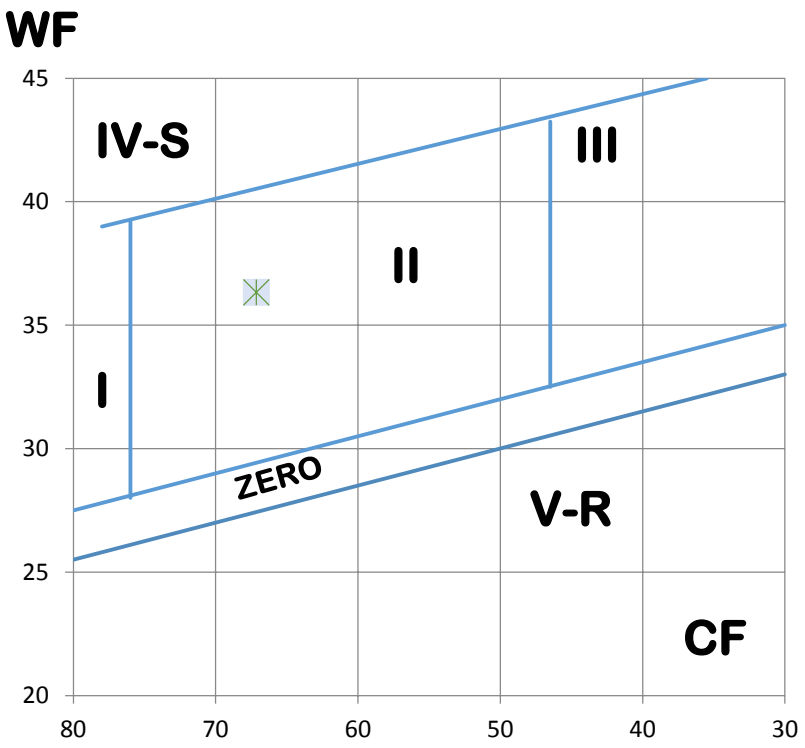

WF = 36
CF = 67

Zone II ? ok

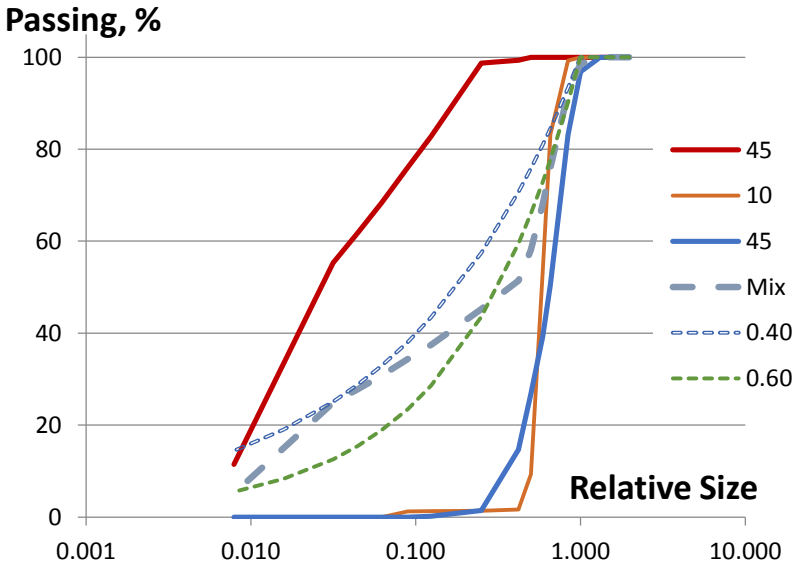

DOT Concrete

1) 28-day Compressive Strength = 4000 psi
2) Slump = 4 in
3) Exposed to F/T, therefore Air Entrainment (AE) should be used:

ACI 211.6T

Step 1: Nominal Maximum Aggregate Size = 0.75 in

Step 2: Select Combined Aggregates

Coarse Aggregate	45	%	
Intermediate Aggregate	10	%	as the best fit to 0.55-power curve
Fine Aggregate	45	%	
Dry-Rodded Bulk Dens.=	125	lb/ft3	

Step 3: Combined Aggregates Voids and SAF

Voids =	23.8	%
SAF =	3.2	

Step 4: Paste and Air Volume

Min Vol. paste and air =	28.6	%				
Use Vol. paste and air =	30.2	%	as	5.5	%	boost

Step 5: Determine W/C ratio

W/C=	0.45	$f'c$=	4358	psi

Step 6: Verify air content

Air Entrainment=	6	%

Step 7: Determine W/P ratio (+Limestone/Stone powder)

W/P=	0.45	

Step 8: Calculate individual components

		Volumes		Mass		
Vol. %	C+FA =	0.103	yd3	521	lb/yd3	
30.2	Cement =	0.084	yd3	443	lb/yd3	
	Fly Ash =	0.019	yd3	78	lb/yd3	15 %
	Water =	0.139	yd3	235	lb/yd3	
	Air =	0.060	yd3			
	Total =	0.302	yd3	756	lb/yd3	

69.8	C. Agg. =	0.314	yd3	1402	lb/yd3		
	I. Agg. =	0.070	yd3	312	lb/yd3		
	F. Agg. =	0.314	yd3	1376	lb/yd3		
	Total =	0.698	yd3	3089	lb/yd3		
Check:	Total =	1.000	yd3	3845	lb/yd3	ok	
	Superplasticizer =			0.782	lb/yd3	0.15	%
	AE =			0.052	lb/yd3	0.01	%

Step 9: Make adjustments and evaluate trial mixtures

Coarse Agg.(wet)=	1423	lb/yd3	
Intermediate Agg.(wet)=	316	lb/yd3	
Fine Agg.(wet)=	1479	lb/yd3	
Superplasticizer (30 %) =	2.607	lb/yd3	30 %

Coarse Adj.=	1.15	%
Intermediate Adj.=	1.15	%
Fine Adj.=	6.75	%
Water Required=	120	lb/yd3

Cement=	443	lb/yd3
Fly Ash =	78	lb/yd3
Water=	120	lb/yd3
Coarse Agg.=	1423	lb/yd3
Intermediate Agg.=	316	lb/yd3
Fine Agg.=	1479	lb/yd3
Superplasticizer =	2.607	lb/yd3
AE =	0.052	lb/yd3
Sum=	3863	lb/yd3

Therefore, amounts for 10 ft3 batch are:

Cement=	164	lb
Fly Ash =	29	lb
Water=	45	lb
Coarse Agg.=	527	lb
Intermediate Agg.=	117	lb
Fine Agg.=	548	lb
Superplasticizer =	0.97	lb
AE =	0.02	lb
Sum=	1431	lb

Step 10: Make adjustments for yield based on trial mix or field test

Slump =	4.5	in.	ok
Air =	6.5	%	ok
Fresh Unit Mass=	3830	lb/yd3	
Yield =	1.008		
$f'c$=	4,250	psi	ok

Mixture proportions for one cubic yard (corrected for yield):

Cement=	440
Fly Ash =	78
Water=	119
Coarse Agg.=	1411
Intermediate Agg.=	314
Fine Agg.=	1466
Superplasticizer =	2.59
AE =	0.05
Sum=	3830 lb/yd3

Air Entrainment= 6 % According to Table A1.5.3.3 ACI 211.1

ACI 211.1

Step 1: Determine Water (W)

According to Table 6.3.3:

W=	305	lb/yd3	
W reduced for plasticizer	275	lb/yd3	0.05 %
W reduced for superplasticizer	233	lb/yd3	0.15 %

Step 2: Determine W/C ratio

According to Table 6.3.4(b) for extreme exposure:

W/C= 0.45 $f'c$= 4358 psi

Step 3: Determine the amount of Cement (C+FA)

	C+FA=	519	lb/yd3
15 %	FA=	78	lb/yd3
	C=	441	lb/yd3

Step 4: Determine Coarse Aggregates

According to Table 6.3.6

Volume of	C. Agg.=	0.65	yd^3
Weight of	C. Agg.=	1755	lb/yd3

Step 5: Estimate of Fine Aggregates

All components minus sand= 2579 lb/yd3

According to Table 6.3.7.1

Fresh Unit Mass= 3840 lb/yd3

Fine Agg. by Mass Method= 1262 lb/yd3

<u>Absolute Volume Method</u>

Vol. of Cement=	0.083	yd^3
Vol. of Fly Ash=	0.019	yd^3
Vol. of Water=	0.138	yd^3
Vol. of C. Agg.=	0.393	yd^3

Vol. of Air=	0.060	yd^3	
Total =	0.694	yd^3	
Vol. of Fine Agg.=	0.306	yd^3	
Weight of Fine Agg.=	1341	lb/yd3	
Superplasticizer =	0.778	lb/yd3	0.15 %
AE =	0.052	lb/yd3	0.01 %

Step 6: Make adjustments and evaluate trial mixtures

Moisture Adjustment:

Coarse Agg.(wet)=	1781	lb/yd3
Fine Agg.(wet)=	1442	lb/yd3
Superplasticizer (30 %) =	2.593	lb/yd3 30 %

Absorption Adjustment:

Coarse Adj.=	1.15	%
Fine Adj.=	6.75	%
Water Required=	121	lb/yd3

Estimated batch for one cubic meter:

Cement=	441	lb/yd3
Fly Ash =	78	lb/yd3
Water=	121	lb/yd3
Coarse Agg.=	1781	lb/yd3
Fine Agg.=	1442	lb/yd3
Superplasticizer =	2.593	lb/yd3
AE =	0.052	lb/yd3
Sum=	3865	lb/yd3

Therefore, amounts for 10 ft3 batch are:

Cement=	163	lb
Fly Ash =	29	lb
Water=	45	lb
Coarse Agg.=	660	lb
Fine Agg.=	534	lb
Superplasticizer =	0.96	lb
AE =	0.02	lb
Sum=	1431	lb

Step 7: Make adjustments for yield based on trial mix or field test

Slump =	3.75	in.	ok
Air =	5.5	%	ok
Fresh Unit Mass=	3875	lb/yd3	
Yield =	0.997		
$f'c$=	4,450	psi	ok

Mixture proportions for one cubic yard (corrected for yield):

Cement=	442	
Fly Ash =	78	
Water=	121	
Coarse Agg.=	1786	
Fine Agg.=	1445	
Superplasticizer =	2.60	
AE =	0.05	
Sum=	3875	lb/yd3